

การพัฒนาอาชีพที่พหิมูโนเซนเซอร์ในการตรวจวัด  
โปรตีนเหมือนโคติเนสซึ่งเป็นตัวบ่งชี้ทางชีวภาพ



วิทยานิพนธ์นี้เป็นส่วนหนึ่งของการศึกษาตามหลักสูตรปริญญาวิทยาศาสตรดุษฎีบัณฑิต  
สาขาวิชาชีวเคมี  
มหาวิทยาลัยเทคโนโลยีสุรนารี  
ปีการศึกษา 2558

**THE DEVELOPMENT OF CAPACITIVE  
IMMUNOSENSORS TO DETECT CHITINASE-LIKE  
PROTEIN BIOMARKERS**

**Wethaka Chaocharoen**



**A Thesis Submitted in Partial Fulfillment of the Requirements for the  
Degree of Doctor of Philosophy in Biochemistry  
Suranaree University of Technology  
Academic Year 2015**

# **THE DEVELOPMENT OF CAPACITIVE IMMUNOSENSORS TO DETECT CHITINASE-LIKE PROTEIN BIOMARKERS**

Suranaree University of Technology has approved this thesis submitted in partial fulfillment of the requirements for the Degree of Doctor of Philosophy.

Thesis Examining Committee

---

(Prof. Dr. James R. Ketudat-Cairns)

Chairperson

---

(Assoc. Prof. Dr. Wipa Suginta)

Member (Thesis Advisor)

---

(Assoc. Prof. Dr. Panote Thavarungkul)

Member

---

(Assoc. Prof. Dr. Albert Schults)

Member

---

(Asst. Prof. Dr. Panida Khunkaewla)

Member

---

(Prof. Dr. Sukit Limpijumnong)

Vice Rector for Academic Affairs  
and Innovation

---

(Assoc. Prof. Dr. Prapun Manyum)

Dean of Institute of Science

เวรกา เจ้าเจริญ : การพัฒนาคาพาซิทีฟอิมมูโนเซนเซอร์ในการตรวจวัดโปรตีนเหมือน  
ไคตินเนสซึ่งเป็นตัวบ่งชี้ทางชีวภาพ (THE DEVELOPMENT OF CAPACITIVE  
IMMUNOSENSORS TO DETECT CHITINASE-LIKE PROTEIN BIOMARKERS)  
อาจารย์ที่ปรึกษา : รองศาสตราจารย์ ดร.วิภา สุจินต์, 173 หน้า

ในการศึกษานี้ได้ทำการพัฒนาคาพาซิทีฟอิมมูโนเซนเซอร์แบบไม่ติดผลึกเพื่อการตรวจวัดโปรตีนที่เป็นตัวบ่งชี้ต่อโรค 2 ชนิดคือ YKL-39 และ YKL-40 ในระบบโพลีอิมมูโนเซนเซอร์ วิชานิพนธ์ฉบับนี้ได้แบ่งการศึกษาออกเป็น 2 ส่วน โดยส่วนแรกทำการศึกษาเกี่ยวกับการผลิตรีคอมบิแนนท์โปรตีน YKL-40 ในระบบการแสดงออกจากเซลล์แบคทีเรีย และเซลล์ของสัตว์เลี้ยงลูกด้วยนม เพื่อใช้สำหรับการผลิตโพลีโคลนอลที่จำเพาะต่อโปรตีน YKL-40 จากการศึกษาพบว่า YKL-40 แอนติบอดีมีความจำเพาะและทำปฏิกิริยาอย่างสูงต่อโปรตีน YKL-40 เมื่อนำ YKL-40 โพลีโคลนอลแอนติบอดีที่ถูกทำให้บริสุทธิ์ มาตรึงบนผิวอิเล็กโทรดทองคำทำงานโดยเทคนิคการเคลือบผิวแบบเรียงตัวชั้นเดียว พบว่าสภาวะที่เหมาะสมในการวิเคราะห์ของระบบอิมมูโนเซนเซอร์ต่อโปรตีน YKL-40 จากแบคทีเรีย ได้แก่ ปริมาณสารตัวอย่าง 200 ไมโครลิตร อัตราการไหล 100 ไมโครลิตรต่อนาที กรดไฮโดรคลอริกเข้มข้น 3.16 มิลลิโมลาร์ (พีเอชเท่ากับ 2.5) เป็นสารรีเจนเนอเรต และบัฟเฟอร์ที่ใช้คือ โซเดียมฟอสเฟตบัฟเฟอร์ความเข้มข้น 10 มิลลิโมลาร์ มีค่าพีเอชที่ 7.0 ในขณะที่ สภาวะที่เหมาะสมในการวิเคราะห์ของระบบอิมมูโนเซนเซอร์ต่อโปรตีน YKL-40 จากเซลล์ของสัตว์เลี้ยงลูกด้วยนม ได้แก่ ปริมาณสารตัวอย่าง 250 ไมโครลิตร อัตราการไหล 100 ไมโครลิตรต่อนาที กรดไฮโดรคลอริกเข้มข้น 3.16 มิลลิโมลาร์ (พีเอชเท่ากับ 2.5) เป็นสารรีเจนเนอเรต และบัฟเฟอร์ที่ใช้คือ โซเดียมฟอสเฟตบัฟเฟอร์ความเข้มข้น 10 มิลลิโมลาร์ มีค่าพีเอชที่ 7.0 โดยภายใต้สภาวะที่เหมาะสมต่อการวิเคราะห์ ทั้งสองระบบของอิมมูโนเซนเซอร์ต่อโปรตีน YKL-40 พบช่วงความเป็นเส้นตรงระหว่าง 0.1 ถึง 1,000 ไมโครกรัมต่อลิตร ในขณะที่ค่าขีดจำกัดที่ต่ำสุดในการวัดอยู่ที่  $0.07 \pm 0.01$  ไมโครกรัมต่อลิตรในอิมมูโนเซนเซอร์ต่อโปรตีน YKL-40 จากแบคทีเรีย และ  $0.08 \pm 0.02$  ไมโครกรัมต่อลิตรในอิมมูโนเซนเซอร์ต่อโปรตีน YKL-40 จากเซลล์ของสัตว์เลี้ยงลูกด้วยนม อิเล็กโทรดทำงานสามารถนำกลับมาใช้ใหม่ได้มากกว่า 40 รอบ สำหรับอิมมูโนเซนเซอร์ต่อโปรตีน YKL-40 จากแบคทีเรีย และ 50 รอบ สำหรับอิมมูโนเซนเซอร์ต่อโปรตีน YKL-40 จากเซลล์ของสัตว์เลี้ยงลูกด้วยนม และระบบยังแสดงความจำเพาะต่อโปรตีน YKL-40 ในตัวอย่างแบบจำลองพบว่า การพัฒนาระบบอิมมูโนเซนเซอร์ให้ค่าเปอร์เซ็นต์การคืนกลับของวิธีการวิเคราะห์ในช่วงร้อยละ 98 ถึง 102 และในการตรวจวัดค่าโปรตีน YKL-40 ใน 4 ตัวอย่างของคนปกติ 5 ตัวอย่างของมะเร็งเต้านม และ 4 ตัวอย่างของมะเร็งสมอง ด้วยวิธีอิมมูโนเซนเซอร์ต่อ

โปรตีน YKL-40 จากเซลล์ของสัตว์เลี้ยงลูกด้วยนม ให้ค่าการตรวจวัดของโปรตีน YKL-40 ที่ตรงกับวิธีมาตรฐาน ELISA อย่างไรก็ตาม วิธีที่พัฒนาขึ้นนี้ให้ค่าช่วงความเป็นเส้นตรงที่กว้างกว่า และมีค่าขีดจำกัดที่ต่ำสุดในการวัดต่ำกว่า อีกทั้งอิเล็กโทรดทำงานสามารถนำกลับมาใช้ใหม่ได้หลายครั้ง

ส่วนที่ 2 เป็นการศึกษาการพัฒนาคาปาซิทีฟอิมมูโนเซนเซอร์เพื่อใช้ในการตรวจวัดโปรตีน YKL-39 ซึ่งเป็นโปรตีนที่ใช้ในการติดตามความก้าวหน้าของโรคข้อเสื่อม โพลีโคนอลแอนติบอดีต่อโปรตีน YKL-39 ถูกใช้ในการตรึงกับอิเล็กโทรดทองทำงานโดยเทคนิค การเคลือบผิวแบบเรียงตัวชั้นเดียวด้วยไทโอยูเรีย สภาวะที่เหมาะสมต่อการวิเคราะห์ของระบบของคาปาซิทีฟอิมมูโนเซนเซอร์ต่อโปรตีน YKL-39 ได้แก่ ปริมาณสารตัวอย่าง 200 ไมโครลิตร อัตราการไหล 100 ไมโครลิตรต่อนาที กรดไฮโดรคลอริกเข้มข้น 3.16 มิลลิโมลาร์ (พีเอชเท่ากับ 2.5) เป็นสารรีเจเนอเรต และบัฟเฟอร์ที่ใช้คือ โซเดียมฟอสเฟตบัฟเฟอร์ความเข้มข้น 25 มิลลิโมลาร์ มีค่าพีเอชที่ 7.0 ภายใต้สภาวะที่เหมาะสมพบช่วงความเป็นเส้นตรงระหว่าง 0.1 ไมโครกรัมต่อลิตร ถึง 1 มิลลิกรัมต่อลิตร ในขณะที่ค่าขีดจำกัดที่ต่ำสุดในการวัดอยู่ที่  $0.07 \pm 0.02$  ไมโครกรัมต่อลิตร อิเล็กโทรดตรึงโพลีโคนอลแอนติบอดีต่อโปรตีน YKL-39 สามารถนำกลับมาใช้ใหม่ได้มากกว่า 49 ครั้งโดยมีค่าส่วนเบี่ยงเบนมาตรฐานสัมพัทธ์ น้อยกว่าร้อยละ 5 ค่าที่ได้ในการตรวจวัดค่าโปรตีน YKL-39 ในตัวอย่างเซลล์ ตัวอย่างแบบจำลอง และน้ำไขข้อของผู้ป่วยโรคข้อเสื่อมพบว่า วิธีคาปาซิทีฟอิมมูโนเซนเซอร์ต่อโปรตีน YKL-39 และ วิธีมาตรฐาน ELISA พบว่าวิธีทั้งสองให้ค่าการตรวจวัดของโปรตีน YKL-39 ที่ตรงกัน

WETHAKA CHAOCHAROEN : THE DEVELOPMENT OF CAPACITIVE  
IMMUNOSENSORS TO DETECT CHITINASE-LIKE PROTEIN  
BIOMARKERS. THESIS ADVISOR : ASSOC. PROF. WIPA SUGINTA,  
Ph.D. 173 PP.

THE DEVELOPMENT OF CAPACITIVE IMMUNOSENSORS TO DETECT  
CHITINASE-LIKE PROTEIN BIOMARKERS

In this study, a label-free capacitive immunosensor to detect two disease markers YKL-39 and YKL-40 has been established in a flow injection system. This thesis is divided into two parts. The first part involves expression of YKL-40 in bacterial and mammalian cell expression systems that were used as for production of anti-YKL-40 polyclonal antibody. The YKL-40 antibodies were highly specific and strongly reacting with YKL-40. The purified YKL-40 polyclonal antibody was immobilized on a gold working electrode via a self-assembled monolayer. Optimum operational conditions of the bacterial- YKL-40 immunosensor were a sample volume of 200  $\mu\text{L}$ , a flow rate of 100  $\mu\text{L}/\text{min}$ , HCl solution, pH 2.5, as regeneration solution and 10 mM sodium phosphate buffer, pH 7.0, as running buffer. For the mammalian- YKL-40 immunosensor, they were a sample volume of 250  $\mu\text{L}$ , a flow rate of 100  $\mu\text{L}/\text{min}$ , HCl solution, pH 2.5, as a regeneration solution and 25 mM sodium phosphate buffer, pH 7.0, as running buffer. Under optimum operational conditions, both YKL-40 immunosensors gave a linear dynamic range between 0.1 and 1,000  $\mu\text{g}/\text{L}$ , with limit of detection of  $0.07\pm 0.01$   $\mu\text{g}/\text{L}$  for the bacterial-YKL-40 immunosensor and  $0.08\pm 0.02$   $\mu\text{g}/\text{L}$  in the mammalian-YKL-40 immunosensor. The

reproducibility of working electrode can be regenerated up to 40 cycles for the bacterial-YKL-40 immunosensor and 50 cycles for the mammalian-YKL-40 immunosensor. The system also showed good selectivity towards YKL-40. In model samples, the newly-developed capacitive immunosensor provided good recovery in a range of 98 to 102%. The serum level of YKL-40 in 4 healthy people, 5 breast cancer patients and 4 glioblastoma patients was detected with the mammalian-YKL-40 immunosensor and the results agreed with the standard ELISA method. However, this developed method offered greater advantages with a broader linear range, lower limit of detection and multiple uses of the antibody-immobilized electrode.

In the second part, a capacitive immunosensor for detection YKL-39 as osteoarthritis biomarker was developed. Antibody against YKL-39 was immobilized on a gold working electrode via a self-assembled thiourea monolayer. Optimum operational conditions were a sample volume of 200  $\mu\text{L}$ , a flow rate of 100  $\mu\text{L}/\text{min}$ , HCl solution, pH 2.5, as a regeneration solution and 25 mM sodium phosphate buffer, pH 7.0, as running buffer. The linear detection range was between 0.1  $\mu\text{g}/\text{L}$  and 1 mg/L with the detection limit of  $0.07 \pm 0.02 \mu\text{g}/\text{L}$ . The immobilized anti-YKL-39 antibody on gold electrode was stable and after regeneration good reproducibility of the signal could be obtained up to 49 times with an RSD lower than 5%. Good agreement was obtained when YKL-39 concentrations of cell lysate, model samples and synovial fluid were determined by the YKL-39 capacitive immunosensor system as compared to the ELISA method.

School of Biochemistry

Academic Year 2015

Student's signature \_\_\_\_\_

Advisor's signature \_\_\_\_\_

## **ACKNOWLEDGEMENTS**

I would like to express my deepest appreciation to my advisor Assoc. Prof. Dr. Wipa Suginta for providing me the opportunity to study towards my Ph.D. degree in Biochemistry and to work on a great project, and for her patience and continuous guidance, unconditional support, and encouragement. I am also deeply grateful to my co-advisor, Assoc. Prof. Dr. Albert Schulte for his valuable guidance, advice on the electrochemical part.

I gratefully recognize the contribution of Assoc. Prof. Dr. Panote Thavarungkul for giving me a chance to do some parts of my research at the Trace Analysis and Biosensor Research Center, Prince of Songkla University, Hat Yai, Songkla, Thailand, providing valuable suggestions, scientific discussions, and excellent guidance. Special thanks are extended to all the Trace Analysis and Biosensor Research Center lab staff and members for providing research information and essential facilities and for their friendship.

I would like to sincerely thank Dr. Araya Ranok for supplying the YKL-40 recombinant plasmid, YKL-39 protein and YKL-39 polyclonal antibody to be used in thesis work.

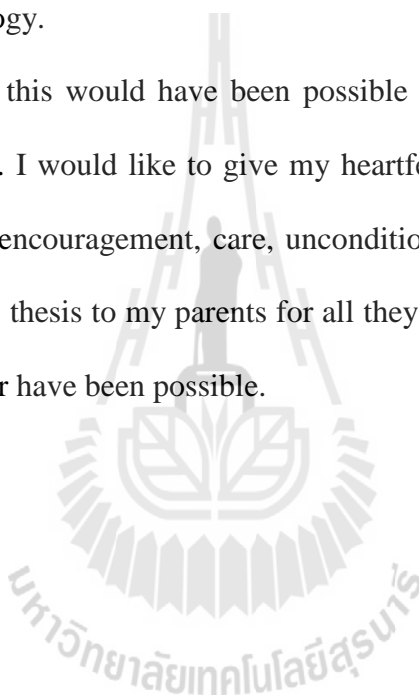
I would like to thank all lecturers and members of the School of Biochemistry, Suranaree University of Technology and especially the members of the Biochemistry and Electrochemistry Research Unit at Suranaree University of Technology, who

passing on to me their biochemistry knowledge and their constant support and helping me throughout the project and in making this journey of mine relatively easy.

This Ph.D. dissertation was supported by a scholarship from the Office of the Higher Education Commission, Thailand through a grant in the program “Strategic Scholarships Fellowship Frontier Research Networks for the Ph.D. Program” (grant no. CHE 510767). Financial support for the work came also through the Suranaree University of Technology.

Finally, none of this would have been possible without the constant love and patience of my family. I would like to give my heartfelt thanks to my family for all their endless support, encouragement, care, unconditional love and endless financial support. I dedicate this thesis to my parents for all they have done for me and without whom this would never have been possible.

Wethaka Chaocharoen



# CONTENTS

	<b>Page</b>
ABSTRACT IN THAI.....	I
ABSTRACT IN ENGLISH .....	III
ACKNOWLEDGEMENTS.....	V
CONTENTS.....	VII
LIST OF TABLES .....	XIII
LIST OF FIGURES .....	XV
LIST OF ABBREVIATIONS.....	XX
<b>CHAPTER</b>	
<b>I INTRODUCTION.....</b>	<b>1</b>
1.1 YKL-40 as a cancer marker .....	1
1.1.1 Methods for the determination of YKL-40 in tissues and body fluids ...	10
1.2 YKL-39 as an ostioarthritis marker .....	13
1.3 The principle of capacitive electrochemical immunosensing.....	19
1.4 Thesis objectives .....	26
<b>II MATERIALS AND METHODS .....</b>	<b>28</b>
2.1 Materials .....	28
2.1.1 Chemicals and reagents .....	29
2.1.2 Instrumentation.....	30
2.2 Methods.....	30
2.2.1 Molecular biology .....	30

## CONTENTS (Continued)

	<b>Page</b>
2.2.1.1 Preparation of competent cells of <i>E. coli</i> strains DH5 $\alpha$ and M15 (pREP).....	30
2.2.1.2 Transformation of plasmid DNA into competent cells .....	30
2.2.1.3 Denaturing sodium dodecyl sulfate polyacrylamide gel electrophoresis (SDS-PAGE) and western blot analysis .....	31
2.2.1.4 Cell culture .....	32
2.2.1.5 Expression and purification of recombinant YKL-40 in <i>E. coli</i> M15 (pREP) (bYKL-40) .....	33
2.2.1.6 Expression and purification of recombinant YKL-40 in 293T cells (mYKL-40) .....	34
2.2.2 Immunology .....	36
2.2.2.1 Polyclonal antibody production.....	36
2.2.2.2 Purification of polyclonal antibody .....	37
2.2.2.3 Characterization of anti-YKL-40 polyclonal antibody.....	38
2.2.2.3.1 Determination of the antibody titers and specificity by western blotting.....	38
2.2.2.3.2 Determination of the antibody titers and specificity by ELISA .....	38
2.2.3 Development of immunosensor specific for YKL-39/40 .....	39
2.2.3.1 Preparation of capacitive YKL-39/40 immunosensors .....	40
2.2.3.2 The workstation for flow-based capacitive YKL-39/40 immunosensing .....	41

## CONTENTS (Continued)

	<b>Page</b>
2.3.2.3 YKL-39/40 measurements with capacitive YKL-39/40 immunosensor .....	42
2.3.2.4 Parameter optimization YKL-39/40 immunosensing .....	44
2.3.2.4.1 Choice of the optimal type of the regeneration solution.....	44
2.3.2.4.2 Choice of the optimal pH of the regeneration solution	48
2.3.2.4.3 Choice of the optimal type of running buffer .....	48
2.3.2.4.4 Choice of the optimal sample volume and flow rate ...	49
2.3.2.4.5 Summary of the performed optimization trials.....	49
2.3.2.5 Stability and selectivity tests with YKL-39/40 immunosensors.	50
2.3.2.6 Limit of detection (LOD) .....	51
2.3.2.7 Determination of YKL-39/40 in model and clinical samples.....	52
2.3.2.7.1 Model samples .....	52
2.3.2.7.2 Clinical samples.....	53
<b>III RESULTS .....</b>	<b>55</b>
3.1 Capacitive immunosensor for detection of bYKL-40.....	55
3.1.1 Expression and purification of YKL-40 in bacteria system (bYKL-40).	55
3.1.2 Production and characterization of bYKL-40 polyclonal antibody .....	57
3.1.3 Capacitive bYKL-40 immunosensing.....	62
3.1.3.1 Preparation of the capacitive bYKL-40 immunosensors.....	62
3.1.3.2 Parameter optimization for capacitive bYKL-40 immunosensing .....	64

## CONTENTS (Continued)

	<b>Page</b>
3.1.3.2.1 Optimization of the regeneration solution .....	65
3.1.3.2.2 Optimization of the type of running buffer.....	67
3.1.3.2.3 Optimization of the pH of sodium phosphate-based running buffer .....	69
3.1.3.2.4 Optimization of the concentration of the running buffer.....	69
3.1.3.2.5 Optimization of the flow rate.....	71
3.1.3.2.6 Optimization of the injected sample volume .....	72
3.1.3.3 The analytical performance of bYKL-40 immunosensors in flow operation .....	74
3.1.3.3.1 Linearity range and limit of detection.....	74
3.1.3.3.2 The stability of anti-bYKL-40 immobilized electrode	76
3.1.3.3.3 The selectivity of capacitive bYKL-40 immunosensors .....	78
3.1.3.4 Determination of YKL-40 in model and spiked serum samples	79
3.1.4 Expression and purification of YKL-40 in mammalian system (mYKL-40) .....	83
3.1.5 Production of mYKL-40 polyclonal antibody .....	85
3.1.6 Capacitive mYKL-40 immunosensor .....	90
3.1.6.1 Preparation of the immunosensors.....	90
3.1.6.2 Optimization of operational conditions .....	91

## CONTENTS (Continued)

	<b>Page</b>
3.1.6.3 The analytical performance of mYKL-40 immunosensors in flow operation .....	96
3.1.6.3.1 Linearity range and limit of detection.....	96
3.1.6.3.2 The stability of capacitive mYKL-40 immunosensors .....	97
3.1.6.3.3 The selectivity of anti-mYKL-40 immunosensors .....	99
3.1.6.4 Determination of YKL-40 in cell lysates .....	104
3.2 Capacitive immunosensor for detection of YKL-39.....	106
3.2.1 Preparation of YKL-39 immunosensors .....	106
3.2.2 Optimization of conditions for YKL-39 operation in the electrochemical flow cell .....	107
3.2.3 YKL-39 immunosensor performance in the electrochemical flow cell	112
3.2.3.1 Linearity range and limit of detection.....	112
3.2.3.2 Stability of capacitive YKL-39 immunosensors.....	113
3.2.4 Enzyme-linked immunosorbent assay for detection of YKL-39 .....	116
3.4.5 Determination of YKL-39 in model and clinical samples .....	117
<b>IV DISCUSSION .....</b>	<b>124</b>
4.1 Capacitive immunosensor for detection of YKL-40.....	124
4.2 Capacitive immunosensor for detection of YKL-39.....	133
<b>V CONCLUSION .....</b>	<b>138</b>

**CONTENTS (Continued)**

	<b>Page</b>
REFERENCES .....	141
APPENDIX.....	156
CURRICULUM VITAE.....	173

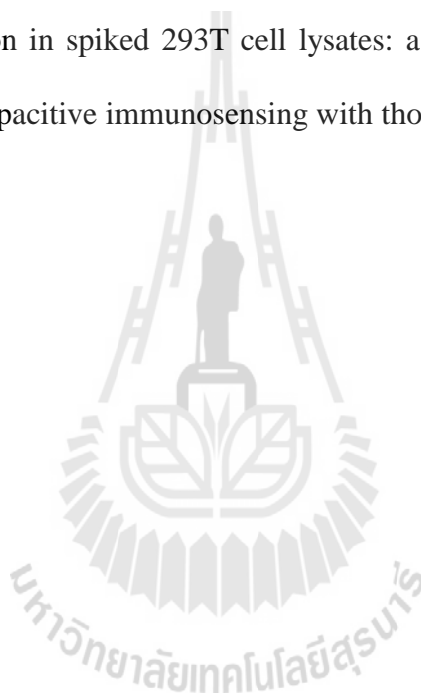


## LIST OF TABLES

Table	Page
1.1 Serum levels of YKL-40 ( $\mu\text{g/L}$ ) in cancer patients and the percentage of patients with elevated serum YKL-40 .....	9
2.1 Starting operational conditions .....	45
2.2 Target parameters for human chitinase-like proteins immunosensor optimization trials .....	50
3.1 Interaction of bYKL-40 and its homologues with purified anti-bYKL-40 polyclonal antibody.....	62
3.2 YKL-40 detection in model samples: a comparison of the results from bYKL-40 capacitive immunosensing with those from ELISA (n=3).....	80
3.3 YKL-40 detection in spiked serum samples: a comparison of the results from bYKL-40 capacitive immunosensing with those from ELISA (n=3) .....	82
3.4 YKL-40 detection in model samples: a comparison of the results from mYKL-40 capacitive immunosensing with those from ELISA (n=3).....	101
3.5 YKL-40 detection in serum samples from a healthy person: a comparison of the results from mYKL-40 capacitive immunosensing with those from ELISA (n=3) .....	103
3.6 YKL-40 detection in serum samples from cancer patients: a comparison of the results from mYKL-40 capacitive immunosensing with those from ELISA (n=3) .....	105
3.7 YKL-40 detection in cell lysates: a comparison of the results from mYKL-40 capacitive immunosensing with those from ELISA (n=3) .....	106

**LIST OF TABLES (Continued)**

<b>Table</b>	<b>Page</b>
3.8 YKL-39 detection in model samples: a comparison of the results from YKL-39 capacitive immunosensing with those from ELISA (n=3) .....	119
3.9 YKL-39 detection in clinical samples: a comparison of the results from YKL-39 capacitive immunosensing with those from ELISA (n=3).....	123
3.10 YKL-39 detection in spiked 293T cell lysates: a comparison of the results from YKL-39 capacitive immunosensing with those from ELISA (n=3) .....	123



## LIST OF FIGURES

Figure	Page
1.1 The crystal structure of YKL-40.....	2
1.2 The proposed signaling pathways of YKL-40 in cellular proliferation, adhesion, and survival.....	4
1.3 Individual serum YKL-40 concentrations in breast cancer patients in relation to survival time .....	6
1.4 SDS-PAGE analysis of YKL-39 and YKL-40 .....	15
1.5 YKL-39 induced arthritis in <i>BALB/c</i> mice.....	17
1.6 The principle of a biosensor.....	19
1.7 Representation of the dielectric layer in front of an antibody-modified gold electrode.....	24
2.1 Illustration of the equipment used for flow injection-based capacitive YKL-39/40 immunosensing.....	42
2.2 A schematic diagram showing the capacitance change caused by binding between antigen and antibody following an YKL-39/40 protein sample injection.....	47
3.1 SDS-PAGE analysis of bYKL-40 expression.....	56
3.2 SDS-PAGE analysis of bYKL-40 purification by Ni-NTA agarose column .....	56
3.3 Polyclonal anti-bYKL-40 antiserum titer .....	58
3.4 Specificity of polyclonal anti-bYKL-40 antiserum .....	59
3.5 Purified anti-bYKL-40 polyclonal antibody.....	60

## LIST OF FIGURES (Continued)

<b>Figure</b>	<b>Page</b>
3.6 bYKL-40 ELISA technique .....	61
3.7 Cyclic voltammograms of a gold electrode at various surface conditions .....	64
3.8 Efficiency of different types of regeneration solutions.....	66
3.9 The influence of the pH of the HCl regeneration solution on the efficiency of removal bYKL-40 from anti-bYKL-40 on a thiol-coated gold electrode.....	67
3.10 The efficiency of bYKL-40 capacitive immunosensors for different types of running buffer .....	68
3.11 The efficiency of capacitive bYKL-40 immunosensors for applications with 10 mM sodium phosphate running buffer at different pH.....	69
3.12 The dependence of the efficiency of bYKL-40 quantification on different salt concentrations of the sodium phosphate buffer, pH 7.0 .....	70
3.13 The dependence of the efficiency of bYKL-40 quantification with capacitive immunosensor readout for different running buffer flow rates.....	72
3.14 The dependence of the efficiency of bYKL-40 capacitive immunosensing on a variation of injected sample volume.....	73
3.15 Representation of a calibration curve as valid for routine capacitive bYKL- 40 immunosensing.....	75
3.16 bYKL-40 immunosensor response to the injection of 0.1 µg/L of bYKL-40 under pre-identified optimal operational conditions .....	75
3.17 Assessment of the stability of the signal during repeated cycles of sample injection and immunosensor regeneration.....	77

## LIST OF FIGURES (Continued)

<b>Figure</b>	<b>Page</b>
3.18 The cyclic voltammograms in ferricyanide-containing electrolyte recorded before (black curve) and after (gray curve) the stability test. ....	77
3.19 Representative selectivity test for capacitive bYKL-40 immunosensors .....	79
3.20 12% SDS-PAGE analysis of mYKL-40 purification by Ni-NTA agaroses.....	84
3.21 mYKL-40 proteins detected by immunoblotting with the anti-YKL-40.....	84
3.22 Reactivity of polyclonal anti-mYKL-40 antiserum .....	86
3.23 The polyclonal anti-mYKL-40 antiserum titers against 2 $\mu$ g of purified mYKL-40.....	86
3.24 Specificity of polyclonal anti-mYKL-40 antiserum .....	87
3.25 Purification of anti-mYKL-40 polyclonal antibody by affinity protein A-agarose column. ....	88
3.26 Purified anti-mYKL-40 polyclonal antibody titers against 2 $\mu$ g of mYKL-40 ..	89
3.27 mYKL-40 Enzyme-linked immunosorbent assay.....	90
3.28 Cyclic voltammograms of a gold electrode at various surface conditions .....	91
3.29 Efficiency of different types of regeneration solutions.....	92
3.30 The influence of the pH of the HCl regeneration solution on the efficiency of removal mYKL-40 from anti-mYKL-40 on a thiol-coated gold electrode ....	93
3.31 The efficiency of mYKL-40 capacitive immunosensors for different types of running buffer .....	94
3.32 The efficiency of capacitive mYKL-40 immunosensors for applications with 10 mM sodium phosphate running buffer at different pH .....	94

## LIST OF FIGURES (Continued)

<b>Figure</b>	<b>Page</b>
3.33 The dependence of the efficiency of mYKL-40 quantification on different salt concentrations of the sodium phosphate buffer, pH 7.0.....	94
3.34 The dependence of the efficiency of mYKL-40 capacitive immunosensing on a variation of injected sample volume. ....	95
3.35 The dependence of the efficiency of mYKL-40 quantification with capacitive immunosensor readout for different running buffer flow rates .....	95
3.36 Representation of a calibration curve as valid for routine capacitive mYKL-40 immunosensing .....	97
3.37 Assessment of the stability of the signal during repeated cycles of sample injection and immunosensor regeneration .....	92
3.38 The cyclic voltammograms in ferricyanide-containing electrolyte recorded before (black curve) and after (gray curve) the stability test .....	98
3.39 Representative selectivity test for capacitive mYKL-40 immunosensors .....	100
3.40 Cyclic voltammograms of a gold electrode at various surface conditions .....	107
3.41 Efficiency of different types of regeneration solutions.....	108
3.42 The influence of the pH of the HCl regeneration solution on the efficiency of removal YKL-39 from anti-YKL-39 on a thiol-coated gold electrode .....	109
3.43 The efficiency of YKL-39 capacitive immunosensors for different types of running buffer .....	109
3.44 The efficiency of YKL-39 capacitive YKL-39 immunosensors for applications with 10 mM sodium phosphate running buffer at different pH....	110

## LIST OF FIGURES (Continued)

<b>Figure</b>	<b>Page</b>
3.45 The dependence of the efficiency of YKL-39 quantification on different salt concentrations of the sodium phosphate buffer, pH 7.0 .....	110
3.46 The dependence of the efficiency of YKL-39 capacitive immunosensing on a variation of injected sample volume .....	111
3.47 The dependence of the efficiency of YKL-39 quantification with capacitive immunosensor readout for different running buffer flow rates .....	111
3.48 Representation of a calibration curve as valid for routine capacitive YKL-39 immunosensing .....	113
3.49 Assessment of the stability of the signal during repeated cycles of sample injection and immunosensor regeneration .....	114
3.50 The cyclic voltammograms in ferricyanide-containing electrolyte recorded before (black curve) and after (gray curve) the stability test.....	114
3.51 Representative selectivity test for capacitive YKL-39 immunosensors .....	116
3.52 YKL-39 ELISA technique .....	117
3.53 Detection of YKL-39 in clinical samples by immunoblot assay .....	121
3.54 Capacitance response of anti-YKL-39-modified electrode .....	122

## LIST OF ABBREVIATIONS

( $\mu$ , n)F	(micro, nano) Farad
(m)V	(milli) Volts
(m, $\mu$ )L	(milli, micro) Liter(s)
(m, $\mu$ )M	(milli, micro) Molar(s)
(m, $\mu$ , n)g	(milli, micro, nano) Gram(s)
( $\mu$ )mol	(micro) Mole(s)
$\Delta$ C	Capacitance change
$^{\circ}$ C	Degrees Celsius
$\mu$ A	Micro Amps
aa	Amino acid(s)
Ab	Antibody
Ag	Antigen
AMCase	Acidic mammalian chitinase
Au	Gold
bp	Base pair(s)
bYKL-40	YKL-40 protein derived from bacterial system
BRE	Biorecognition element(s)
C	Capacitance
cDNA	Complementary deoxyribonucleic acid
CHI3L1, YKL-40	Chitinase 3-like-1
CHI3L2, YKL-39	Chitinase 3-like-2
CHIT	Chitotriosidase
CLPs	Chitinase-like proteins

**LIST OF ABBREVIATIONS (Continued)**

cm	Centimeter
DMEM	Dulbecco's Modified Eagle's Medium
DNA	Deoxynucleic acid
EDTA	Ethylenediamine tetraacetate
ELISA	Enzyme linked-immunosorbent assay
FAK	Focal adhesion kinase
FCS	Fetal Calf Serum
GH	Glycoside hydrolase
GH-18	Glycoside hydrolase family 18
hr (s)	Hour(s)
HRP	Horseradish peroxidase
IFN- $\gamma$	Interferon gamma
IgG	Immunoglobulin G
IL-4	Interleukin 4
IPTG	Isopropyl- $\beta$ -D-thiogalactopyranoside
kDa	Kilo Dalton(s)
LB	Luria-Bertani lysogeny broth
min	Minute(s)
mYKL-40	YKL-40 protein derived from mammalian system
MW	Molecular weight
Ni-NTA	Ni-nitrilotriacetic acid
nm	Nanometer(s)
OA	Osteoarthritis
OD	Optical density

**LIST OF ABBREVIATIONS (Continued)**

PAGE	Polyacrylamide gel electrophoresis
PBS	Phosphate buffered saline
PBST	Phosphate buffered saline containing Tween-20
pH	Negative logarithm of hydrogen ion activity
PMSF	Phenylmethylsulfonylfluoride
RA	Rheumatoid arthritis
RE	Reference electrode
RIA	Radioimmunoassay
rpm	Rotations per minute
RPMI-1640	Roswell Park Memorial Institute
s	Second(s)
SAMs	Self-assembled monolayers
SDS	Sodium dodecyl sulfate
SI-CLP	Stabilin-1-interacting chitinase-like protein
TEMED	Tetramethylenediamine
TGF- $\beta$	Transforming growth factor beta
TMB	3,3',5,5'-tetramethylbenzidine
TNF- $\alpha$	Tumor necrosis factor alpha
Tris	Tris-(hydroxymethyl)-aminoethane
UV	Ultraviolet
v/v	Volume/volume
w/v	Weight/volume
WE	Working electrode

# CHAPTER I

## INTRODUCTION

### 1.1 YKL-40 as a cancer marker

YKL-40 was originally identified a glycoprotein secreted *in vitro* in large amounts by the human osteosarcoma cell line MG-63 (Johansen, Williamson and Rice *et al.*, 1992). The named protein “YKL-40” based on its three NH<sub>2</sub>-terminal amino acids tyrosine (Y), lysine (K), and leucine (L) and its molecular weight of 40 kDa (Johansen *et al.*, 1992). It is also known as Chitinase-3-like protein 1 (CHI3L1) (Rehli, Krause and Andreesen, 1997), or human cartilage glycoprotein-39 (HC gp-39) (Hakala, White and Recklies, 1993). The complete amino acid sequence of the human YKL-40 was published in 1993. It belongs to family 18 glycosyl hydrolases (Hakala *et al.*, 1993).

The crystallographic three-dimensional structure of human YKL-40 displays the typical fold found in all family 18 glycosyl hydrolases (Fuseti, Pijning, Kalk *et al.*, 2003). The structure is divided into two globular domains: a big core domain consists of a ( $\beta/\alpha$ )<sub>8</sub> domain structure with a triose-phosphate isomerase (TIM) barrel fold, and a small  $\alpha/\beta$  domain, composed of five antiparallel  $\beta$ -strands and one  $\alpha$ -helix that is inserted in the loop between strand  $\beta$ 7 and helix  $\alpha$ 7 of the TIM barrel. The TIM barrel domain of YKL-40 contains a GlcNAc binding groove responsible for binding with chitin fragments (Fuseti *et al.*, 2003). YKL-40 catalytically inactive since two

amino acid residues (Asp140-Glu) that are normally found in the catalytic motif D138xD140xE of true chitinases are mutated to alanine and leucine, respectively (Figure 1.1) (Houston, Recklies, Krupa *et al.*, 2003). YKL-40 also contains a heparin binding motif (GRRDKQH, residues 143-149) (Shackelton, Mann, and Millis, 1995) located on a surface loop (Fusetti *et al.*, 2003). YKL-40 contains five cysteine, four of which are involved in two disulfide bonds (C<sup>26</sup>-C<sup>51</sup> and C<sup>300</sup>-C<sup>364</sup>) (Fusetti *et al.*, 2003).

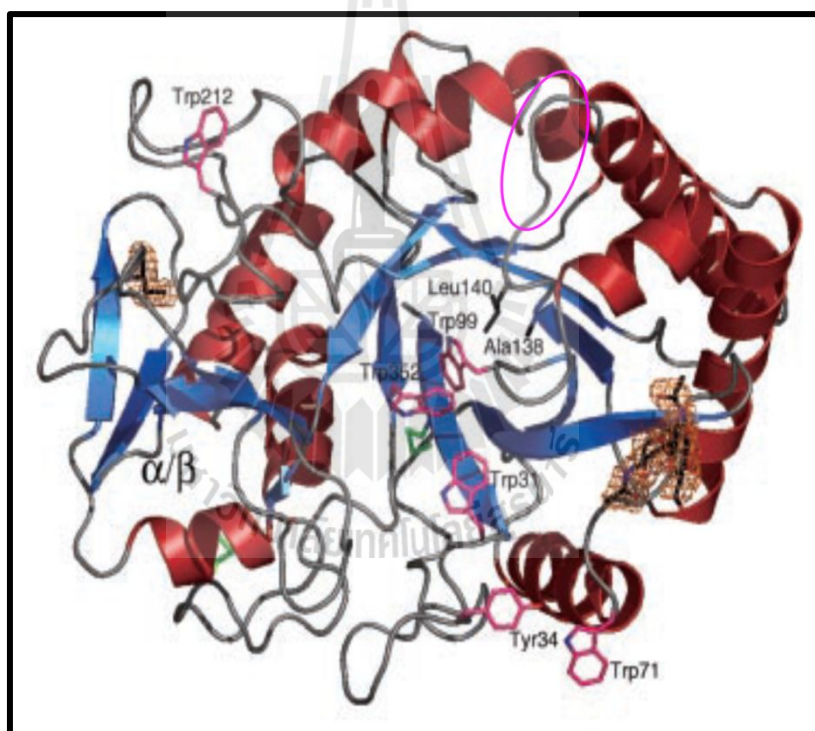


**Figure 1.1** The crystal structure of YKL-40. Red color in the ribbon representation indicates  $\alpha$ -helices and blue indicates  $\beta$ -strands. The side chain of Leu140 is shown as black stick. The two disulfide bonds are shown in green. Solvent-exposed aromatic residues lining the binding cleft are shown as sticks with magenta carbons and pink circle representation indicates the heparin binding motif (Houston *et al.*, 2003).

A number of studies demonstrate elevated YKL-40 expression in cancer tissues from breast (Johansen, Christensen, Riisbro *et al.*, 2003), colorectal (Cintin, Johansen, Christensen *et al.*, 1999), small cell lung (Johansen, Drivsholm, Price *et al.*, 2004), ovary (Dupont, Tanwar, Thaler *et al.*, 2004), glioblastoma (Tanwar, Gilbert, and Holland *et al.*, 2002), and prostate (Brasso, Christensen, Johansen *et al.*, 2006). However, exact physiological functions of YKL-40 protein are still unclear. A recent review article suggested that YKL-40 may play a role in the proliferation and differentiation of malignant cells, by protecting cancer cells from undergoing apoptosis, as well as stimulating angiogenesis. YKL-40 may have effects on extracellular tissue remodeling, and stimulate fibroblasts surrounding the tumor tissue (Johansen, 2006). In addition, YKL-40 may as well play a role in inflammation of non-malignant tissues.

In 2009, Shao and co-worker reported that YKL-40 involves in the regulatory pathways that mediate vascular effects (Shao, Hamel, Petersen *et al.*, 2009). Through tumor angiogenesis, YKL-40 binds to the heparin sulfates of Syndecan-1, a major proteoglycan on the epithelial cell surface, and activates (phosphorylates) focal adhesion kinase (FAK) together with integrin  $\alpha\beta3$ . This induces angiogenesis through the subsequent activation of MAP/Erk kinase (Shao *et al.*, 2009). FAK can also activate phosphatidylinositol 3 kinase (PI3K)/Akt signaling pathways that are critical for cell survival, differentiation, and fibrogenesis (Horowitz, Rogers, Sharma *et al.*, 2007) (Figure 1.2).

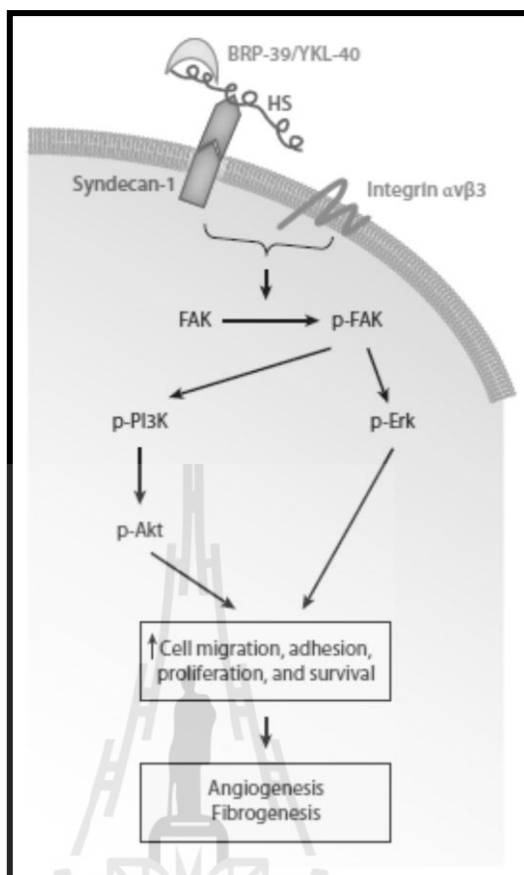


**Figure 1.2** The proposed signaling pathways of YKL-40 in cellular proliferation, adhesion, and survival. BRP-39 binds to the heparan sulfate of Syndecan-1, a major cell surface proteoglycan. Along with integrin  $\alpha\beta 3$ , the binding activates focal adhesion kinase (FAK). Phosphorylated FAK (p-FAK) activates downstream signaling molecules, including MAP or Erk (p-Erk) kinase, phosphatidylinositol 3 kinase (p-PI3K), and Akt (p-Akt) (Lee, Da Silva, Dela Cruz *et al.*, 2011).

The plasma levels of YKL-40 were normally determined by commercial enzyme-linked immunoassays (ELISA). In a report by Harvey and co-worker (1998) using the ELISA kit provided by Quidel, Santa Clara, CA, USA, (the plasma levels of YKL-40 from both male and female were highly correlated with ages ( $p < 0.001$ ) and the median plasma YKL-40 level in healthy subjects ( $n = 245$ ) was  $40 \mu\text{g/L}$  (Harvey,

Weisman, O'Dell *et al.*, 1998; Johansen, Jensen, Roslind *et al.*, 2006; Johansen, Lottenburger, and Nielsen, 2008; Johansen, Bojesen, Mylin *et al.*, 2009).

In another report, Johansen and co-worker reported that patients with breast cancer had significantly increased serum YKL-40. They measured the level of YKL-40 from breast cancer patients and found that the median serum YKL-40 in patients with visceral and bone metastases were 328 and 157.1  $\mu\text{g/L}$ , respectively. Such values were significantly higher than the value of healthy subjects (99  $\mu\text{g/L}$ ,  $p < 0.001$ ). The survival rates after 18 months were 24% for patients with high level of serum YKL-40 ( $>207 \mu\text{g/L}$ ) and 60% for patients with normal level of serum YKL-40. The highest level of YKL-40 were found in patients with short survival, while normal levels of YKL-40 were found in longer survival patients as shown in Figure 1.3 (Johansen, Cintin, Jørgensen *et al.*, 1995). The results suggested that serum YKL-40 might be used as a prognostic marker in breast cancer patients. In another study, associations were observed with the preoperative serum YKL-40 out of 271 patients with primary breast cancer in relation to relapse-free survival and overall survival. The median follow-up time was 5.9 years. The median serum YKL-40 concentration in the patients was 57  $\mu\text{g/L}$  (range, 22 to 688  $\mu\text{g/L}$ ) compared to the serum YKL-40 in healthy females. Of which, 19% of the patients had high serum YKL-40. Patients with high serum YKL-40 had shorter relapse-free interval and survival than patients with normal serum YKL-40 (Johansen *et al.*, 2003).

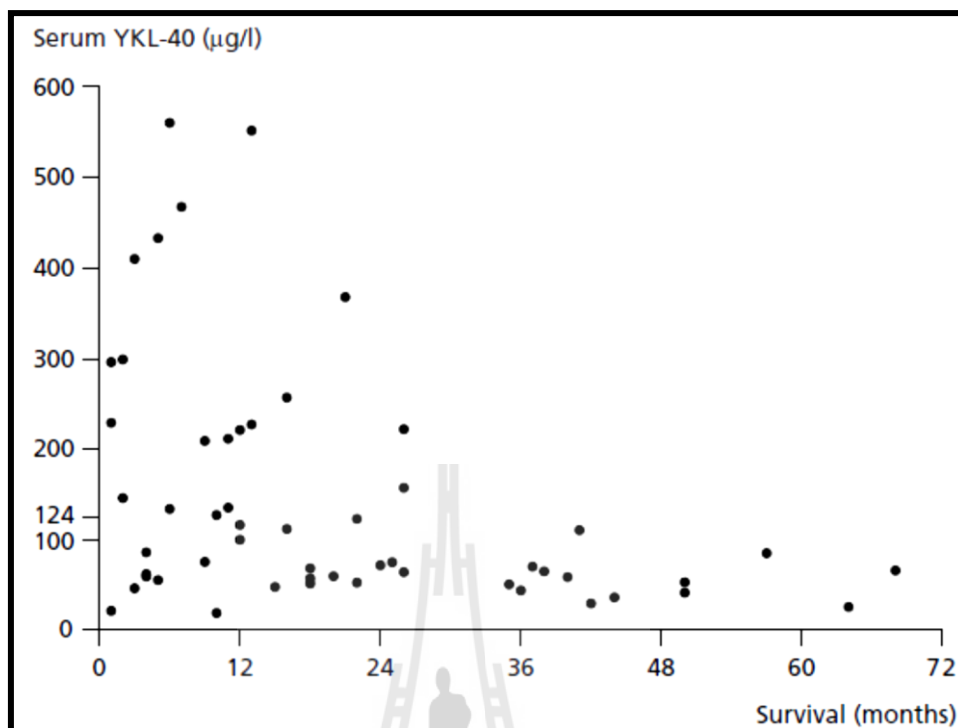


**Figure 1.3** Individual serum YKL-40 concentrations in breast cancer patients in relation to survival time. The serum YKL-40 was determined by radioimmunoassay (Johansen *et al.*, 2006).

Serum YKL-40 was also determined in 603 patients with colorectal cancer (Cintin *et al.*, 1999). The median serum YKL-40 concentration in the cancer patients was 180 µg/L (range, 56 to 2709 µg/L). Survival after operation was registered, and the median of the follow-up time was 61 months. Three hundred and forty patients died, for which 16% of the patients with Dukes' A (tumor confined within the bowel wall, no lymph-node metastases), 26% with Dukes' B (tumor extending through the bowel wall, no lymph-node metastases), 19% with Dukes' C (regional lymph-node metastases) and 39% with Dukes' D (disseminated disease) had high serum YKL-40 levels. Analysis of serum YKL-40 as a continuous variable showed an association between increased serum YKL-40 and short survival ( $p < 0.0001$ ). Patients with high

preoperative serum YKL-40 concentration had significantly shorter survival than patients with normal YKL-40 (Cintin *et al.*, 1999). Serum YKL-40 decreased significantly after curative operation for colorectal cancer in patients with high preoperative serum YKL-40 (Cintin, Johansen, Christensen *et al.*, 2002), indicating that serum YKL-40 may reflect tumor burden.

In ovarian cancer, the serum YKL-40 levels were determined by ELISA for 46 healthy subjects, 61 high-risk individuals, 33 patients with benign gynecologic processes, and 50 preoperative patients subsequently diagnosed with predominantly early-stage ovarian cancer. The results showed that the median YKL-40 level was 28  $\mu\text{g/L}$  (range, 15 to 166  $\mu\text{g/L}$ ) for healthy subjects, 36  $\mu\text{g/L}$  (range, 9 to 69  $\mu\text{g/L}$ ) for high-risk individuals without prior cancer, 44.5  $\mu\text{g/L}$  (range, 5 to 133  $\mu\text{g/L}$ ) for high-risk patients with prior breast cancer, and 38  $\mu\text{g/L}$  (range, 5 to 67  $\mu\text{g/L}$ ) for individuals with benign gynecologic processes. The median of preoperative YKL-40 level for ovarian cancer patients was 94  $\mu\text{g/L}$  (range, 17 to 517  $\mu\text{g/L}$ ). Twenty of 31 early-stage patients (stage I and II) had elevated serum YKL-40 level (Dupont *et al.*, 2004). The median level of plasma YKL-40 in the stage III patient was 168  $\mu\text{g/L}$  (range, 32 to 1808  $\mu\text{g/L}$ ) and significantly higher compared to the plasma level in healthy women (median 35  $\mu\text{g/L}$ , range 20 to 130  $\mu\text{g/L}$ ). In addition, preoperative serum YKL-40 was elevated in 74% to 91% of patients with ovarian cancer stage III (tumor growth involving one or both ovaries with wide-spread intraperitoneal metastases) and stage IV (disseminated disease) and 55% of ovarian cancer patient had high plasma YKL-40 at the time of relapse and had significantly shorter survival than patients with normal level (Høgdall, Johansen, Kjaer *et al.*, 2003; Dehn, Høgdall, Johansen *et al.*, 2003).

For small cell lung cancer, the serum YKL-40 level in 131 patients was determined by RIA, giving the median level serum of YKL-40 in the patients to be 172  $\mu\text{g/L}$  (range, 48 to 2481  $\mu\text{g/L}$ ) and significantly elevated ( $p < 0.001$ ) compared with the level in the healthy age-matched controls (median 102  $\mu\text{g/L}$ , range 38 to 514  $\mu\text{g/L}$ ). The results also showed that 22% of the patients with low grade cancer and 40% of the patients with high grade cancer had elevated serum YKL-40. The median survival time was only 5.1 months for patients with elevated serum YKL-40 and 9 months for patients with normal serum YKL-40. Also, patients with elevated serum YKL-40 had increased hazard for death within the first 6 months after the start of chemotherapy compared to patients with normal serum YKL-40 (Johansen *et al.*, 2004).

In case of prostate carcinoma, the serum level of YKL-40 in 93 healthy Danish men older than 25 years (median age of 51 years, range 26 to 73 years) was determined by ELISA assay. The median serum YKL-40 in the control group was 47  $\mu\text{g/L}$  (range 20 to 184  $\mu\text{g/L}$ ), whereas the median serum concentration of YKL-40 in the patients with prostate carcinoma was 112  $\mu\text{g/L}$  (range 20 to 2080  $\mu\text{g/L}$ ) was significantly higher compared to the levels in healthy men and 43% of patients with metastatic prostate cancer ( $p < 0.001$ ) (Brasso *et al.*, 2006).

For glioblastoma, YKL-40 mRNA was detected in the glioblastoma samples with a range of 3- to 62-fold higher than mRNA level in normal brain samples. The serum level of YKL-40 in glioblastoma patients in 45 patients was 130  $\mu\text{g/L}$ , and ranges from 38 to 654  $\mu\text{g/L}$ . The analysis on serum YKL-40 in glioblastoma patients was found to be correlated with the presence of tumor and tumor grade or burden. Seventy two percentage of patients with glioblastoma multiform and 57% with lower

grade gliomas had high serum YKL-40 (Tanwar *et al.*, 2002). The data of some of the clinical studies on the serum YKL-40 level of cancer patients and the percentage of patients with elevated high serum YKL-40 is summarized in Table 1.1.

**Table 1.1** Serum levels of YKL-40 ( $\mu\text{g/L}$ ) in cancer patients and the percentage of patients with elevated serum YKL-40.

<b>Diagnosis</b>	<b>n</b>	<b>YKL-40 (<math>\mu\text{g/L}</math>)</b>	<b>High YKL-40 (%)*</b>	<b>Reference</b>
Breast cancer	271	57 (22-688)	19	(Johansen <i>et al.</i> , 2003)
Colorectal cancer	603	180 (56-2709)	26	(Cintin <i>et al.</i> , 1999)
Ovarian cancer	50	94 (17-517)	72	(Dupont <i>et al.</i> , 2004)
Small cell lung cancer	131	172 (48-2481)	32	(Johansen <i>et al.</i> , 2004)
prostate cancer	153	112 (20-2080)	43	(Brasso <i>et al.</i> , 2006)
Glioblastoma	45	130 (38-654)	72	(Tanwar <i>et al.</i> , 2002)

\* The percentage (%) of patients with elevated serum YKL-40 compared to the age-adjusted serum YKL-40 level in healthy subjects.

Based on the literature review, YKL-40 has been received attention as a potential prognostic marker for cancer development and health prospects of cancer patients. Diagnostic application of this protein needs sensitive analytical approach for the detection of YKL-40 in cancer serum samples. In this study, we describe establishment of YKL-40 detection using electrochemical-based immunosensor.

### **1.1.1 Methods for the determination of YKL-40 in tissues and body fluids**

Several methods have been proposed for quantitative analysis of YKL-40 in blood serum samples and some details are provided as listed below:

#### **Immunohistochemical analysis**

Immunohistochemical procedures for the detection of YKL-40 protein expression in biopsies of human tissues have been described using routine staining methods for frozen or formalin-fixed paraffin-embedded tissues. An affinity purified rabbit antibody against human YKL-40 (Johansen, Møller, Price *et al.*, 1997; Johansen, Baslund, Garbarsch *et al.*, 1999; Johansen, Christoffersen, Møller *et al.*, 2000; Volck, Price, Johansen *et al.*, 1998; Volck, Østergaard, Johansen *et al.*, 1999; Volck, Johansen, Stoltenberg *et al.*, 2001; Kawasaki, Hasegawa, Kondo *et al.*, 2001) or a mouse monoclonal antibody against human YKL-40 (Baeten, Boots, Steenbakkens *et al.*, 2000) were used as primary antibodies. The methodology was proven functional for different human tissues: such as liver (Johansen *et al.*, 1997; 2000), bone marrow (Volck *et al.*, 1998), inflamed arteries (Johansen *et al.*, 1999), cartilage (Volck *et al.*, 1999, 2001), synovial membrane (Baeten *et al.*, 2000; Volck *et al.*, 2001), peripheral blood mononuclear cells (Baeten *et al.*, 2000) and atherosclerotic vessels (Nishikawa and Millis, 2003).

#### **Detection of serum YKL-40 by different enzyme-linked immuno assays**

The first human YKL-40 assay was a radioimmunoassay (RIA) using a rabbit polyclonal antibody against human YKL-40 (Johansen, Jensen, and Price *et al.*, 1993). The assay runs over two days, involves 20 hr of incubation at room

temperature and requires sample dilution. The sensitivity of the RIA is 10 µg/L and the percentage of recovery 100.3% (Johansen *et al.*, 1993).

A sandwich-type enzyme-linked immunosorbent assay (ELISA) for measurements of human YKL-40 was later developed and is now commercially available from Quidel, Santa Clara, CA, USA. This assay uses a 96-well plate coated with streptavidin and a biotinylated murine monoclonal antibody against human YKL-40, an alkaline phosphatase (AP)-conjugated rabbit polyclonal antibody to YKL-40, and a chromogenic substrate. In the first step, standards, and test specimens are added to the avidin coated wells along with the captured solution containing a biotinylated F<sub>(ab)</sub> fragment of a murine monoclonal antibody to YKL-40. The monoclonal antibody binds to YKL-40 standards, or specimens, while the biotin binds to the avidin on the microwell plate, leading to immobilization of the antibody. After an incubation period, a wash cycle removes any unbound materials. In the second step, alkaline phosphatase conjugated rabbit anti-YKL-40 is added to each well. The enzyme conjugated anti-YKL-40 binds to the immobilized YKL-40 captured in the first step. After an incubation period, a wash cycle removes any unbound conjugates. In the third step, *p*-nitrophenyl phosphate, a chromogenic substrate solution, is added to the wells. The bound alkaline phosphatase reacts with the substrate, forming yellow color. After an incubation period, the reaction is stopped chemically, and the color intensity is measured spectrophotometrically at A<sub>450</sub>. The color intensity of the reaction mixture is proportional to the concentration of YKL-40 present in the test specimens, standards and controls. Results are calculated from the generated standard curve using linear regression analysis. The ELISA is finished within 4 hr, is carried out at room temperature and does not require sample dilution

(only if the concentration of YKL-40 in the sample is very high). The lower limit of quantification is 20  $\mu\text{g/L}$  and the linear range is 20 to 300  $\mu\text{g/L}$ . The sensitivity of the ELISA from previous study is 8  $\mu\text{g/L}$  and the percentage of recovery 102% (Harvey *et al.*, 1998).

Another commercial ELISA kit for determining YKL-40 serum is available from Shanghai BlueGene Biotech CO., LTD (Ma, Wang, Du *et al.*, 2012). The YKL-40 enzyme linked immunosorbent assay is called a competitive ELISA. The microtiter plate provided in this kit is pre-coated with anti-YKL-40. Standards or samples are added to the microtiter plate wells. Then, YKL-40 conjugated with HRP (YKL-40-HRP) was added, mixed and incubated 1 hr. After incubation, the wells are thoroughly washed to remove all unbound components. The wells are then incubated with a chromogenic substrate for horse radish peroxidase (HRP) enzyme. The product of the enzyme-substrate reaction forms a blue colored complex. Finally, a stop solution is added to 1 N HCl to the reaction, which will then turn yellow. The intensity of color is measured spectrophotometrically at 450 nm in a microplate reader. The intensity of the color is inversely proportional to the YKL-40 concentration since YKL-40 from samples and YKL-40-HRP conjugated compete for the anti-YKL-40 antibody binding site. Since the number of sites is limited, as more sites are occupied by YKL-40 from the sample, fewer sites are left to bind the YKL40-HRP conjugate. This method recommends the lower limit of quantification to be 2.5  $\mu\text{g/L}$  and linear range 2.5 to 250  $\mu\text{g/L}$ .

Non-commercial ELISA was also developed and used for a small-scale detection of YKL-40 in clinical trials. The YKL-40 ELISA was carried out by coating a 96-well plate with a mouse monoclonal antibody against human YKL-40 and a HRP

conjugated mouse monoclonal antibody against human YKL-40 was used as a detection antibody. The linear range of this approach was reported to be 0-300 µg/L (Vos, Steenbakkens, Miltenburg *et al.*, 2000).

Later, an indirect competition ELISA was developed for detecting serum YKL-40 in guinea pigs using polyclonal anti-guinea pig YKL-40 antibody produced in hens and extracted from the egg yolk. This assay can also determine rabbit YKL-40, but not rat or mice YKL-40. The lower limit of detected was reported to be 10 µg/L and a linear range was 10 to 320 µg/L (De Ceuninck, Pastoureau, Agnellet *et al.*, 2001).

Since the existing method for detection of low level of YKL-40 is still not optimal, analytical properties to improve sensitivity, detection limit, time of analysis, and cost are required. A lower detection limit and sensitivity would, for instance, be in support of a better detection of the gradually appearing increase in the body level of YKL-40. Over the past two decades, the quality of biosensor has improved a dramatically and this analytical tool is currently accepted and qualified for improving bio-analyte detection in clinical samples. The principles of biosensor will be introduced and its functional features will be described.

## **1.2 YKL-39 as an ostioarthritis marker**

YKL-39 (also known as chitinase3-like2, CHI3L2) is a non-glycosylated YKL-40 homolog. It was originally isolated as one of the major proteins secreted in primary culture of human articular chondrocytes and accounts for 4% of the total proteins secreted in chondrocyte-conditioned medium (Hu, Trinh, Figueira *et al.*, 1996). YKL-39 is more closely related in size and sequence to YKL-40 than other

members of the GH-18 family with more than 50% identity. Similar to YKL-40, the name of YKL-39 was given based on its three *N*-terminal amino acids: tyrosine (Y), lysine (K) and leucine (L) and its apparent molecular weight of 39 kDa. YKL-39 was co-purified with YKL-40 (Hu *et al.*, 1996). When the secreted protein YKL-40 from human articular chondrocyte culture was harvested and then fractionated by Sephacryl S-300 HR chromatography, the *N*-terminal sequencing data displayed the presence of two amino acid sequences, one of which had the sequence of YKLVXYYTSWSQYR (YKL-40), whereas the other had the sequence of YKLVXYFTNWSQDR (later being identified as YKL-39) (Hu *et al.*, 1996). Functional characterization showed that YKL-40 was different from YKL-39, in that YKL-40 contains the heparin binding sequence at the *C*-terminus. Therefore, YKL-40 can bind to heparin with high affinity, whereas YKL-39 does not contain heparin binding sequence. SDS-PAGE analysis showed that YKL-39 had a molecular mass slightly smaller than YKL-40 (Figure 1.4, Lane 1a and 2a). Staining of the SDS-PAGE gel for carbohydrate showed that YKL-39 is not a glycoprotein (Figure 1.4, Lane 2b), but YKL-40 is a glycoprotein (Figure 1.4, Lane 1b).

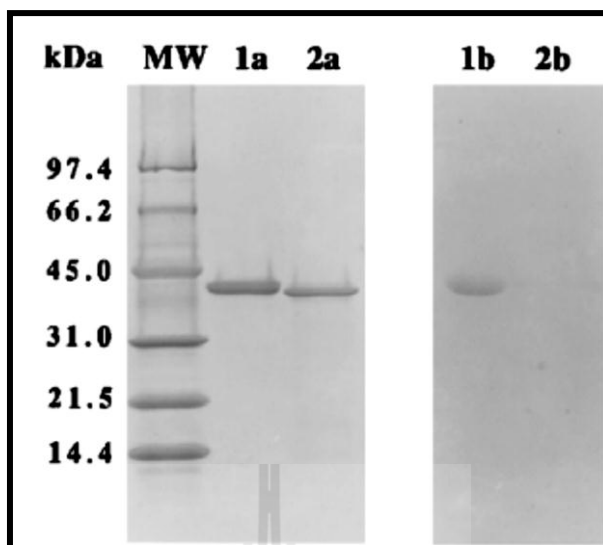


**Figure 1.4** SDS-PAGE analysis of YKL-39 and YKL-40; (left-hand panel) Coomassie Brilliant Blue stain; (right-hand panel). Glycoprotein stains using the Sigma glycoprotein detection. Lane MW, molecular mass standards; Lane 1a and 1b, YKL-40; Lane 2a and 2b, YKL-39 (Hu *et al.*, 1996).

A complete YKL-39 cDNA encodes a single polypeptide chain of 385 amino acids, which contains the 21-amino acid signal peptide. The mature protein, after removal of the signal peptide, has a length of 364 amino acids and a calculated molecular mass of 40,825 Da. Within the conserved sequence motif region, the glutamic acid, which is essential for catalytic activity of human chitinases, is substituted with isoleucine, thus making YKL-39 lack chitinase activity (Hu *et al.*, 1996).

In addition to be predominantly expressed in chondrocytes and synoviocytes (Hu *et al.*, 1996), YKL-39 mRNA was also detected in lung and heart and glioblastoma cells, but not in brain, spleen, pancreas, and liver (Kavsan, Dmitrenko, Boyko *et al.*, 2008 and Hu *et al.*, 1996).

YKL-39 is currently recognized as a biochemical marker for the activation of chondrocytes and the progress of the osteoarthritis in human (Knorr, Obermayr, Bartnik *et al.*, 2003). Real time PCR and DNA microarray analysis suggested that YKL-39 mRNA is significantly up-regulated in cartilage of patients with osteoarthritis and the YKL-39 mRNA expression was correlated with collagen type 2 up-regulations, while YKL-40 mRNA showed no significant up-regulation in osteoarthritis cartilage (Steck, Breit, Breusch *et al.*, 2002). Another study showed that the mRNA expression of YKL-39 was up-regulated both in early degenerative and late stage osteoarthritis, while YKL-40 was significantly down-regulated during the progression of osteoarthritis (Knorr *et al.*, 2003). Proteomic analysis identified YKL-39, but not YKL-40, to be secreted by human osteoarthritic cartilage in culture (De Ceuninck, Marcheteau, Berger *et al.*, 2005). YKL-39 has been proposed to contribute to the disease progression and may be an induction of autoimmune response of osteoarthritis (Sekine, Masuko-Hongo, Matsui *et al.*, 2001; Du *et al.*, 2005). ELISA and western blotting analysis showed that YKL-39 antibodies were detected 8% in human serum in patients with rheumatoid arthritis (RA), while only 1% of patients with RA had autoantibodies. The detection of autoantibody during initial cartilage degeneration in osteoarthritis in early stage knee osteoarthritis suggested a specific immune response to YKL-39 (Du *et al.*, 2005) and that YKL-39 may be used as a candidate biomarker to monitor the progression of ostioartitris. Other lines of evidence have supported the important roles of YKL-39 in osteoarthritis. For example, immunization with recombinant YKL-39 induced arthritis in different strains of mice tested, which *BALB/c* mice was most susceptible (Sakata, Masuko-Hongo, Tsuruha *et al.*, 2002). Histological examination revealed synovial

proliferation and irregularity of the cartilage surface in *BALB/c* mice (Figure 1.5). After injection of purified YKL-39, not only anti-YKL-39 antibody was detected, but also the antibody against type II collagen, suggesting the spreading of autoimmune reactions (Sakata *et al.*, 2002). This animal model suggested that YKL-39 acted as an inducer of autoimmune processes related to arthritis. Another biological activity of YKL-39 is it may play a role in tissue remodeling (Sakata *et al.*, 2002). Participation of YKL-39 in tissue remodeling was suggested on the basis of its high level in chondrocyte cultures and close homology to YKL-40 that was shown to induce cell proliferation and migration. Moreover, recently report showed that YKL-39 also activated cell signaling regulated by ERK1/ERK2 kinases in human embryonic kidney (HEK293) and human glioblastoma (U87) cells (Areshkov and Kavsan, 2010). As well as YKL-39 also found in the synovial fluid of an ostioarthritis patient, Jurkat cell lysate, and U937 cell lysate (Ranok, Khunkaewla and Suginta, 2013).



**Figure 1.5** YKL-39 induced arthritis in *BALB/c* mice. The right foot pad of a control mouse (left-hand panel) and the right foot pad of an YKL-39 (50  $\mu$ g) immunized *BALB/c* mouse 30 days after the first immunization (right-hand panel) (Sakata *et al.*, 2002).

Osteoarthritis is the most common type of arthritis and is seen especially among older people. Sometimes it is called degenerative joint disease. Osteoarthritis can affect any joint, but it occurs most often in knees, hips, lower back and neck, small joints of the fingers and the bases of the thumb and big toe. Osteoarthritis mostly affects cartilage, the hard but smooth tissue that covers the ends of bones where they meet to form a joint. The diagnosis of osteoarthritis is currently based on radiographic criteria (e.g. joint space width) and clinical symptoms (e.g. pain and loss of function). However, the limitations of radiography (e.g. technical issues, precision and sensitivity) have led to research into alternative parameters to detect osteoarthritic changes in the joints in an early stage of the disease in a quantitative, reliable, and sensitive manner. The measurement of biochemical markers in blood, urine or synovial fluid samples could reflect dynamic and quantitative changes in joint remodeling and therefore disease progression (Mobasheri and Henrotin, 2010; Lamers, van Nesselrooij, Kraus *et al.*, 2005). The C-terminal telopeptide of collagen type II (CTX-II, Kim, Park, Min *et al.*, 2013), cartilage oligomeric matrix proteins (COMPs, Hong, Park, Jang *et al.*, 2012), various matrix metalloproteinases (Bay-Jensen, Liu, Byrjalsen *et al.*, 2011; Gargiulo, Gamba, Poli *et al.*, 2014) and finally YKL-39 (Knorr *et al.*, 2003; Steck *et al.*, 2002; Ranok *et al.*, 2013) were identified as potentially measurable biomarkers for osteoarthritis. The standard analytical method for the detection biomarkers in body fluids is the ELISA technique, which requires an antibody against the chosen indicator molecule and an enzyme-labeled secondary antibody to generate the final signal. However, ELISA methods are time consuming and involve relatively expensive equipment. To improve the alternative method for

detection in early stage in ostioarthritis patient we chose the YKL-39, the biomarker for early stage of ostioarthritis patient (Knorr *et al.*, 2003), by capacitive immunosensor.

### 1.3 The principle of capacitive electrochemical immunosensing

Capacitive immunosensors are a special form of biosensors, which are analytical tools using specific biological recognition elements (BRE) (e.g. enzymes, tissue, microorganisms, antibodies, cell receptors etc.) in intimate contact on a suitable physicochemical transducer device that converts the interaction of the BRE with substrate into a quantifiable electric signal. Biosensors usually generate an electronic signal which is proportional to the concentration of a specific analyte or a group of analytes (Sharma, Shegal, and Kumar, 2003). The general working principle of biosensors is shown in Figure 1.6 in a schematic drawing.

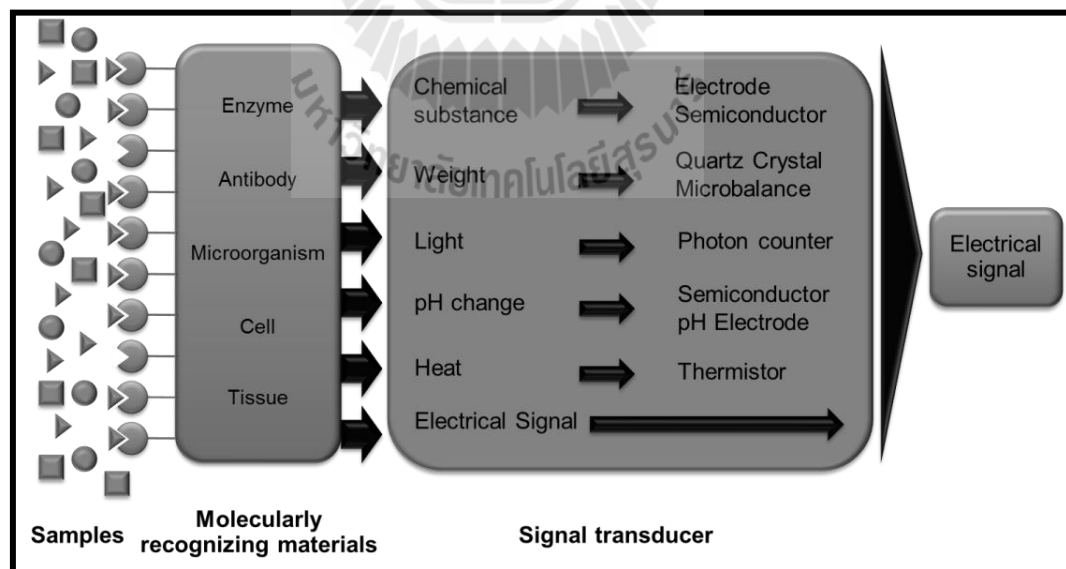


**Figure 1.6** The principle of a biosensor.

Biosensors can be divided into two categories, namely the catalytic and the affinity-based biosensors. Bio-catalytic biosensors use isolated enzymes or whole cells with their totality of enzymes as BREs that catalyze a signaling biochemical reaction with the substrate of the immobilized enzyme, which usually then is the analyte. In enzyme-based biosensors, for example, substrate molecules are continuously converted into the corresponding product molecules; regeneration of the BRE needs interaction with a co-factor, which accordingly changes chemical (redox) state and the upcoming converted co-factor is a side product of the enzymatic action on substrate (Yang, 2012). Monitored with a suitable transducer of enzyme-biosensors as analytically useful signal is then the consumption of substrate, the generation of product of enzyme activity, or the co-factor in initial or final version state (Byfield and Abuknesha, 1994; Dong and Chen, 2002). Common analytes for enzyme biosensors are small organic molecules, and most popular case is the glucose oxidase-based glucose biosensor that is used by the millions of people around the world with diabetes for measuring on hourly basis their blood sugar levels.

Bio-affinity-based biosensors, designed to monitor substrate/BRE conjugation and not chemical turnover, use binding proteins such as lactins, receptors, nucleic acids, membranes, whole cells, antibodies, or antibody-related substances, for specific bimolecular recognition (Rogger, 2000). According to the type of the BREs, affinity biosensor can be classified as DNA biosensors, receptor biosensors and immunosensors.

Immunosensors are compact analytical devices in which the event of formation of antigen antibody complexes is detected and converted, by means of a transducer, to an electrical signal, which can be processed, recorded and displayed.

Immunosensors are divided into two main categories; label-free (direct method) and labeled (indirect method). The labeled immunosensors are derived from the immunoassay technology, where signal generation is significantly facilitated. This type of sensor requires the target analyte or secondary antibody to be labeled, and can undoubtedly be potent; however, there are significant issues associated with the process of labeling, attaining reproducible changes at the surface and in the inherently multistep nature of analyses. Label-free immunosensors rely on the detection of physical change during the immune complex formation. Such changes have been measured using optical, piezoelectric and electrochemical transducers. Label-free approaches benefit considerably from being single step, fast, and cheap and they make real time measurement possible.

In electrochemical immunosensors, the event of the formation of antigen-antibody complex is converted into an electrical signal: amperometry, voltammetry or electrochemical impedance spectroscopy (EIS) are schemes that can help to translate the binding event into a readable measure (Centi *et al.*, 2009). The most common type of amperometric/voltammetric immunosensors can be regarded as ELISA tests with electrochemical detection, where redox species generated by a redox enzyme (enzymatic label) are converted into a measurable current. Whereas, EIS is a label-free method that measures electrode capacitance changes produced by restructuring of the interfacial Helmholtz double-layer on antigen binding. EIS immunosensing is an effective and sensitive method to probe the interfacial properties of modified electrode and to monitoring the binding of the antigen-antibody but EIS requires specific hardware and software and the acquired data is complex. A simpler method to detecting the binding of the antigen-antibody due to capacitance changes is the

analysis of the current response on application of a potential pulse (Berggren, Bjarnason, and Johansson, 2001; Berggren and Johansson, 1997 and Limbut, Kanatharana, Mattiasson *et al.*, 2006a,b).

Capacitive immunosensors have been report by Newman and co-worker as early as 1986. They reported that antibody-antigen reaction, which occur at the device surface, produce significant and reversible capacitance change on the time scale of several minutes. Unfortunately no further information is given, so that the results cannot be interpreted in relation to concentrations of the background electrolyte and the analyte, nor other physical and chemical environmental conditions (Newman *et al.*, 1986). The methodology is based on the principle that for an electrolytic capacitor, the interfacial capacitance depends on the thickness and dielectric behavior of a dielectric layer on the surface of a metal (Gebbert *et al.*, 1992).

The capacitance and the sensitivity of the device are related to the thickness of the dielectric. The electric capacitance between two parallel plate separated a distance  $d$  is given by Eq. 1.1.

$$C = \epsilon_0 \epsilon A/d \quad \text{Eq. 1.1}$$

Where  $\epsilon_0$  is permittivity of free space,  $\epsilon$  is the dielectric constant of material between the plates,  $d$  is distance between two plates and  $A$  is the surface area.

Electrochemical immunosensors can be considered as electrolytic capacitors, with one “capacitor plate” represented by the charges accumulated at the antibody modified metal surface of the electrode covered with an insulator and the other

“plate” being represented by the Helmholtz layer of counter-ions in electrolyte. The binding of antigen to immobilized antibodies will, as shown in Figure 1.7, move the two constituting layers of the capacitance apart from each other, causing, in accordance with Eq. 1.1, the capacitance to decrease since the distance of the “plates” increase. The capacitance change between before and after antigen capture is concentration dependent and thus allows quantification of antigen. This type of capacitance measurements will be described in full detail later in Chapter II, Section 2.3.2.3.

In order to make the capacitive immunosensor, the antibody has to be properly attached to the transducer with the boundary condition that the biological function (equal to the ability to conjugate with the corresponding antigen) is preserved. This process is commonly known as antibody immobilization. Proper immobilization is an important step in capacitive immunosensor since the electrode surface has to be equipped with the antibody and at the same time entirely electrically insulated. Different immobilization techniques have been developed and antibodies may be immobilized on capacitive sensors via the use of modified semiconductor surfaces (Barraud, Perrot, Billard *et al.*, 1993; Bataillard, Gardies, Jaffrezic-Renault *et al.*, 1988), metal oxides surfaces (Gebbert, Alvarez-Icaza, Stoecklein *et al.*, 1994), or self-assembled monolayers (SAMs) of sulfur compounds on gold (Berggren and Johansson, 1997; Berggren, Bjarnason, and Johansson, 1998).

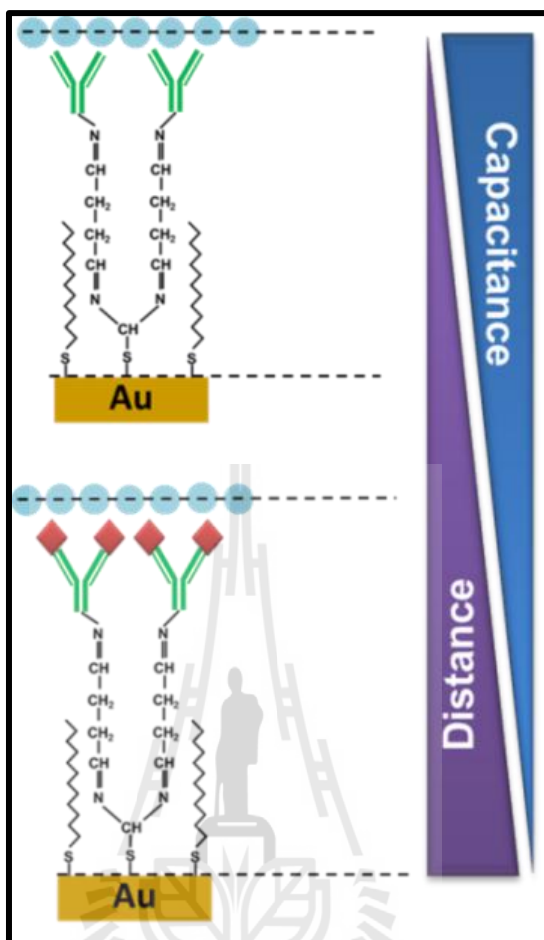


**Figure 1.7** Representation of the dielectric layer in front of an antibody-modified gold electrode. One layer (“plate”) is the charged surface of the antibody modified metal electrode with an insulator itself and the second layer (“plate”) is formed by ions of opposite charge that accumulate at the electrolyte/electrode interface via electrostatic attraction (blue circle). The thickness of the dielectric layer (= distance of the two “plates”) increases when antigens binds to antibody and squeezes in between, causing the capacitance to decrease. A measured capacitance change thus is an indication of antigen capture, and the concentration dependence of the effect makes quantification of antigen possible.

SAMs of alkane-thiols on gold turned into a versatile model system for electrochemists in the last decade as through clever design of bifunctional HS-(C)<sub>n</sub>-X compounds intentional electrode surface modification in a well-defined and reproducible way became accessible and opened elegant opportunities for the buildup of molecular architectures on this type of sensor surface (Schweiss, Werner, and Knoll, 2003). In particular, the simplicity of an automatic formation of a SAMs and the related ease of sulfur bond-based antibody immobilization made it an attractive strategy for achieving better control in the orientation and molecular organization of biomolecules at interfaces (Akram, Stuart, and Wong, 2004).

The stability of SAMs arises from the strong chemical absorption of the sulfur-atom on metal interfaces in combination with intermolecular interaction between the protruding alkyl chains (Wink, van Zuilen, Bult *et al.*, 1997). The bond between sulfur and gold atoms is very strong and SAMs are thus stable in air, water and organic solvent at room temperature (Berggren and Johansson, 1997; Bain, Evall, and Whitesides, 1989; Chaki and Vijayamohanan, 2002). The SAMs technique is a simple way to obtain a reproducible and well-ordered layer suitable for further modification with antibodies, and improved detection sensitivity, speed, and reproducibility are the gains (Fu, Yuan, Tang *et al.*, 2005). In electrolytes, self-assembled monolayer on Au are usually quite stable in the potential window of -400 to +1400 mV vs. SCE in dilute acidic solution, which is well suitable for applications in electrochemical sensing (Finklea, Avery, Lynch *et al.*, 1987).

Thiourea (NH<sub>2</sub>CSNH<sub>2</sub>), a reasonably cheap thiol reagent with low environmental impact and strong adsorption on gold. It has amino groups (R-NH<sub>2</sub>) that can be covalently coupled to -NH<sub>2</sub> entities in the antibody protein structure via

exposure to the chemical cross-linker glutaraldehyde. The application of thiourea as starting layer for the formation of capacitive immunosensors has recently been introduced and the novel functional compound performed very well in the completed sensors with good reliability in the formation of the antibody-modified sensing layer and support of good analytical figures of merit for sensor operation in a flow injection-based capacitive immunosensing system (Limbut *et al.*, 2006a, b). Based on the good reported behavior of self-assembled thiourea monolayer as basis for capacitive immunosensors, this particular surface modification was the choice in this thesis for the establishment of the target YKL-40 and YKL-39 capacitive immunosensors.

#### **1.4 Thesis objectives**

Main goal of this thesis was the development of capacitive immunosensors for the direct sensitive and selective detection of the chitinase-like proteins YKL-39 and YKL-40 using specific antibodies immobilized on a self-assembled thiourea monolayer on gold surfaces as analytical tool in a flow-based analysis system. Tasks included thorough performance tests with of the YKL-39/40 capacitive immunosensors for the determination of their corresponding analyte levels in model and clinical samples and a comparison with data from applications of commonly-used enzyme-linked immunosorbent assay (ELISA).

The six major objectives of this research.

1. To express and purify human YKL-40.
2. To produce polyclonal antibodies specific for human YKL-40.
3. To develop a capacitive immunosensor for human YKL-40.

4. To test the human YKL-40 capacitive immunosensor in clinical samples.
5. To develop a capacitive immunosensor for human YKL-39.
6. To test the human YKL-39 capacitive immunosensor in clinical samples.



## CHAPTER II

### MATERIALS AND METHODS

#### 2.1 Materials

##### 2.1.1 Chemicals and reagents

All chemicals reagent used were analytical grade. A protein A agarose column and HRP-conjugated anti-rabbit IgG were obtained from GenScript Inc., Piscataway, NJ, USA. The pQE-Tri System expression vector, a Ni-nitrilotriacetic acid (Ni-NTA) agarose column and *Escherichia (E.) coli* stain M15 (pREP) and DH5 $\alpha$  were purchased from Qiagen Ltd., Manchester, UK. Ampicillin, phenylmethylsulphonyl fluoride (PMSF), imidazole and TritonX-100 were products of USB Corporation, Cleveland, OH, USA. Isopropyl thio- $\beta$ -D-galactoside (IPTG), Freund's complete adjuvant, Freund's incomplete adjuvant, Tris-HCl, Tris-base and lysozyme were from Sigma Aldrich, St. Louis, MO, USA. 3,3',5,5'-tetramethylbenzidine (TMB), the substrate for ELISA assays, was purchased from Invitrogen, Carlsbad, CA, USA. Glutaraldehyde, 1-dodecanethiol, potassium ferricyanide (K<sub>3</sub>[Fe(CN)<sub>6</sub>]), and 4-(2-hydroxyethyl)-1-piperazineethanesulfonic acid (HEPES) were purchased from Acros Organic, Bridgewater, NJ, USA. Protein concentrations were measured with a Pierce<sup>®</sup> BCA Protein Assay kit from Thermo Scientific, Rockford, IL, USA. Skimmed milk powder was product of Himedia (Himedia Laboratories Pvt. Ltd., Mumbai, India). All

other basic chemical reagents (e.g. NaCl, KCl, Na<sub>2</sub>HPO<sub>4</sub>, KH<sub>2</sub>PO<sub>4</sub>, Urea, HCl, H<sub>2</sub>SO<sub>4</sub> and thiourea) were from Carlo Erba Reagents, Cornaredo (MI), Italy and unless otherwise mentioned were of analytical grade. Alumina slurries with a particle size of 1 and 5 μm, as used for gold sensor surface polishing, were obtained from Metkon Instruments Ltd., Bursa, Turkey. A Hiprep 26/10 desalting column was supplied by GE HealthCare, Hatfield, UK and Vivaspin-20 ultrafiltration membranes came from Vivascience AG, Hannover, Germany. All aqueous solutions were prepared with purified water from a reverse osmosis-deionizing system (Cascada™ Lab Water Systems, PALL Life Science, Ann Arbor, MI, USA). Buffers were filtered through Whatman® cellulose nitrate membrane with pore size 0.20 μm from GE HealthCare, Hatfield, UK. Fetal Calf Serum (FCS), Roswell Park Memorial Institute (RPMI-1640) medium, and Dulbecco's Modified Eagle's Medium (DMEM) were obtained from Gibco® (Grand Island, NY, USA). Other chemicals and molecular reagents used but not listed here were purchased from a variety of suppliers.

### 2.1.2 Instrumentation

ELISA analysis was performed using a Biochrom® Anthos Multi Read 400 Microplate Reader (Biochrom Ltd., Cambridge, UK). All electrochemical immunosensor recordings were made with an EA163 potentiostat and e-corder 410 data acquisition device, from eDAQ, Denistone East, Australia. The system for flow injection-based sample measurements used a peristaltic pump (Miniplus® 3 from Gilson, Middleton, WI, USA), a manual injection valve (Biologic MV-6® from Bio-Rad, Hercules, CA, USA) and a three-electrode radial flow cell with customized 3-mm-diameter gold disk electrodes (ALS Co., Ltd., Tokyo, Japan).

## **2.2 Methods**

### **2.2.1 Molecular biology**

#### **2.2.1.1 Preparation of competent cells of *E. coli* strains DH5 $\alpha$ and M15 (pREP)**

*E. coli* from glycerol stock was streaked onto a Luria broth (LB, 10 g/L tryptone, 5 g/L yeast extract, 5 g/L sodium chloride) agar plate containing 50  $\mu$ g/mL kanamycin and 100  $\mu$ g/mL ampicillin for the M15 (pREP) strain or without antibiotic for the DH5 $\alpha$  strain. A single colony was picked into 5 mL LB media containing antibiotics as listed above. The cells were grown at 37°C for 16-18 hr. with shaking at 200 rpm. Then, 0.5 mL of starter culture was inoculated into 50 mL LB prepared in a 250 mL flask and incubated at 37°C with shaking until the OD<sub>600</sub> reached 0.5-0.6. The culture was cooled on ice for 15 min, then transferred to pre-cooled centrifuge tubes, and cell pellet was collected by centrifugation at 3,000 rpm for 10 min. Cells were gently and slowly resuspended with 10 mL of cold 0.1 M CaCl<sub>2</sub> and placed on ice for 20 min. The cells were centrifuged as before and resuspended with 0.5 mL of cold 0.1 M CaCl<sub>2</sub> and placed on ice for 1 hr. Finally, cold glycerol was added to the cells to the final concentration of 15%. Then, they were resuspended and 50  $\mu$ L aliquots were stored in pre-cooled tubes at -80°C.

#### **2.2.1.2 Transformation of plasmid DNA into competent cells**

Plasmid DNA (20 ng) was added into the 50  $\mu$ L of competent cells, mixed by tapping and immediately place on ice for 30 min. The cells were heat shocked at 42°C for exactly 45 s and then immediately put on ice for 10 min. Then, 0.9 mL of LB medium was added into the cell mixture and the tube was incubated in a 37°C shaker

for 1 hr. Then, 100-200  $\mu\text{L}$  of the cells were spread on an LB plate containing the appropriate antibiotics and incubated at  $37^\circ\text{C}$  overnight.

### **2.2.1.3 Denaturing sodium dodecyl sulfate polyacrylamide gel electrophoresis (SDS-PAGE) and western blot analysis.**

SDS-PAGE was carried out following Laemmli (1970). Protein samples were prepared by mixing with 3X loading buffer (150 mM Tris-HCl, pH 6.8, 5% (v/v) of 2-mercaptoethanol, 6% (w/v) SDS, 30% (v/v) glycerol and 0.03% (w/v) bromophenol blue), and then boiled for 5 min. The samples will be centrifuged at 12,000 rpm for 5 min, and then 10-15  $\mu\text{L}$  supernatant is loaded onto 12% SDS-PAGE gel (3.345 mL of distilled water, 2.5 mL of 1.5 M Tris-HCl, pH 8.8, 4 mL of 30% acrylamide/bisacrylamide solution, 100  $\mu\text{L}$  of 10% (w/v) SDS, 50  $\mu\text{L}$  of 10% (w/v) ammonium persulfate, and 5  $\mu\text{L}$  TEMED. The 4% stacking gel was prepared by mixing 3 mL of distilled water, 1.25 mL of 0.5 M Tris-HCl, pH 6.8, 0.67 mL of 30% acrylamide/bisacrylamide solution, 50  $\mu\text{L}$  of 10% (w/v) SDS, 25  $\mu\text{L}$  of 10% (w/v) ammonium persulfate, and 5  $\mu\text{L}$  of TEMED) with a discontinuous Tris-glycine buffer system set in a Mini-PROTEAN<sup>®</sup> 3 cell (BioRAD). A constant potential of 120 V is applied across the SDS-PAGE gel for 1 hr. using Tris-glycine, pH 8.3, as a running buffer. After electrophoresis, the gel were stained with 0.025% coomassie brilliant blue R250 (40% methanol, 7% acetic acid) for 30 min, and then destained with a destaining solution (40% methanol, 7% acetic acid) until the background is clear. Molecular weights of proteins were estimated by comparing with the pink plus prestained protein ladder (GeneDirex, Taiwan) that contains 11 proteins that resolve in the range of 10-175 kDa. Whereas western blotting technique, after run

SDS-PAGE, then transfer proteins in the gel onto nitrocellulose membrane by semi-dry transfer device (Trans-blot SD semi-dry cell transfer; Bio-Rad, Hercules, CA, USA). After transfer, incubate membrane in 5% skimmed milk in 1X PBS, pH 7.2 for one hour at room temperature. Add the primary antibody (anti-YKL-40 or anti-YKL-39) to membrane and incubate 1-2 hr. at room temperature. Remove antibody solution and wash membrane three times for 5 min each with 0.1% Tween-20 in 1X PBS, pH 7.2 (PBST) and then add Horseradish peroxidase conjugated-goat-anti-rabbit Igs (secondary antibody) to membrane and incubate for 1 hr. at room temperature with shaking. Remove antibody solution and wash membrane three times for 5 min each with PBST. Remove solution from the membrane. Apply chemiluminescent substrate reagent to cover all surface of the membrane. Incubate at room temperature for 3 min and detect the protein band by developing with X-ray film at various times, in dark room.

#### **2.2.1.4 Cell culture**

All human cell lines were of American cell culture collection. Human T cell lines (Jurkat), human leukemic monocyte lymphoma cell line (U937) and human leukemia cell line (THP-1) were cultured in Roswell Park Memorial Institute (RPMI-1640) medium, supplemented with 10% heat inactivated fetal calf serum (FCS), 40 µg/mL gentamycin and 2.5 µg/mL amphotericin B in a humidified atmosphere of 5% CO<sub>2</sub> at 37°C. Human embryonic kidney cells (293T) were cultured in Dulbecco's Modified Eagle's Medium (DMEM) with the condition as mentioned above. After cell passages of three times a week, the cells were collected, and washed three times with 1X PBS, pH 7.2 by centrifugation at 1,500 rpm for 5 min. Then  $1 \times 10^7$  cells were

lysed on ice for 30 min in 1 mL of lysis buffer (50 mM Tris-HCl, pH 8.2, 100 mM NaCl, 2 mM EDTA, 0.02% (w/v) NaN<sub>3</sub>, 1% (v/v) TritonX-100, 1 mM phenylmethylsulphonylfluoride (PMSF), 5 mM iodoacetamide, and 10 µg/mL aprotinin) at 4°C for 30 min. Clear lysate was collected by centrifugation at 13,000 rpm, 4°C for 30 min, and used for further experiment.

#### **2.2.1.5 Expression and purification of recombinant YKL-40 in *E. coli* strain M15 (pREP) (bYKL-40)**

*E. coli* strain M15 (pREP) competent cells were transformed with pQE-tri system plasmids that contained YKL-40 gene and cultured in 5 mL LB medium supplemented with ampicillin (100 µg/mL), incubated at 37°C, 200 rpm shaking. The overnight culture were diluted to a ratio of 1:100 with LB medium supplemented with ampicillin (100 µg/mL), and further grown at 37°C until OD<sub>600</sub> reaches 0.6. The culture was pre-incubated at 25°C for 30 min, then isopropyl β-D-1-thiogalactopyranoside (IPTG) was added to a final concentration of 0.5 mM, and then the bacterial culture was incubated at 25°C for additional 16 hr. with 150 rpm shaking. With this protocol, the recombinant bYKL-40 was expressed in inclusion bodies. The IPTG-induced cells was harvested by centrifugation at 4,500 rpm at 4°C for 45 min. Cell pellet was kept at -80°C until used or re-suspended in lysis buffer (50 mM Tris-HCl buffer, pH 8.0, containing 300 mM NaCl, 1 mM PMSF, 1.0 mg/mL lysozyme and 1% (v/v) TritonX-100) and then lysed on ice using a Sonopuls Ultrasonic homogenizer with a 6-mm diameter probe (50% duty cycle; amplitude setting, 20%; 30 s, 6 to 8 times). Cells debris was removed by centrifugation at 12,000 rpm at 4°C for 30 min, while white pellet containing bYKL-40 was collected. The

insoluble protein was further solubilized 8 M urea, and cell pellet was removed the cell pellet by centrifugation at 12,000 rpm at 4°C for 60 min. Then, the solubilized/denatured bYKL-40 protein was further purified by Ni-NTA affinity chromatography run under gravity. To bind the His<sub>8</sub>-tagged proteins to the Ni-NTA resin, 5 mL of Ni-NTA agarose resin, which had been equilibrated with equilibration buffer, containing 8 M urea, was added to 40 mL of the solubilized protein extract and then gently shaken on ice for 1 hr. The protein-bound resin was washed with 10 column volumes of equilibration buffer, followed by 5 column volumes of wash buffer 1 (10 mM imidazole in equilibration buffer) and 5 column volumes of wash buffer 2 (20 mM imidazole in equilibration buffer). Finally, the bound protein was eluted with elution buffer (250 mM imidazole in equilibration buffer). Fractions containing YKL-40 were pooled and then subjected to several rounds of membrane centrifugation using Vivaspin-20 ultrafiltration membrane concentrators (Mr 10000 cut-off) for complete removal of imidazole. The purity of the purified YKL-40 was verified by SDS-PAGE and the final protein concentration was determined using the Pierce<sup>®</sup> BCA Protein Assay kit by (Novagen, Darmstadt, Germany).

#### **2.2.1.6 Expression and purification of recombinant YKL-40 in 293T cells (mYKL-40)**

293T cell line was cultured in DMEM medium, the day before transfection, 500,000 cells of were seeded into 6 well in 3 mL of DMEM medium without antibiotics so that cells were 70-90% confluent at the time of transfection. For each transfection sample, prepare complexes as follows: (solution a) Dilute 2 µg of mYKL-40/pCMV/hygro-His recombinant plasmid (Sino Biological Inc., Beijing, China) in

250  $\mu$ L of DMEM medium without FCS and antibiotic, mix gently. (solution b) Mix 8  $\mu$ L of lipofectamine<sup>®</sup> 2000 with 250  $\mu$ L of DMEM medium without FCS and antibiotic. Incubate for 5 min at room temperature. After that combine the diluted DNA (solution a) with diluted lipofectamine<sup>®</sup> 2000 (solution b) (total volume = 500  $\mu$ L). Mix gently and incubate for 20 min at room temperature. Then, add the 250  $\mu$ L of complexes to each well containing cells and medium. Mix gently by rocking the plate back and forth. Incubate cells at 37°C in a CO<sub>2</sub> incubator for 48 hr. and collect the supernatant that contain YKL-40 protein. Then, the culture supernatant was further purified by affinity chromatography on a Ni-NTA agarose column run under gravity. To bind the His<sub>10</sub>-tagged protein to the Ni-NTA resin, 25  $\mu$ L of Ni-NTA resin, which had been equilibrated with equilibration buffer (50 mM NaH<sub>2</sub>PO<sub>4</sub>, 300 mM NaCl, adjust pH to 8.0 using NaOH) was added to 10 mL of culture supernatant and then gently shaken on ice for 1 hr. The resin-bound protein was centrifuged at 1,000 rpm for 5 min at 4°C, the supernatant was removed and then the protein-bound resin was washed with 1 mL of equilibration buffer, 1 mL of wash buffer 1 (10 mM imidazole in equilibration buffer) and 1 mL of wash buffer 2 (20 mM imidazole in equilibration buffer) repeat for each step of washing five times. Finally, the bound protein was eluted with elution buffer (250 mM imidazole in equilibration buffer). Fractions containing YKL-40 were pooled and follow by the buffer exchange to 1X PBS, pH 7.2 using dialysis bag (Standard RC tubing, MW cut-off 12-14 kDa, Spectrum Laboratories, Inc., CA, US) for removal of imidazole. The purity of the purified YKL-40 was verified by SDS-PAGE and the final protein concentration was determined using the Pierce<sup>®</sup> BCA Protein Assay kit.

## 2.2.2 Immunology

### 2.2.2.1 Polyclonal antibody production

YKL-40 polyclonal antibody production was carried out using in-gel protein method (Amero, James, and Elgin, 1988). Firstly, purified YKL-40 protein (20 to 25  $\mu\text{g}$  per well) was separated by 12% SDS-PAGE. Following the electrophoresis, the gel was stained with 0.025% coomassie brilliant blue R250 for 30 min, and then destained with destaining solution until the background was clear. After destaining thoroughly with distilled water for overnight, the YKL-40 band was excised from gel, homogenized with 250  $\mu\text{L}$  of 1X PBS, pH 7.2 and then mixed with 250  $\mu\text{L}$  of Freund's complete adjuvant (Sigma, St. Louis, Mo, USA). The protein mixture was used to as immunogen by subcutaneous injecting into a female New Zealand white rabbit, 10 weeks age. The immunization was repeated twice every second week. Below is the work plan for polyclonal anti-YKL-40 antiserum production.

Week 0: Collection of pre-immune serum (10 mL).

Week 1: First immunization with  $\sim 100 \mu\text{g}$  of YKL-40 protein in Freund's complete adjuvant.

Week 3: First boosting with  $\sim 100 \mu\text{g}$  of YKL-40 protein in Freund's incomplete adjuvant.

Week 4: Second boosting with  $\sim 100 \mu\text{g}$  of YKL-40 protein in Freund's incomplete adjuvant.

Week 5: Third boosting with  $\sim 100 \mu\text{g}$  of YKL-40 protein in Freund's incomplete adjuvant.

Week 6: Collection of blood serum (30 mL).

Week 7: Collection of blood serum (30 mL).

Week 8: Collection of blood serum (30 mL).

Week 9: Collection of blood serum (30 mL).

The blood serum was collected from the central ear artery with a 21-gauge needle. The blood serum was allowed to clot and retract at 4°C overnight, and the serum was retrieved by centrifugation at 4,500 rpm for 15 min. The titer of antiserum was determined by indirect ELISA and Western blotting.

#### **2.2.2.2 Purification of polyclonal antibody**

The immunized serum was purified by affinity chromatography on a protein A agarose column run under gravity (GenScript Corporation, USA). Serum sample was diluted with Binding buffer (0.15 M NaCl, 20 mM Na<sub>2</sub>HPO<sub>4</sub>, pH 8.0) at a ratio of 1:1 to ensure that proper ionic strength and pH are maintained for optimal binding, and further filtered through a 0.20 µm filter to remove cells. The diluted serum sample was applied onto protein A resin gravity column which was equilibrated with 10 column volumes Binding buffer. Bound IgG resin was washed with 30 column volumes binding Buffer. Bound antibodies were eluted with 10 column volumes Elution Buffer (0.1 M glycine, pH 2.5) and were further immediately neutralized to pH 7.4 with 1 M Tris-HCl, pH 8.5 at a ratio of 1:10 volume of total eluted. The eluted fraction was then applied onto Hiprep 26/10 Desalting column (GE-Healthcare) for buffer exchanging to 1X PBS, pH 7.2. The purity of anti-YKL-40 was verified by SDS-PAGE. Antibody concentration was determined by Pierce<sup>®</sup> BCA Protein Assay kit. Purified antiserum aliquots were stored at -40°C.

### **2.2.2.3 Characterization of anti-YKL-40 polyclonal antibody**

#### **2.2.2.3.1 Determination of the antibody titers and specificity by western blotting**

Titer and specificity of the anti-YKL-40 polyclonal antibody were determined by western blotting. Two micrograms of the purified YKL-40 was resolved on a 12% SDS-PAGE, and then electrophoretically transferred onto a nitrocellulose membrane by the semi-dry transfer blotting technique. After blotting, non-specific binding was blocked by incubation with 5% (w/v) skimmed milk in 1X PBS, pH 7.2 for 1 hr. at room temperature. The blocked membrane was rinsed once with 1X PBS, pH 7.2 before cutting into 6 strips, each 1 cm wide. Each strip was incubated for 1 hr. at room temperature with two-fold serial dilutions (1:5,000, 1:10,000, 1:20,000, 1:40,000, 1:80,000, and 1:160,000) of anti-YKL-40 serum. Cross-reactivity against other YKL-40 homologues, including YKL-39, AMCase and bacterial chitinase, was used to test antibody cross-reactivity. The antibody-antigen interaction was detected with HRP-conjugated goat-anti-rabbit IgG using the enhanced chemiluminescence method (Thorpe *et al.*, 1985).

#### **2.2.2.3.2 Determination of the antibody titers and specificity by ELISA**

For ELISA analysis, each well of a 96-well plate was loaded with 50  $\mu$ L of YKL-40, YKL-39, AMCase or bacterial chitinase, each well contained 1 to 500  $\mu$ g/L protein in 0.2 M sodium carbonate buffer, pH 9.6. The coated plate was incubated overnight at 4°C. After that supernatant was discarded, and the loaded plate was blocked with 200  $\mu$ L per well of 2% (w/v) skimmed milk in 1X PBS, pH 7.2 (blocking buffer). After 1 hr. of incubation at 25°C, the treated plate was washed once with 300  $\mu$ L per well of 0.05% (v/v) Tween-20 in 1X PBS, pH 7.2 (PBST). In a

routine, 50  $\mu\text{L}$  of 15.6  $\mu\text{g/L}$  anti-YKL-40 antisera (prepared in blocking buffer) was added to each well. The plate was incubated at 25°C for 1 hr., followed by 4 washes with PBST. HRP conjugated-goat-anti-rabbit IgG was added, incubated at 25°C for 1 hr, followed by wash 5 times with PBST to remove the unbound antibody. To develop color after the peroxidase reaction, 100  $\mu\text{L}$  of TMB substrate was added to each well after four washes. The reaction was then stopped by adding 100  $\mu\text{L}$  of 1 N HCl solution. The intensity of the developed color was determined spectrophotometrically using a microplate reader used at a wavelength of 450 nm. For titration experiments, the wells of a microtiter plate were treated with 50  $\mu\text{L}$  of YKL-40 solution of various concentrations (2 fold-dilutions from 1 to 500  $\mu\text{g/L}$ ) with incubation overnight at 4°C. The remaining steps of ELISA were carried out as described above.

### **2.2.3 Development of immunosensor specific for YKL-39/40**

The desired capacitive immunosensor specific for the two human chitinase-like proteins (YKL-39 and YKL-40) were developed by immobilizing the corresponding polyclonal antibodies against human chitinase-like proteins on the surface of gold working electrode using a self-assembled thiourea monolayer and a glutaraldehyde crosslinking strategy for protein surface anchoring. Detailed information on the antibody immobilization on gold electrodes and on the application of the YKL-39/40 immunosensors for capacitive antigen monitoring and quantification will be provided in the following sections.

### 2.2.3.1 Preparation of capacitive YKL-39/40 immunosensors

The capacitive immunosensors were result of a literature-known procedure that worked with a sequence of mechanical and electrochemical cleaning, self-assembled thiourea monolayer formation and glutaraldehyde-assisted chemical antibody immobilization (Chaocharoen *et al.*, 2015; Berggren *et al.*, 2001; Berggren and Johannsson, 1997; Limbut *et al.*, 2006a, b). In brief, gold electrodes (3-mm diameter, 99.9% purity) were very thoroughly polished on soft polishing pads that were soaked with alumina slurries of decreasing particle size (5, 1 and 0.5 micron, respectively). The sequential polishing steps were interrupted by intense water rinsing and, after final polishing, a 15 min ultrasonication in water. Smoothened gold electrode surfaces dried in a stream of N<sub>2</sub> gas before they were further electrochemically cleaned in a 0.5 M H<sub>2</sub>SO<sub>4</sub> electrolyte with 25 repetitions of a 100 mV/s potential scan from 0 to 1.5 V vs. Ag/AgCl reference electrode. Rinsing with deionized water and drying in a stream of N<sub>2</sub> gas made the electrodes ready for the application of the immobilization chemistry. A cleaned gold electrode was actually immersed at room temperature for 24 hr into a 250 mM thiourea. This allowed the selected bifunctional thiol, it has sulfur and amino groups in the structure, thiol self-assembled on the electrode disk via covalent Au-S bond formation; the amino groups remained to be untouched and, pointed off the surface, were the target for the following glutaraldehyde assisted crosslinking with equivalent entities in the antibody structure. Thiourea-modified electrodes were thoroughly rinsed with deionized water to remove excess thiourea and then dried with N<sub>2</sub> gas. Final step was the coupling of the antibody (either YKL-39 or YKL-40) to the primed gold electrode. Start was a 20 min treatment with 5% (v/v) glutaraldehyde in 10 mM sodium phosphate buffer, pH

7.0. Rinsing with 10 mM sodium phosphate buffer, pH 7.0 removed excess glutaraldehyde. The amino groups of the self-assembled thiourea layer on the Au electrode got at this stage covalently linked to the glutaraldehyde molecules and, after being dried in a stream of N<sub>2</sub> gas, the electrode was prepared for the last reaction, namely the exposure to antibody of choice and final -CHO/-NH<sub>2</sub> crosslinking. To do so, 20 μL of 1 mg/mL antibody were placed on the surface of the Au electrode and -CHO/-NH<sub>2</sub> reaction was allowed to take place overnight at 4°C. As a last step in the preparation, covalently antibody-modified electrodes were placed for 20 min in a 10 mM ethanolic 1-dodecanethiol solution in order to cover remaining bare areas of the gold surface and create the well-insulated condition that is needed for success with a capacitive readout of antigen capture. Routinely, electrodes were kept at 4°C in a closed box filled with nitrogen gas, when not used for measurements.

Success with gold electrode cleaning and stable antibody modification was checked via voltammetric tests in 5 mM solutions of potassium ferricyanide in 100 mM KCl. Cyclic voltammograms of the aqueous Fe (III) redox species were recorded at the end of the each stage of electrode treatment with a scan range of +0.7 to -0.2 V vs. Ag/AgCl reference electrode and a scan rate of 0.1 V/s. Judgments on the quality of particular steps in the electrode preparation were possible by interpretation of the Fe (III) reduction current signatures, in terms of peak magnitude and position.

### **2.3.2.2 The workstation for flow-based capacitive YKL-39/40 immunosensing**

All measurements of YKL-39 and YKL-40 with a capacitive readout of antigen-antibody affinity binding were carried out in a flow injection system as illustrated on Figure 2.1. Working electrode in the electrochemical flow cell of the

arrangement was the antibody-modified gold electrode while the stainless steel tube liquid outlet of the flow-through electrochemical cell was connected to the potentiostat as the counter electrode. Placed opposite of the detecting disk of the immunosensor was a common Ag/AgCl reference electrode. The three-electrode electrochemical cell was operated by a computer-controlled potentiostat (EA 163/ED410, eDAQ, Australia), which was responsible for potential application, current measurements, and timely data acquisition and storage.

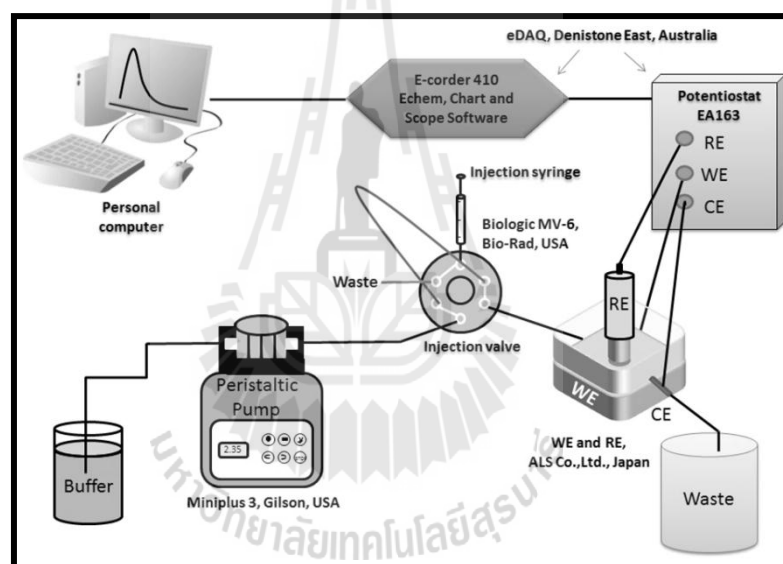


**Figure 2.1** Illustration of the equipment used for flow injection-based capacitive YKL-39/40 immunosensing.

### 2.3.2.3 YKL-39/40 measurements with capacitive YKL-39/40 immunosensor

The apparatus for capacitive YKL-39 and YKL-40 capacitive immunosensing has been detailed in the previous section. The capacitance of the electrode surface used a signal for analyte determination and, upon calibration, quantification, was computed from the current response of the corresponding

immunosensors induced by repetitively applied potential steps of 50 mV and a few ms length. For the type of sensors used here for analysis, the current actually decays exponentially and the drop can mathematically be expressed via Eq. 2.1:

$$i(t) = E/R_s \exp (-t/R_s C) \quad \text{Eq. 2.1}$$

where  $i(t)$  is the current in the circuit between the counter and working electrode as a function of time,  $E$  the potential applied to the immunosensor surface vs. the Ag/AgCl reference electrode,  $R_s$  the dynamic resistance of the immobilization layer,  $t$  the time that elapsed after the potential step was applied, and  $C$  is the total capacitance measured at the capacitive immunosensor electrode/solution interface. Taking the logarithm of Eq. 2.1 leads to

$$\ln i(t) = \ln E/R_s - (1/R_s C) t \quad \text{Eq. 2.2}$$

The value of the potential amplitude is known and the value of the y-intercept is provided by the software used to generate the linear least-square fitting of  $\ln i(t)$  versus  $t$ . Accordingly,  $R_s$ , can be computed and the obtained value further used to calculate the capacitance from the slope of the regression line. In a typical analytical trial, the potential pulses were executed once every minute while the running buffer went through the flow cell and the capacitance values, extracted from the acquired current traces as described above, were plotted as function of time. When a sample solution with analyte is injected into the flow line, the YKL-39 or YKL-40 molecules move downstream towards the electrochemical flow cell and the capacitive

immunosensor, where binding to the immobilized antibody happens on the gold electrode surface. As outlined earlier, the antigen capture is causing a decrease in capacitance; however, a stable value is reached at the point of maximum capture for a given concentration of analyte. The induced change in capacitance due to the antigen binding is gained by subtracting the capacitance after the binding events from its value before the binding (Chaocharoen *et al.*, 2015; Berggren *et al.*, 2001; Berggren and Johannsson, 1997 and Limbut *et al.*, 2006a, b). Since capacitance change is proportional to the concentration of antigen, calibration curves can be constructed in calibration trials and later used for analyte quantification in model or real samples quantification trials.

#### **2.3.2.4 Parameter optimization YKL-39/40 immunosensing**

All experimental parameters affecting the performance of the capacitive immunosensor were looked at and optimized to yield optimal analytical performance. Evaluated were type and concentration of regeneration solution, type of running buffer, pH of running buffer, concentration of running buffer, sample volume and flow rate. Optimization measurements were performed in triplicate by changing the variable under inspection while keeping all others fixed. When an optimum condition for the particular parameter was identified, the next parameter was made subject of optimization. The starting conditions for the optimization trials are shown in Table 2.1. The selection of the optimal value for a certain parameter took a good balance between the sensitivity of the measurement and the analysis time for individual samples into account.

**Table 2.1** Starting operational conditions.

<b>Parameter</b>	<b>Options</b>
<b>1. Type of regeneration solution</b>	low pH: HCl
<b>2. pH of regeneration solution</b>	pH 1.0
<b>3. Type of buffer</b>	sodium phosphate buffer
<b>4. pH of buffer</b>	pH 7.0
<b>5. Concentration of buffer</b>	10 mM
<b>6. Sample volume</b>	200 $\mu$ L
<b>7. Flow rate</b>	100 $\mu$ L/min

#### 2.3.2.4.1 Choice of the optimal type of the regeneration solution

One important issue for success with qualitative and quantitative immunosensor analysis is whether the surface can after exposure to one antigen binding run be regenerated without significant loss of activity (Thévenot, Toth, Durst *et al.*, 2001). Ideally, the regeneration of the working electrode should disrupt all antibody/antigen conjugates without adversely affecting the activity of the covalently immobilized antibody molecules and should also not destroy the self-assembled thiourea monolayer that provides the firm antibody bond to the gold surface. Gentle but effective regeneration allows immunosensor surfaces to be reused for quantification trials many times, saving both time and money (van der Merwe, 2000).

Following suggestions from published reports, the regeneration solutions tested in this work were divided into three categories, namely a high ionic strength solution (Pei, Cheng, Wang *et al.*, 2001), a low pH solution (Chou, Hsu, Hwang *et al.*,

2002), and high pH solution (Park, Kim, and Kim, 2000). The particular choices were actually 1 M NaCl or 1 M KCl (high ionic strength), Glycine/HCl pH 2.5 and HCl solution of pH 1.0 or 2.0 (low pH) and 5 mM or 50 mM NaOH (high pH).

Using the conditions 3 – 7 in Table 2.1 for other parameters than the type of the regeneration solution, small aliquots of a standard solution of the two human chitinase-like proteins were injected in course of the optimization trials into the capacitive immunosensor system and via the continuous flow of buffer transported into the flow cell of the detection system. Upon arrival, binding between the antigens and their corresponding immobilized antibody happened and caused the analytically relevant decreases in sensor capacitance. The different regeneration solutions were then affected and used to break the antigen-antibody bond and force antigen to be flushed away in the flowing stream of the running buffer. A good regeneration solution was expected to let the sensor capacitance return to baseline level (the one before sample injection) in order to prepare the sensing tool for the next sample injection (Figure 2.2). An optimal regeneration solution would reproducibly reestablish the starting sensor surface condition by removing all captured antigen and restoring the original capacitance signal of the modified electrode before any antigen exposure effectively. The optimum regeneration solution was selected by considering the quality of the restored activity of modified electrode after regeneration. The percentage of residual activity is calculated from the capacitance change ( $\Delta C$ ) resulting from the binding between antigen-antibody before ( $\Delta C_1$ ) and after regeneration ( $\Delta C_2$ ), as described by Figure 2.2 and Eq. 2.3. Based on this definition, an ideal 100% restored activity refers to the situation where the capacitances of the immunosensor before sample injection and after regeneration were

absolutely the same. However, the regeneration was capable to restore the capacitance of the immunosensor surface to values above 90%, the binding efficiency can be considered as suitable (van der Merwe, 2000). Chosen of course for the analytical applications to the quantification of model and real samples here was the regeneration buffer with the highest value of the percentage of restored activity.

$$\% \text{ restored activity} = (\Delta C_2 / \Delta C_1) \times 100$$

**Eq. 2.3**

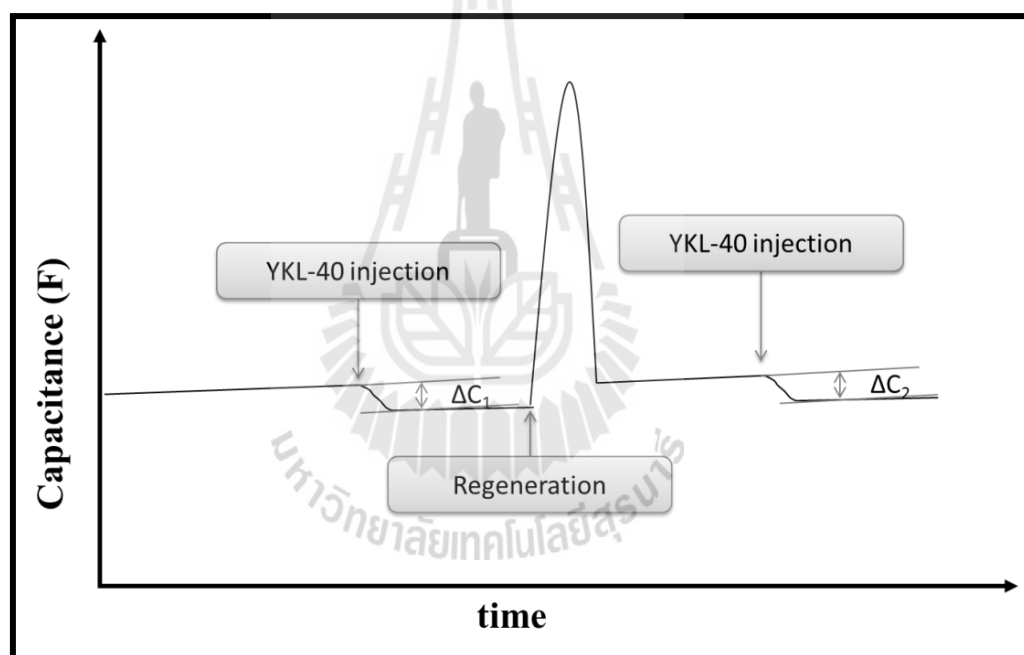


**Figure 2.2** A schematic diagram showing the capacitance change caused by binding between antigen and antibody following an YKL-39/40 protein sample injection. Injection of regeneration solution removes bound antigen from antibodies immobilized on gold electrode surface. When the base-line signal is recovered a new analysis cycle can be applied.

#### **2.3.2.4.2 Choice of the optimal pH of the regeneration solution**

The regeneration conditions could affect the performance and the lifetime of completed immunosensors because the antigen-antibody conjugation has to be broken and, as side effect, the antibody bond to the self-assembled thiol layer and/or the attachment of the thiol layer to the gold electrode surface may be weakened and/or even destroyed, too. In addition to the type of regeneration solution also the best level of acidity (pH) of the regeneration solution was tested in order treat in gentle but effective way with the reach of high percentage of restored activity. Tested here were HCl solutions with a pH of 3.0, 2.5, 2.0, 1.5, and 1.0.

#### **2.3.2.4.3 Choice of the optimal type of running buffer**

It is essential to find the best type of the running buffer solution that is continuously guided through the electrochemical flow cell of the capacitive immunosensor system. Based on experiences reported by others for similar immunosensing schemes, the buffers that have been explored here included 10 mM of sodium phosphate buffer, 10 mM of HEPES buffer and 10 mM Tris-HCl buffer at pH 7.0 (Loyprasert, Thavarungkul, Asawatreratanakul *et al.*, 2008). Measured in the trials were the concentration-dependent responses of the YKL39/40 protein-modified gold electrodes to their corresponding analyte levels over a range of 1 ng/L to 100 mg/L. The sensitivity (slope) of the linear part of plots between capacitance change and logarithm of trialed antigen concentration was used as guiding criteria for the selection of the most suitable running buffer, which was then further optimized in terms of pH and ionic strength (Bezerra, de Lima Filho, Montenegro *et al.*, 2003).

#### **2.3.2.4.4 Choice of the optimal sample volume and flow rate**

In the applied flow injection-type of YKL-39/40 protein analysis the volume of the sample that was injected into the stream of running buffer and also the flow rate for the running buffer were expected to have an effect on the quality level of the analyte quantification. Larger volumes would expose the sensor in a measuring run to more antigen molecules and saturation of the limited number of antibody entities may have been reached at lower concentration; variation of the flow rate would, on the other hand, affect the time available for the formation of the antibody/antigen conjugation. Both mentioned parameter would logically affect the linear range and/or sensitivity of the chosen detection scheme. Test trials were thus executed with sample injections ranging from 50, 100, 150, 200, 250, 300 to 400  $\mu\text{L}$  and with flow rates of 50, 100, 150, 200, 300 and 400  $\mu\text{L}/\text{min}$ .

#### **2.3.2.4.5 Summary of the performed optimization trials**

The parameters to be optimized and the explored settings are summarized in Table 2.2. With the optimal parameter applied, the analytical performance of the system was evaluated and the limit of detection, linear range, sensitivity, specificity and reducibility for both the YKL-39 and YKL-40 capacitive immunosensor analysis was assessed.

**Table 2.2** Target parameters for human chitinase-like proteins immunosensor optimization trials.

Parameter	Options
<b>1. Type of regeneration solution</b>	high ionic strength, low pH, high pH
<b>2. pH of regeneration solution</b>	pH 1.0, 1.5, 2.0, 2.5, 3.0 and 3.5 10 mM of sodium phosphate buffer, pH 7.0
<b>3. Type of running buffer</b>	10 mM of HEPES buffer, pH 7.0 10 mM of Tris-HCl buffer, pH 7.0
<b>4. pH of running buffer</b>	pH 6.0, 6.5, 7.0, 7.5, and 8.0
<b>5. Concentration of running buffer</b>	5, 10, 25, 50, and 100 mM
<b>6. Sample volume</b>	50, 100, 150, 200, 250, 300 and 400 $\mu$ L
<b>7. Flow rate</b>	50, 100, 150, 200, 300 and 400 $\mu$ L/min

#### 2.3.2.5 Stability and selectivity tests with YKL-39/40 immunosensors

All organic, biological and other materials used for sensor construction may be prone to deterioration with time, especially when used in continuous flow of measuring buffer and with repetitive changes of exposures to running and regeneration buffers and sample solutions. Degradation (denaturation) is through environmental stress is obviously a major risk for the biological protein (antibody) component of the employed immunosensor and limited sensor lifetimes may thus be likely and would call for frequent sensor replacements (Eggins, 1996).

Under identified optimum analysis condition the stability of immobilized electrode was studied by repetitive injections of standard solution of the two targeted

YKL-39/40 proteins into the immunosensor system and sequences of detection and sensor regeneration. Identified and used as hint of the sensor stability was the number of injections that could be done with the response of the immunosensor system remaining at a percentage of restored activity above 95%.

Selectivity tests were carried out to get an idea how reliably the target analytes could be detected in the presence of possibly interfering species that are structurally and/or chemically similar to the proteins of interest. Relevant interferences for this work were other members of the family GH-18 proteins, namely YKL-39 (for YKL-40 analysis), YKL-40 (for YKL-39 analysis), and AMCcase (for both analyses). Standard solutions of YKL-39, YKL-40 and AMCcase with concentrations of 1 ng/L to 100 mg/L were analyzed in triplicate with the proposed methodology in the capacitive immunosensor system, under the optimum conditions. Obtained calibration curves of each protein were plotted and compared.

#### **2.3.2.6 Limit of detection (LOD)**

The limit of detection is defined as the amount or the content of an analyte corresponding to the lowest measurement signal which with a certain statistical confidence may be interpreted as indicating that the analyte is present in the solution/analytical sample, but not necessarily allowing exact quantification (AOAC, 2004). Limit of detection can be calculated using follow equation:

$$\text{LOD} = (3 \times \text{SD}_b)/m \qquad \text{Eq. 2.4}$$

where LOD is limit of detection,  $SD_b$  is the standard deviation of 20 measurement of blank results and  $m$  is the slope of the calibration curve.

The running buffer was injected into capacitive immunosensor system for twenty times under the optimum conditions. The standard deviation was calculated. The slope of the calibration curve obtained from the injection of standard solution of YKL-39/40 at concentration between 0.1  $\mu\text{g/L}$  and 1  $\text{mg/L}$  into the capacitive immunosensor system in triplicate under the optimum conditions. The limit of detection was then calculated using Eq. 2.4.

#### **2.3.2.7 Determination of YKL-39/40 in model and clinical samples**

To demonstrate the use of the developed capacitive immunosensor, the system was tested for model and clinical samples. The latter were for YKL-40 trials derived from blood samples of a healthy person and breast cancer and glioblastoma patients and for YKL-39 represented the synovial fluids of people with recognized appearance of osteoarthritis. All samples were determined by the capacitive immunosensor system and, for comparison, via application of the common ELISA technique.

##### **2.3.2.7.1 Model samples**

To demonstrate the quality of the established YKL-39/40 capacitive immunosensing in a flow injection system, standard solutions of the two proteins were injected at various but known concentrations and determined with the scheme operated under optimum conditions. Prior to triplicate sample analysis, the calibration curves were prepared as plots of the capacitance change versus log of the analyte

concentration. The value of the capacitance change for a particular sample was used to compute their protein content from the predetermined calibration curve. This allowed calculation of the percentage of recovery of analyte by the follow equation Eq. 2.5:

$$\text{Recovery (\%)} = (C_{\text{Found}} / C_{\text{Added}}) \times 100 \quad \text{Eq. 2.5}$$

#### 2.3.2.7.2 Clinical samples

For YKL-40 capacitive immunosensors, a set of clinical blood samples and two types of cell lysates were analysed under optimum conditions for their relevant protein content. The blood serum came actually from 4 healthy persons (in the following labeled as H1-H4), 5 breast cancer patients (in the following labeled as B1-B5), and 4 Glioblastoma patient (in the following labeled as G1-G4) while cell lysates were from THP-1 and 293T cells. Prior to the triplicate analytical immunosensor and ELISA trials, serum samples were routinely diluted 10 times with the standard running buffer to reduce the matrix effect. The change in the capacitance of particular samples was used to calculate the concentration of YKL-40 from predetermined calibration curves. Compared were the blood serum and cell lysate levels of YKL-40 from the immunosensor measurements with the outcome of the ELISA.

For YKL-39 capacitive immunosensors, the clinical samples and cell lysate that were tested under optimum conditions included four synovial fluids from osteoarthritis patient, a Jurkat cell lysate, a U937 cell lysate and a 293T cell lysate. All samples were in a parallel approach also inspected via an ELISA. Prior to triplicate quantification trials, the serum samples were diluted 10 times with running

buffer to reduce matrix effects and signal disturbance by other (proteins) species. The capacitance change of a particular sample was translated into an analyte concentration via calibration curve utilization. Values from the electrochemical YKL-39 screen were compared with the ones from the ELISA.



## CHAPTER III

### RESULTS

#### 3.1 Capacitive immunosensor for detection of bYKL-40

##### 3.1.1 Expression and purification of YKL-40 in bacteria system (bYKL-40)

The full-length YKL-40 DNA was cloned into pQE-Tri System expression vector, which was ready to be expressed in *E. coli* strain M15 (pREP). The recombinant protein was expressed with the 21-amino acid *N*-terminal signal sequence attached, to aid protein targeting to the bacterial cell envelope and His<sub>8</sub>-tagged at *C*-terminal. The bYKL-40 with signal peptide contains 381 amino acid residues and has a predicted MW of 42,338 Da.

Recombinant YKL-40 was expressed in *E. coli* strain M15 (pREP). Induction for 16 hr. with 0.5 M IPTG, cell pellet was collected and bYKL-40 was extraction by lysis buffer (Figure 3.1, Lane 1), the bulk of the induced bYKL-40 was insoluble that suggest the bYKL-40 was present in inclusion bodies. The insoluble fraction further solubilized with 8 M urea that fraction were contained bYKL-40 (Figure 3.1, Lane 2). 12% SDS-PAGE analysis revealed several protein bands. To obtain highly purified bYKL-40 for antibody production and immunosensing preparation, the soluble bYKL-40 fraction was further purified by Ni-NTA affinity column. Figure 3.2 shows the 12% SDS-PAGE of the purified protein, which migrated as a single band around 40 kDa (Lane 5), consistent with molecular mass expected for bYKL-40 lacking the 20 amino-acid signal peptide and has a predicted MW of 40,488 Da.

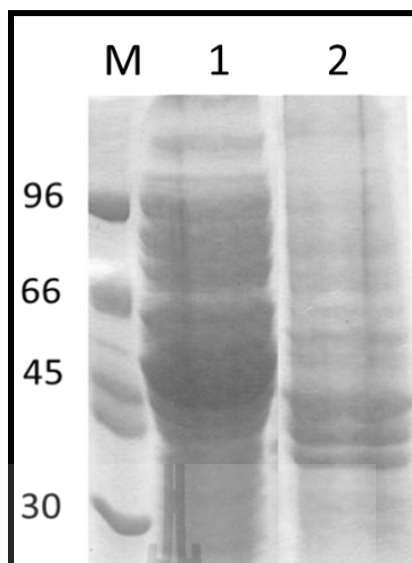


**Figure 3.1** SDS-PAGE analysis of bYKL-40 expression. Lane M, protein marker; Lane 1, bYKL-40 expression in cell pellet extracted with lysis buffer; Lane 2, YKL-40 expression in cell pellet extracted with 8 M urea.

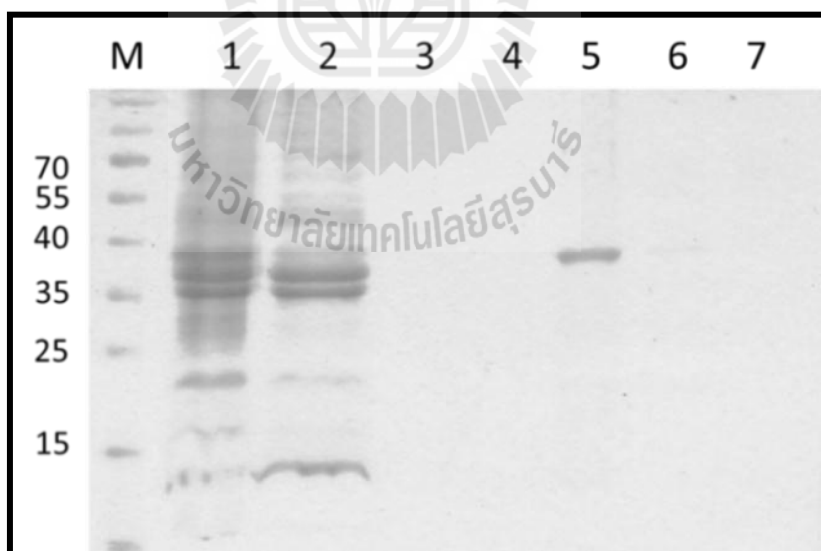


**Figure 3.2** SDS-PAGE analysis of bYKL-40 purification by Ni-NTA agarose column. Lane M, protein marker; Lane 1, soluble bYKL-40 fraction; Lane 2, Flow through; Lane 3, wash fraction with 10 mM imidazole; Lane 4, wash fraction with 20 mM imidazole; Lane 5-7, eluted fractions with 250 mM imidazole.

### 3.1.2 Production and characterization of bYKL-40 polyclonal antibody

Purified bYKL-40 protein was used for the production of bYKL-40 polyclonal antibody. The polyclonal anti-bYKL-40 antiserum and antibody titers were determined by western blot assay (Figure 3.3). The polyclonal anti-bYKL-40 antiserum reacted strongly with the bYKL-40 target protein at dilutions up to 1:80,000 and a faint signal was detectable even at 1:160,000 dilutions. In contrast, no signal was detected from the pre-immune serum, even at the highest concentration tested (1:5,000 dilutions). Evaluations of cross-reactivity against other members of GH-18 were tested by western blot assay at 1:40,000 dilutions of polyclonal anti-bYKL-40 antiserum. Western blots analysis (Figure 3.4A and B) revealed no interaction of the polyclonal anti-bYKL-40 antiserum with YKL-40 homologues, such as YKL-39, AMCase and chitinase A. These results confirming that polyclonal anti-bYKL-40 antiserum was specific for bYKL-40.

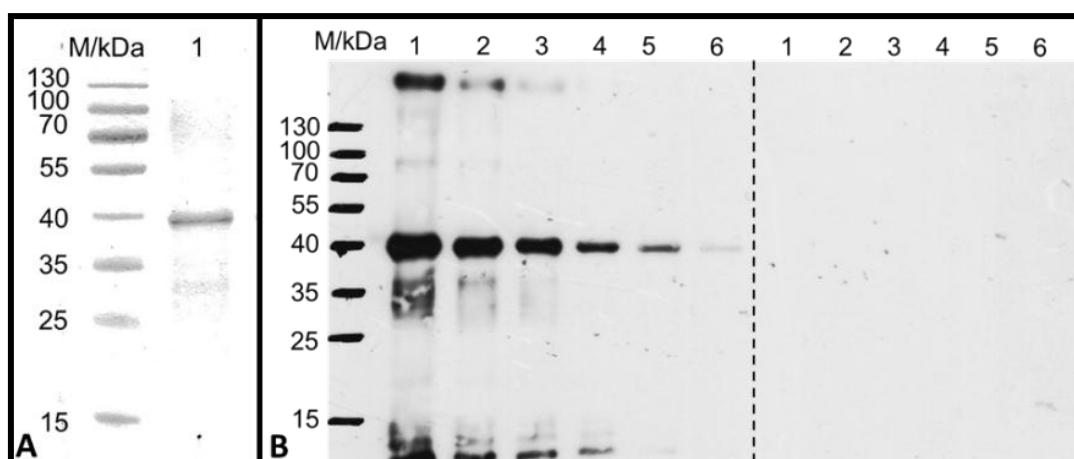


**Figure 3.3** Polyclonal anti-bYKL-40 antiserum titer. (A) 12% SDS-PAGE, coomassie-blue stained: Lane 1, 2  $\mu$ g of purified bYKL-40. (B) bYKL-40 protein detected by western blot assay with the polyclonal anti-bYKL-40 antiserum (left-hand panel). Lane M, standard protein markers; Lane 1–6, 2  $\mu$ g of purified bYKL-40 detected with various dilutions (1:5,000, 1:10,000, 1:20,000, 1:40,000, 1:80,000 and 1:160,000) of polyclonal anti-bYKL-40 antiserum. The same dilutions of pre-immune serum were used as negative control (right-hand panel).

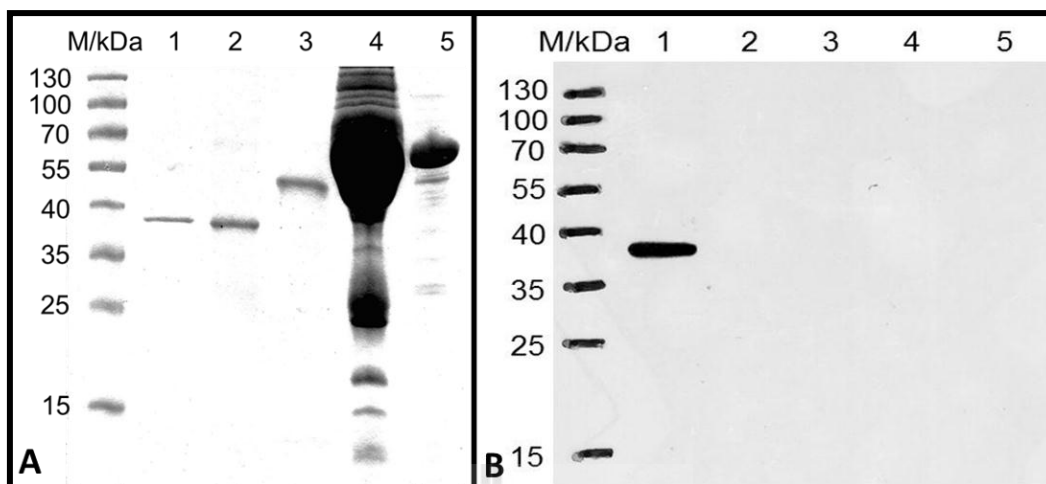


**Figure 3.4** Specificity of polyclonal anti-bYKL-40 antiserum. (A) Coomassie-blue stained 12% SDS-PAGE. (B) Immunoblot with polyclonal anti-bYKL-40 antiserum (1:40,000 dilution); pre-immune serum was used as a negative control (not shown). Lane 1, purified bYKL-40 (1.2  $\mu$ g); Lane 2, YKL-39 (3.2  $\mu$ g); Lane 3, AMCase (2.9  $\mu$ g); Lane 4, human serum (231  $\mu$ g) and Lane 5, chitinase A (10.4  $\mu$ g).

The polyclonal anti-bYKL-40 antiserum was fractionated by affinity chromatography using protein A agarose column run under gravity. SDS-PAGE analysis (Figure 3.5A) showed the purity of the anti-bYKL-40 polyclonal antibody, and confirmed that it was a protein A-specific IgG isotype. The immunoglobulin migrated above the 130 kDa marker under non-reducing condition (Figure 3.5A, Lane 2), while reducing condition the sample produced two protein bands, of about 55 kDa and 22 kDa (Figure 3.5A, Lane 1), as expected for IgG (heavy chain; 50 kDa, light chain; 25 kDa) and whole molecule; 150 kDa. In Western blot analysis the purified anti-bYKL-40 polyclonal antibody reacted strongly with bYKL-40 down to 0.175 mg/L, whereas the pre-immune serum showed no reaction (Figure 3.5B).

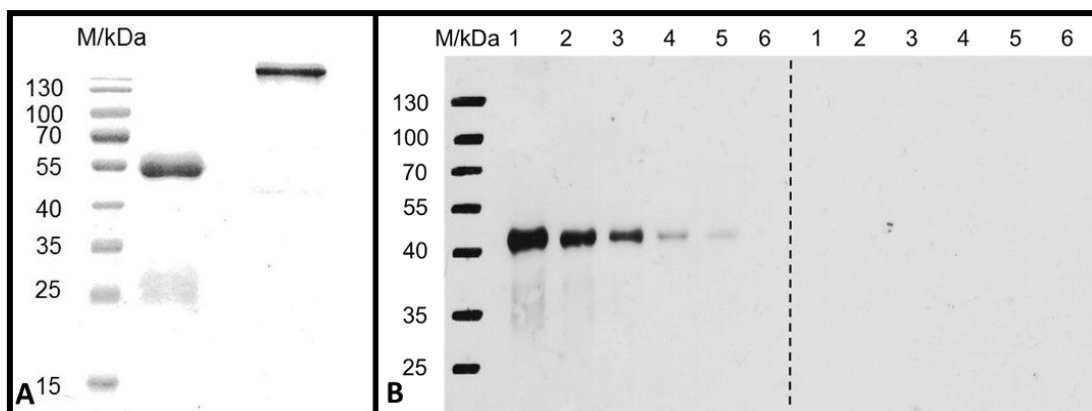


**Figure 3.5** Purified anti-bYKL-40 polyclonal antibody. (A) SDS-PAGE analysis of purified anti-bYKL-40 polyclonal antibody: Lane 1, under reducing condition; Lane 2, non-reducing condition: coomassie-blue stained gel. (B) Antibody titers against bYKL-40 (2 µg): Lane M, standard protein markers; Lane 1–6, serial dilutions of the purified antibody to 2, 1, 0.500, 0.250, 0.175 and 0.078 mg/L, respectively (left-hand panel). Unfractionated pre-immune serum was used as a negative control (right-hand panel).

Cross-reactivity of the purified anti-bYKL-40 polyclonal antibody with related proteins was tested by indirect ELISA technique. Figure 3.6 shows binding of purified anti-bYKL-40 polyclonal antibody (50 µL, 15.6 µg/L) to bYKL-40 (curve a); the hyperbolic plot of the interaction signal with increasing antigen load in the microtiter plate well was characteristic of a specific interaction. With YKL-39 (curve b), AMCcase (curve c) and chitinases A (curve d), no significant signal was obtained. The binding of each antigen was further tested with a fixed antigen load (50 µL, 125 µg/L) and constant anti-bYKL-40 polyclonal antibody (50 µL, 15.6 µg/L). A summary of this test is shown in Table 3.1. The signal for bYKL-40 was about 11-, 12.5- and 50-fold larger than that for YKL-39, AMCcase and chitinases A, respectively.

The ELISA showed a linear range from 2.5 to 125  $\mu\text{g/L}$  (Figure 3.6, inset). The linear regression equation is  $y = (0.008 \pm 0.001) x + (0.101 \pm 0.005)$  and correlation coefficient was 0.997. The lower limit of detection was 2.5  $\mu\text{g/L}$ .

These results confirmed that the purified anti-bYKL-40 polyclonal antibody was highly specific for bYKL-40 target protein and thus suitable for use in bYKL-40 capacitive immunosensor based flow injection system.

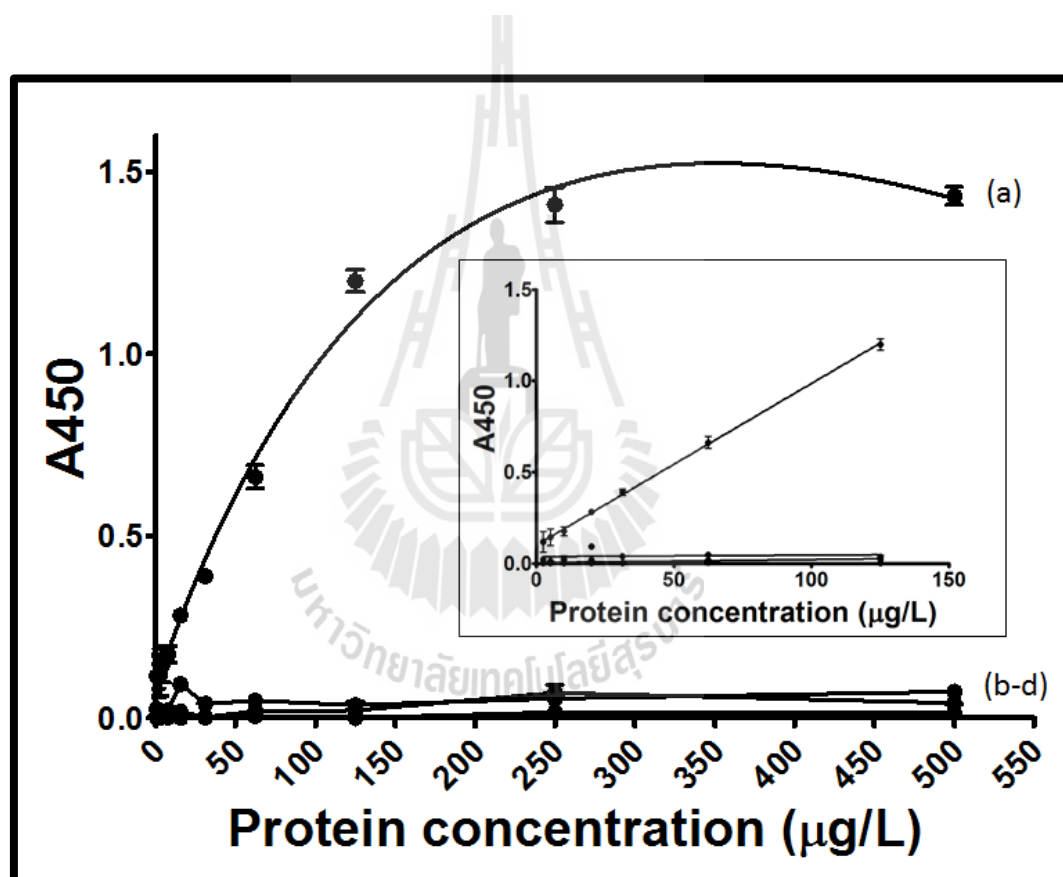


**Figure 3.6** bYKL-40 ELISA technique. Binding of purified anti-bYKL-40 polyclonal antibody (50  $\mu\text{L}$ , 15.6  $\mu\text{g/L}$ ) to different concentrations of surface-attached bYKL-40 related proteins: bYKL-40 (a); YKL-39 (b); AMCase (c) and chitinases A (d). Inset shows the calibration curve of bYKL-40 obtained from the ELISA technique.

**Table 3.1** Interaction of bYKL-40 and its homologues with purified anti-bYKL-40 polyclonal antibody.

	$A_{450}$ **	Reactivity***
<b>bYKL-40*</b>	1.17±0.03	1.00
<b>YKL-39*</b>	0.10±0.01	11.63
<b>ChiA*</b>	0.02±0.02	54.05
<b>AMCase*</b>	0.09±0.01	12.41

\* ELISA used a well load of 50  $\mu$ L of 125  $\mu$ g/L antigen and 50  $\mu$ L of 15.6  $\mu$ g/L antibody aid affinity testing.

\*\* ( $A_{450}$ ) is the absorbance at wavelength of 450 nm.

Values are averages of triplicate measurement.

\*\*\* Values normalized against bYKL-40.

### 3.1.3 Capacitive bYKL-40 immunosensing

#### 3.1.3.1 Preparation of the capacitive bYKL-40 immunosensors

For capacitive immunosensors the insulating property of the self-assembled monolayer on the electrode surface is of vital importance. To investigate the gradual change of the electrical conductivity a bare gold disk electrode in course of the transition into a bYKL-40 capacitive immunosensor via thiol layer placement and subsequent covalent antibody immobilization cyclic voltammetry measurements were performed at different stages of the electrode modification in a 5 mM  $K_3[Fe(CN)_6]$ /0.1 M KCl solution at a scan rate of 0.1 V/s vs. Ag/AgCl reference electrode, with the voltage varied from +0.7 to -0.2 V. The acquired collection of

voltammograms of such an electrode test trial is shown in Figure 3.7. At the clean gold disk electrode surface (curve a), the redox compound produced the expected pair of cathodic and anodic current peaks that relate to the reduction of Fe (III) to Fe (II) in the forward potential scan and subsequent re-oxidation of the Fe (II) to Fe (III) in the reverse potential scan. The magnitude of the two redox peaks decreased considerably upon placement of the self-assembled layer of thiourea since the molecular electrode coating is non-conductive and block the electron-transfer interaction of the Fe (III) in the solution with the charged gold disk (curve b). When glutaraldehyde was allowed to react with the amine groups of the thiourea and then anti-bYKL-40 was linked covalently on the electrode via reaction with of surface-bound remaining aldehyde groups with amine groups in the antibody structure, the insulating property of the gold electrode surface further decreased for the same reason as in the initial step of thiol monolayer formation (curve c and d, respectively). Finally, the modified electrode surface was exposed to a short treatment with 1-dodecanethiol in order to let this small thiol cover any still uncovered gold surface via self-assembly and establish complete insulation; evidence for the gain of a well-insulated bYKL-40 modified gold disk electrode (“the bYKL-40 capacitive immunosensor”) it that the current peaks virtually disappear fully (curve e).

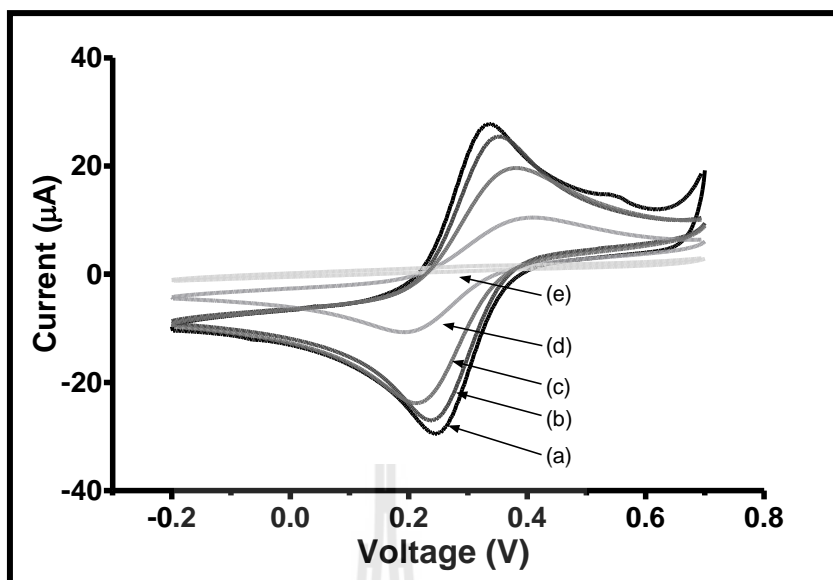


**Figure 3.7** Cyclic voltammograms of a gold electrode at various surface conditions. (a) clean (b) coated with a self-assembled thiourea monolayer, (c) after glutaraldehyde exposure of the thiourea film, (d) after anti-bYKL-40 bonding to the glutaraldehyde-treated thiourea film and (e) after final treatment with 1-dodecanethiol.

### 3.1.3.2 Parameter optimization for capacitive bYKL-40 immunosensing

The experimental parameters possibly influencing the performance of the bYKL-40 capacitive immunosensor included the type and pH of the regeneration solution, the type, concentration and pH of the running buffer, the injected sample volume and the flow rate, and they were all optimized to reach a satisfactory level of YKL-40 in model and real samples. In each optimization test the capacitance changes of bYKL-40 capacitive immunosensors, following either individual or sequential multiple injections of 10 µg/L of bYKL-40 were evaluated as earlier described through an analysis of the recorded current response to ms-long potential steps. All measurements were executed in triplicate, with one parameter varied while the others ones were fixed. The starting operational conditions for the optimization trials are

shown in Table 2.1, Chapter II, Section 2.3.2.4. The following sections present the results of the parameter optimization, starting with the adaptation of the regeneration buffer and finishing with an adjustment of the flow rate.

### 3.1.3.2.1 Optimization of the regeneration solution

Injection of 10  $\mu\text{g/L}$  of standard bYKL-40 solution caused antigen conjugation to antibody on the sensor surface, producing a capacitance change. The modified surface had to be regenerated by the removal of bound bYKL-40 before the measurement of the next sample was possible. Since the affinity binding of bYKL-40 and immobilized anti-bYKL-40 is of non-covalent nature the complex was liable to dissociation through exposure to a regeneration solution that was in support of bond weakening and release of antigen that then could be flushed away by the stream of the buffer. The efficiency of the tested regeneration solutions was determined by a calculation of a restored activity of the immobilized anti-bYKL-40, as it was described in Eq. 2.3 in Chapter II, Section 2.3.2.4.1.

Three types of regeneration solutions were studied including neutral solutions of high ionic strength (1 M KCl, 1 M NaCl) or high (5 or 50 mM NaOH) and low pH (50 mM glycine/HCl buffer, pH 2.5 and HCl solution, pH 1.0). The results in terms of the gained clearance of the antibody from bound antigen are for the set of regeneration tests shown in Figure 3.8. Treatment of used immunosensors with neutral solutions of high ionic strength (1 M KCl, 1 M NaCl) gave actually the lowest percentage of restored activity ( $24.5 \pm 2.1$  and  $12.4 \pm 1.3$ , respectively) and high pH (5 or 50 mM NaOH) produced rather low percentage of restored activity values ( $30.3 \pm 0.6$  and  $40.7 \pm 0.1$ , respectively), too. Better was regeneration in acidic

regeneration solutions such as 50 mM glycine/HCl buffer, pH 2.5 and HCl solution, pH 1.0. Here percentages of restored activity were  $59.1\pm 1.4$  and  $67.5\pm 0.2$ , respectively. Accordingly, regeneration with HCl solution of pH 1.0 was the most effective treatment because it offered the highest percentage of restored activity.

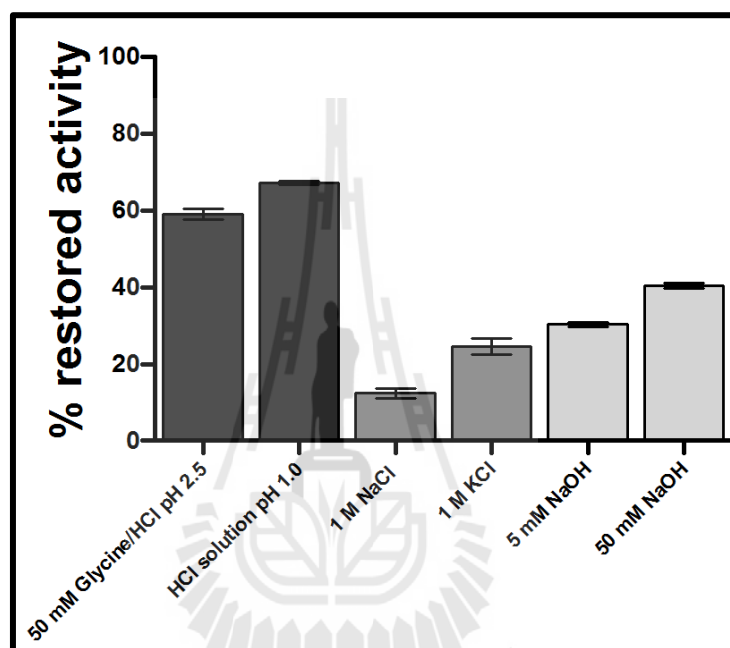


**Figure 3.8** Efficiency of different types of regeneration solutions. Percentage of restored activity is an expression that scales the amount of immobilized bYKL-40 antibody that got released from bYKL-40 antigen that had been captured in course of a measurement cycle; the higher the percentage of residual activity, the more antibody was freed and successfully primed for capturing antigen again in the next analytical sample injection run.

The effect of pH of HCl solution was then studied for values of 1.0, 1.5, 2.0, 2.5 and 3.0. The percentage of restored activity increased from  $80.1\pm 0.9$  to  $99.4\pm 0.5$  when the pH was decreased from 3.0 to 2.5 (Figure 3.9). At a pH lower than

2.5, the percentage of restored activity decreased, which may be because of a destructive impact of such a strong acid on either the self-assembled thiourea monolayer or the antibody, or both. Based on the above, the HCl solution, pH 2.5 offered the best regeneration with the recovery of antibody approaching an almost ideal 100%. This solution was thus used as the regular regeneration solution in all subsequent optimization trials and all other analytical bYKL-40 quantifications.

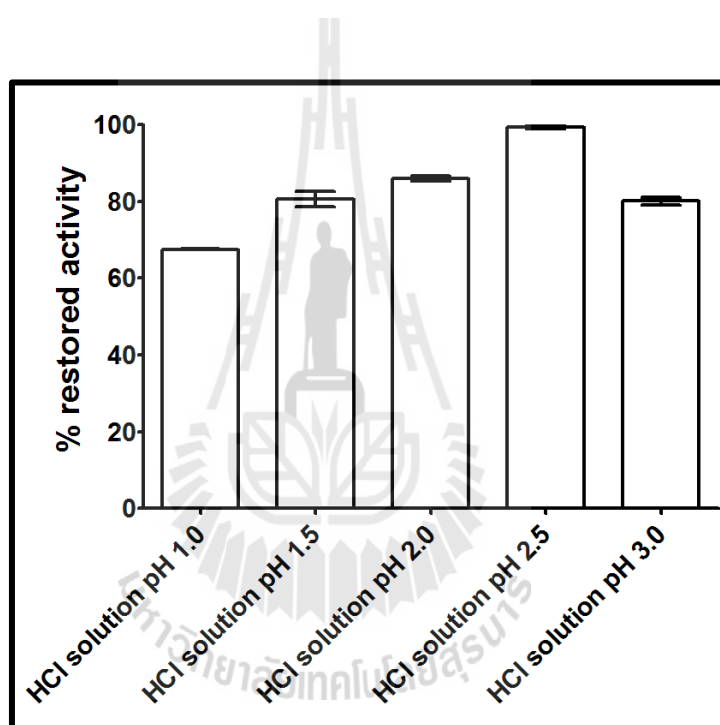


**Figure 3.9** The influence of the pH of the HCl regeneration solution on the efficiency of removal bYKL-40 from anti-bYKL-40 on a thiol-coated gold electrode.

### 3.1.3.2.2 Optimization of the type of running buffer

The running buffer in the flow analysis system is at the same time the electrolyte in the electrochemical flow cell during the potential step-based capacitance measurements. It was therefore expected that the nature of the running buffer would affect the quality of a capacitive signal generation. Three types of running buffer

solutions, each with pH 7.0 and 10 mM of buffer concentration were tested as the constantly flowing liquid in the tubes of the flow system, namely sodium phosphate, HEPES and Tris-HCl buffers. A look at the sensitivity (slope) of plots between capacitance change in response to antigen injections and the logarithm of its concentration in the linear range (0.1  $\mu\text{g/L}$  to 1 mg/L, Figure 3.10) showed that 10 mM sodium phosphate buffer, pH 7.0 provided the highest sensitivity value and, for given injections, the largest specific capacitance changes. Therefore this type of buffer was used as the standard running solution for all work with the bYKL-40 capacitive immunosensors.

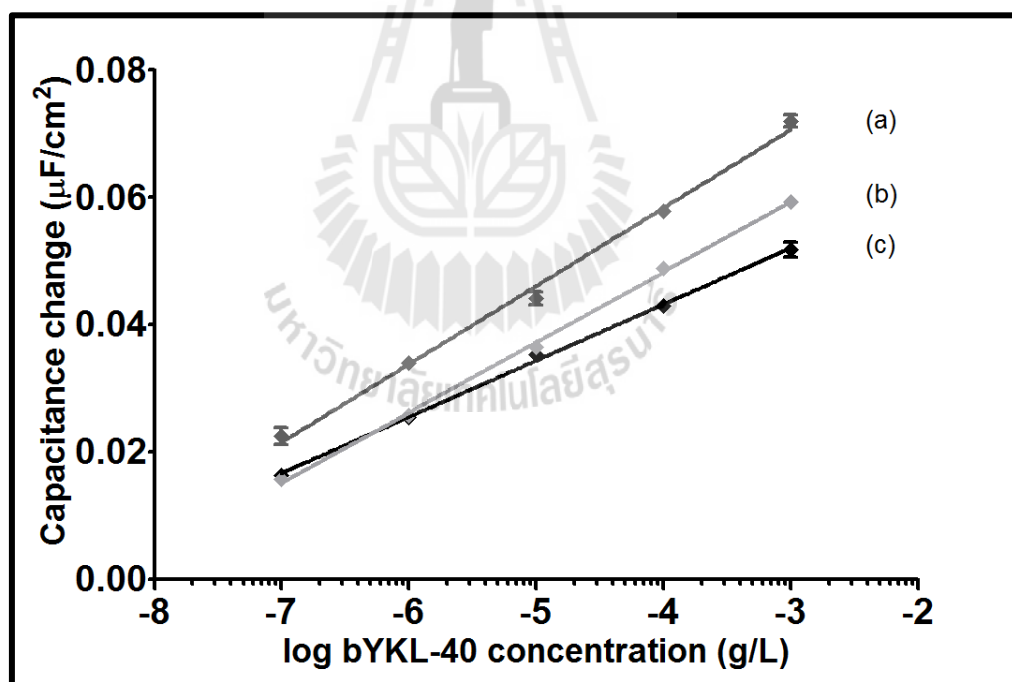


**Figure 3.10** The efficiency of bYKL-40 capacitive immunosensors for different types of running buffer. (a) 10 mM sodium phosphate buffer, pH 7.0; (b) 10 mM HEPES buffer, pH 7.0; (c) 10 mM Tris-HCl buffer, pH 7.0.

### 3.1.3.2.3 Optimization of the pH of sodium phosphate-based running buffer

The influence of pH during the binding reaction was studied between 6.5 and 8.0 for the fixed concentration of bYKL-40 (10  $\mu\text{g/L}$ ) in 10 mM sodium phosphate buffer of different pH (6.5, 7.0, 7.5, and 8.0). Figure 3.11 shows that the change of capacitance increased with a move in pH from 6.0 to 7.0 and then decreased as the pH increased further. This suggested that the response of capacitive bYKL-40 immunosensors in terms of a capacitance change due to antigen-antibody binding was maximal at pH 7.0. Accordingly, the sodium phosphate buffer was routinely adjusted to pH 7.0.

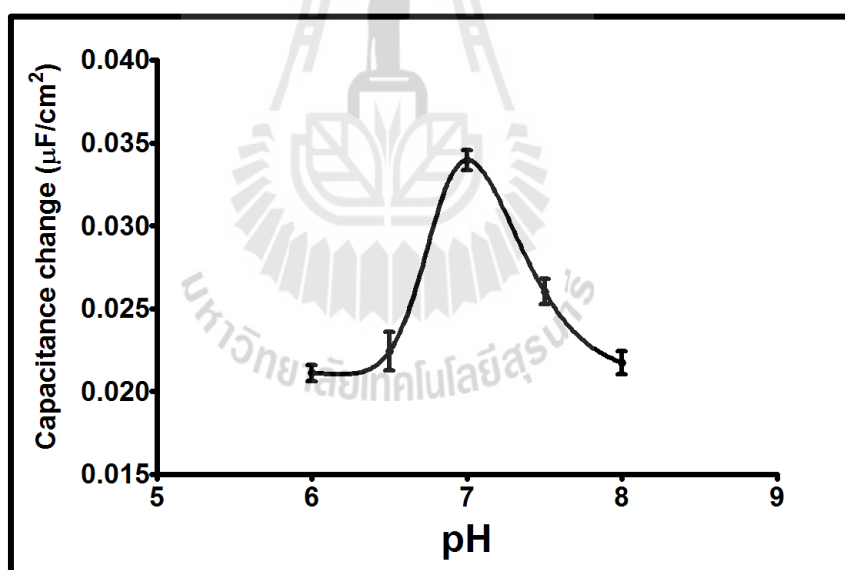


**Figure 3.11** The efficiency of capacitive bYKL-40 immunosensors for applications with 10 mM sodium phosphate running buffer at different pH.

### 3.1.3.2.4 Optimization of the concentration of the running buffer

The ionic strength of a buffer increases with its salt concentration and the ionic strength were expected to influence the non-covalent antigen-antibody binding

and hence capacitive signal generation for the chosen type of immunosensor. In view of that 5, 10, 50 and 100 mM sodium phosphate running buffer solutions, pH 7.0 were tested in analytical runs for samples with the same level of bYKL-40 (10  $\mu\text{g/L}$ ) and the observed capacitance changes to bYKL-40/anti-bYKL-40 conjugation were compared. The outcome is shown in Figure 3.12, which provides the evidence that the change in sensor capacitance upon sample injection got bigger when moving from 5 to 10 mM buffer salt concentration and then decreased with a further salt level raise. The highest signal, under otherwise identical conditions, was clearly observed for the 10 mM sodium phosphate running buffer, pH 7.0 and this solution was thus chosen for quantitative analysis with the developed capacitive bYKL-40 immunosensing.

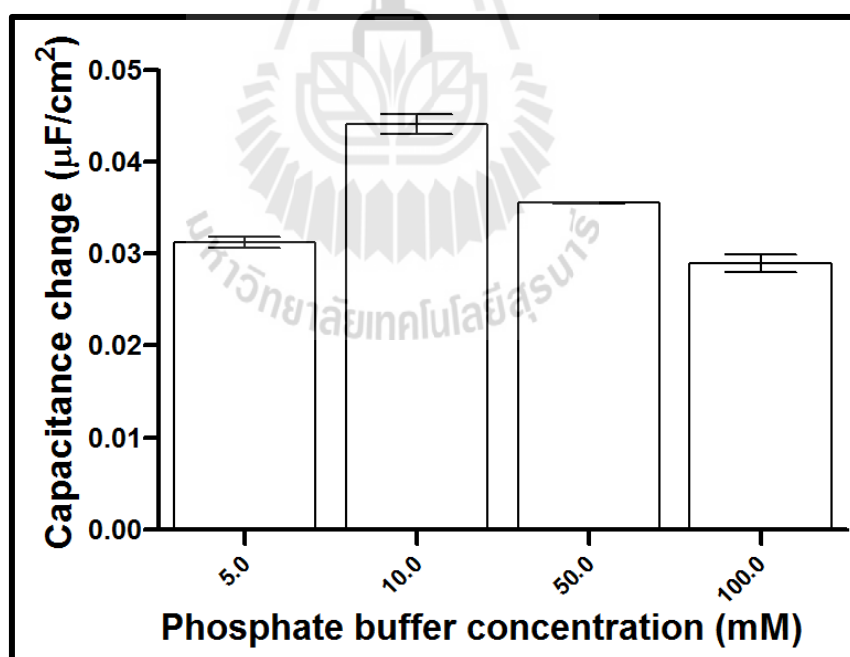


**Figure 3.12** The dependence of the efficiency of bYKL-40 quantification on different salt concentrations of the sodium phosphate buffer, pH 7.0.

### 3.1.3.2.5 Optimization of the flow rate

In a flow injection capacitive immunosensor system the flow rate of the running buffer passing through the electrochemical flow cell is a main factor affecting the yield of interaction between bYKL-40 and immobilized anti-bYKL-40. For a given sample injection, choice of a faster (slower) flow rate will correspond to a shorter (longer) time given for antigen capture and smaller (larger) immunosensor capacitance changes are the result of the variation. Thus, an adaptation of the parameter is providing a chance for signal optimization. The result of a capacitive bYKL-40 immunosensing with flow rates of 50 to 400  $\mu\text{L}/\text{min}$ , worked with for bYKL-40 injections of 10  $\mu\text{g}/\text{L}$  in 10 mM sodium phosphate buffer, pH 7.0, confirmed this expectation (Figure 3.13). The lowest flow rate of 50  $\mu\text{L}/\text{min}$  offered for the bYKL-40 antigen the maximum time for finding of and binding to its conjugation partner anti-bYKL-40 on the gold electrode and indeed produced the highest change in specific capacitance. And the signal decreased when the flow rate was increased. However, as the difference between the signals observed at 50 and 100  $\mu\text{L}/\text{min}$  was not significantly different, preference as choice for routine application of the methodology was not given to the best 50  $\mu\text{L}/\text{min}$  but 100  $\mu\text{L}/\text{min}$  to compromise with the related to a short overall analysis time.

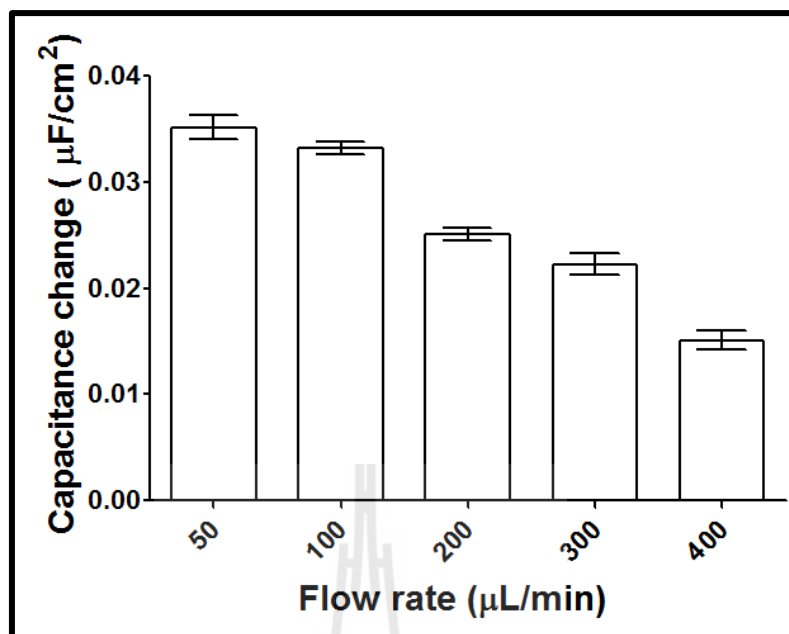


**Figure 3.13** The dependence of the efficiency of bYKL-40 quantification with capacitive immunosensor readout for different running buffer flow rates.

### 3.1.3.2.6 Optimization of the injected sample volume

Increasing (decreasing) the sample volumes that are injected into the analytical system will increase (decrease) the number of bYKL-40 analyte molecules brought to the immunosensor surface by the buffer stream. Obviously a sample volume variation will thus have an impact on the magnitude of the triggered capacitance change on the capturing immunosensor surface. The dependence of the sensor signal on sample volume was inspected in capacitive bYKL-40 immunosensor trials for injections of 100 to 400 μL of 10 μg/L of bYKL-40 standard solution. The results of the set of measurements are summarized in Figure 3.14. The change in capacitance signal actually increased with a change of the sample volume from 100 to 200 μL. A further increase in sample volume did not lead to a continuation of the effect and the capacitance change instead stayed about constant. Accordingly, 200 μL

was chosen in all quantification trials as the sample volume as it relates to short analysis time and at the same time saves precious analyte.

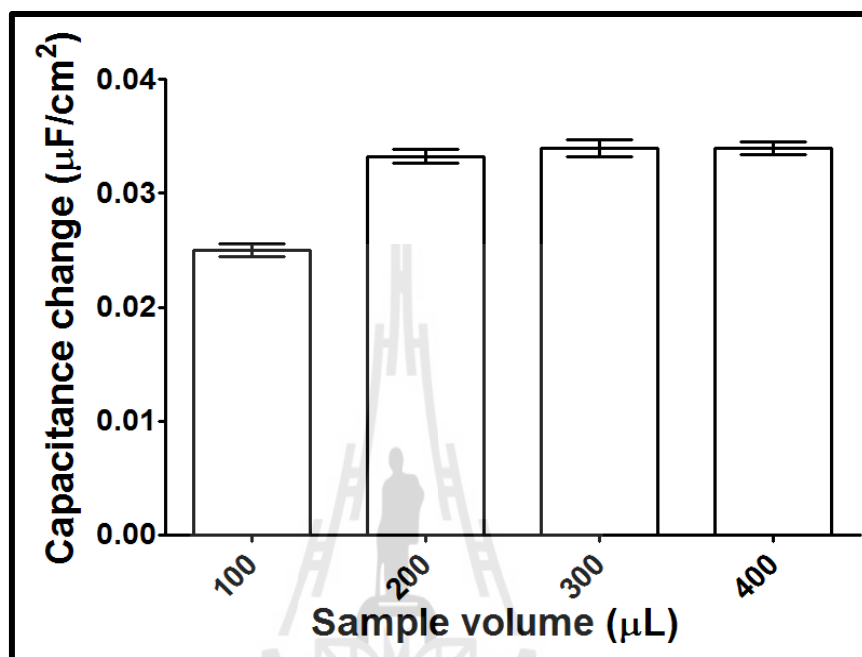


**Figure 3.14** The dependence of the efficiency of bYKL-40 capacitive immunosensing on a variation of injected sample volume.

In summary capacitive bYKL-40 immunosensor work best for analyte identification and quantification when applied with a 10 mM sodium phosphate running buffer, pH 7.0, HCl solution, pH 2.5 as regeneration solution, 100 μL/min as flow rate and a 200 μL as a sample volume. These values became thus the standard settings for the following assessments of the analytical merits of the analytical scheme and all applications to model and real sample analyses, too.

### 3.1.3.3 The analytical performance of bYKL-40 immunosensors in flow operation

#### 3.1.3.3.1 Linearity range and limit of detection

Sequential injections of bYKL-40 standard solutions of concentrations from 0.01  $\mu\text{g/L}$  to 10  $\text{mg/L}$ , inspected in triplicate for each concentration and with intermediate regeneration as described, were performed under optimal conditions to determine the linear dynamic range of the capacitive assay for bYKL-40 quantification. Figure 3.15 shows the results of a typical calibration experiment, with the capacitance change plotted against the logarithm of the bYKL-40 concentration. A linear response was reproducibly obtained within the range of 0.1  $\mu\text{g/L}$  to 1  $\text{mg/L}$ . The linear regression equation was  $y = (12.3 \pm 0.3) \log(x) + (107.4 \pm 1.4)$  and the correlation coefficient settled at 0.995. To investigate the limit of detection the running buffer (10 mM sodium phosphate buffer, pH 7.0) was injected into the immunosensor for twenty times under the optimum conditions. The standard deviation of 20 blank results was obtained at 0.30 and slope of the regression line (from 0.1 to 10  $\mu\text{g/L}$ ) was obtained at 12.11. So, the limit of detection was calculated from Eq. 2.4 that is limit of detection equal to  $0.07 \pm 0.01 \mu\text{g/L}$ . A representative trace of the capacitance response of the sensor to 0.1  $\mu\text{g/L}$  of bYKL-40 is shown in Figure 3.16, to demonstrate the capability of the developed sensing scheme to indeed work at very low analyte levels.

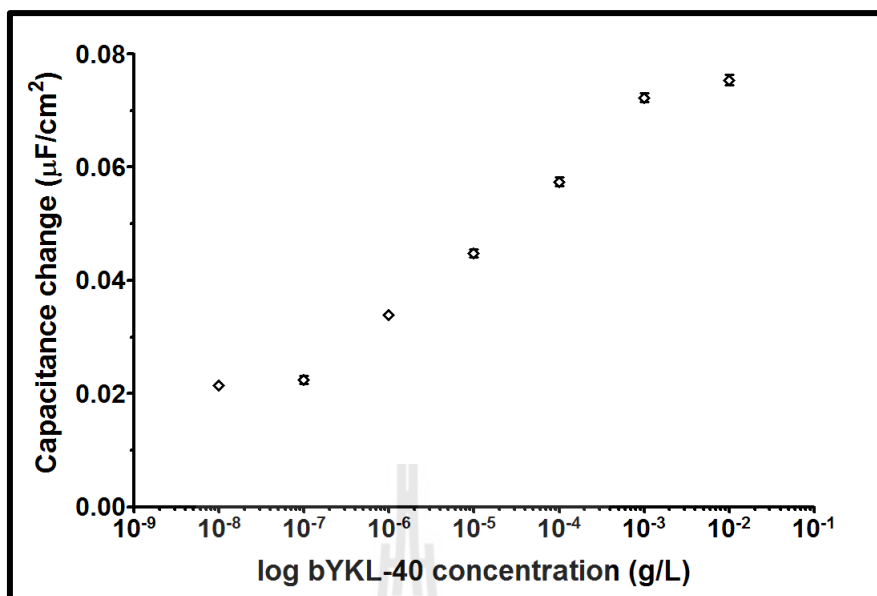


**Figure 3.15** Representation of a calibration curve as valid for routine capacitive bYKL-40 immunosensing. Screened was the sensor response to injections of bYKL-40 standard solutions of concentrations from 0.01  $\mu\text{g/L}$  to 10  $\text{mg/L}$ , under pre-identified optimal operational conditions.

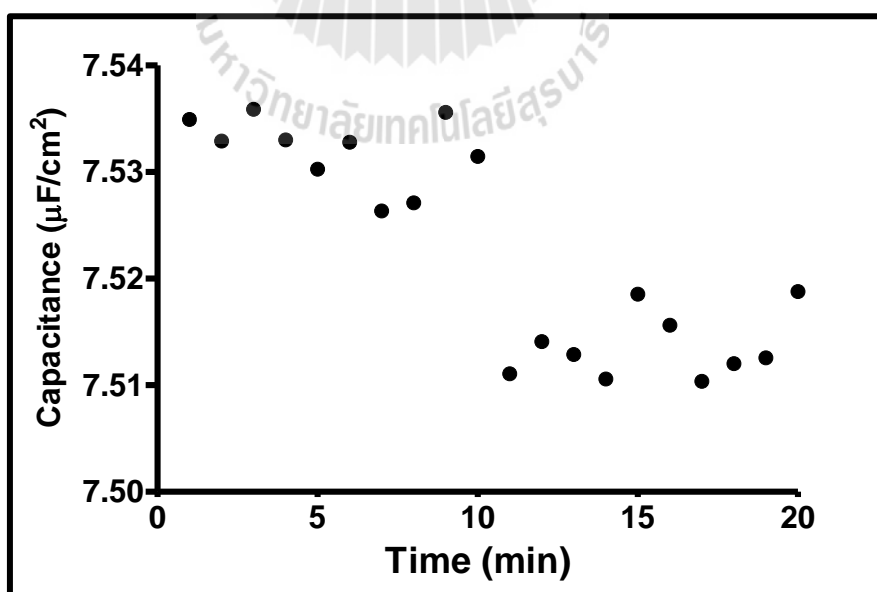


**Figure 3.16** bYKL-40 immunosensor response to the injection of 0.1  $\mu\text{g/L}$  of bYKL-40 under pre-identified optimal operational conditions.

### 3.1.3.3.2 The stability of anti-bYKL-40 immobilized electrode

The reproducibility of the capacitive bYKL-40 immunosensors in flow operation in continuous use was investigated at pre-identified optimal operational conditions by repetitively detecting the change of the capacitance triggered by injections of a fixed concentration of bYKL-40 standard solution (10  $\mu\text{g/L}$ ) with also repeated sensor surface regenerations to remove bYKL-40 from the anti-bYKL-40 immobilized on the electrode in between the injections. The performance of the modified electrode was evaluated for more than 3 days with about 15 sample injections per day. Figure 3.17 shows a plot of the percentage of restored activity of the anti-bYKL-40 immobilized electrode as function of number injection. As desired, the induced capacitance changes were highly reproducible and the percentage of restored immunosensor activity settled at an average level of  $100.1 \pm 1.7\%$  with a 1.67% R.S.D. The stable behavior lasted for 40 cycles of sample injection and surface regeneration, then the percentage of restored activity dropped rapidly to much lower, actually unacceptable. To additional proof that the self-assembled thiol monolayer as carrier of the antibody did not get destroyed during long term analysis, the thiol/bYKL-40 modified gold electrodes were tested via cyclic voltammetry before and after a stability trial. No significantly difference in the appearance of the cyclic voltammograms were observed (Figure 3.18), indicating that the self-assembled thiourea monolayer remained to be intact upon repeated cyclic exposures to sample and regeneration solutions, at least for the number of injections studied in the long-term tests. Therefore, the decrease in response of bYKL-40 immunosensors is most likely caused by a degradation of the antibody entities of the tool and their loss in

ability to well conjugate with the arriving corresponding antigen molecules rather than by a delamination and/or damage of the thiol monolayer.

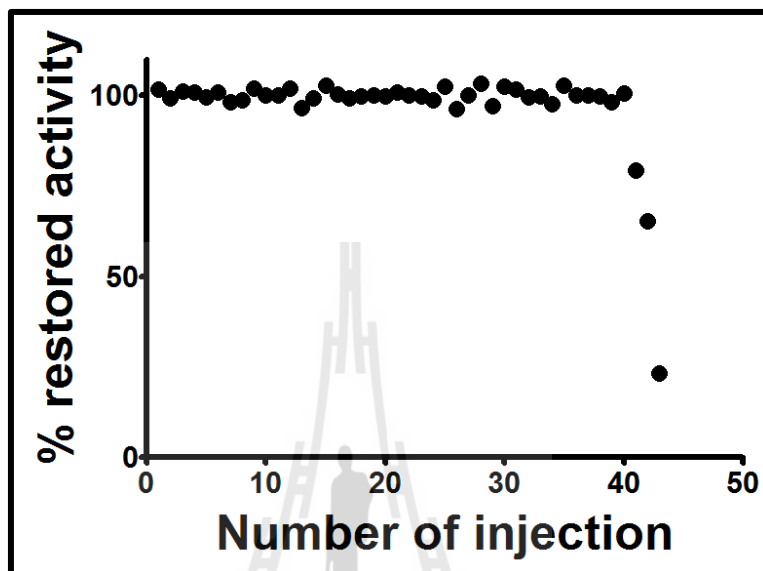


**Figure 3.17** Assessment of the stability of the signal during repeated cycles of sample injection and immunosensor regeneration.

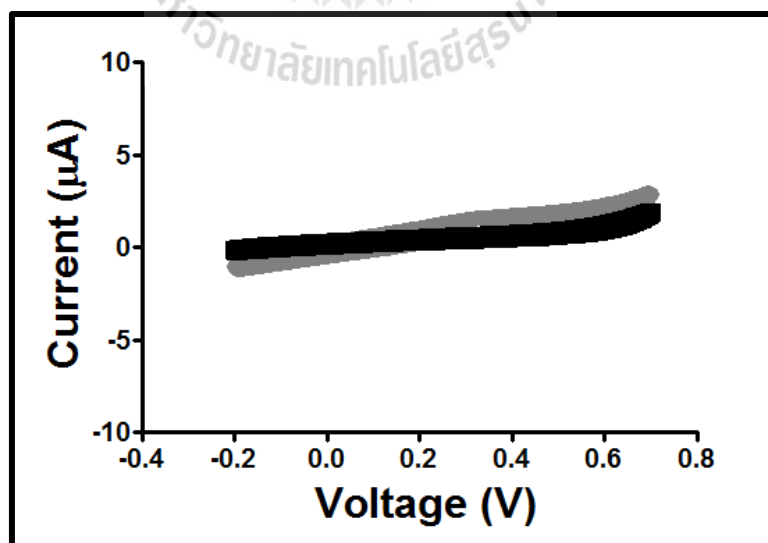


**Figure 3.18** The cyclic voltammograms in ferricyanide-containing electrolyte recorded before (black curve) and after (gray curve) the stability test.

### 3.1.3.3.3 The selectivity of capacitive bYKL-40 immunosensors

Inspected was also the effect of substances that might interfere with the response of bYKL-40 in the capacitive immunosensor system, when present in the sample solution. Two homolog proteins of YKL-40, namely YKL-39 and AMCase, were used as potent interferences to test the selectivity of the capacitive immunosensor system at a concentration range of 0.01  $\mu\text{g/L}$  to 10  $\text{mg/L}$ . Both candidates for interference produced, however, only very small capacitive responses of bYKL40 immunosensors, when compared with the one of the target analyte and designated antibody binding partner bYKL-40 (Figure 3.19). The responses of bYKL-40 demonstrated pronounced concentration dependence but the responses of YKL-39 and AMCase did not change with increase in their concentration with values about the same as triggered by running buffer injections. Apparently the presence of the two species does not interfere with the detection of bYKL-40 and bYKL-40 capacitive immunosensor have indeed the particularly good selectivity to bYKL-40 that is predicted for a tailored antibody/antigen bio-conjugate couple.

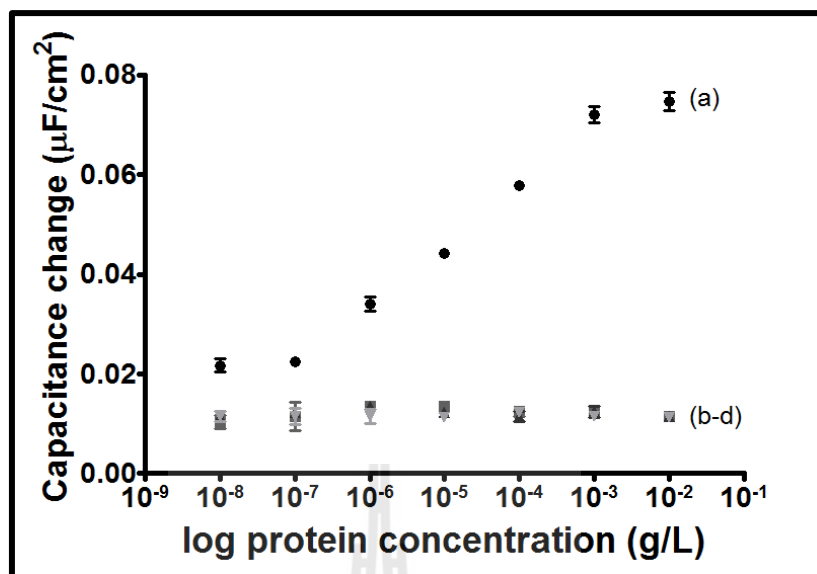


**Figure 3.19** Representative selectivity test for capacitive bYKL-40 immunosensors. The anti-bYKL-40 modified gold electrode was exposed either to the target analyte bYKL-40 and other members of the GH-18 (YKL-39 and AMCCase) and thus potential candidates as interfering species. The capacitance change was evaluated under pre-identical optimal operational conditions. (a), bYKL-40; (b), YKL-39; (c), AMCCase and (d), injections of blank running buffer solution.

#### 3.1.3.4 Determination of YKL-40 in model and spiked serum samples

To demonstrate the use of the developed bYKL-40 capacitive immunosensor system for accurate analyte quantification, the system was applied to model and spiked serum samples of known concentration of YKL-40 and percentage of recovery calculations were used for judgment of the quality of the measurements, its was described in Eq. 2.5 in Chapter II, Section 2.3.2.7.1. All samples were analyzed with the flow-based capacitive bYKL-40 immunosensing scheme and also with the common ELISA, and the data from the two complementary assessments were compared.

The immunosensors responses to particular sample injections were used to extract the actual YKL-40 concentration from the calibration curve that was obtained through work with YKL-40 standard solutions. Table 3.2 show the data for triplicate quantifications of spiked buffer solutions with added YKL-40 of a 0.5 to 50  $\mu\text{g/L}$  level. It is well obvious that the set point levels were reproduced with a good percentage of recovery and the statistically analysis (One-Way ANOVA,  $p < 0.05$ ), demonstrated that there was not significantly difference between data from the bYKL-40 capacitive immunosensor and the common ELISA.

**Table 3.2** YKL-40 detection in model samples: a comparison of the results from bYKL-40 capacitive immunosensing with those from ELISA (n=3).

Added ( $\mu\text{g/L}$ )	Immunosensor		ELISA	
	Found	Recovery	Found	Recovery
	( $\mu\text{g/L}$ )	(%)	( $\mu\text{g/L}$ )	(%)
0.50	0.50 $\pm$ 0.01	99.15 $\pm$ 2.63	N.d.	N.d.
2.50	2.50 $\pm$ 0.04	100.27 $\pm$ 2.66	2.57 $\pm$ 0.05	102.12 $\pm$ 2.21
10.00	10.28 $\pm$ 0.16	102.16 $\pm$ 1.57	10.33 $\pm$ 0.12	103.42 $\pm$ 1.42
50.00	50.82 $\pm$ 2.62	101.75 $\pm$ 2.70	50.48 $\pm$ 0.15	102.11 $\pm$ 3.11

N.d. = Not detection

The applicability of the capacitive biosensor for competitive YKL-40 analysis became further evident by measuring the analyte in spiked serum samples, which were spiked with 25, 50, 80 and 100  $\mu\text{g/L}$  of bYKL-40. Spiked serum samples

were 10 dilution times with running buffer to minimize a possible influence of components of the more demanding real sample matrix. Again, the capacitance response to particular sample injections was used to calculate the actual YKL-40 sample concentration of from the pre-determined calibration curve for the immunosensor in use. ELISA measurements on all tested samples delivered data for comparison and validation. Table 3.3 shows a summary of the results that were obtained in course of the spiked serum tests. Evident is that bYKL-40 capacitive immunosensor can measure the concentration of YKL-40 in spiked serum samples accurately and in good agreement with the ELISA. The percentage of recovery of the spiked YKL-40 levels in the four serum samples was between about  $99.17 \pm 5.70\%$  to  $106.68 \pm 2.39\%$  and  $99.44 \pm 0.43\%$  to  $101.92 \pm 3.22\%$ , respectively. As for the model samples, the statistical analysis (One-Way ANOVA,  $p < 0.05$ ) did not reveal any significantly difference between the data from bYKL-40 capacitive immunosensing and ELISA.

Altogether, above results demonstrated success with the establishment of flow injection-based capacitive bYKL-40 immunosensing and a good analytical performance for analyte quantification in both model and spiked blood serum samples.

Normally, the healthy person was expression levels of YKL-40 protein in serum around  $40 \mu\text{g/L}$  (Johansen *et al.*, 1995 and 2003, and Dupont *et al.*, 2004). For the results of spiked serum samples in Table 3.3 shows the bYKL-40 capacitive immunosensor system and ELISA technique did not detect YKL-40 protein in non-spiked serum of healthy person but both systems can detected only spiked concentration of bYKL-40 in serum of healthy person. These results indicated that our

anti-bYKL-40 polyclonal antibody, which produced from bacteria system, did not react with YKL-40 protein in human serum form. So, we change protocol for production of YKL-40 protein from bacteria expression system to mammalian expression system. An alternative method for the expression of the YKL-40 protein is the use of a mammalian cell expression system. The main advantages of this optional expression system are that the signals for synthesis, processing and secretion of eukaryotic proteins are properly and efficiently recognized by the mammalian cells. In a continuation of the work already reported, access to the YKL-40 protein through mammalian expression system and use the obtained alternative protein for immunosensor preparation and application was thus explored.

**Table 3.3** YKL-40 detection in spiked serum samples: a comparison of the results from capacitive immunosensing with those from ELISA (n=3).

Added ( $\mu\text{g/L}$ )	Immunosensor		ELISA	
	Found	Recovery	Found	Recovery
	( $\mu\text{g/L}$ )	(%)	( $\mu\text{g/L}$ )	(%)
0.00	N.d.	-	N.d.	-
25.00	25.09 $\pm$ 1.20	100.38 $\pm$ 4.79	25.51 $\pm$ 0.81	101.92 $\pm$ 3.22
50.00	49.59 $\pm$ 2.85	99.17 $\pm$ 5.70	50.83 $\pm$ 0.72	101.53 $\pm$ 1.33
80.00	85.35 $\pm$ 1.91	106.68 $\pm$ 2.39	79.51 $\pm$ 0.31	99.44 $\pm$ 0.43
100.00	101.17 $\pm$ 3.51	101.17 $\pm$ 3.51	101.14 $\pm$ 0.55	101.14 $\pm$ 0.55

N.d. = Not detection

### 3.1.4 Expression and purification of YKL-40 in mammalian system (mYKL-40)

The recombinant plasmid of full-length YKL-40 DNA cloned into pCMV/hygro-His expression vector was obtained from Sino biological Inc., Beijing, China, which was ready to be expressed in 293T cell line. The recombinant protein was expressed with the 21-amino acid *N*-terminal signal sequence attached and His<sub>10</sub>-tagged at *C*-terminal.

Recombinant YKL-40 was expressed in 293T cell line. After transfected recombinant plasmid to 293T cell line, culture medium that contains mYKL-40 protein was collected. The mYKL-40 fraction was further purified by affinity chromatography using a Ni-NTA agarose column run under gravity flow. The Figure 3.20 shows 12% SDS-PAGE analysis of mYKL-40 purification by Ni-NTA agarose, which migrated as a single band around 40 kDa (Lane 4 and 5), consistent with molar mass expected for mYKL-40 lacking the 21 amino acid signal peptide and has a predicted MW of 40,488 Da. The Figure 3.21 shows western blot analysis of the purified protein by commercial anti-YKL-40 (Quidel Corporation, San Diego, CA, USA); the results show the positive band of mYKL-40 protein in Elution fraction 1, 2 and 3. These results show the successfully expressed and purified mYKL-40 protein. Subsequently the purified mYKL-40 protein was used as immunogenic for mYKL-40 polyclonal antibody production by injected into subcutaneous of white New Zealand rabbit, 10 weeks age.

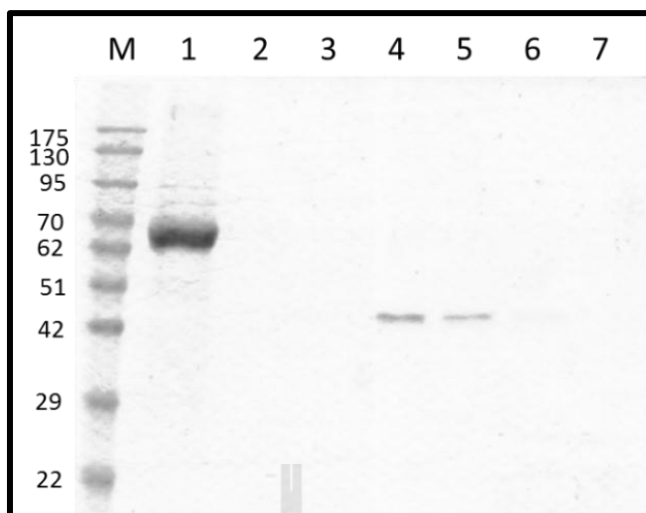


**Figure 3.20** 12% SDS-PAGE analysis of mYKL-40 purification by Ni-NTA agarose. Lane M, protein marker; Lane 1, culture medium fraction; Lane 2, wash with 10 mM imidazole; Lane 3, wash with 20 mM imidazole; Lane 4-7, Elute with 250 mM imidazole.

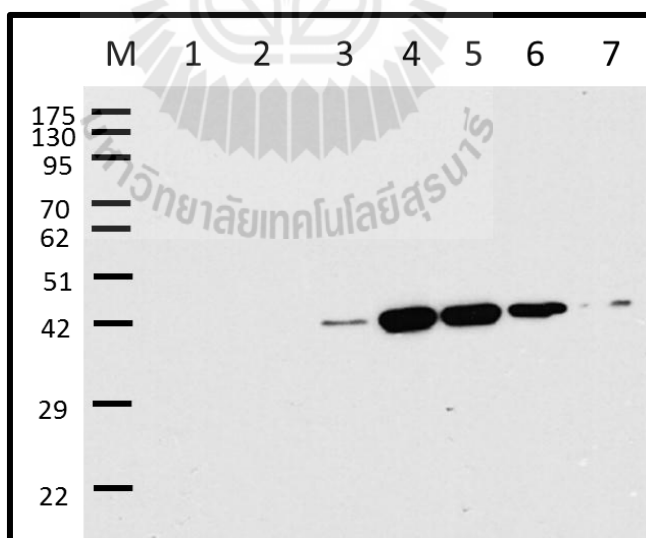


**Figure 3.21** mYKL-40 proteins detected by immunoblotting with the anti-YKL-40. Lane M, protein marker; Lane 1, culture medium fraction; Lane 2, wash with 10 mM imidazole; Lane 3, wash with 20 mM imidazole; Lane 4-7, elute with 250 mM imidazole.

### 3.1.5 Production of mYKL-40 polyclonal antibody

Purified mYKL-40 protein was used for the production of mYKL-40 polyclonal antibodies. The polyclonal anti-mYKL-40 antiserum was determined by western blot assay (Figure 3.22). The result shows the polyclonal anti-mYKL-40 antiserum and commercial anti-mYKL-40 was reacted strongly with the mYKL-40 target protein, shown in Figure 3.22B, Lane 2 and 3, respectively. In contrast, no signal was detected from the pre-immune serum (Figure 3.22B, Lane 1). The polyclonal anti-mYKL-40 antiserum titers were determined by western blot assay (Figure 3.23). The polyclonal anti-mYKL-40 antiserum reacted strongly with the mYKL-40 target protein at dilutions up to 1:40,000 and a faint signal were detectable even at 1:80,000 dilutions. In contrast, no signal was detected from the pre-immune serum, even at the highest concentration tested (1:2,500 dilutions). Evaluation of cross-reactivity against other members of GH-18 used a 1:40,000 dilutions of polyclonal anti-mYKL-40 antiserum. The western blots analysis (Figure 3.24B) revealed no interaction of the polyclonal anti-mYKL-40 antiserum with mYKL-40 homologues such as YKL-39, AMCase and chitinases A, confirming that the polyclonal anti-mYKL-40 antiserum specific for the target protein, mYKL-40.

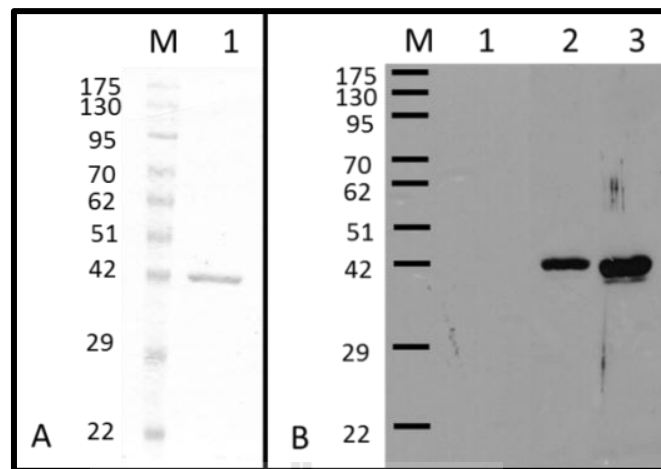


**Figure 3.22** Reactivity of polyclonal anti-mYKL-40 antiserum. (A) 12% SDS-PAGE analysis of 2  $\mu$ g of purified mYKL-40: Lane 1, coomassie-blue stained. (B) mYKL-40 protein detected by western blot assay. Lane M, protein markers; Lane 1, pre-immune serum; Lane 2, polyclonal anti-mYKL-40 antiserum; Lane 3, commercial anti-YKL-40.

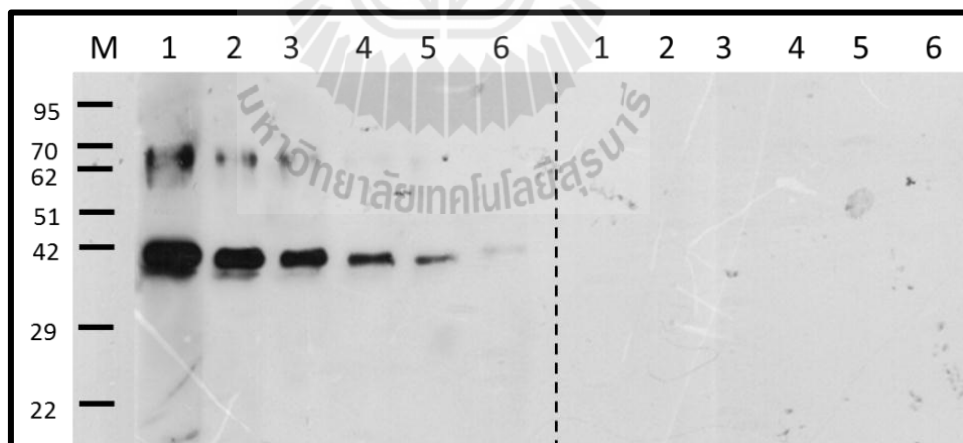


**Figure 3.23** The polyclonal anti-mYKL-40 antiserum titers against 2  $\mu$ g of purified mYKL-40. Lane M, protein markers; Lane 1–6, 2  $\mu$ g of purified mYKL-40 protein detected with various dilutions (1:2,500, 1:5,000, 1:10,000, 1:20,000, 1:40,000 and 1:80,000) of polyclonal anti-mYKL-40 antiserum (left-hand panel). The same dilutions of pre-immune serum were used as a negative control (right-hand panel).

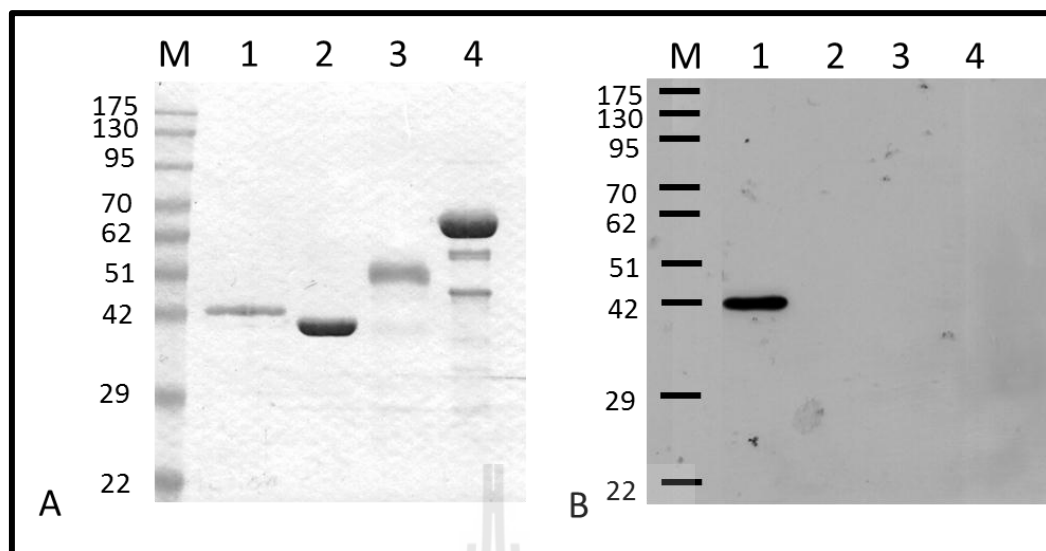


**Figure 3.24** Specificity of polyclonal anti-mYKL-40 antiserum. (A) Coomassie-blue stained 12% SDS-PAGE. (B) Western blot analysis with polyclonal anti-mYKL-40 antiserum (1:40,000 dilution); pre-immune serum was used as a negative control (not shown). Lane 1, purified mYKL-40 protein (2  $\mu$ g); Lane 2, YKL-39 (3  $\mu$ g); Lane 3, AMCase (3  $\mu$ g) and Lane 4, chitinases A (10  $\mu$ g).

Polyclonal anti-mYKL-40 antiserum was purified by affinity chromatography on protein A agarose column run under gravity flow. The SDS-PAGE analysis (Figure 3.25) showed the purity of the anti-mYKL-40 polyclonal antibody, and confirmed that it is a protein A-specific IgG isotype. The immunoglobulin migrated above the 130 kDa marker under non-reducing conditions (Figure 3.25, Lane 2), while reduction of the sample produced two protein bands, of about 55 kDa and 22 kDa (Figure 3.25, Lane 1), as expected for IgG isotype. IgG antibodies are large molecules of about 150 kDa, contains heavy chains of about 50 kDa and light chains of about 25 kDa. To check the reactivity of purified anti-mYKL-40 polyclonal antibody was determined by western blot assay. The western blot analysis of the

purified anti-mYKL-40 polyclonal antibody show the anti-mYKL-40 reacted strongly with mYKL-40 down to 0.250 mg/L, whereas the pre-immune serum showed no detected signal (Figure 3.26).

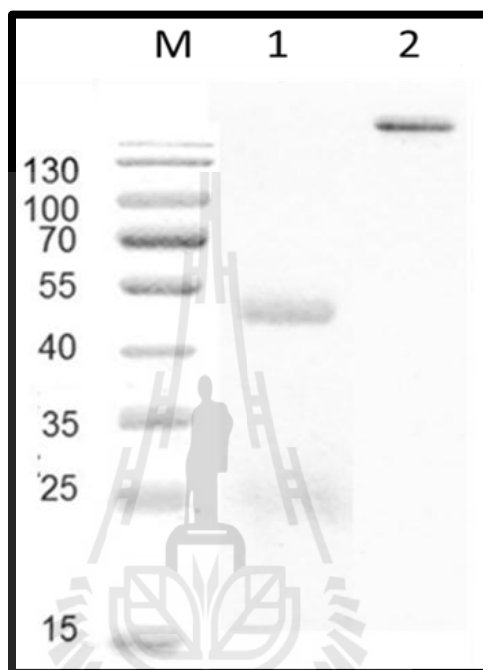


**Figure 3.25** Purification of anti-mYKL-40 polyclonal antibody by affinity protein A-agarose column run under gravity flow. 12% SDS-PAGE analysis of purified anti-mYKL-40 polyclonal antibody; Lane 1, under reducing conditions and Lane 2, non-reducing conditions: coomassie-blue stained gel.

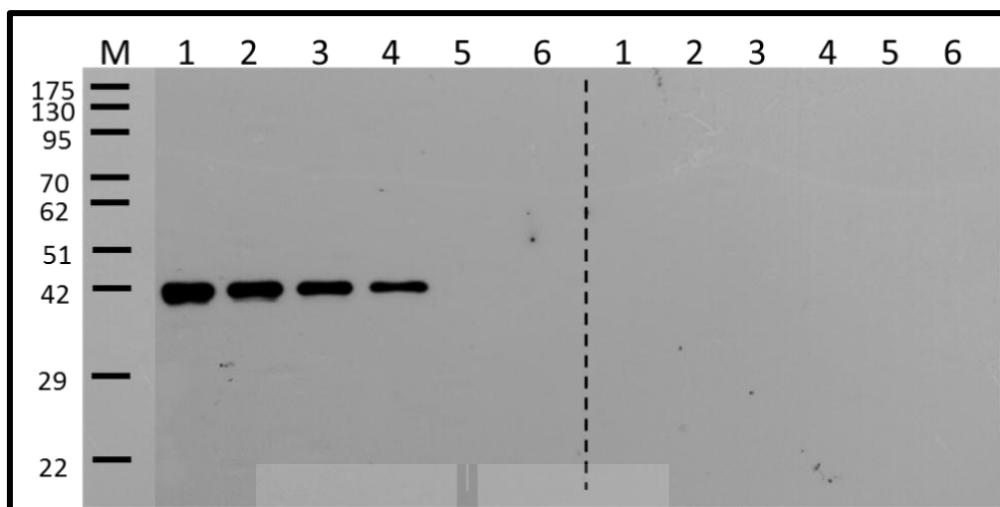


**Figure 3.26** Purified anti-mYKL-40 polyclonal antibody titers against 2  $\mu$ g of mYKL-40. Lane M, protein markers; Lane 1–6, serial dilutions of the purified antibody to 2, 1, 0.500, 0.250, 0.175 and 0.078 mg/L, respectively (left-hand panel). Unfractionated pre-immune serum was used as a negative control (right-hand panel).

To confirm the specificity of purified anti-mYKL-40 polyclonal antibody with related proteins was tested by using another commonly technique that is ELISA. Figure 3.27 shows the binding of anti-mYKL-40 polyclonal antibody to mYKL-40 and homologous proteins. Figure 3.27 represent the binding curve of mYKL-40, showing concentration dependence of the anti-mYKL-40 polyclonal antibody towards the mYKL-40 protein and homologous proteins. The mYKL-40 (curve a) shown the hyperbolic plot of the interaction signal with increasing mYKL-40 protein concentration is characteristic of a specific antigen-antibody interaction. Whereas, other members of GH-18 (YKL-39 and AMCcase) shown the no significant signal was obtained, YKL-39 (curve b) and AMCcase (curve c). This well confirmed that the anti-mYKL-40 polyclonal antibody was highly specific for mYKL-40 protein, target protein.

The linearity range of mYKL-40 ELISA was obtained from 2.5 to 320  $\mu\text{g/L}$  and the limit of detection is 2.5  $\mu\text{g/L}$ . The linear regression equation is  $y = (0.005 \pm 0.001)x + (0.019 \pm 0.006)$  at the correlation coefficient at 0.997.

These results confirmed that the purified anti-mYKL-40 was highly specific for mYKL-40 protein and thus suitable for use in mYKL-40 capacitive immunosensor based flow injection system.

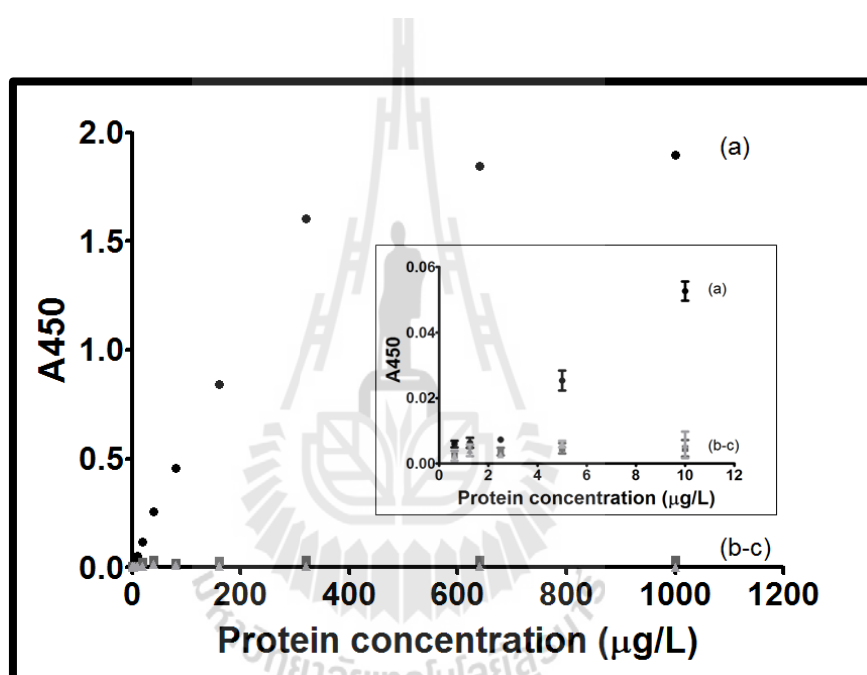


**Figure 3.27** mYKL-40 Enzyme-linked immunosorbent assay. Binding of anti-mYKL-40 IgG (50  $\mu\text{L}$ , 10  $\mu\text{g/L}$ ) to different amounts of surface-attached mYKL-40 related proteins: mYKL-40 (curve a); YKL-39 (curve b); and AMCCase (curve c). Inset show the signal response at low concentration of mYKL-40.

### 3.1.6 Capacitive mYKL-40 immunosensor

#### 3.1.6.1 Preparation of the immunosensors

As above described in detail (section 3.1.3.1), the insulating properties of modified gold electrode have been inspected after individual preparation steps via

cyclic voltammograms in ferricyanide-containing electrolytes. The gradual disappearance of the Fe (III)/Fe (II) redox peaks in the voltammograms again was taken as evidence of thiol monolayer assembly, antibody immobilization, and complete insulation reach via residual exposed electrode surface coverage with 1-dodecanethiol (Figure 3.28).

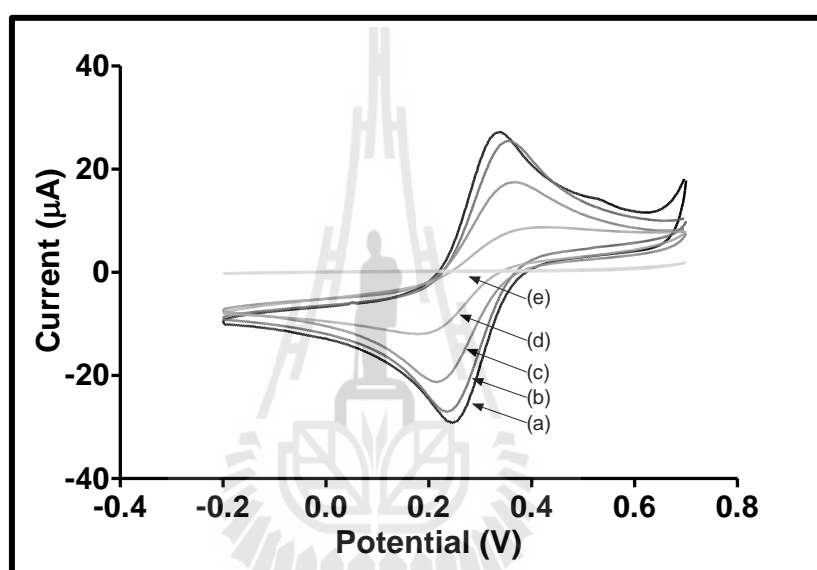


**Figure 3.28** Cyclic voltammograms of a gold electrode at various surface conditions. (a) clean (b) coated with a self-assembled thiourea monolayer, (c) after glutaraldehyde exposure of the thiourea film, (d) after anti-mYKL-40 bonding to the glutaraldehyde-treated thiourea film and (e) after final treatment with 1-dodecanethiol.

### 3.1.6.2 Optimization of operational conditions

Again, the experimental parameters affecting the performance of the capacitive immunosensor (now just with an YKL-40 antibody from the mammalian cell expression system) in the already introduced flow injection system was investigated and optimized to yield optimal analytical performance. Evaluations

considered the regeneration solution, the running buffer, injected sample volume and flow rate. All measurements were carried out as above described in detail for the bYKL-40 protein derived from the bacterial cell expression system and were again performed in triplicate. The data of the optimization trials with mYKL-40 immunosensors incorporating anti-mYKL-40 polyclonal antibody produced via mYKL-40 derived from the mammalian cell expression system are summarized in Figures 3.29 - 3.35. Optimal conditions for the operation of the alternative type of capacitive mYKL-40 immunosensor were: regeneration solution, HCl solution, pH 2.5; running buffer, 25 mM sodium phosphate buffer, pH 7.0; sample volume, 250  $\mu$ L and flow rate, 100  $\mu$ L/min.

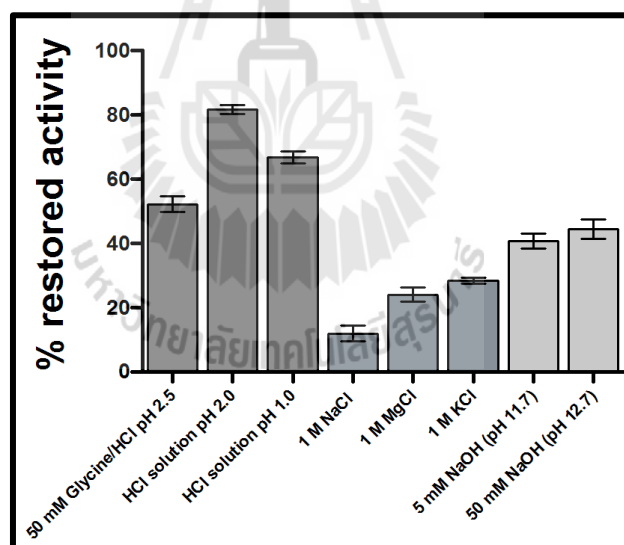


**Figure 3.29** Efficiency of different types of regeneration solutions. Percentage of restored activity is an expression that scales the amount of immobilized anti-mYKL-40 antibody that got released from mYKL-40 antigen that had been captured in course of a measurement cycle; the higher the percentage of restored activity, the more antibody was freed and successfully primed for capturing antigen again in the next analytical sample injection run.

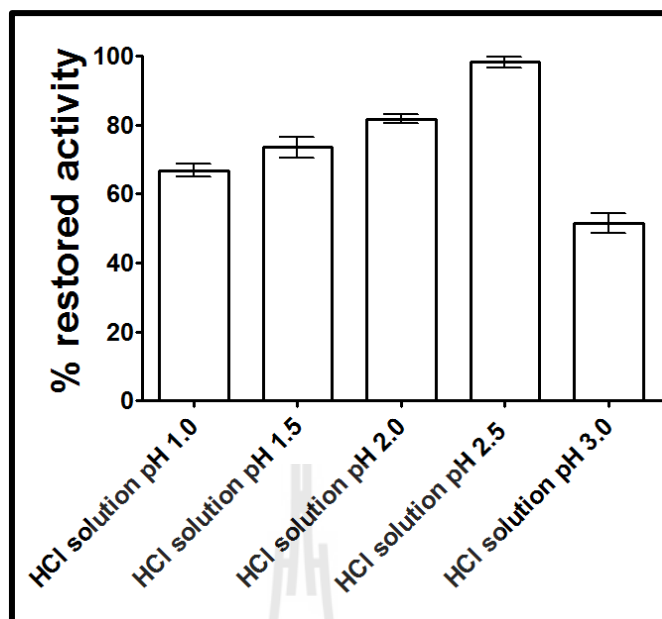


**Figure 3.30** The influence of the pH of the HCl regeneration solution on the efficiency of removal mYKL-40 from anti-mYKL-40 on a thiol-coated gold electrode.

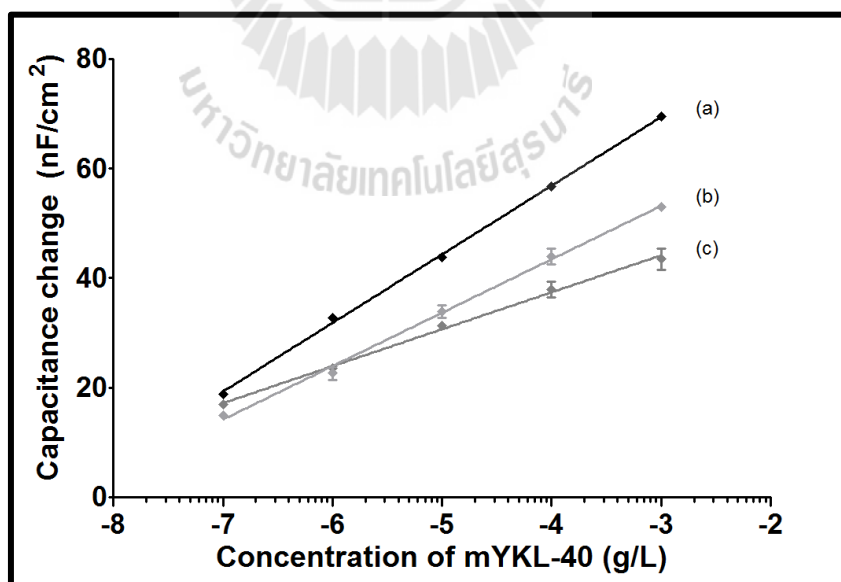


**Figure 3.31** The efficiency of mYKL-40 capacitive immunosensors for different types of running buffer. (a) 10 mM sodium phosphate buffer pH 7.0; (b) 10 mM HEPES buffer pH 7.0; (c) 10 mM Tris-HCl buffer pH 7.0.

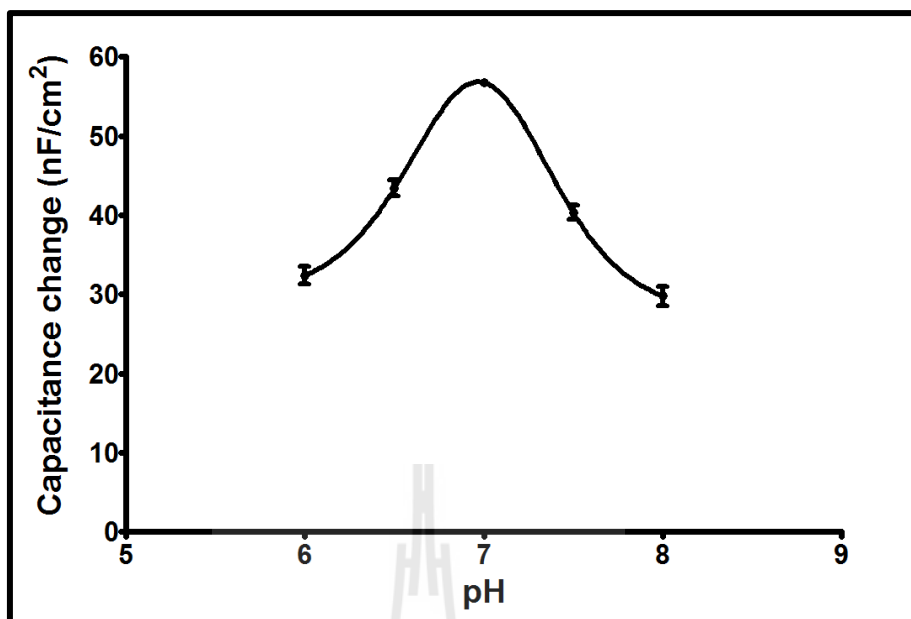


**Figure 3.32** The efficiency of mYKL-40 capacitive immunosensors for applications with 10 mM sodium phosphate running buffer at different pH.

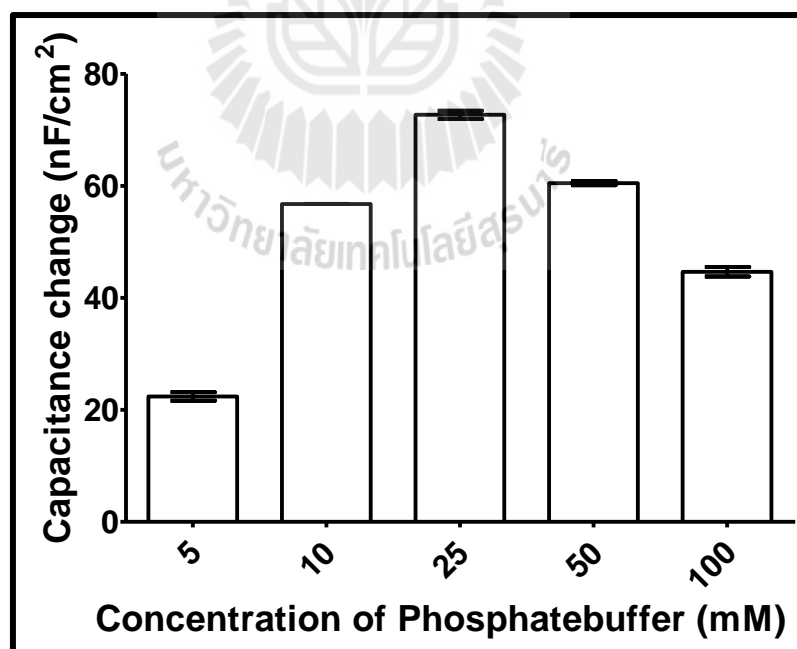


**Figure 3.33** The dependence of the efficiency of mYKL-40 quantification on different salt concentrations of the sodium phosphate buffer, pH 7.0.

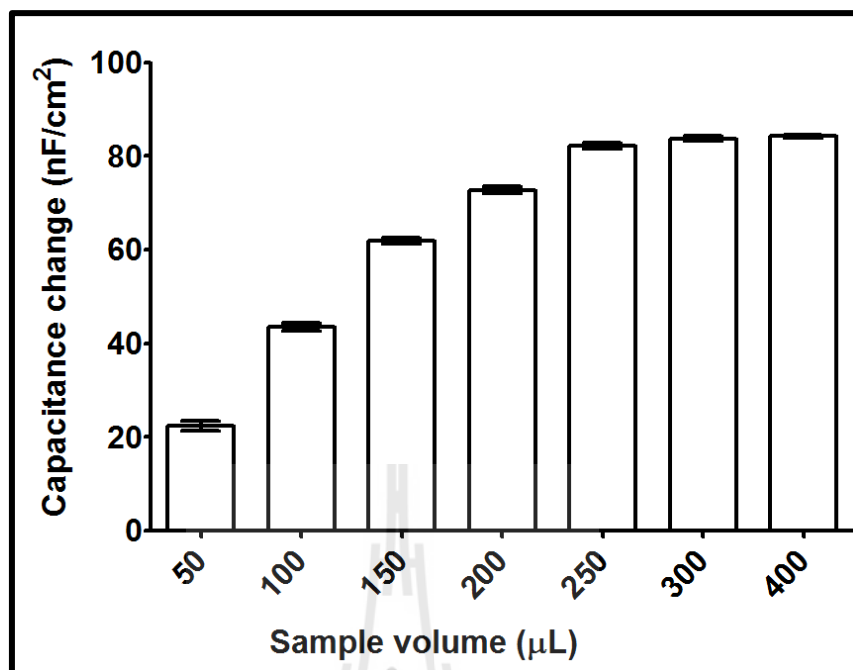


**Figure 3.34** The dependence of the efficiency of mYKL-40 capacitive immunosensing on a variation of injected sample volume.

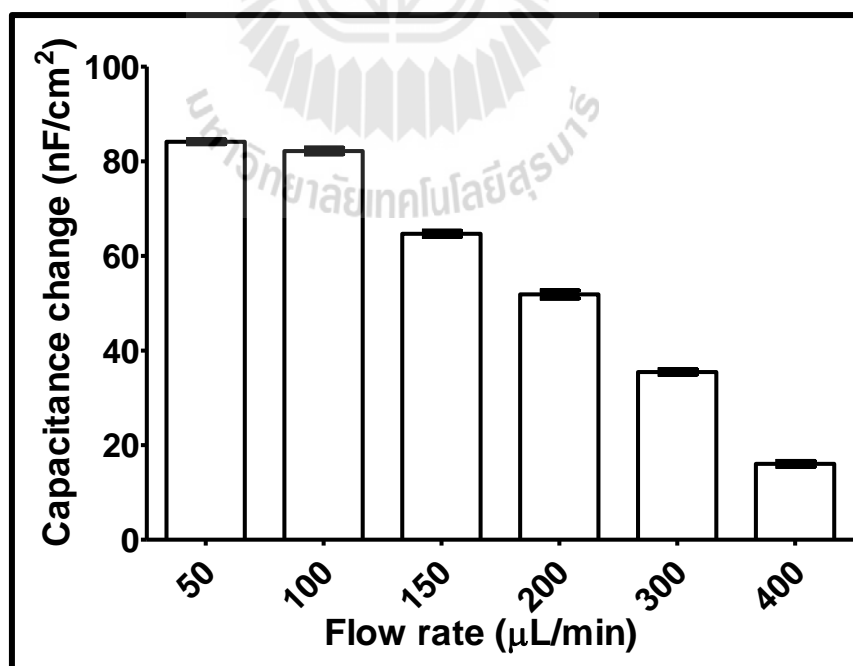


**Figure 3.35** The dependence of the efficiency of mYKL-40 quantification with capacitive immunosensor readout for different running buffer flow rates.

### **3.1.6.3 The analytical performance of mYKL-40 immunosensors in flow operation**

#### **3.1.6.3.1 Linearity range and limit of detection**

Tested via triplicate injections of standard solutions of mYKL-40 in the range 1 ng/L to 100 mg/L the immunosensor system with the antibody/antigen obtained from the mammalian expression system offered under the pre-identical optimal operational conditions a linear range between 0.1  $\mu\text{g/L}$  to 1 mg/L (Figure 3.36). The corresponding linear equation of the regression line  $y = (19.9 \pm 0.5) \log(x) + (156.3 \pm 0.6)$  and the plot had a correlation coefficient of 0.992. At concentration above 1 mg/L the capacitance signal became constant because of the saturation of all immobilized antibody entities with mYKL-40 antigen. To investigate the limit of detection the running buffer (25 mM sodium phosphate buffer, pH 7.0) was injected into the immunosensor for twenty times under the optimum conditions. The standard deviation of 20 blank results was obtained at 0.55 and slope of the regression line (from 0.1 to 10  $\mu\text{g/L}$ ) was obtained at 19.90. So, the limit of detection was calculated from Eq.2.4 that is the limit of detection was about  $0.08 \pm 0.02 \mu\text{g/L}$ .

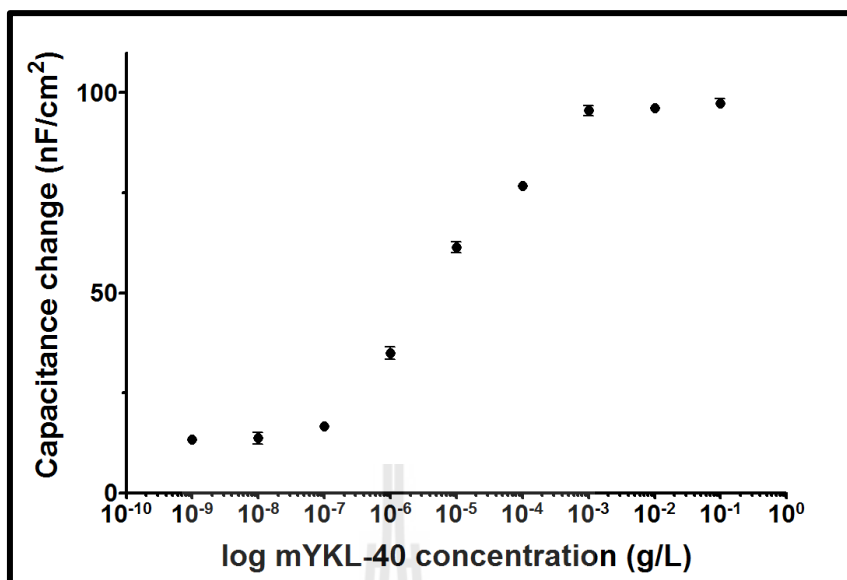


**Figure 3.36** Representation of a calibration curve as valid for routine capacitive mYKL-40 immunosensing. Screened was the sensor response to injections of mYKL-40 standard solutions of concentrations from 1 ng/L to 100 mg/L under pre-identified optimal operational conditions.

### 3.1.6.3.2 The stability of capacitive mYKL-40 immunosensors

In similar manner as before done for the immunosensors with a bYKL-40 antibody/antigen couple originating from bacterial cell expression the new option gained from the mammalian cell expression was also subjected to a stability trial. Figure 3.37 shows a display of a plot of the percentage of restored activity of for the anti-mYKL-40 electrode as a function of the number of regeneration cycles at the time of measurement. Evident is that for more than 3 days, which is the equivalent of 50 cycles of analyte injection and immunosensor detection and regeneration, the percentage of restored activity of was at a very good level of  $98.8 \pm 0.9\%$  (0.85% RSD) of the original capacitance change. And again the acquisition of equality of cyclic voltammograms for sensors before and after the long-term stability test demonstrated

self-assembled monolayer intactness and pointed toward structural and/or chemical antibody modification and related loss of antigen binding ability (Figure 3.38).

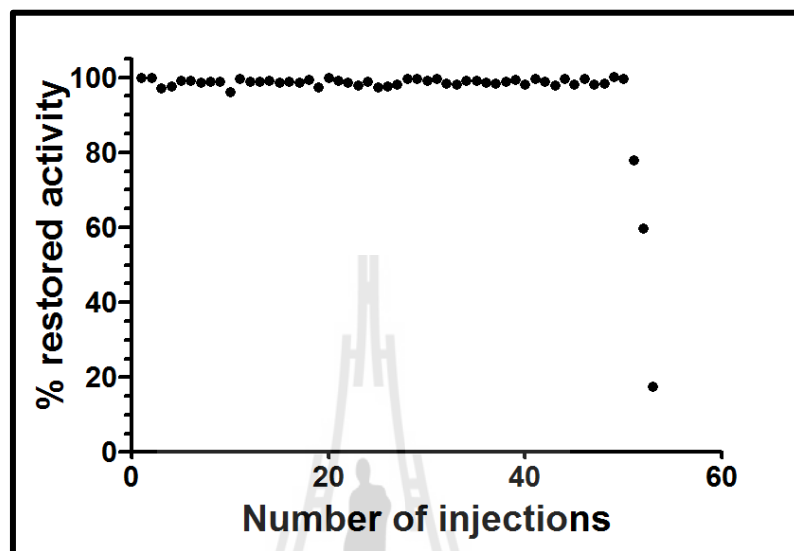


**Figure 3.37** Assessment of the stability of the signal during repeated cycles of sample injection and immunosensor regeneration.

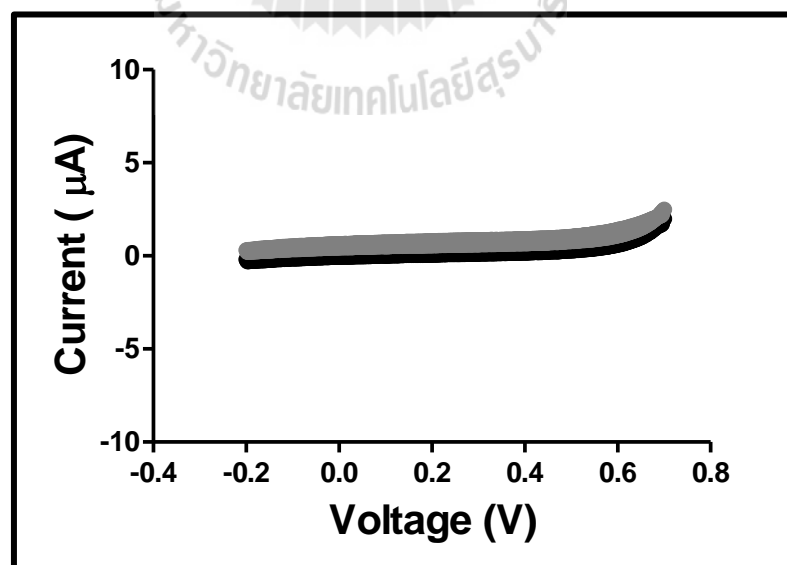


**Figure 3.38** The cyclic voltammograms in ferricyanide-containing electrolyte recorded before (black curve) and after (gray curve) the stability test.

### 3.1.6.3.3 The selectivity of anti-mYKL-40 immunosensors

Following the strategy handled for the selectivity tests on immunosensors with antibody from the bacterial cell expression, the mYKL-40 antibody based on the mammalian cell expression was tested in the flow-based capacitive immunosensor system with samples that had on top of the target analyte also its homologous proteins (YKL-39 and AMCCase). Tests were of course done as a sort of calibration run with the capacitive immunosensor system used for the concentration range from 1 ng/L to 100 mg/L), under the pre-identified optimal operational conditions. The two homologous protein samples tested in the mYKL-40 capacitive immunosensor system produced capacitance changes not larger than injections of running buffer solution. Injections of samples with the target analyte, mYKL-40, however, changed the capacitance nicely in concentration-dependent manner (Figure 3.39). Conclusion was thus that YKL-39 and AMCCase presence does not cause interference problems, even though the proteins are structurally and chemically very closely related to the target antigen. The identified specificity made tests in model and real samples practical. They are described in the following sub-chapter.

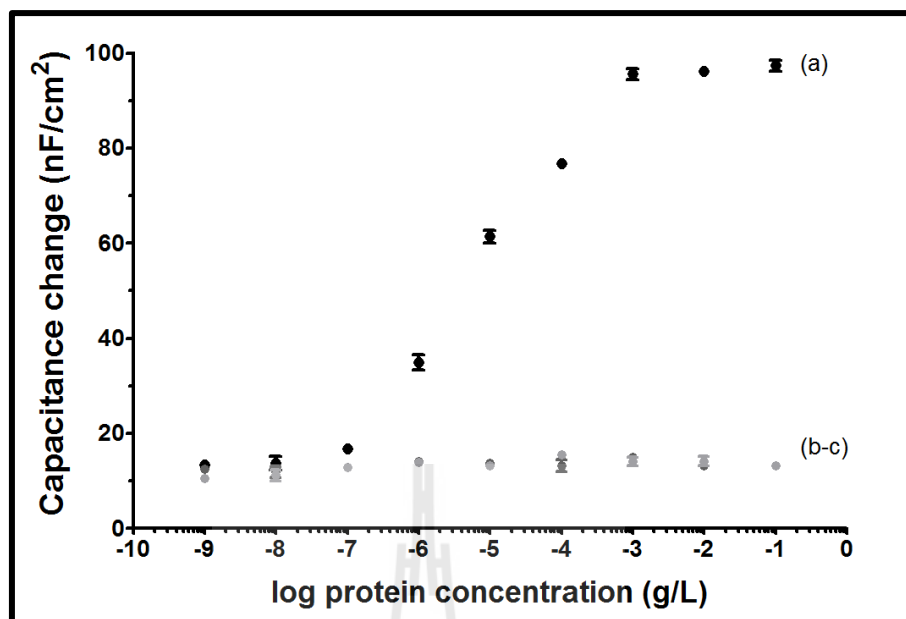


**Figure 3.39** Representative selectivity test for capacitive mYKL-40 immunosensors. The anti-mYKL-40 modified gold electrode was exposed either to the target analyte mYKL-40, and other members of the GH-18 (YKL-39 and AMCCase) and thus potential candidates as interfering species. The capacitance change was evaluated under the pre-identified optimal operational conditions. (a), mYKL-40; (b), YKL-39; and (c), AMCCase.

#### 3.1.6.4 Determination of YKL-40 in model and clinical samples

Triplicate quantification was approached with the capacitive immunosensors for model samples that were spiked with three different YKL-40 concentrations in the range of 30 to 150  $\mu\text{g/L}$ . In parallel analytical trials the concentrations of the three samples were also determined by an in-house and a commercial ELISAs (BlueGene Biotech CO., LTD). Obtained data proved a good agreement of the YKL-40 levels reported by the three methods. The percentage of recovery for the quantifications by the capacitive immunosensor and the in-house and the commercial ELISAs were

100.1±0.6 to 102.2±1.9%, 98.9±0.6 to 99.9±0.2% and 100.5±2.1 to 100.6±0.6%, respectively (Table 3.4). Data inspection by statistical analysis pointed out that there were no systematic differences between the results from the three methodologies (One-Way ANOVA,  $p < 0.05$ ). Sensors were then further applied for YKL-40 assessments in clinical samples of healthy people, suitable cell lysate samples and samples from people with cancer.

**Table 3.4** YKL-40 detection in model samples: a comparison of the results from mYKL-40 capacitive immunosensing with those from ELISA (n=3).

Added ( $\mu\text{g/L}$ )	Immunosensor		In-house ELISA		Commercial ELISA	
	Found	Recovery	Found	Recovery	Found	Recovery
	( $\mu\text{g/L}$ )	(%)	( $\mu\text{g/L}$ )	(%)	( $\mu\text{g/L}$ )	(%)
<b>0</b>	N.d.	-	N.d.	-	N.d.	-
<b>30</b>	30.7±0.7	102.2±1.9	29.7±0.2	98.9±0.6	30.1±0.8	100.5±2.1
<b>40</b>	40.8±1.0	101.9±2.1	39.7±0.6	99.2±1.2	40.3±0.3	100.6±0.6
<b>150</b>	150.2±1.2	100.1±0.6	149.8±0.4	99.9±0.2	150.1±0.8	100.8±0.9

N.d. = Not detection

The clinical application of capacitive mYKL-40 immunosensors was first explored for four hospital serum samples from healthy persons, labeled here simply as H1-H4. Prior to analysis, the serum samples were diluted 10 times to reduce the possible impact of other proteins in the complex serum matrix on capacitive signal

generation at the immunosensor and in the ELISA, both in-house and commercial. The outcome of the three trials is shown in Table 3.5, which provides the evidence that the concentrations determined by the capacitive immunosensor, in-house ELISA and commercial ELISA are in good agreement with each other and they were in accordance with reported values in the literature. The actual level of YKL-40 in the four healthy person range of 60 to 75  $\mu\text{g/L}$ . The quality of analysis was confirmed through measurements of by spiked serum samples that had been up scaled with 50  $\mu\text{g/L}$  of YKL-40. As expected the measured level of YKL-40 in the spiked healthy person samples shifted to higher levels and with exact values from 100 to 125  $\mu\text{g/L}$  (found concentration + spiked concentration) the percentage of recovery were very close to the ideal 100%. In summary all three analysis techniques applied in the trials could actually reveal correctly the native YKL-40 in healthy human serum; no significantly difference in the values were observed (One-Way ANOVA,  $p < 0.05$ ). Apparently, the developed mYKL-40 immunosensor system was suitable for the detection of target YKL-40 in healthy human serum.

**Table 3.5** YKL-40 detection in serum samples from a healthy person: a comparison of the results from mYKL-40 capacitive immunosensing with those from ELISA (n=3).

<b>Healthy person</b>	<b>Immunosensor (<math>\mu\text{g/L}</math>)</b>	<b>In-house ELISA (<math>\mu\text{g/L}</math>)</b>	<b>Commercial ELISA (<math>\mu\text{g/L}</math>)</b>
<b>H1</b>	75.4 $\pm$ 1.4	74.5 $\pm$ 1.9	75.1 $\pm$ 0.8
<b>H2</b>	60.4 $\pm$ 1.1	59.9 $\pm$ 1.9	60.2 $\pm$ 0.1
<b>H3</b>	66.3 $\pm$ 1.4	66.5 $\pm$ 3.8	66.7 $\pm$ 0.2
<b>H4</b>	51.7 $\pm$ 2.5	51.9 $\pm$ 5.0	51.7 $\pm$ 0.4
<b>H1 + 50 <math>\mu\text{g/L}</math></b>	125.0 $\pm$ 2.3	126.5 $\pm$ 3.8	124.9 $\pm$ 0.6
<b>H2 + 50 <math>\mu\text{g/L}</math></b>	109.4 $\pm$ 1.3	109.2 $\pm$ 3.3	111.3 $\pm$ 0.7
<b>H3 + 50 <math>\mu\text{g/L}</math></b>	116.8 $\pm$ 0.4	115.9 $\pm$ 1.9	117.0 $\pm$ 0.5
<b>H4 + 50 <math>\mu\text{g/L}</math></b>	100.8 $\pm$ 0.9	101.2 $\pm$ 3.3	101.0 $\pm$ 0.2

Known from the literature review was that YKL-40 levels were higher in serum samples of patients with, for instance, breast cancer, colorectal cancer, ovarian cancer, small cell lung cancer, prostate cancer, and glioblastoma. Inspected here for their YKL-40 content were the blood serum samples from 5 breast (named B1-B5) and 4 glioblastoma (named G1-G4) cancer patients, again via mYKL-40 capacitive immunosensing and in-house and commercial ELISAs. The nine serum samples were kind provision of the Maharat Nakhon Ratchasima Hospital in Nakhon Ratchasima, Thailand and they were as a routine diluted at 10 times with running buffer to minimize matrix effects. Table 3.6 is a presentation of the outcome of the trial on the cancer patient's blood serum. Noticed can be that the concentrations that determined

by the capacitive immunosensor, in-house ELISA and commercial ELISA are close to each other. In fact, the YKL-40 levels of the five breast cancer patients ranged from about 40 (low) to 400 (high)  $\mu\text{g/L}$  while the four glioblastoma patients had blood serum with 50 (low) to 650 (high)  $\mu\text{g/L}$  of YKL-40. Recovery tests were carried out with spiked samples (B3 + 50  $\mu\text{g/L}$  of YKL-40 and G1+ 50  $\mu\text{g/L}$  of YKL-40) and the percentage of recovery for both attempts were close to the ideal 100%. Evidence was thus gained that not only the native YKL-40 level of healthy human blood serum can be determined accurately but also the elevated equivalents due to cancer. No significantly difference became evident between the suggested electrochemical capacitive immunosensor screen and an ELISA with optical readout (One-Way ANOVA,  $p < 0.05$ ).

### 3.1.6.5 Determination of YKL-40 in cell lysates

Michelsen *et al.* (2010) reported the YKL-40 expression by THP-1 (human leukemia cell line) cells while 293T cells had not been linked with YKL-40 generation. THP-1 and 293T cell lysates were thus nice samples for comparative performance tests with the mYKL-40 capacitive immunosensor and the in-house and commercial ELISAs. The results of the application of the three assays on the two cell lysates are shown in Table 3.6. In good agreement with the expectation all schemes reported similar YKL-40 concentrations in the THP-1 cell lysate, and did not detect noticeable levels of the analyte in 293T cell lysates. This was further supported of the impression that capacitive mYKL-40 immunosensing is a trustful novel analytical approach for the detection and quantification of this biomarker molecule. Since 293T cell lysates was confirmed to be YKL-40 free this liquid offered the chance of control

quantifications in a more complex sample matrix with a defined adjustment of the protein analyte. Accordingly, 293T cell lysates were spiked with 50  $\mu\text{g/L}$  of YKL-40 and jointly all the capacitive electrochemical and the optical ELISAs revealed the adjusted level with good percentage of recovery (see Table 3.7).

**Table 3.6** YKL-40 detection in serum samples from cancer patients: a comparison of the results from mYKL-40 capacitive immunosensing with those from ELISA (n=3).

Clinical Samples	Immunosensor	In-house ELISA	Commercial ELISA
	( $\mu\text{g/L}$ )	( $\mu\text{g/L}$ )	( $\mu\text{g/L}$ )
B1	42.5 $\pm$ 0.8	43.3 $\pm$ 1.9	42.2 $\pm$ 0.5
B2	87.1 $\pm$ 0.1	87.3 $\pm$ 1.9	86.3 $\pm$ 1.1
B3	399.8 $\pm$ 2.4	399.3 $\pm$ 2.3	400.5 $\pm$ 2.6
B4	212.9 $\pm$ 1.4	212.7 $\pm$ 3.8	214.8 $\pm$ 1.4
B5	47.3 $\pm$ 1.3	47.3 $\pm$ 1.9	47.6 $\pm$ 1.1
B3 + 50 $\mu\text{g/L}$	449.4 $\pm$ 4.2	450.0 $\pm$ 3.3	451.8 $\pm$ 3.9
G1	654.6 $\pm$ 1.5	654.0 $\pm$ 3.3	653.0 $\pm$ 0.7
G2	143.7 $\pm$ 2.6	143.3 $\pm$ 1.9	144.0 $\pm$ 1.0
G3	47.7 $\pm$ 0.7	47.3 $\pm$ 1.9	46.9 $\pm$ 0.3
G4	96.3 $\pm$ 1.6	95.3 $\pm$ 1.9	95.9 $\pm$ 0.5
G1 + 50 $\mu\text{g/L}$	705.6 $\pm$ 4.7	700.7 $\pm$ 1.9	709.2 $\pm$ 2.9

**Table 3.7** YKL-40 detection in cell lysates from cancer patient: a comparison of the results from mYKL-40 capacitive immunosensing with those from ELISA (n=3).

<b>Samples</b>	<b>Immunosensor (<math>\mu\text{g/L}</math>)</b>	<b>In-house ELISA (<math>\mu\text{g/L}</math>)</b>	<b>Commercial ELISA (<math>\mu\text{g/L}</math>)</b>
THP-1	87.3 $\pm$ 1.5	86.0 $\pm$ 3.3	86.4 $\pm$ 2.2
293T	N.d.	N.d.	N.d.
293T + 50 $\mu\text{g/L}$	49.7 $\pm$ 0.2	50.5 $\pm$ 1.9	49.2 $\pm$ 0.3

N.d. = Not detection

## 3.2 Capacitive immunosensor for detection of YKL-39

### 3.2.1 Preparation of YKL-39 immunosensors

As above described in detail for the inspections in course of YKL-40 preparation (Chapter III, Section 3.1.3.1), the insulating properties of modified gold electrode have been inspected after individual preparation steps of YKL-39 immunosensor fabrication via cyclic voltammetry in ferricyanide-containing electrolytes. The gradual disappearance of the Fe (III)/Fe (II) redox peaks in the voltammograms again was taken as evidence of thiol monolayer assembly, antibody immobilization, and complete insulation reach via residual exposed electrode surface coverage with 1-dodecanethiol (Figure 3.40).

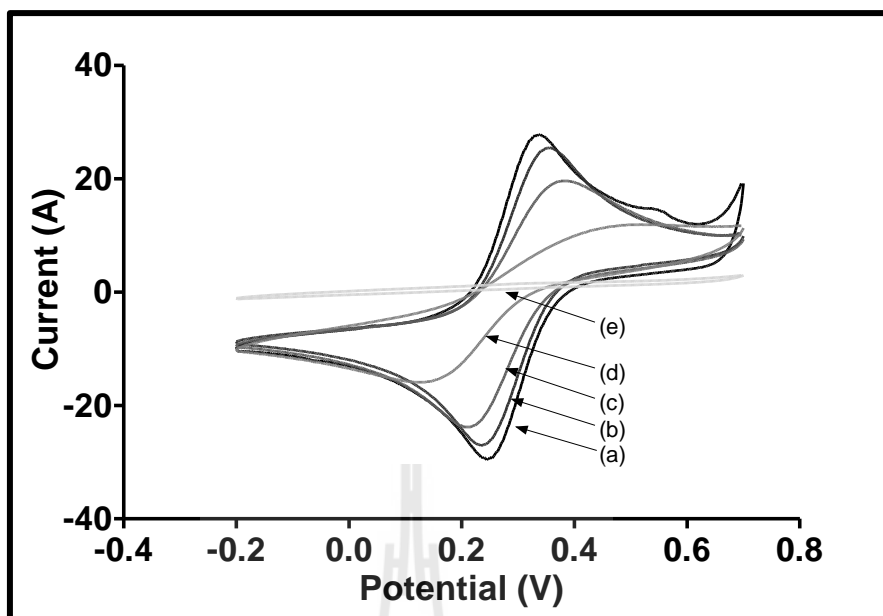


**Figure 3.40** Cyclic voltammograms of a gold electrode at various surface conditions. (a) clean (b) coated with a self-assembled thiourea monolayer, (c) after glutaraldehyde exposure of the thiourea film, (d) after anti-YKL-39 bonding to the glutaraldehyde-treated thiourea film and (e) after final treatment with 1-dodecanethiol.

### 3.2.2 Optimization of conditions for YKL-39 operation in the electrochemical flow cell

As for YKL-40 immunosensors, the experimental parameters affecting the performance of the capacitive immunosensor (now just with an YKL-39 antibody on the sensor surface) in the already introduced flow injection system was investigated and optimized to yield optimal analytical performance. Evaluations considered the regeneration solution, the running buffer, injected sample volume and flow rate. All measurements were carried out as above described in detail for the YKL-40 protein and were again performed in triplicate. The data of the optimization trials with YKL-39 immunosensors incorporating YKL-39 antibody are summarized in Figures 3.41 -

3.47. Optimal conditions for the operation of capacitive YKL-39 immunosensors were: regeneration solution, HCl solution, pH 2.5; running buffer, 25 mM sodium phosphate buffer, pH 7.0; sample volume, 200  $\mu$ L and flow rate, 100  $\mu$ L/min.

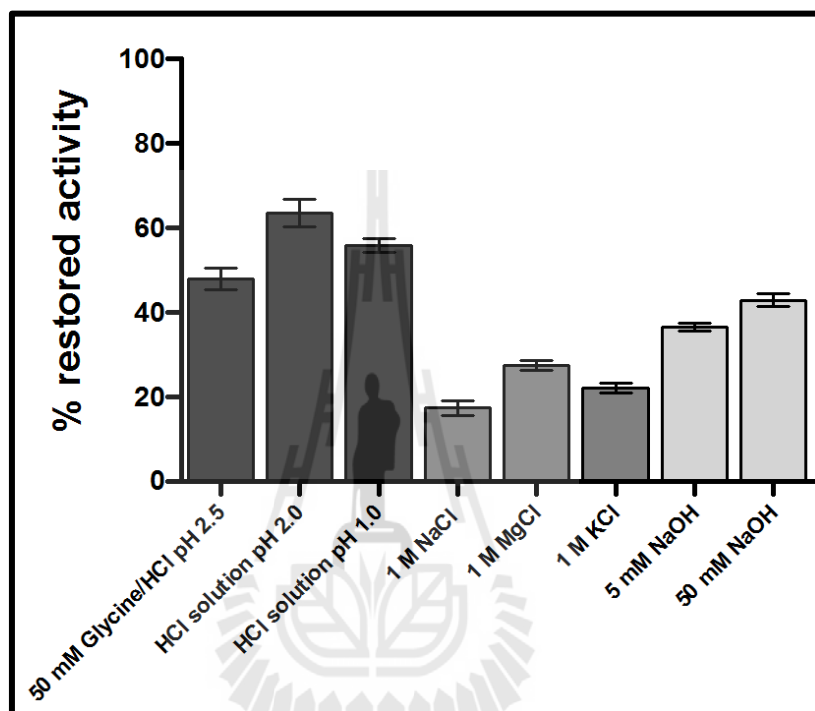


**Figure 3.41** Efficiency of different types of regeneration solutions. Percentage of restored activity is an expression that scales the amount of immobilized YKL-39 antibody that got released from YKL-39 antigen that had been captured in course of a measurement cycle; the higher the percentage of residual activity, the more antibody was free and successfully primed for capturing antigen again in the next analytical sample injection run.

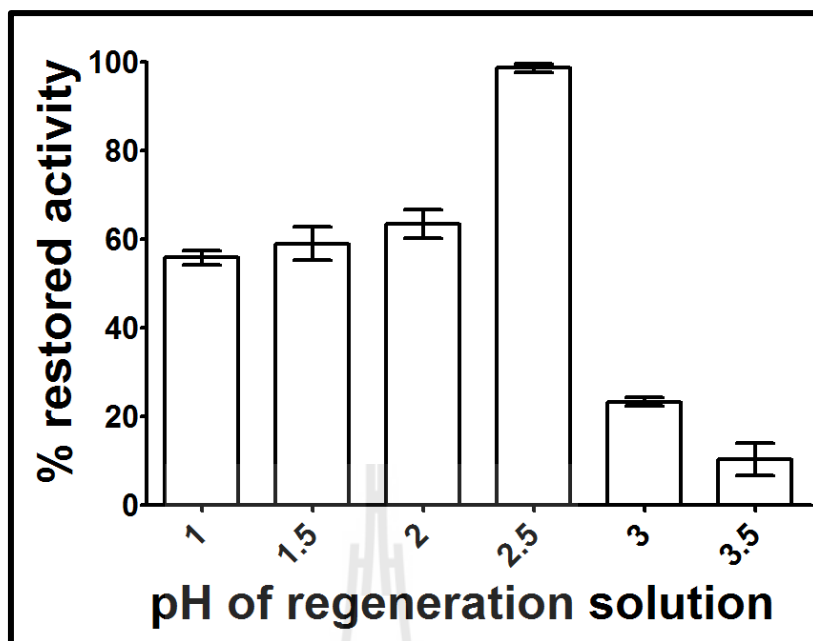


**Figure 3.42** The influence of the pH of the HCl regeneration solution on the efficiency of removal YKL-39 from anti-YKL-39 on a thiol-coated gold electrode.

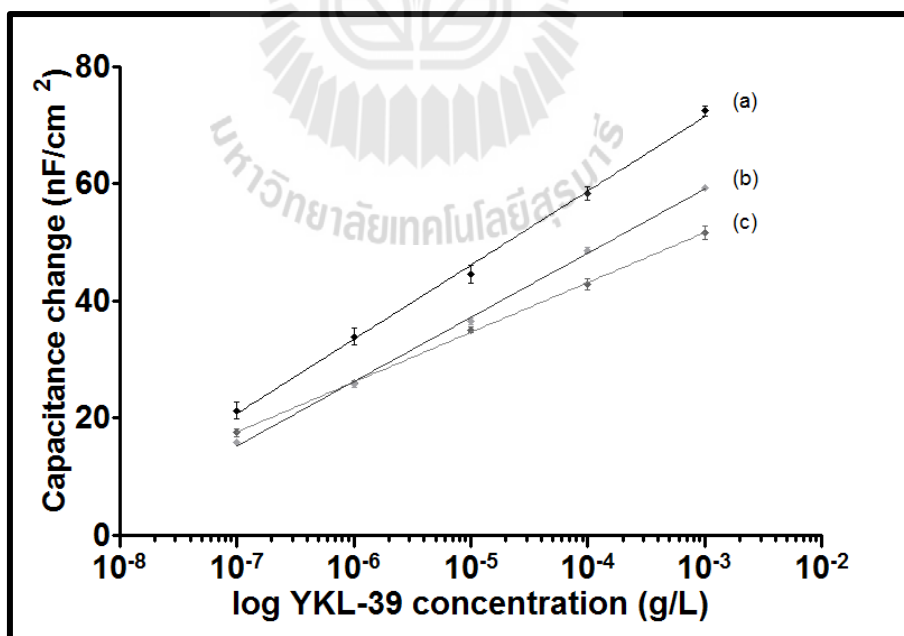


**Figure 3.43** The efficiency of YKL-39 capacitive immunosensors for different types of running buffer. (a) 10 mM sodium phosphate buffer, pH 7.0; (b) 10 mM HEPES buffer, pH 7.0; (c) 10 mM Tris-HCl buffer, pH 7.0.

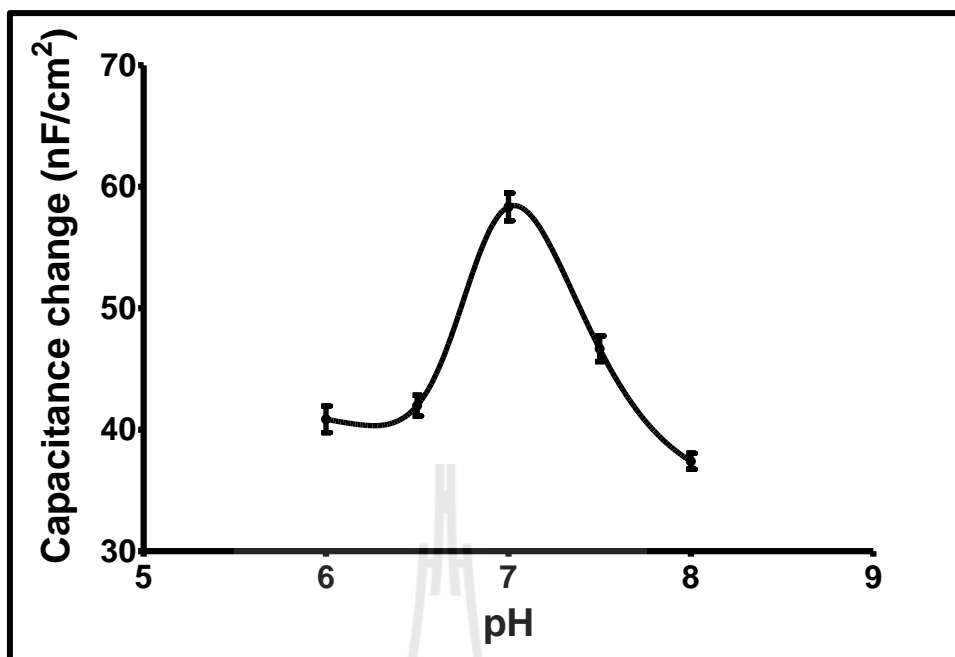


**Figure 3.44** The efficiency of YKL-39 capacitive YKL-39 immunosensors for applications with 10 mM sodium phosphate running buffer at different pH.

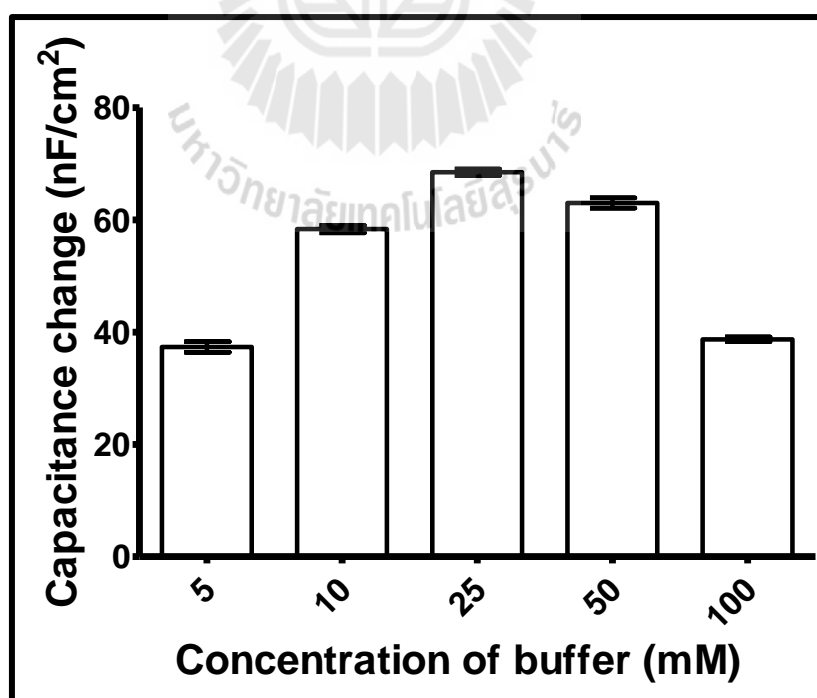


**Figure 3.45** The dependence of the efficiency of YKL-39 quantification on different salt concentrations of the sodium phosphate buffer, pH 7.0.

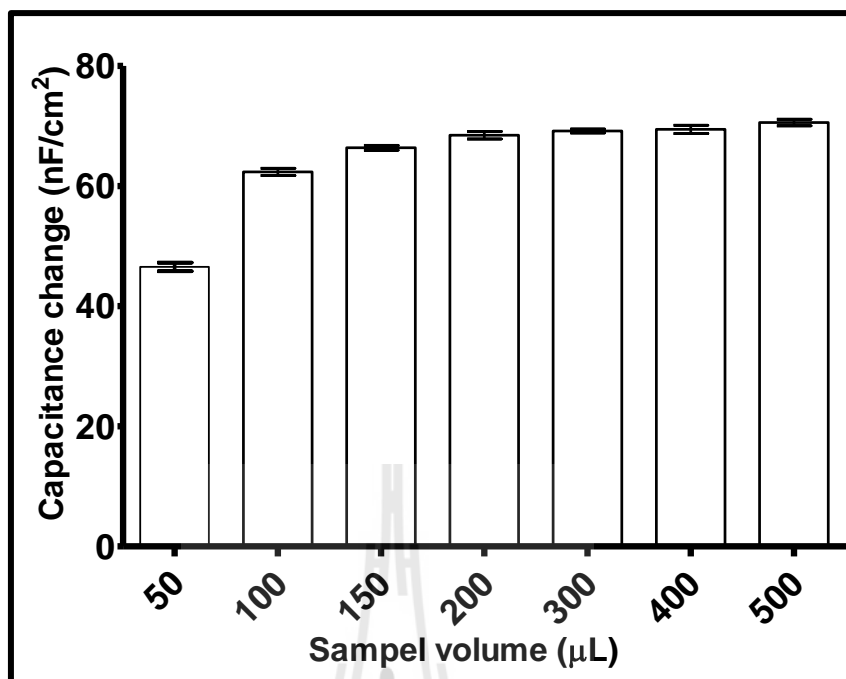


**Figure 3.46** The dependence of the efficiency of YKL-39 capacitive immunosensing on a variation of injected sample volume.

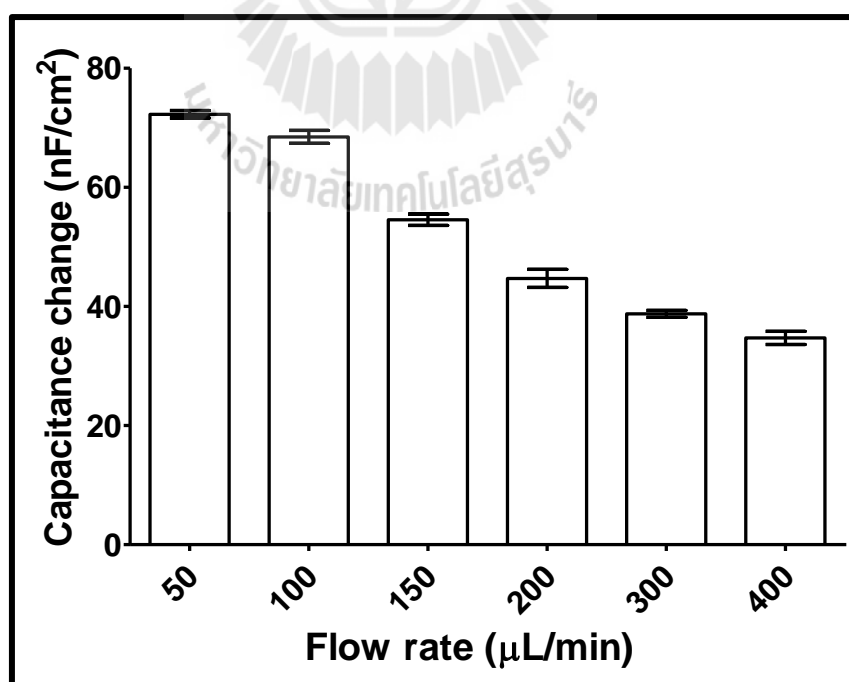


**Figure 3.47** The dependence of the efficiency of YKL-39 quantification with capacitive immunosensor readout for different running buffer flow rates.

### 3.2.3 YKL-39 immunosensor performance in the electrochemical flow cell

After the operational conditions for capacitive YKL-39 immunosensors were optimized, they were exposed at the identified best settings to analytical performance tests in the flow-based electrochemical workstation.

#### 3.2.3.1 Linearity range and limit of detection

To identify the practical linear range YKL-39 standard solutions of 1 ng/L to 100 mg/L were quantified by the capacitive immunosensor system. An example of the obtained calibration curves is shown in Figure 3.48. The triplicate measurements of all analyte concentrations revealed a linearity in between 0.1  $\mu\text{g/L}$  and 1 mg/L; the linear regression equation  $y = (16.1 \pm 0.4) \log(x) + (137.2 \pm 2.4)$  had a very good correlation coefficient of 0.99. As already observed for the anti-YKL-40/YKL-40 immunosensors, the magnitude of the capacitance change of YKL-39 in response to antigen injection reached plateau level for concentrations above 1 mg/L, because of the saturation of antibody entities on the sensor surface. To investigate the limit of detection the running buffer (25 mM sodium phosphate buffer, pH 7.0) was injected into the immunosensor for twenty times under the optimum conditions. The standard deviation of 20 blank results was obtained at 0.41 and slope of the regression line (from 0.1 to 10  $\mu\text{g/L}$ ) was obtained at 16.09. So, the limit of detection was calculated from Eq.2.4 that is the limit of detection was about  $0.07 \pm 0.02 \mu\text{g/L}$ .

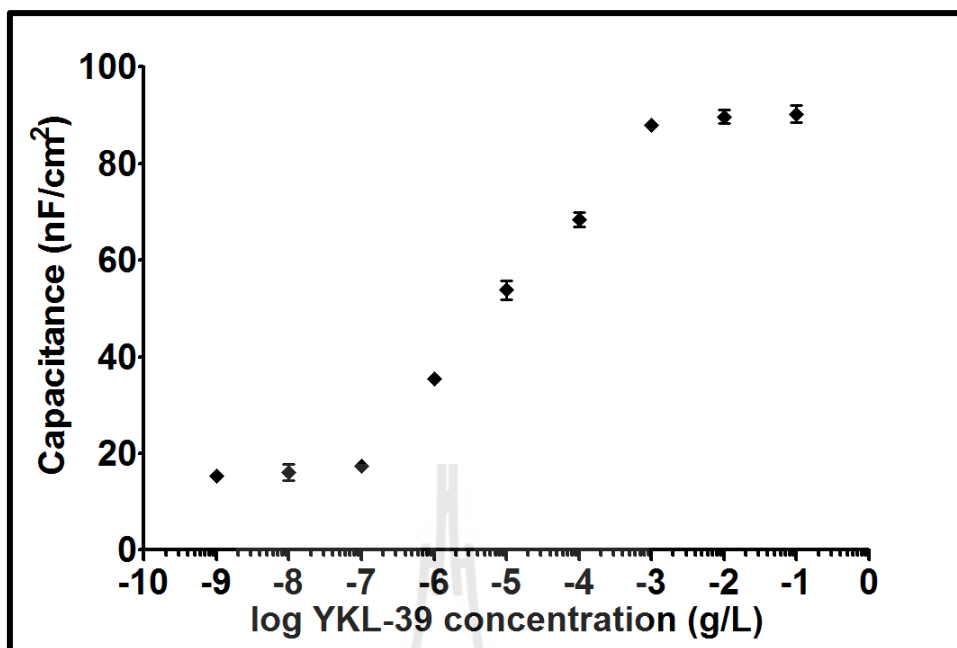


**Figure 3.48** Representation of a calibration curve as valid for routine capacitive YKL-39 immunosensing. Screened was the sensor response to injections of YKL-39 standard solutions of concentrations from 1 ng/L to 100 mg/L under pre-identified optimal operational conditions.

### 3.2.3.2 Stability of capacitive YKL-39 immunosensors

In similar manner as before done for YKL-40 capacitive immunosensors, YKL-39 was also subjected to a stability trial. Figure 3.49 shows a display of a plot of the percentage of restored activity of the anti-YKL-39 immobilized electrode as a function of the number of regeneration cycles at the time of measurement. Evident is that for more than 3 days (an equivalent of 49 cycles of analyte injection and immunosensor detection and regeneration) the percentage of restored activity was at a very good level of  $99.5 \pm 1.5\%$  (1.5% RSD) of the original capacitance change. The acquisition of almost identical cyclic voltammograms for sensors before and after the long-term stability test was an evidence of self-assembled thiolurea monolayer

intactness and indicated structural and/or biological function of antibody degradation as reason for a loss of antigen binding ability (Figure 3.50).

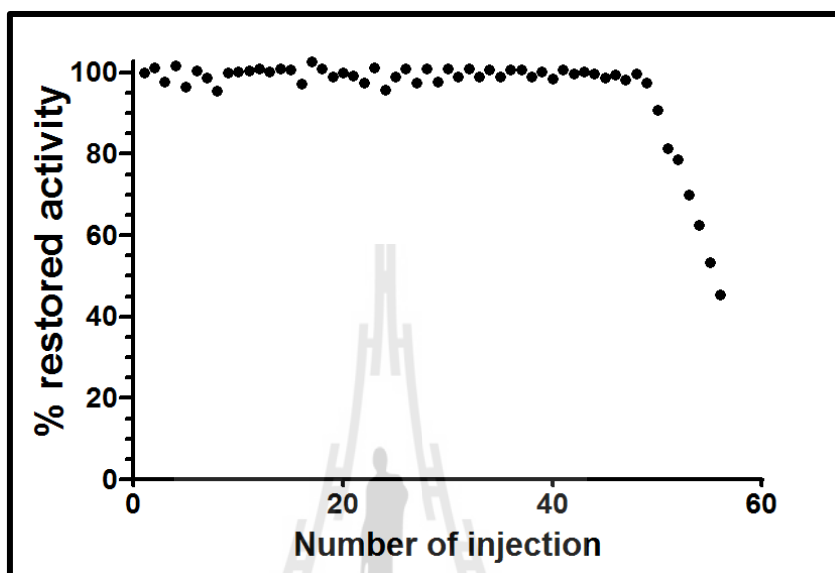


**Figure 3.49** Assessment of the stability of the signal during repeated cycles of sample injection and immunosensor regeneration.

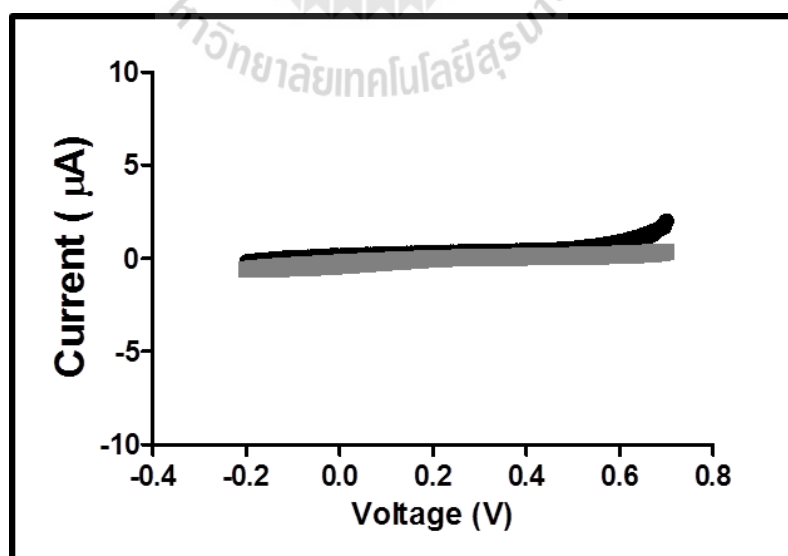


**Figure 3.50** The cyclic voltammograms in ferricyanide-containing electrolyte recorded before (black curve) and after (gray curve) the stability test.

### 3.2.3.3 The selectivity of YKL-39 immunosensors

Following the strategy handled for the selectivity tests on YKL-40 capacitive immunosensors, the YKL-39 capacitive immunosensors were tested in the flow-based capacitive immunosensor system with samples that had on top of the target analyte also the homolog proteins YKL-40 and AMCCase present. Tests were actually analytical calibration runs with the capacitive immunosensor system tried for the concentration range from 1 ng/L to 100 mg/L, under the optimal operation conditions. While YKL-40 and AMCCase in the tests did not produce capacitance changes larger than seen for injections of bare buffer solution, injections of the target analyte YKL-39 changed the capacitance as expected in noticeable and concentration-dependent manner (Figure 3.51). Conclusion was thus at this stage that YKL-40 and AMCCase presence do not cause interference problems, even though the two proteins are structurally and chemically very closely related to the target antigen YKL-39. The identified specificity made tests in model and real samples practical. They are described in the following sub-chapter.

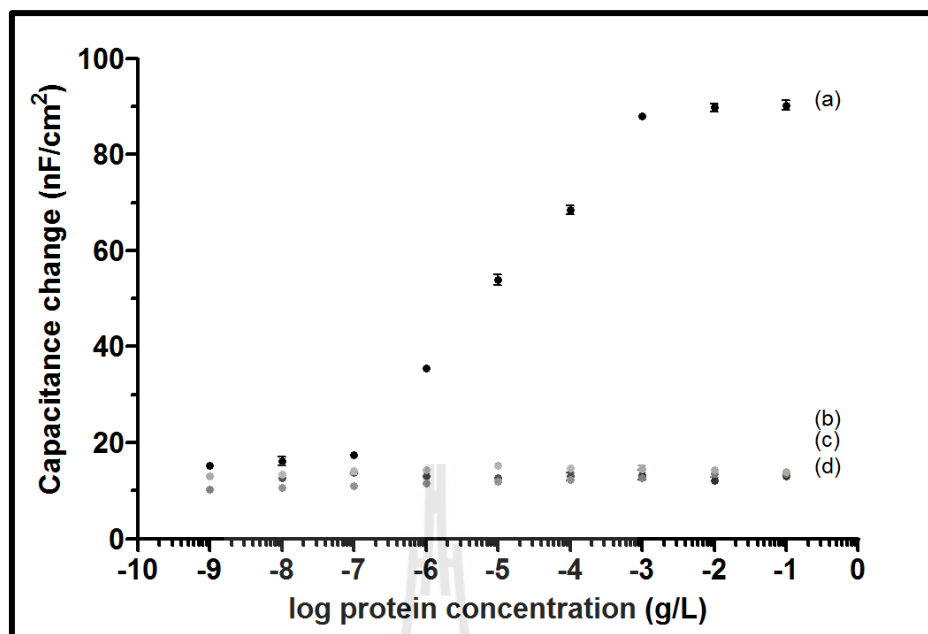


**Figure 3.51** Representative selectivity test for capacitive YKL-39 immunosensors. The anti-YKL-39 modified gold electrode was exposed either to its the target analyte YKL-39 and the proteins GH-18 members ( YKL-40 and AMCCase) and thus potential candidates as interfering species. The capacitance change, was evaluated under optimal assay conditions. (a), YKL-39; (b), YKL-40; and (c), AMCCase; (d), injections of blank running buffer solution.

### 3.2.4 Enzyme-linked immunosorbent assay for detection of YKL-39

The common method used for the detection of YKL-39 is ELISA technique. YKL-39 standard solutions of concentration range from 1 to 500  $\mu\text{g/L}$  were used for ELISA to investigate the linearity range and limit of detection. The linearity of the response was determined by plotting the calibration curve between  $A_{450}$  absorbance and YKL-39 concentration. Linearity was obtained from 2.5 to 125  $\mu\text{g/L}$  with the linear regression equation;  $y = (0.006 \pm 0.001) x + (0.04 \pm 0.01)$ , regression coefficient at 0.992 (Figure 3.52). The detection limit of the YKL-39 ELISA was 2.5  $\mu\text{g/L}$ .

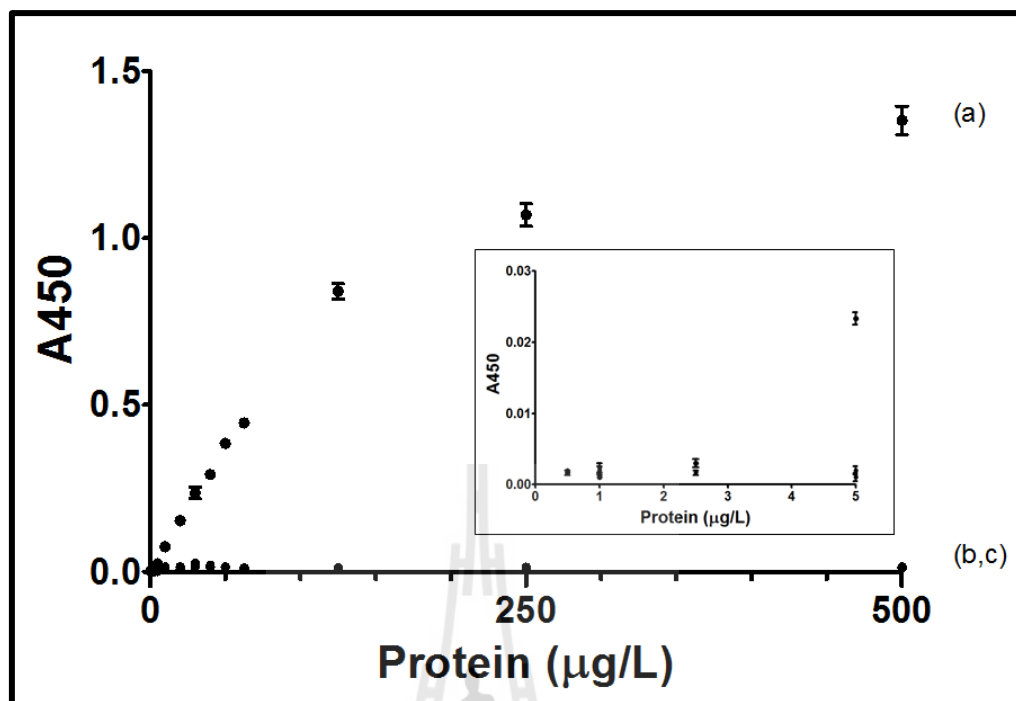


**Figure 3.52** YKL-39 ELISA technique. Binding of purified anti-YKL-39 IgG (50  $\mu\text{L}$ , 15  $\mu\text{g/L}$ ) to different concentrations of surface-attached YKL-39 related proteins: YKL-39 (a); YKL-39 (b); AMCase (c) and chitinases A (d). Inset shows the signal response at low concentration of YKL-39 and related protein.

### 3.4.5 Determination of YKL-39 in model and clinical samples

To get a first idea about the ability of YKL-39 immunosensor to quantify YKL-39 protein in samples with reasonable accuracy, a series of model samples were analyzed by using YKL-39 capacitive immunosensors and the results were compared with the YKL-39 ELISA. The model samples spanned the concentration range of 0.5 to 150  $\mu\text{g/L}$  and they were tested by the immunosensor system at the pre-identified optimum operational settings. The capacitance response to individual sample injections was used to compute corresponding sample concentration of YKL-39 from the calibration curve. The results from the trial on of model samples are shown in

Table 3.8. Capacitive YKL-39 immunosensors detected their target YKL-39 with a good percentage of recovery close to the ideal 100% and in agreement with the data from the comparative ELISA measurements. While capacitive immunosensing was able to handle the lowest (0.5 µg/L) and highest (150 µg/L) model sample YKL-39 levels, the ELISA failed for this two situations because the concentrations were out of the more limited linear range of the optical screen. This failure nicely demonstrated that the advantage of capacitive immunosensing of YKL-39 in terms of the gain of a broader linear range. For all other samples the application of statistically analysis (One-Way ANOVA,  $p < 0.05$ ) revealed that there were no systematic differences between the results obtained from capacitive YKL-39 immunosensing and ELISA. Based on the outcome of the model samples analysis, the methodology of YKL-39 capacitive immunosensing was applied with confidence for the quantitative analysis of the YKL-39 content in real/clinical samples (synovial fluid of osteoarthritis patients and cell lysates).

**Table 3.8** YKL-39 detection in model samples: a comparison of the results from YKL-39 capacitive immunosensing with those from ELISA (n=3).

Added ( $\mu\text{g/L}$ )	Immunosensor		ELISA	
	Found ( $\mu\text{g/L}$ )	Recovery (%)	Found ( $\mu\text{g/L}$ )	Recovery (%)
0.50	0.52 $\pm$ 0.01	103.93 $\pm$ 1.40	N.d.	N.d.
2.50	2.52 $\pm$ 0.03	100.75 $\pm$ 1.18	2.49 $\pm$ 0.08	99.56 $\pm$ 3.08
5.00	5.02 $\pm$ 0.19	100.47 $\pm$ 3.83	5.24 $\pm$ 0.13	104.89 $\pm$ 2.67
50.00	51.23 $\pm$ 0.32	102.47 $\pm$ 0.65	48.80 $\pm$ 1.39	99.60 $\pm$ 2.68
150.00	149.99 $\pm$ 2.48	100.00 $\pm$ 1.65	105.24 $\pm$ 0.80	70.16 $\pm$ 0.53

N.d. = Not detection

Four synovial fluids from osteoarthritis patients were obtained from Maharat Nakhon Ratchasima Hospital, Nakhon Ratchasima, Thailand and they were analyzed with capacitive YKL-39 immunosensing and the ELISA. Both analytical techniques were also used for YKL-39 quantifications in the cell lysates of Jurkat, U937, and 293T cells. Prior to quantification trials, YKL-39 presence was screened for by using an immunoblot assay. Figure 3.53B shows the immunoblot for detection of YKL-39 in the synovial fluid samples from osteoarthritis patients and in the chosen cell lysates. Obvious are strongly react with YKL-39 protein band for the synovial fluids and also for Jurkat and U937 cell lysates while the lysate of 293T cells did not produce a visible specific band for the YKL-39 protein.

Prior to quantitative analysis with the electrochemical or ELISA scheme, the synovial fluids and cell lysates were 10 times diluted with 25 mM sodium phosphate

buffer, pH 7.0 to minimize an adverse influence of non-targeted matrix components on signal generation. 200  $\mu$ L of the diluted samples were then injected into the immunosensor system under optimum conditions. Figure 3.54 displays the capacitance response of the anti-YKL-39 modified electrode upon injections of the various samples. The base-line capacitance of the sensor surface exposed to flowing running buffer was first recorded and stored (left-hand side, Figure 3.54). After samples injection, appearance of conjugate formation between YKL-39 and anti-YKL-39 should cause the sensor capacitance to decrease. All four synovial fluids, and the Jurkat and U937 cell lysates indeed induced a considerable capacitance decrease, whereas 293T cell lysates injection virtually left the capacitance signal unchanged (the capacitance signal same with blank control). These observations are in good agreement with the findings made via western blot analysis (Figure 3.53B). The YKL-39 levels from the determination of the various samples are shown in Table 3.9. Both used methods measured the levels of YKL-39 in synovial fluid of osteoarthritis patients and Jurkat and U937 cell lysates similarly. The absence of YKL-39 in 293T cell lysates was also signaled by both analytical schemes. A comparison of the data from capacitive immunosensing and ELISA via One-Way ANOVA analysis ( $p < 0.05$ ) suggested that they determined the level of YKL-39 with good statistical correlation.

In a final trial YKL-39 at levels of 20 and 30  $\mu$ g/L where added to otherwise YKL-39 free 293T cell lysates and the spiked concentrations were determined or percentage of recovery assessments by the YKL-39 capacitive immunosensor and the ELISA. The results of these measurements are shown in Table 3.10. The valid percentage of recovery was close to the ideal 100% for both techniques, which was

further evidence that capacitive YKL-39 immunosensing functions well as alternative option to the common ELISA.

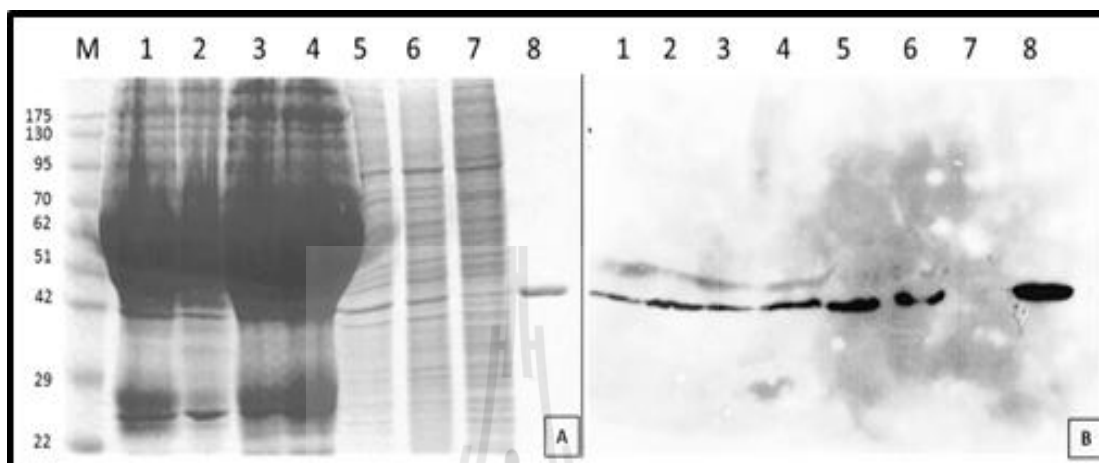


**Figure 3.53** Detection of YKL-39 in real/clinical samples by immunoblot assay. Lane M, protein marker; Lane 1 – 4, synovial fluid from four osteoarthritis patient; Lane 5, Jurkat cell lysates; Lane 6, U937 cell lysates; Lane 7, 293T cell lysates; Lane 8, YKL-39 (2  $\mu$ g) were resolved on a 12% SDS-PAGE. (A) Coomassie-blue stained gel. (B) Immunoblot detected with anti-YKL-39 polyclonal antibody (1:10,000 dilution).

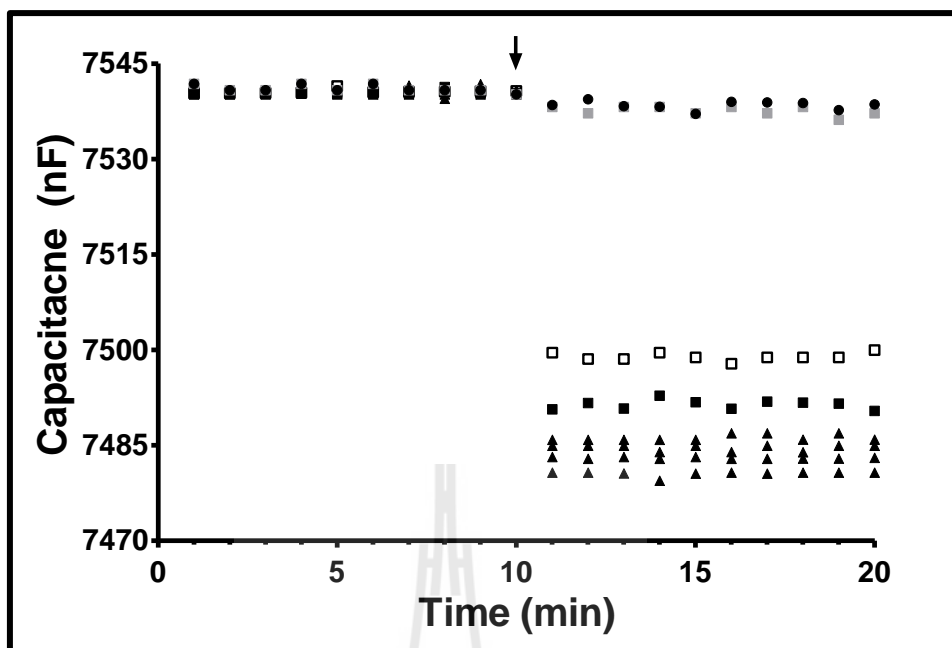


**Figure 3.54** Capacitance response of anti-YKL-39-modified electrode. The samples were injection (black arrow) into the flow buffer produce a decreasing of capacitance.

●, Blank (running buffer); ■, Jurkat cell lysates; □, U937 cell lysates, ■, 293T cell lysates; ▲ *osteoarthritis* patient 1 - 4.

**Table 3.9** YKL-39 detection in clinical samples: a comparison of the results from YKL-39 capacitive immunosensing with those from ELISA (n=3).

Samples	Immunosensor	ELISA
	( $\mu\text{g/L}$ )	( $\mu\text{g/L}$ )
Synovial fluid # 1	59.4 $\pm$ 2.4	58.3 $\pm$ 3.4
Synovial fluid # 2	106.3 $\pm$ 0.8	107.0 $\pm$ 2.5
Synovial fluid # 3	68.1 $\pm$ 1.3	67.7 $\pm$ 1.2
Synovial fluid # 4	89.0 $\pm$ 2.7	88.8 $\pm$ 1.6
Jurkat	26.4 $\pm$ 0.4	25.2 $\pm$ 3.1
U937	10.6 $\pm$ 0.3	9.8 $\pm$ 0.8
293T	N.d.	N.d.

N.d. = Not detection

**Table 3.10** YKL-39 detection in spiked 293T cell lysate: a comparison of the results from YKL-39 capacitive immunosensing with those from ELISA (n=3).

Added ( $\mu\text{g/L}$ )	Immunosensor		ELISA	
	Found	Recovery	Found	Recovery
	( $\mu\text{g/L}$ )	(%)	( $\mu\text{g/L}$ )	(%)
0	N.d.	-	N.d.	-
20	20.2 $\pm$ 0.4	100.8 $\pm$ 2.2	20.5 $\pm$ 0.5	102.4 $\pm$ 1.8
30	29.7 $\pm$ 0.2	99.1 $\pm$ 0.7	30.4 $\pm$ 0.5	101.2 $\pm$ 1.2

N.d. = Not detection

## CHAPTER IV

### DISCUSSION

#### 4.1 Capacitive immunosensor for detection of YKL-40

Firstly, YKL-40 protein was expressed in bacterial and mammalian expression systems. The recombinant YKL-40 was expressed in the *E. coli* M15 (pREP) strain and 293T cell line. In bacterial expression system, the bulk of induce YKL-40 protein was insoluble, suggesting that it was present in inclusion bodies. The insoluble YKL-40 protein was solubilized in 8 M urea and the YKL-40 fraction was further purified by using Ni-NTA agarose column. Whereas in mammalian expression system, the YKL-40 protein was solubilized in culture medium and the YKL-40 protein was further purified by affinity chromatography using a Ni-NTA agarose column. The molecular weight of the purified YKL-40 estimated from SDS-PAGE was consistent with the molar weight expected for human YKL-40 lacking the 20 amino acid signal peptide, with the predicted MW of 40,488 Da.

The both of purified YKL-40 protein were used for the production of anti-YKL-40 polyclonal antibody. The both of polyclonal antiserum strongly reacted with YKL-40 and evaluation of cross-reactivity against other member of GH-18 revealed no interaction of the both of polyclonal antiserum with YKL-40 homologues such as YKL-39, AMCcase and bacteria chitinases. The results confirmed that the raised both of polyclonal antiserum was specific for the YKL-40 protein. The both of anti-YKL-

40 antiserum were fractionated by affinity chromatography on protein A agarose. SDS-PAGE analysis showed that the purified anti-YKL-40 migrated behind the 130 kDa protein marker under non-reducing condition, indicating the whole molecule of IgG isotype (MW ~150 kDa), while two bands of about 55 kDa and 25 kDa were observed under denaturing condition indicating the heavy chain (MW ~50 kDa) and light chain (MW ~25 kDa) of the IgG isotype. Western blot analysis of the purified bacterial-anti-YKL-40 antibody and mammalian-anti-YKL-40 antibody reacted strongly with YKL-40 down to 0.175 mg/L and 0.250 mg/L, respectively, whereas pre-immune serum showed no reaction. Cross reactivity of both of purified anti-YKL-40 antibody showed no signal with YKL-39, AMCCase and bacteria chitinase. This indicated that YKL-40 protein was highly specific and strongly reactive polyclonal antibodies against the protein of interest and hence suitable for use in electrochemical YKL-40 immunodetection.

The YKL-40 antibody was immobilized on gold disk working electrodes by covalent coupling with thiourea and glutaraldehyde. The electrochemical characteristics of modified electrodes were investigated after each assembly step. The quality of the thiol-based electrode surface insulation was examined with an exposure to a solution of 5 mM  $K_3[Fe(CN)_6]$  in 100 mM KCl and an acquisition of the cyclic voltammograms for the reversible  $[Fe(CN)_6]^{3-}/[Fe(CN)_6]^{4-}$  redox conversion. The cleaned gold working electrode routinely showed the expected oxidation and reduction peaks of the redox couple. The redox peaks decreased more and more when first thiourea was self-assembled on the clean gold surface, the glutaraldehyde was fixed to the thiol layer, and finally anti-YKL-40 was covalently linked and added to the surface layout. This trend was a sign that the insulating properties of the electrode

increased with cumulative levels of surface modification. However, the remaining small electrochemical activity of the immunosensor surface after antibody immobilization could still be a problem with capacitance-based measurements of antigen binding. The modified electrode surface was thus treated with 1-dodecanethiol to block residual bare gold surface and tune the immunosensor for the pure capacitive current recordings in YKL-40 quantification trials.

To gain highest performance of the newly-established bacterial-YKL-40 capacitive immunosensing setting, several parameters were optimized.

Regeneration step to stabilize and regain the current signals for multiple uses of the prepared electrode seem to be critical. It was found that low pH (HCl) gave the highest percentage of residual activity. This probably causes the antigen bind to the antibody through weak interactions, such as hydrogen bonds (Subramanian, Irudayaraj, and Ryan, 2006) as well as electrostatic interactions, hydrophobic interaction and Van der Waals interactions (Byfield and Abuksha, 1994). Such bonds can be removed lowering/raising pH in cause of protonation and deprotonation (Limbut, Hedström, Thavarungkul *et al.*, 2007). HCl solution was also used as the regeneration solution by other immunosensing set up such as Loyprasert *et al.*, (2008). In their report, HCl solution pH 2.5 (3.16 mM) show to provide the recovery, with the residual activity reaching almost 100% after 43 cycles of regeneration. The percentage of residual activity was decreased with the increase concentration of HCl solution, which may cause by the denaturation of the antibody due to low pH solution (Blackburn, Shah, Kenten *et al.*, 1991).

When types of running buffer were tested, 10 mM sodium phosphate buffer, pH 7.0 gave the highest capacitance response and sensitivity because the ionic

strength of sodium phosphate buffer was higher than that of Tris-HCl and HEPES, which was directly related to the ionic strength (Skoog, West, and Hollar, 1996; Bezerra *et al.*, 2003) and the binding affinity between the two binding partners that is known to be pH-dependent (Boehm, Corper, Wan *et al.*, 2000). The association and dissociation affinity binding the Ag-Ab interactions are favored by low ionic strength and neutral pH of buffer whereas high ionic strength and extreme pH of buffer cause the antigen-antibody dissociation (Ramos-Vara, 2005).

In flow injection capacitive immunosensor system, the flow rate is one of the factors affecting the yield of the interactions occurring on the electrode surface. At low flow rate the antigen had longer time to bind with the antibody. Hence, the change of capacitance increased when the flow rate decreased. In our results, the maximum capacitive responses were observed between 50 and 100  $\mu\text{L}/\text{min}$ . However 100  $\mu\text{L}/\text{min}$  was chosen to reduce the data acquiring time to 35 min compared to 60 min when the lower flow rate was applied.

The last parameter to be tested was sample volume. Large sample volume that was injected into the capacitive immunosensor system led to an increase the amount of YKL-40 molecules, thereby increasing the probability of interactions on the anti-YKL-40 immobilized electrode. A sample volume of 200  $\mu\text{L}$  was test to be the best.

In summary the optimum condition of bacterial-YKL-40 immunosensor are carrier buffer 10 mM sodium phosphate buffer, pH 7.0, regeneration solution HCl solution at pH 2.5, flow rate 100  $\mu\text{L}/\text{min}$  and sample volume 200  $\mu\text{L}$ . Whereas mammalian-YKL-40 immunosensor are carrier buffer 25 mM sodium phosphate buffer, pH 7.0, regeneration solution HCl solution, pH 2.5, flow rate 100  $\mu\text{L}/\text{min}$  and

sample volume 250  $\mu\text{L}$ . These optimum operational conditions were used to evaluate the performance of the system.

Sequential injections of YKL-40 standard solution (concentrations varied from 0.01  $\mu\text{g/L}$  to 10  $\text{mg/L}$ ) were injected into the capacitive immunosensor system under the optimal operational condition. The both of YKL-40 immunosensors, gave a linear dynamic range between 0.1  $\mu\text{g/L}$  and 1  $\text{mg/L}$ , following the equation  $y = (12.3 \pm 0.3) \log x + (107.4 \pm 1.4)$ , with the limit of detection was  $0.07 \pm 0.01 \mu\text{g/L}$  in bacterial-YKL-40 immunosensor and  $y = (19.9 \pm 0.5) \log (x) + (156.3 \pm 0.6)$ , with the limit of detection was  $0.08 \pm 0.02 \mu\text{g/L}$  in mammalian-YKL-40 immunosensor. At higher concentrations the signal became constant, indicating that all immobilized anti-YKL-40 molecules were occupied with the YKL-40 antigen.

The reproducibility and signal stability of the anti-YKL-40 modified electrode were investigated by continuously detecting changes in capacitance at fixed concentration of YKL-40 after applying HCl solution, pH 2.5 in the regeneration step. The electrode could be used up to 40 times and suitable for 3 days in bacterial-YKL-40 immunosensor whereas, 50 times and suitable for 4 days for mammalian-YKL-40 immunosensor with the percentage of residual activity of higher than 95% (%RSD < 5). To prove that the percentage of residual activity was decreased due to the self-assembled monolayer on anti-YKL-40 modified electrode being destroyed by the regeneration solution. The electrode was tested by cyclic voltammogram measurement. The voltammogram of anti-YKL-40 modified electrode before and after used were nearly the same, indicating that the self-assembled monolayer still remained on the gold surface but after 40 times of electrode recycling, the decrease of

the percentage of residual activity was seen, most likely caused by the loss of the anti-YKL-40 antibody activity.

When the YKL-40 homologs (YKL-39 and AMCCase) were used to test the selectivity of the system, only slight changes in the capacitance change were observed as compared with the changes obtained from YKL-40. The results showed that the both of anti-YKL-40 modified electrode were specific to only to the target analyte.

The reliability of the bacterial-YKL-40 immunosensor was accessed by spiking different concentrations of YKL-40 (0.5 to 50  $\mu\text{g/L}$ ) using the flow injection system. The values obtained from the capacitive immunosensor were measured the samples concentrations of YKL-40 were found in the same range of the injected concentrations (0.5 to 50  $\mu\text{g/L}$ ), and the percentages of recovery from the capacitive immunosensor and were in the range of  $99.15 \pm 2.63$  to  $102.16 \pm 1.57$ . When serum YKL-40 samples were determined, the concentrations and the percentages of recovery obtained from the capacitive immunosensor were well correlated with those from the ELISA technique (One-Way ANOVA,  $p < 0.05$ ).

The reliability of the mammalian-YKL-40 immunosensor system, the model samples was spiked at different concentrations of YKL-40 (30 to 150  $\mu\text{g/L}$ ); the concentration of YKL-40 was determined by capacitive immunosensor and ELISA technique. The concentrations and the percentages of recovery obtained from the capacitive immunosensor were well correlated with those from the ELISA technique (One-Way ANOVA,  $p < 0.05$ ). There is no evidence for systematic difference between the results obtained from the capacitive immunosensor system, in-house ELISA and commercial ELISA. These results indicated that the developed YKL-40 capacitive immunosensor is well suited for analysis for YKL-40 in clinical samples.

However, the bacterial-YKL-40 capacitive immunosensor did not detect levels of YKL-40 in healthy serum (see Table 3.5); normally, the serum levels of YKL-40 in healthy person was about 40  $\mu\text{g/L}$  (Johansen *et al.*, 1995 and 2003, and Dupont *et al.*, 2004). Hence, mammalian-YKL-40 immunosensor was selected for all detections in clinical samples.

In the initial clinical trials with YKL-40 immunosensors serum samples from 4 healthy persons, namely H1-H4, were screened for their YKL-40 content. The provided blood serum was measured in 10 times dilution to reduce the matrix effect from other dissolved protein. The three analysis techniques confirmed the YKL-40 concentration in the serum of the healthy persons as 51 to 75  $\mu\text{g/L}$ . A statistical data analysis furthermore revealed that there was no significant difference between the electrochemical and the conventional optical YKL-40 assaying, since the One-Way ANOVA,  $p < 0.05$ , fulfilling the criteria for absence of problematic significant differences. In brief, the developed YKL-40 immunosensor system presents a suitable option for the detection of YKL-40 level in human serum.

Since evaluated levels of YKL-40 has been reported in several types of cancer such as breast cancer, colorectal cancer, ovarian cancer, small cell lung cancer, prostate cancer, and glioblastoma. So, we chose two type of cancer (breast cancer and glioblastoma) as a model for testing with YKL-40 immunosensor system with clinical samples. The level of YKL-40 in breast cancer patients were 40 to 400  $\mu\text{g/L}$  and glioblastoma patients were 50 to 650  $\mu\text{g/L}$ . To confirm the level of YKL-40 in breast cancer patients (B3) and glioblastoma patients (G1) by spiked 50  $\mu\text{g/L}$  of the YKL-40 into the obtained concentration. The values were comparable between the capacitive and other two ELISA techniques (One-Way ANOVA,  $p < 0.05$ ) as shown in Table

3.6, indicating that the consistency of the estimated YKL-40 concentrations in clinical samples. Similar results were observed with the estimated YKL-40 from human cells lines, which confirmed of reliable performance our immunosensing setup.

However, the biological function of YKL-40 in cancer diseases is still unknown. It has been hypothesized that YKL-40 is a growth factor of cancer cells or protects them from undergoing apoptosis. High preoperative serum level of YKL-40 in patients with primary breast cancer was an independent prognostic variable of short recurrence-free interval and short overall survival when axillary lymph node and estrogen receptor status, age, tumor size and histology, menopausal status, and serum YKL-40 were included in the multivariate Cox analysis (Johansen *et al.*, 2003). However, elevated levels of serum YKL-40 in patients with breast cancer at the time of first recurrence predicted shorter time to progression and shorter overall survival (Jensen *et al.*, 2003). High preoperative serum level of YKL-40 in patients with colorectal cancer was also a prognostic variable of short recurrence-free interval and short overall survival (Cintin *et al.*, 1999). In patients with stage III ovarian cancer, a high preoperative plasma concentration of YKL-40 was an independent prognostic variable of short survival (Høgdall *et al.*, 2003) and patients with early stage ovarian cancer and high serum YKL-40 had a poor prognosis (Dupont *et al.*, 2004). Similar results were found in patients with a recurrence of ovarian cancer (Denh *et al.*, 2003). An elevated serum YKL-40 level was also an independent prognostic variable of short survival in patients with metastatic prostate cancer (Brasso *et al.*, 2006), in patients with metastatic renal cell carcinoma (Geertsens, Johansen, van der Maase *et al.*, 2003), and in patients with metastatic malignant melanoma (Schmidt, Johansen, Gehl *et al.*, 2006). In patients with small cell lung cancer, a high serum YKL-40 at the time of

diagnosis and before chemotherapy was a variable for death within the following 6 months (Jensen *et al.*, 2004). There are no studies of serum YKL-40 levels in patients with glioblastoma and prognosis, but high YKL-40 gene protein (Pelloski, Mahajan, Maor *et al.*, 2005) expressions in glioblastoma tumor samples were related to short survival. Furthermore, high YKL-40 protein expression in glioblastoma tumor samples was associated with poorer radiation response and shorter time to progression (Pelloski *et al.*, 2005). In all eight types of solid cancer tested until now, a high serum YKL-40 level was related to poor prognosis. These results suggest that serum YKL-40 may be a useful “prognostic biomarker”.

One study of curatively operated colorectal cancer patients has evaluated serum YKL-40 levels during the follow-up after surgery (Cintin *et al.*, 2002). It was found that patients with elevated serum YKL-40 6 months after the operation had significantly shorter recurrence-free intervals and overall survival than patients with normal serum YKL-40 at 6 months postoperative. This result was independent of serum carcinoembryonic antigen levels at 6 months postoperative. Multivariate Cox analysis scoring serum YKL-40 as a time-dependent covariant and including age, Dukes' stage, gender, and tumor localization showed that a high serum YKL-40 postoperatively in curatively operated colorectal cancer patients increased the risk of recurrence within the following 6 months by 6.9-fold, and the risk of death within the following 6 months by 8.5-fold (Cintin *et al.*, 2002). The results of this study indicate that serum concentrations of YKL-40 may be useful for the monitoring of cancer patients.

In summary, the elevated plasma YKL-40 levels, compared to age-matched healthy subjects, are found in cancer patients with 13 different types of cancer have

shown that high pretreatment plasma levels of YKL-40 is related to poor prognosis. Highest plasma YKL-40 levels are found in patients with metastatic cancer and plasma levels of YKL-40 provides independent information of recurrence and progression free survival and of overall survival. The potential values of plasma YKL-40 as a biomarker in monitoring and screening of cancer need more studies, and its value in combinations with other biomarkers has to be determined. It is likely that plasma YKL-40 should be combined in panels of biomarkers for optimal clinical use, since most biomarkers will probably individually lack optimal sensitivity and specificity. A study of patients with pancreatic cancer suggests that this may be useful. However, YKL-40 is not cancer specific, and high plasma YKL-40 levels are also found in patients with diseases characterized by inflammation, tissue remodelling and fibrosis. Co-morbidity should therefore always be considered in cancer patients.

#### **4.2 Capacitive immunosensor for detection of YKL-39**

To obtain the best possible analytical performance, the experimental parameters affecting YKL-39 capacitive immunosensor system were optimized. Optimum conditions were: carrier buffer 25 mM sodium phosphate buffer, pH 7.0, regeneration solution HCl solution, pH 2.5, flow rate 100  $\mu\text{L}/\text{min}$  and sample volume 200  $\mu\text{L}$ . These operational conditions were used in all trials evaluating the performance of the system.

To identify the practical linear range, YKL-39 standard solutions of 1 ng/L to 100 mg/L were quantified by the immunosensor system. In the calibration curves (plots of the capacitance change normalized to the geometric sensor area and the logarithm of YKL-39 concentration) the linear regression line drawn by standard

software followed the equation  $y = (16.1 \pm 0.4) \log x + (137.2 \pm 2.4)$  with a correlation coefficient of 0.99. Linearity between the capacitance change and the logarithm of YKL-39 concentration was valid from 0.1  $\mu\text{g/L}$  to 1  $\text{mg/L}$ . The computed limit of detection of capacitive YKL-39 immunosensor was about  $0.07 \pm 0.02 \mu\text{g/L}$ .

Reproducibility was investigated at optimum conditions by continuously detecting the change of capacitance at the same concentration of standard YKL-39 (10  $\mu\text{g/L}$ ) with subsequent regeneration (HCl solution, pH 2.5) after each measurement to remove YKL-39 from the immobilized anti-YKL-39 on the electrode. The capacitance change after regeneration was used to calculate the percentage of restored activity of an anti-YKL-39 immobilized electrode. It became clear that a modified YKL-39 sensor can be regenerated and reused with good reproducibility for up to 49 times. The electrode was tested by cyclic voltammetry before first and after last sample injection. The two voltammograms were similar. This means that the decrease in the restored activity after the 49<sup>th</sup> injection was not due to the loss and/or destruction of the self-assembled monolayer but probably caused by the loss of anti-YKL-39 activity.

Two protein homologues of YKL-39 (YKL-40 and AMCCase) were used to test the selectivity of the capacitive immunosensor system at concentration of 1  $\text{ng/L}$  to 100  $\text{mg/L}$ . As expected for an YKL-39 immunosensor, the capacitive response to YKL-39 increased with the analyte concentration. In contrast, the responses of YKL-40 and AMCCase were the same for all tested concentrations and in line with the residual response triggered by injections of blank solution (running buffer). Therefore it can be concluded that there a presence of the most critical interferences would not interfere with the detection of YKL-39 and the YKL-39 capacitive immunosensor

system indeed gained high specificity to YKL-39 protein from the choice of antibody/antigen conjugation for signal generation.

The routine option for the detection of YKL-39 is ELISA technique. From the calibration curves (the 450 absorbance vs. concentration) the linearity of optical YKL-39 ELISA assaying was revealed as 2.5 to 125  $\mu\text{g/L}$  and the detection limit of the method was 2.5  $\mu\text{g/L}$ . The comparison of the linearity range and the detection limit of YKL-39 capacitive immunosensing and YKL-39 ELISA screening, suggested a wider linear range and lower limit of detection for the electrochemical approach.

Standard concentrations of YKL-39 in range of 0.5 to 250  $\mu\text{g/L}$  were injected in form of model samples into the immunosensor system, of course under the optimum condition. Model samples were detected accurately and with good percentage of recovery for the concentration 0.5, 5, 25, 50 and 250  $\mu\text{g/L}$ , whereas the indirect ELISA technique could handle only concentrations of 5, 25, and 50  $\mu\text{g/L}$  with good percentage of recovery. Apparently, the established capacitive YKL-39 immunosensing offered an enhanced quality of quantification over a wider range of analyte levels, which is an asset if working with clinical samples of unknown YKL-39 content.

YKL-39 is currently recognized as a promising biochemical marker for the activation of chondrocytes and the progress of the osteoarthritis in human (Knorr *et al.*, 2003). YKL-39 protein was, for instance, found at elevated level in synovial fluid from osteoarthritis patient and Jurkat and U937 cell lysates (Ranok *et al.*, 2013). It was thus made a task to check the synovial fluid from a number of confirmed osteoarthritis patients, as well as lysates from Jurkat and U937 cells with the new YKL-39 selective capacitive immunosensors for the biomarkers levels and compare

the acquired data with the outcome of comparative assessments with an ELISA screen. In a pre-screen by an immunoblot assay, YKL-39 was detected in the synovial fluid all four samples from the osteoarthritis patients, in the Jurkat and also U937 cell lysates; the lysate from 293T cells, however, did not produce the specific band of the target protein.

Since synovial fluid and cell lysates are complex mixtures of a variety of biochemical species the liquids were not straight used for capacitive and ELISA analysis but subjected to a 10 fold dilution with 25 mM sodium phosphate buffer, pH 7.0 first in order to minimize contributions of non-targeted matrix components to signal generation. Both the electrochemical capacitive and the optical ELISA methods quantified YKL-39 in the synovial fluid of osteoarthritis patients between 59 and 106  $\mu\text{g/L}$ . Their application to an analysis of Jurkat and U937 cell lysates revealed 26 and 10  $\mu\text{g/L}$ , respectively, whereas, the 293T cell lysate was reported to be YKL-39 free. Finally, the two methods reported the absence of YKL-39 in 293T cell lysates. Altogether, these results were in good agreement with own immunoblot control measurement and also confirmed what was known from the literature survey of the subject. 293T cell lysates spiked with 20 and 30  $\mu\text{g/L}$  of YKL-39 presented another type of model sample that the proposed immunosensor scheme was applied to adjust YKL-39 concentrations of 20 and 30  $\mu\text{g/L}$  were quantified with the capacitive immunosensors and control ELISA with a percentage of recovery that was close to 100%. The values were comparable between the capacitive and ELISA techniques (One-Way ANOVA,  $p < 0.05$ ) as shown in Table 3.9 and 3.10. This commonly good recovery was another proof that capacitive YKL-39 immunosensors were well-

working analytical tools for quantitative and qualitative identification of the presence of a renowned osteoarthritis biomarker in real biological sample environment.

The observed equivalency in performance for all measurements on the samples of this study is good evidence that capacitive electrochemical immunosensing in general functions well and has the potential to be used as a competitive alternative option for laboratories aiming on an effective analysis of disease markers related to human chitinase-like proteins.



## CHAPTER IV

### CONCLUSION

The recombinant YKL-40 polypeptide lacking its 20-amino acid signal sequence was successfully expressed in an insoluble form with *E. coli* strain M15 (pREP) as host. The protein was expressed as a His8/YKL-40 fusion protein with the total molecular weight of approximately 40 kDa. The insoluble YKL-40 protein was solubilized in 8 M urea and further purified by Ni-NTA agarose affinity column chromatography. Purified YKL-40 protein was used for the production of YKL-40 polyclonal antibody. The anti-YKL-40 strongly reacted with YKL-40 target protein and evaluation of cross-reactivity against other members of GH-18 (YKL-39, AMCase, and bacteria chitinases) revealed no interaction of the polyclonal antibody.

Purified anti-YKL-40 antibody was immobilized on disk-shaped smoothly polished gold working electrodes by covalent coupling the protein to a thin thiourea film via glutaraldehyde as chemical crosslinking reagent. The resulting YKL-40 immunosensors were employed as novel analytical tools in an electrochemical flow cell and used to quantify YKL-40 antigen levels of injected samples by an analysis of their capacitive current response to ms-long simulative potential pulses. Optimum conditions for capacitive YKL-40 immunosensing were the use of 10 mM sodium phosphate buffer, pH 7.0, as running buffer in the tubes of the flow system, use of HCl solution, pH 2.5, as regeneration solution that broke antibody/antigen conjugates

apart after a sample injection and antigen capture, and the choice of a flow rate and sample volume of 100  $\mu\text{L}/\text{min}$  and 200  $\mu\text{L}$ , respectively. The basic performance of the system and its power for the accurate quantitative detection of YKL-40 were evaluated under optimal conditions. The linear dynamic range of the capacitive YKL-40 screen spread from 0.1  $\mu\text{g}/\text{L}$  to 1  $\text{mg}/\text{L}$ , while its limit of detection was found to be  $0.07 \pm 0.01 \mu\text{g}/\text{L}$ . Specificity tests revealed that anti-YKL-40 modified gold disk electrodes reacted with changes in capacitance only against an exposure to YKL-40, while even structurally similar protein relatives could not trigger a measurable sensor response. Stability tests, on the other hand, disclosed a functional applicability up to 40 times of YKL-40 sample injections or about three days continuous operation in the flow-based electrochemical workstation. Capacitive YKL-40 immunosensor identified in the flow detection mode their protein target in spiked model samples with excellent recovery rates and in very good agreement with comparative data from parallel assessment via ELISA testing. The content of spiked serum samples was recovered accurately and was consistent with the outcome of ELISA-based tests. Finally, the effective application of the developed capacitive YKL-40 immunosensing for the analysis of blood serum samples from some breast cancer and glioblastoma patients and lysates from model cells with and without the possibility of cellular YKL secretion was successful and confirmed through close matches with complementary ELISA data the strong potential of the methodology as a useful tool for analytical YKL-40 cancer biomarker screening.

YKL-39 antigen and antibody was available from previous research work in the group and the affinity couple was, the relevance of YKL-39 as potential osteoarthritis biomarker in mind, explored for capacitive YKL-39 immunosensor

construction and application of completed versions for YKL-39 screens in model (spiked buffer) and real (synovial fluid of osteoarthritis patients) samples. When used with pre-identified optimal assay conditions, the linearity of the sensor response, the sensor stability and the recovery rates for model sample determinations was as good for YKL-39 immunosensors as for the YKL-40 variant described above (here: linear range from 0.1  $\mu\text{g/L}$  to 1  $\text{mg/L}$ ; operational stability up to 49 sample injections and percentage of recovery close to ideal 100%). Apparently, the method can measure the YKL-39 content of synovial fluid of osteoarthritis patients and cell lysates of Jurkat, U937 and 293T in good agreement with complementary ELISA. Thus, capacitive YKL-39 immunosensing holds great promises as complementary optional tool for an early detection of joint osteoarthritis, which currently cannot be achieved at the onset or early development stages because of a lack of a powerful enough analytical techniques for this biomarker.



**REFERENCES**

## REFERENCES

- Akram, M., Stuart, M. C. and Wong, D. K. Y. (2004). Direct application strategy to immobilise a thioctic acid self-assembled monolayer on a gold electrode. **Anal. Chim. Acta.** 504(2): 243-251.
- Amero, S. A., James, T. C. and Elgin, S. C. (1988). Production of antibodies using proteins in gel bands. **Methods Mol. Biol.** 3: 355-362.
- Areshkov, P. A. and Kavsan, V. M. (2010). Chitinase 3-like protein 2 (CHI3L2, YKL-39) activates phosphorylation of extracellular signal-regulated kinases ERK1/ERK2 in human embryonic kidney (HEK293) and human glioblastoma (U87 MG) cells. **Tsitol. Genet.** 44(1): 3-9.
- Baeten, D., Boots, A. M. H., Steenbakkens, P. G. A., Elewaut, D., Bos, E., Verheijden, G. F. M., Verbruggen, G., Miltenburg, A. M. M., Rijnders, A. W. M., Veys, E. M. and de Keyser, F. (2000). Human cartilage gp-39+, CD16+ monocytes in peripheral blood and synovium. Correlation with joint destruction in rheumatoid arthritis. **Arthritis Rheum.** 43(6): 1233-43.
- Bain, C. D., Evall, J. and Whitesides, G. M. (1989). Formation of monolayers by the coadsorption of thiols on gold: variation in the head group, tail group, and solvent. **J. Am. Chem. Soc.** 111: 7155-7164
- Barraud, A., Perrot, H., Billard, V., Martelet, C. and Therasse, J. (1993). Study of immunoglobulin G thin layers obtained by the Langmuir-Blodgett method: application to immunosensors. **Biosens. Bioelectron.** 8(1): 39-48.

- Bataillard, P., Gardies, F., Jaffrezic-Renault, N., Martelet, C., Colin, B. and Mandrand, B. (1988). Direct detection of immunospecies by capacitance measurements. **Anal. Chem.** 60(21): 2374-2379.
- Bay-Jensen, A. C., Liu, Q., Byrjalsen, I., Li, Y., Wang, J., Pedersen, C., Leeming, D. J., Dam, E. B., Zheng, Q., Qvist, P. and Karsdal, M. A. (2011). Enzyme-linked immunosorbent assay (ELISAs) for metalloproteinase derived type II collagen neoepitope, CIIM-increased serum CIIM in subjects with severe radiographic osteoarthritis. **Clin. Biochem.** 44: 423-429.
- Berggren, C. and Johansson, G. (1997). Capacitance Measurements of Antibody–Antigen Interactions in a Flow System. **Anal. Chem.** 69(18): 3651-3657.
- Berggren, C., Bjarnason, B. and Johansson, G. (1998). An immunological interleukine-6 capacitive biosensor using perturbation with a potentiostatic step. **Biosens. Bioelectron.** 13(10): 1061-1068.
- Berggren, C., Bjarnason, B. and Johansson, G. (2001). Capacitive Biosensors. **Electroanalysis.** 13(3): 173-180.
- Bezerra, V. S., de Lima Filho, J. L., Montenegro, M. C., Araújo, A. N. and da Silva, V. L. (2003). Flow-injection amperometric determination of dopamine in pharmaceuticals using a polyphenol oxidase biosensor obtained from soursop pulp. **J. Pharm. Biomed. Anal.** 33(5): 1025-31.
- Blackburn, G. F., Shah, H. P., Kenten, J. H., Leland, J., Kamin, R. A., Link, J., Peterman, J., Powell, M. J., Shah, A., Talley, D. B., Tyagi, S. K., Wilkins, E., Wu, T. G. and Massey, R. J. (1991). Electrochemiluminescence detection for

development of immunoassays and DNA probe assays for clinical diagnostics.

**Clin. Chem.** 37(9): 1534-1539.

Boehm, M. K., Corper, A. L., Wan, T., Sohi, M. K., Sutton, B. J., Thornton, J. D., Keep, P. A., Chester, K. A., Begent, R. H. and Perkins, S. J. (2000). Crystal structure of the anti-(carcinoembryonic antigen) single-chain Fv antibody MFE-23 and a model for antigen binding based on intermolecular contacts. **Biochem. J.** 346(Pt 2): 519-528.

Brasso, K., Christensen, I. J., Johansen, J. S., Teisner, B., Garnero, P., Price, P. A. and Iversen, P. (2006). Prognostic value of PINP, bone alkaline phosphatase, CTX-I, and YKL-40 in patients with metastatic prostate carcinoma. **Prostate.** 66(5): 503-513.

Byfield, M. P. and Abuknesha, R. A. (1994). Biochemical aspects of biosensor. **Biosens. Bioelectron.** 9: 373-400.

Chaki, N. K. and Vijayamohan, K. (2002). Self-assembled monolayers as a tunable platform for biosensor applications. **Biosens. Bioelectron.** 17(1-2): 1-12.

Chaocharoen, W., Suginta, W., Limbut, W., Ranok, A., Numnuam, A., Khunkaewla, P., Kanatharana, P., Thavarungkul, P. and Schulte, A. (2015). Electrochemical detection of the disease marker human chitinases-3-like protein 1 by matching antibody-modified gold as label-free immunosensors. **Bioelectrochemistry.** 101: 106-113.

Chou, S. F., Hsu, W. L., Hwang, J. M. and Chen, C. Y. (2002). Determination of alpha-fetoprotein in human serum by a quartz crystal microbalance-based immunosensor. **Clin. Chem.** 48(6 Pt 1): 913-918.

- Cintin, C., Johansen, J. S., Christensen, I. J., Price, P. A., Sorensen, S. and Nielsen, H. J. (2002). High serum YKL-40 level after surgery for colorectal carcinoma is related to short survival. **Cancer**. 95(2): 267-274.
- Cintin, C., Johansen, J. S., Christensen, I. J., Price, P. A., Sørensen, S. and Nielsen, H. J. (1999). Serum YKL-40 and colorectal cancer. **Br. J. Cancer**. 79(9-10): 1494-1499.
- De Ceuninck, F., Marcheteau, E., Berger, S., Caliez, A., Dumont, V., Raes, M., Anract, P., Leclerc, G., Boutin, J. A. and Ferry, G. (2005). Assessment of some tools for the characterization of the human osteoarthritic cartilage proteome. **J. Biomol. Tech.** 16(3): 256-265.
- De Ceuninck, F., Pastoureau, P., Agnellet, S., Bonnet, J. and Vanhoutte, P. M. (2001). Development of an enzyme-linked immunoassay for the quantification of YKL-40 (cartilage gp-39) in guinea pig serum using hen egg yolk antibodies. **J. Immunol. Methods**. 252: 153-161.
- Dehn, H., Høgdall, E. V., Johansen, J. S., Jørgensen, M., Price, P. A., Engelholm, S. A. and Høgdall, C. K. (2003). Plasma YKL-40, as a prognostic tumor marker in recurrent ovarian cancer. **Acta. Obstet. Gynecol. Scand.** 82(3): 287-293.
- Dong, S. and Chen, X. (2002). Some new aspects in biosensor. **Rev. Mol. Biotechnol.** 81: 303-323.
- Dupont, J., Tanwar, M. K., Thaler, H. T., Fleisher, M., Kauff, N., Hensley, M. L., Sabbatini, P., Anderson, S., Aghajanian, C., Holland, E. C. and Spriggs, D. R. (2004). Early detection and prognosis of ovarian cancer using serum YKL-40. **J. Clin. Oncol.** 22(16): 3330-3339.

- Eggins, B. R. (1996). *Biosensor: and introduction*. John Wiley and Sons, Inc., New York, USA.
- Finklea, H. O., Avery, S., Lynch, M. and Furtch T. (1987). Blocking oriented monolayers of alkyl mercaptans on gold electrodes. **Langmuir**. 3(3): 409-413.
- Fu, Y., Yuan, R., Tang, D., Chai, Y. and Xu, L. (2005). Study on the immobilization of anti-IgG on Au-colloid modified gold electrode via potentiometric immunosensor, cyclic voltammetry, and electrochemical impedance techniques. **Colloids Surf. B Biointerfaces**. 40(1): 61-66.
- Fusetti, F., Pijning, T., Kalk, K. H., Bos, E. and Dijkstra, B. W. (2003) Crystal structure and carbohydrate-binding properties of the human cartilage glycoprotein-39. **J. Biol. Chem**. 278(39): 37753-37760.
- Gargiulo, S., Gamba, P., Poli, G. and Leonarduzzi, G. (2014). Metalloproteinases and metalloproteinase inhibitors in age-related diseases. **Curr. Pharm. Des**. 20(18): 2993-3018.
- Gebbert, A., Alvarez-Icaza, M., Peters, H., Jäger, V., Bilitewski, U. and Schmid, R. D. (1994). On-line monitoring of monoclonal antibody production with regenerable flow-injection immuno systems. **J. Biotechnol**. 32(3): 213-220.
- Gebbert, A., Alvarez-Icaza, M., Stoecklein, W. and Schmid, R. D. (1992). Real-time monitoring of immunochemical interactions with a tantalum capacitance flow-through cell. **Anal. Chem**. 64(9): 997-1003.
- Geertsen, P., Johansen, J. S., von der Maase, H., Jensen, B. V. and Price, P. A. (2003). High pretreatment serum level of YKL-40 is related to short survival in patients with advanced renal cell carcinoma treated with high-dose continuous intravenous infusion of interleukin-2. **Proc ASCO**. 22: 1603.

- Hakala, B. E., White, C. and Recklies, A. D. (1993). Human cartilage gp-39, a major secretory product of articular chondrocytes and synovial cells, is a mammalian member of a chitinase protein family. **J. Biol. Chem.** 268(34): 25803-25810.
- Harvey, S., Weisman, M., O'Dell, J., Scott, T., Krusemeier, M., Visor, J. and Swindlehurst, C. (1998). Chondrex: new marker of joint disease. **Clin. Chem.** 44(3): 509-516.
- Høgdall, E. V. S., Johansen, J. S., Kjaer, S. K., Price, P. A., Christensen, L., Blaakaer, J., Bock, J. E., Glud, E. and Høgdall, C. K. (2003). High plasma YKL-40 level in patients with ovarian cancer stage III is related to shorter survival. **Oncol. Rep.** 10(24): 1535-1538.
- Hong, S. Y., Park, Y. M., Jang, Y. H., Min, B. H. and Yoon, H. C. (2012). Quantitative lateral-flow immunoassay for the assessment of the cartilage oligomeric matrix protein as a marker of osteoarthritis. **Bio. Chip. J.** 6: 213-220.
- Horowitz, J. C., Rogers, D. S., Sharma, V., Vittal, R., White, E. S. Cui, Z. and Thannickal, V. T. (2007). Combinatorial activation of FAK and AKT by transforming growth factor- $\beta$ 1 confers an anoikis-resistant phenotype to myofibroblasts. **Cell Signal.** 19(4): 761-771.
- Houston, D. R., Recklies, A. D., Krupa, J. C. and van Aalten, D. M. (2003). Structure and ligand-induced conformational change of the 39-kDa glycoprotein from human articular chondrocytes. **J. Biol. Chem.** 278(32): 30206-30212.
- Hu, B., Trinh, K., Figueira, W. F. and Price, P. A. (1996). Isolation and sequence of a novel human chondrocyte protein related to mammalian members of the chitinase protein family. **J. Biol. Chem.** 271(32): 19415-19420.

- Johansen, J. S., Baslund, B., Garbarsch, C., Hansen, M., Stoltenberg, M., Lorenzen, I. and Price, P. A. (1999). YKL-40 in giant cells and macrophages from patients with giant cell arteritis. **Arthritis Rheum.** 42(12): 2624-2630.
- Johansen, J. S., Bojesen, S. E., Mylin, A. K., Frikke-Schmidt, R., Price, P. A. and Nordestgaard, B. G. (2009). Elevated plasma YKL-40 predicts increased risk of gastrointestinal cancer and decreased survival after any cancer diagnosis in the general population. **J. Clin. Oncol.** 27(4): 572-578.
- Johansen, J. S., Christensen, I. J., Riisbro, R., Greenall, M., Han, C., Price, P. A., Smith, K., Brunner, N. and Harris, A. L. (2003). High serum YKL-40 levels in patients with primary breast cancer is related to short recurrence free survival. **Breast Cancer Res. Treat.** 80(1): 15-21.
- Johansen, J. S., Christoffersen, P., Møller, S., Price, P. A., Henriksen, J. H., Garbarsch, C. and Bendtsen, F. (2000). Serum YKL-40 is increased in patients with hepatic fibrosis. **J. Hepatol.** 32(6): 911-920.
- Johansen, J. S., Cintin, C., Jørgensen, M., Kamby, C. and Price, P. A. (1995). Serum YKL-40: a new potential marker of prognosis and location of metastases of patients with recurrent breast cancer. **Eur. J. Cancer.** 31(A): 1437-1442.
- Johansen, J. S., Drivsholm, L., Price, P. A. and Christensen, I. J. (2004). High serum YKL-40 level in patients with small cell lung cancer is related to early death. **Lung Cancer.** 46(3): 333-340.
- Johansen, J. S., Jensen, B. V., Roslind, A., Nielsen, D. and Price, P. A. (2006). Serum YKL-40, a new prognostic biomarker in cancer patients? **Cancer Epidemiol Biomarkers Prev.** 15(2): 194-202.

- Johansen, J. S., Jensen, H. S. and Price, P. A. (1993). A new biochemical marker for joint injury. Analysis of YKL-40 in serum and synovial fluid. **Br. J. Rheumatol.** 32(11): 949-955.
- Johansen, J. S., Lottenburger, T. and Nielsen, H. J. (2008). Diurnal, weekly, and long-time variation in serum concentrations of YKL-40 in healthy subjects. **Cancer Epidemiol. Biomarkers Prev.** 17(10): 2603-2608.
- Johansen, J. S., Møller, S., Price, P. A., Bendtsen, F., Junge, J., Garbarsch, C. and Henriksen, J. H. (1997). Plasma YKL-40: a new potential marker of fibrosis in patients with alcoholic cirrhosis? **Scand. J. Gastroenterol.** 32(6): 582-590.
- Johansen, J. S., Williamson, M. K., Rice, J. S. and Price, P. A. (1992). Identification of proteins secreted by human osteoblastic cells in culture. **J. Bone. Miner. Res.** 7(5): 501-512.
- Johansen, J. S. (2006). Studies on serum YKL-40 as a biomarker in diseases with inflammation, tissue remodelling, fibroses and cancer. **Dan. Med. Bull.** 53: 172-209.
- Kavsan, V., Dmitrenko, V., Boyko, O., Filonenko, V., Avdeev, S., Areshkov, P., Marusyk, A., Malisheva, T., Rozumenko, V. and Zozulya, Y. (2008). Overexpression of YKL-39 Gene in Glial Brain Tumors. **Scholarly Research Exchange.** 2008.
- Kawasaki, M., Hasegawa, Y., Kondo, S. and Iwata, H. (2001). Concentration and localization of YKL-40 in hip joint diseases. **J. Rheumatol.** 28(2): 341-345.
- Kim, S. J., Park, Y. M., Min, B. H., Lee, D.-S. and Yoon, H. C. (2013). Quantitative lateral-flow immunoassay for the assessment of the cartilage oligomeric matrix protein as a marker of osteoarthritis. **Bio. Chip J.** 7: 399-407.

- Knorr, T., Obermayr, F., Bartnik, E., Zien, A. and Aigner, T. (2003). YKL-39 (chitinase 3-like protein 2), but not YKL-40 (chitinase 3-like protein 1), is up regulated in osteoarthritic chondrocytes. **Ann. Rheum. Dis.** 62(10): 995-998.
- Laemmli, U. K. (1970). Cleavage of structural proteins during the assembly of the head of bacteriophage T4. **Nature.** 227(5259): 680-685.
- Lamers, R. J., van Nesselrooij, J. H., Kraus, V. B., Jordan, J. M., Renner, J. B., Dragomir, A. D., Luta, G., van der Greef, J. and DeGroot, J. (2005). Identification of an urinary metabolite profile associated with osteoarthritis. **Osteoarthr. Cartilage.** 13(9): 762-768.
- Lee, C. G., Da Silva, C. A., Dela Cruz, C. S., Ahangari, F., Ma, B., Kang, M. J., He, C. H., Takyar, S. and Elias, J. A. (2011). Role of chitin and chitinase/chitinase-like proteins in inflammation, tissue remodeling, and injury. **Annu. Rev. Physiol.** 73: 479-501.
- Limbut, W., Kanatharana, P., Mattiasson, B., Asawatreratanakul, P. and Thavarungkul, P. (2006a). A comparative study of capacitive immunosensors based on self-assembled monolayers formed from thiourea, thioctic acid, and 3-mercaptopropionic acid. **Biosens. Bioelectron.** 22(2): 233-240.
- Limbut, W., Kanatharana, P., Mattiasson, B., Asawatreratanakul, P. and Thavarungkul, P. (2006b). A reusable capacitive immunosensor for carcinoembryonic antigen (CEA) detection using thiourea modified gold electrode. **Anal. Chim. Acta.** 561(1-2): 55-61.
- Loyprasert, S., Thavarungkul, P., Asawatreratanakul, P., Wongkittisuksa, B., Limsakul, C. and Kanatharana, P. (2008) Label-free capacitive immunosensor

- for microcystin-LR using selfassembled thiourea monolayer incorporated with Ag nanoparticles on gold electrode. **Biosens. Bioelectron.** 24: 78-86.
- Ma, W. H., Wang, X. L., Du, Y. M., Wang, Y. B., Zhang, Y., Wei, D. E., Guo, L. L. and Bu, P. L. (2012). Association between human cartilage glycoprotein 39 (YKL-40) and arterial stiffness in essential hypertension. **BMC Cardiovasc. Disord.** 12: 35.
- Newman, A. L., Hunter, K. W. and Stanbro, W. D. (1986). The capacitive affinity sensor: a new biosensor. **Proc. 2nd Int. Meeting on Chemical Sensor, Bordeaux.** 596-598.
- Nishikawa, K. C. and Millis, A. J. T. (2003). Gp38k (CHI3L1) is a novel adhesion and migration factor for vascular cells. **Exp Cell Res.** 287(1): 79-87.
- Park, I. S., Kim, W. Y. and Kim, N. (2000). Operational characteristics of an antibody-immobilized QCM system detecting *Salmonella spp.* **Biosens. Bioelectron.** 15(3-4): 167-172.
- Pei, R., Cheng, Z., Wang, E. and Yang, X. (2001). Amplification of antigen-antibody interactions based on biotin labeled protein-streptavidin network complex using impedance spectroscopy. **Biosens. Bioelectron.** 16(6): 355-361.
- Pelloski, C. E., Mahajan, A., Maor, M., Chang, E. L., Woo, S., Gilbert, M., Colman, H., Yang, H., Ledoux, A., Blair, H., Passe, S., Jenkins, R. B. and Aldape, K. D. (2005). YKL-40 expression is associated with poorer response to radiation and shorter overall survival in glioblastoma. **Clin. Cancer Res.** 11: 3326-3334.
- Ranok, A., Khunkaewla, P. and Suginta, W. (2013). Human cartilage chitinase 3-like protein 2: cloning, expression, and production of polyclonal and monoclonal

- antibodies for osteoarthritis detection and identification of potential binding partners. **Monoclon. Antib. Immunodiagn. Immunother.** 32(5): 317-325.
- Rehli, M., Krause, S. W. and Andreesen, R. (1997). Molecular characterization of the gene for human cartilage gp-39 (CHI3L1), a member of the chitinase protein family and marker for late stages of macrophage differentiation. **Genomics.** 43(2): 221-225.
- Rogers, K. R. (2000). Principles of affinity-based biosensors. **Mol. Biotechnol.** 14(2): 109-29.
- Sakata, M., Masuko-Hongo, K., Tsuruha, J., Sekine, T., Nakamura, H., Takigawa, M., Nishioka, K. and Kato, T. (2002). YKL-39, a human cartilage-related protein, induces arthritis in mice. **Clin. Exp. Rheumatol.** 20(3): 343-350.
- Schmidt, H., Johansen, J. S., Gehl, J., Geertsen, P., Fode, K. and von der Maase, H. (2006). Elevated serum level of YKL-40 in an independent prognostic factor for poor survival in patients with metastatic melanoma. **Cancer.** 106(5): 1130-1139.
- Schweiss, R., Werner, C. and Knoll, W. (2003). Impedance spectroscopy studies of interfacial acid–base reactions of self-assembled monolayers. **J. Electroanal. Chem.** 540: 145-151.
- Sekine, T., Masuko-Hongo, K., Matsui, T., Asahara, H., Takigawa, M., Nishioka, K. and Kato, T. (2001). Recognition of YKL-39, a human cartilage related protein, as a target antigen in patients with rheumatoid arthritis. **Ann. Rheum. Dis.** 60(1): 49-54.
- Shackelton, L. M., Mann, D. M. and Millis, A. J. T. (1995). Identification of a 38-kDa heparin binding glycoprotein (gp38k) in differentiating vascular smooth

- muscle cells as a member of a group of proteins associated with tissue remodeling. **J Biol Chem.** 270(22): 13076-13083.
- Shao, R., Hamel, K., Petersen, L., Cao, Q. J., Arenas, R. B., Bigelow, C., Bentley, B. and Yan, W. (2009). YKL-40, a secreted glycoprotein, promotes tumor angiogenesis. **Oncogene.** 28(50): 4456-4468.
- Sharma, S. K., Shegal, N. and Kumar, A. (2003). Biomolecules for development of biosensors and their applications. **Current Applied Physics.** 3: 307-316.
- Skoog, D. A., West, D. M. and Hollar, J. F. (1996). Fundamental of analytical chemistry (7th Edition). Saunders College Publishing, Philadelphia, USA.
- Steck, E., Breit, S., Breusch, S. J., Axt, M. and Richter, W. (2002). Enhanced expression of the human chitinase 3-like 2 gene (YKL-39) but not chitinase 3-like 1 gene (YKL-40) in osteoarthritic cartilage. **Biochem. Biophys. Res. Commun.** 299(1): 109-115.
- Subramanian, A., Irudayaraj, J. and Ryan, T. (2006). A mixed self-assembled monolayer-based surface plasmon immunosensor for detection of *E. coli* O157:H7. **Biosens. Bioelectron.** 21(7): 998-1006.
- Tanwar, M. K., Gilbert, M. R. and Holland, E. C. (2002). Gene expression microarray analysis reveals YKL-40 to be a potential serum marker for malignant character in human glioma. **Cancer Res.** 62(15): 4364-4368.
- Thévenot, D. R., Toth, K., Durst, R. A. and Wilson, G. S. (2001). Electrochemical biosensors: recommended definitions and classification. **Biosens. Bioelectron.** 16(1-2): 121-131.
- Thorpe, G. H., Kricka, L. J., Moseley, S. B. and Whitehead, T. P. (1985). Phenols as enhancers of the chemiluminescent horseradish peroxidase-luminol-hydrogen

- peroxide reaction: application in luminescence-monitored enzyme immunoassays. **Clin. Chem.** 31(8): 1335-1341.
- Van der Merwe, P. A. (2000). Surface Plasmon Resonance. In Protein-Ligand Interactions: A Practical Approach. Oxford University, Oxford, England.
- Volck, B., Johansen, J. S., Stoltenberg, M., Garbarsch, C., Price, P. A., Østergaard, M., Østergaard, K., Løvgreen-Nielsen, P., Sonne-Holm, S. and Lorenzen, I. (2001). Studies on YKL-40 in knee joints of patients with rheumatoid arthritis and osteoarthritis. Involvement of YKL-40 in the joint pathology. **Osteoarthritis Cartilage.** 9(3): 203-214.
- Volck, B., Østergaard, K., Johansen, J. S., Garbarsch, C. and Price, P. A. (1999). The distribution of YKL-40 in osteoarthritic and normal human cartilage. **Scand. J. Rheum.** 28(3): 171-179.
- Volck, B., Price, P. A., Johansen, J. S., Sørensen, O., Benfield, T., Calafat, J., Nielsen, H. J. and Borregaard, N. (1998). YKL-40, a mammalian member of the bacterial chitinases family, is a matrix protein of specific granules in human neutrophils. **Proc. Assoc. Am. Physicians.** 110(4): 351-60.
- Vos, K., Steenbakkens, P., Miltenburg, A. M. M., Bos, E., van den Heuvel, M. W., van Hogezaand, R. A., de Vries, R. R. P., Breedveld, F. C. and Boots, A. M. H. (2000). Raised human cartilage glycoprotein-39 plasma levels in patients with rheumatoid arthritis and other inflammatory conditions. **Ann. Rheum. Dis.** 59: 544-548.
- Wink, T., van Zuilen, S. J., Bult, A. and van Bennekom, W. P. (1997). Self-assembled monolayers for biosensors. **Analyst.** 122: 43R-50R.

Yang, H. (2012). Enzyme-based ultrasensitive electrochemical biosensors. **Curr. Opin. Chem. Biol.** 16(3-4): 422-428.





**APPENDIX**

## APPENDIX

### PUBLICATION

Chaocharoen, W., Suginta, W., Limbut, W., Ranok, A., Numnuam, A., Khunkaewla, P., Kanatharana, P., Thavarungkul, P. and Schulte, A. (2015). Electrochemical detection of the disease marker human chitinases-3-like protein 1 by matching antibody-modified gold as label-free immunosensors. **Bioelectrochemistry**. 101: 106-113.





Contents lists available at ScienceDirect

Bioelectrochemistry

journal homepage: [www.elsevier.com/locate/bioelechem](http://www.elsevier.com/locate/bioelechem)

## Electrochemical detection of the disease marker human chitinase-3-like protein 1 by matching antibody-modified gold electrodes as label-free immunosensors



Wethaka Chaocharoen<sup>a</sup>, Wipa Suginta<sup>a</sup>, Warakorn Limbut<sup>b,c,d</sup>, Araya Ranok<sup>a</sup>, Apon Numnuam<sup>b,c,e</sup>, Panida Khunkaewla<sup>a</sup>, Proespichaya Kanatharana<sup>b,c,e</sup>, Panote Thavarungkul<sup>b,c,f,\*</sup>, Albert Schulte<sup>a,\*</sup>

<sup>a</sup> Biochemistry–Electrochemistry Research Unit, Schools of Chemistry and Biochemistry, Suranaree University of Technology, Nakhon Ratchasima 30000, Thailand

<sup>b</sup> Trace Analysis and Biosensor Research Center, Prince of Songkla University, Hat Yai, Songkhla 90112, Thailand

<sup>c</sup> Center of Excellence for Innovation in Chemistry, Faculty of Science, Prince of Songkla University, Hat Yai, Songkhla 90112, Thailand

<sup>d</sup> Department of Applied Science, Faculty of Science, Prince of Songkla University, Hat Yai, Songkhla 90112, Thailand

<sup>e</sup> Department of Chemistry, Faculty of Science, Prince of Songkla University, Hat Yai, Songkhla 90112, Thailand

<sup>f</sup> Department of Physics, Faculty of Science, Prince of Songkla University, Hat Yai, Songkhla 90112, Thailand

### ARTICLE INFO

#### Article history:

Received 28 January 2014

Received in revised form 27 June 2014

Accepted 6 July 2014

Available online 30 July 2014

#### Keywords:

Human chitinase-3-like protein 1

Chitinase-like proteins

Capacitive immunosensor

Disease marker

Biomarker

### ABSTRACT

Tissue inflammation, certain cardiovascular syndromes and the occurrence of some solid tumors are correlated with raised serum concentrations of human chitinase-3-like protein 1 (YKL-40), a mammalian chitinase-like glycoprotein, which has become the subject of current research. Here we report the construction and characterization of an electrochemical platform for label-free immunosensing of YKL-40. Details of the synthesis of YKL-40 and production of anti-YKL-40 immunoglobulin G (IgG) are provided and cross-reactivity tests presented. Polyclonal anti-YKL-40 IgG was immobilized on gold electrodes and the resulting immunosensors were operated in an electrochemical flow system with capacitive signal generation. The strategy offered a wide linear detection range (0.1 µg/L to 1 mg/L) with correlation coefficients ( $R^2$ ) above 0.99 and good sensitivity ( $12.28 \pm 0.27$  nF/cm<sup>2</sup> per decade of concentration change). Additionally, the detection limit of  $0.07 \pm 0.01$  µg/L was well below that of optical enzyme-linked immunosorbent assays (ELISAs), which makes the proposed methodology a promising alternative for YKL-40 related disease studies.

© 2014 Elsevier B.V. All rights reserved.

### 1. Introduction

Molecular disease markers are important tools for mechanistic disease studies and also key components of diagnostic or prognostic systems for the clinical analysis of critical body conditions. Recently, human chitinase-3-like-protein 1 (YKL-40), a human chitinase-like protein and family-18 glycosyl hydrolase, was identified as a promising biomarker, with elevated concentrations associated with pathologies such as infection, inflammation, fibrosis and cancer [1–7]. Until now YKL-40 analysis has relied exclusively on optical enzyme-linked immunosorbent assays (ELISAs) with detection limits of about 20 µg/L [8], and to the best of our knowledge no alternative YKL-40 immunosensing scheme has been reported.

For clinical applications, immunosensing needs to be cheap, simple and efficient. It therefore requires a supply of high-grade antibodies and antigens, together with a sensitive and robust method for detecting

antibody–antigen binding in sample solutions. Electroanalysis of antibody–antigen (Ab–Ag) interaction is a promising approach, offering high sensitivity detection with compact equipment that is compatible with economical, mass-produced sensor platforms. Usually, the antibody is immobilized on the electroactive surface of the working electrode (the “immunosensor”) of a three-electrode electrochemical cell and antigen binding detected by amperometry, voltammetry or electrochemical impedance spectroscopy (EIS) [9]. Amperometry and voltammetry measure the protein interaction indirectly, using enzyme-labeled secondary antibodies that generate a concentration-dependent Faradaic current through catalytic formation of a redox product. EIS, on the other hand, is a label-free screening method that measures electrode capacitance changes produced by restructuring of the interfacial Helmholtz double-layer on antigen binding [9,10]. EIS-based immunosensing with modern electrochemical workstations is quite effective; however, special hardware and software are needed and data analysis depends upon a rather complex treatment of alternating current signals. A simpler method of detecting antigen-induced electrode capacitance changes is the analysis of the current response on application of a potential pulse [11,12].

\* Corresponding author. Tel.: +66 44 22 6187; fax: +66 44 22 4185.

\*\* Corresponding author. Tel.: +66 74 28 8008; fax: +66 74 44 6657.

E-mail addresses: [panote.t@psu.ac.th](mailto:panote.t@psu.ac.th) (P. Thavarungkul), [schulte@su.ac.th](mailto:schulte@su.ac.th) (A. Schulte).

In developing a novel electrochemical YKL-40 immunosensor with a detection limit significantly lower than that of optical ELISA, we report procedures for the preparation of the YKL-40 antigen and of YKL-40-specific polyclonal IgG, characterization of the antibody and antigen and some promising results from a flow injection analysis system, with antigen binding monitored by electrode capacitance measurements through potential pulsing.

## 2. Experimental

### 2.1. Chemical reagents and other materials

Human cDNA, a protein A agarose column and HRP-conjugated anti-rabbit IgG were obtained from GenScript Inc., Piscataway, NJ, USA. The pQETri System expression vector, a Ni-nitrilotriacetic acid (NTA) agarose column and *Escherichia (E.) coli* M15 (pREP) were purchased from Qiagen Ltd., Manchester, UK. The restriction enzymes *SacI* and *XhoI* were from Promega, Madison, USA. The PCR primer came from GENEBIODESIGN Co., Ltd., Taipei, Taiwan and related verification of the recombinant plasmid by automated DNA sequencing was carried out by First BASE Laboratories Sdn Bhd, Seri Kembangan, Malaysia. Ampicillin, phenylmethylsulphonyl fluoride (PMSF), imidazole and Triton X-100 were products of USB Corporation, Cleveland, OH, USA. Isopropyl thio- $\beta$ -D-galactoside (IPTG), Freund's complete adjuvant, Freund's incomplete adjuvant, Tris-HCl, Tris-base and lysozyme were from Sigma Aldrich, St. Louis, MO, USA. 3,3',5,5'-tetramethylbenzidine (TMB), the substrate for ELISA assays, was purchased from Invitrogen, Carlsbad, CA, USA. Glutaraldehyde, 1-dodecanethiol, potassium ferricyanide ( $K_3[Fe(CN)_6]$ ), and 4-(2-hydroxyethyl)-1-piperazineethanesulfonic acid (HEPES) were purchased from Acros Organic, Bridgewater, NJ, USA. Protein concentrations were measured with a Pierce® BCA Protein Assay kit from Thermo Scientific, Rockford, IL, USA. All other basic chemical reagents (e.g. NaCl, KCl,  $Na_2HPO_4$ ,  $KH_2PO_4$ , Urea, HCl,  $H_2SO_4$  and thiourea) were from Carlo Erba Reagents, Cornaredo (MI), Italy and unless otherwise mentioned were of analytical grade.

Alumina slurries with a particle size of 1 and 5  $\mu$ m, as used for gold sensor surface polishing, were obtained from Metkon Instruments Ltd., Bursa, Turkey. A Hiprep 26/10 desalting column was supplied by GE HealthCare, Hatfield, UK and Vivaspine-20 ultrafiltration membranes came from Vivascience AG, Hannover, Germany. All aqueous solutions were prepared with purified water from a reverse osmosis-deionizing system (Cascada™ Lab Water Systems, PALL Life Science, Ann Arbor, MI, USA). Buffers were filtered through Whatman® cellulose nitrate membrane with pore size 0.20  $\mu$ m from GE HealthCare, Hatfield, UK.

### 2.2. Instrumentation

ELISA analysis was performed using a Biochrom® Anthos MultiRead 400 Microplate Reader (Biochrom Ltd., Cambridge, UK). All electrochemical immunosensor recordings were made with an EA163 potentiostat and e-corder 410 data acquisition device, from eDAQ, Denistone East, Australia. The system for flow injection-based sample measurements used a peristaltic pump (Miniplus® 3 from Gilson, Middleton, WI, USA), a manual injection valve (Biologic MV-6® from Bio-Rad, Hercules, CA, USA) and a three-electrode radial flow cell with customized 3-mm-diameter gold (Au) disk electrodes (ALS Co., Ltd., Tokyo, Japan). Supplementary Fig. 1S is a schematic representation of the entire YKL-40 detection system used in this study.

### 2.3. Preparation of recombinant human YKL-40 antigen

Human cDNA was used as the template for PCR amplification. Two flanking primers were designed according to the YKL-40 sequence, retrieved from the GENBANK database (Accession no. AAA16074). The oligonucleotides used for amplification of full-length YKL-40 DNA were 5'-AGAGCTCGGTGTGAAGGCGTCTCAAAC-3' for the forward and 5'-TCTCGAGCGTTGCAGCGAGTGCATC-3' for the reverse primer. The PCR product of expected size (1.1 kbp) was cloned in the pQETri System expression vector using *SacI* and *XhoI* cloning sites (sequences underlined) following the manufacturer's protocol. The nucleotide sequences of both sense and anti-sense strands of the YKL-40 DNA fragment were confirmed by automated DNA sequencing.

Recombinant YKL-40 was expressed in *E. coli* M15(pREP) as a C-terminally (His)<sub>6</sub>-tagged polypeptide. Cells were grown at 37° in Luria Bertani (LB) medium containing 100  $\mu$ g/mL ampicillin until the OD<sub>600</sub> of the cell culture reached 0.6. Expression was induced by the addition of isopropyl thio- $\beta$ -D-galactoside (IPTG) to a final concentration of 0.5 mM. After 16 h of induction at 25°, the cell pellet was collected by centrifugation and resuspended in lysis buffer (50 mM Tris-HCl buffer, pH = 8.0, containing 300 mM NaCl, 1 mM phenylmethylsulphonyl fluoride (PMSF), 1.0 mg/mL lysozyme and 1% (v/v) triton X-100), and then lysed on ice using a Sonopuls Ultrasonic homogenizer with a 6-mm-diameter probe (50% duty cycle; amplitude setting, 20%; 30 s, 6–8 times). After centrifugation, the pellet containing insoluble YKL-40 was solubilized in 8 M urea before purification of the dissolved protein by affinity chromatography on a Ni-NTA agarose column run under gravity. YKL-40 was eluted with 250 mM imidazole. Fractions containing YKL-40 were pooled and then subjected to several rounds of membrane centrifugation using Vivaspine-20 ultrafiltration membrane concentrators ( $M_r$  10000 cut-off) for complete removal of

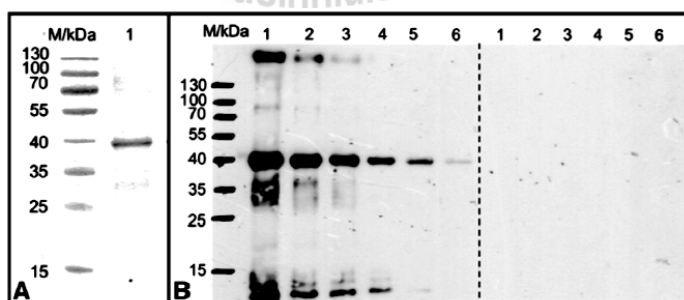
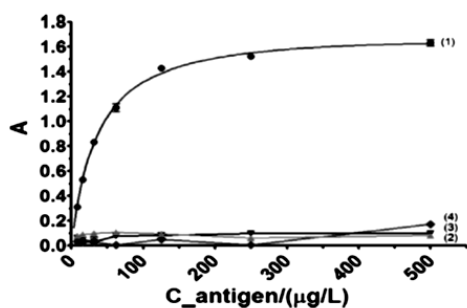


Fig. 1. Purification of recombinant YKL-40. (A) SDS-PAGE of affinity-purified YKL-40 (lane 1, 2  $\mu$ g); Coomassie-blue stained 12% polyacrylamide gel. (B) YKL-40 protein detected by immunoblotting with the anti-YKL-40 serum (left-hand panel). Lane: M, standard protein markers; 1–6, purified YKL-40 protein (2  $\mu$ g) detected with various dilutions (1:5000, 1:10000, 1:20000, 1:40000, 1:80000 and 1:160000) of antiserum. The same dilutions of pre-immune serum were used as a negative control (right-hand panel).



**Fig. 4.** Enzyme-linked YKL-40 immunosorbent assay (ELISA). Binding of purified anti-YKL-40 IgG (50  $\mu$ L, 15.6  $\mu$ g/L) to different amounts of surface-attached YKL-40 related proteins: human YKL-40 (1, red); human YKL-39 (2, green); human AMCase (3, blue) and bacterial chitinase (ChiA, 4, pink). The horizontal axis shows the total amount of the antigen of choice used for microtiter plate well loading. The half maximal effective concentration (EC50) was obtained by statistical analysis of the data set as  $44.6 \pm 0.01$   $\mu$ g/L for a half maximal absorbance ( $\lambda = 450$  nm) of 0.972. (For interpretation of the references to color in this figure legend, the reader is referred to the web version of this article.)

### 2.5. Assembly of YKL-40 immunosensors

The 3-mm-diameter disk-shaped Au electrodes for the flow cell were polished with 5  $\mu$ m and then 1  $\mu$ m alumina slurries, rinsed with purified water and dried in a stream of  $N_2$  gas. Polished electrodes were cleaned electrochemically in 0.5 M  $H_2SO_4$  by cycling their potential 25 times, at 0.1 V/s, between 0 and +1.5 V versus Ag/AgCl/1 M KCl. They were then rinsed thoroughly with water, dried and their quality checked by cyclic voltammetry in 5 mM  $K_3[Fe(CN)_6]$  solution. Anti YKL-40 IgG was immobilized on the cleaned Au electrodes using a published protocol [13], in which the Au disks were coated with a self-assembling monolayer of thiourea, which allowed anti-YKL-40 fixation through glutaraldehyde-mediated crosslinking. Subsequent treatment with 1-dodecanethiol ensured complete insulation of the Au surface and eliminated non-specific binding [14]. The effect of immobilization on the electrochemical activity of the Au electrodes was inspected by cyclic voltammetry in 5 mM  $K_3[Fe(CN)_6]$  in 0.1 M KCl solution at a scan rate of 0.1 V/s.

### 2.6. Capacitive YKL-40 immunosensing

YKL-40 detection used the commercial three-electrode flow cell connected to the eDAQ electrochemical workstation. The working electrodes were anti-YKL-40 modified Au disks, while an Ag/AgCl/1 M KCl system and the steel tube outlet of the flow cell served as the reference and counter electrodes, respectively. Measurements were made and data stored using the tailored software package of the eDAQ system. A stream of measuring buffer through the flow cell was maintained at a defined and constant flow rate with a peristaltic pump and a manual injection valve allowed injection of YKL-40 samples of up to 400  $\mu$ L. YKL-40 quantification was through the capacitance change in

**Table 1**  
Interaction of YKL-40 and homologues with purified anti-YKL-40.

	$A_{450}^{a,c}$	Reactivity <sup>d</sup>
YKL-40 <sup>b</sup>	$1.171 \pm 0.03$	1.00
YKL-39 <sup>b</sup>	$0.101 \pm 0.01$	0.09
ChiA <sup>b</sup>	$0.022 \pm 0.02$	0.02
AMCase <sup>b</sup>	$0.094 \pm 0.01$	0.08

<sup>a</sup> Values are means of triplicate measurements.

<sup>b</sup> ELISA used well loading of 50  $\mu$ L of 125  $\mu$ g/L antigen and 50  $\mu$ L of 15.6  $\mu$ g/L antibody.

<sup>c</sup>  $A_{450}$  is the measured absorbance at wavelength of 450 nm.

<sup>d</sup> Values normalized against YKL-40.

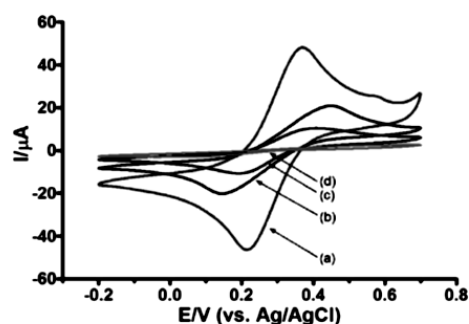


**Fig. 5.** Cyclic voltammetry of thiol- and YKL-40 antibody-modified gold electrodes. Cyclic voltammograms were recorded for the working electrodes with 5 mM  $K_3[Fe(CN)_6]$  in 0.1 M KCl solution at a scan rate of 0.1 V/s. Potentials are relative to the Ag/AgCl reference electrode. (a, red), unmodified gold electrode; (b, green), thiourea-modified gold electrode; (c, blue), thiourea/glutaraldehyde/anti-YKL-40-modified gold electrode; (d, mauve), thiourea/glutaraldehyde/anti-YKL-40/CH<sub>3</sub>(CH<sub>2</sub>)<sub>11</sub>SH-modified gold electrode. (For interpretation of the references to color in this figure legend, the reader is referred to the web version of this article.)

the anti-YKL-40-modified Au electrode, produced by antigen binding. Capacitance values for the immunosensor surfaces with and without bound antigen were computed from recordings of the biosensor current in response to +50 mV potential steps of 6.4 ms width. Choice of the parameter combination was based on experience from previous work with capacitive immunosensing [e.g. 11–13,15–22], which showed that the particular pulse height and length lead to exponentially decaying capacitive current traces that are long and strong enough for determination of true immunosensor capacitance values with low standard deviation and good stability; for the interested reader further information on the methodology of the potential step-based sensor capacitance detection has been provided as part of the supplemental content. Buffer solutions containing known concentrations of YKL-40 were used for studying the concentration dependence of its interaction with anti-YKL-40 and for evaluation of recovery rates. A set of human serum samples of 25, 50, 80 and 100  $\mu$ g/L was created by adding appropriate aliquots of YKL-40 stock solution; however, before analysis spiked serum samples were diluted five-fold with standard running buffer, to minimize matrix effects.

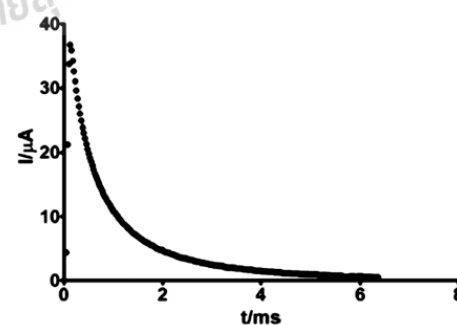


**Fig. 6.** Immunosensor response in a potential step experiment. The current (I) vs. time (t) trace was induced by the application of an electric potential step  $U = 50$  mV of duration  $t_p = 6.4$  s to the anti-YKL-40-modified electrode in the flow system. The time required for the current to fall to 0.632 of the initial value after pulse application (equal to the time constant,  $\tau_c$ , of the cell circuitry) is in this specific case 0.82 ms.

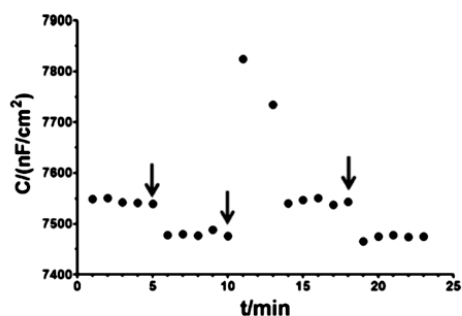


Fig. 7. Plot of the YKL-40 immunosensor capacitance,  $C$ , in  $\mu\text{F}/\text{cm}^2$ , as a function of time. Two separate injections of purified YKL-40 (1 mg/L, red arrows) into the flow buffer produced a decrease in capacitance, as a result of antigen binding. Injection of regeneration solution (3 mM HCl, green arrows) between the YKL-40 applications released the antigen and restored the baseline capacitance. The electrode capacitance was unchanged when antigen-free pure buffer was injected in control experiments (not shown). The experiment was carried out at 25°. (For interpretation of the references to color in this figure legend, the reader is referred to the web version of this article.)

### 3. Results and discussion

#### 3.1. YKL-40 antigen and antibody preparation and characterization

The YKL-40 gene was successfully amplified from human cDNA and the PCR product cloned into the pQETri expression system. Nucleotide sequencing showed that no mutations had occurred during the gene amplification process (data not shown). Induction for 16 h with IPTG resulted in good expression of the YKL-40 recombinant plasmid by the *E. coli* M15 (pREP) host cells, yielding about 3.0 mg of purified protein per liter of cell culture. The bulk of the induced YKL-40 protein was insoluble, suggesting that it was present in inclusion bodies. The insoluble fraction was solubilized with 8 M urea and his<sub>6</sub>-tagged YKL-40 purified by affinity chromatography on Ni-NTA-agarose. Fig. 1A shows SDS-PAGE of the purified protein, which migrated as a single band around 40 kDa, consistent with the molar mass expected for human YKL-40 lacking the 20 amino acid signal peptide (40488 Da).

Table 2

YKL-40 immunosensor regeneration after discrete sample exposures: identification of the type and pH of the regeneration solution for optimal removal of captured antigen.

Regeneration solution	Percentage of average residual activity <sup>a,b,c</sup>
<b>Low pH</b>	
50 mM glycine/HCl pH = 2.5	59.1 ± 1.4
100 mM HCl (pH = 1.0)	67.5 ± 0.2
31.6 mM HCl (pH = 1.5)	80.6 ± 2.0
10 mM HCl (pH = 2.0)	86.0 ± 0.7
3.2 mM HCl (pH = 2.5)	99.4 ± 0.5
1 mM HCl (pH = 3.0)	80.1 ± 1.0
<b>High pH</b>	
5 mM NaOH (pH = 11.7)	30.3 ± 0.6
50 mM NaOH (pH = 12.7)	40.7 ± 0.1
<b>High ionic strength</b>	
1 M NaCl	12.4 ± 1.3
1 M KCl	24.5 ± 2.1

<sup>a</sup> Values are means of the triplicate assessment of YKL-40 samples of 10  $\mu\text{g}/\text{L}$  at 25°.

<sup>b</sup> Percentage of residual activity defined as  $\Delta C_2/\Delta C_1 \times 100$ , with  $\Delta C_1$  and  $\Delta C_2$  equal to the capacitance change observed before and after regeneration.

<sup>c</sup> The original data responsible for completing this table is part of the Supplementary content and presented in Figs. S3–S4.

Purified YKL-40 protein was used for the production of polyclonal anti-YKL-40 serum, and antibody titers were determined by immunoblotting (Fig. 1B). The antiserum reacted strongly with the YKL-40 target at dilutions up to 1:80000 and a faint signal was detectable even at 160000-fold dilution. In contrast, no signal was detected from the pre-immune serum, even at the highest concentration tested (5000-fold dilution). Evaluation of cross-reactivity against other family-18 glycosyl hydrolases used a 1:40000 dilution of anti-YKL-40 serum. Western blots (Fig. 2A and B) revealed no interaction of the polyclonal antiserum with YKL-40 homologues such as human YKL-39, human AMCase and bacterial chitinase, confirming specificity for the target protein, YKL-40.

Polyclonal anti-YKL-40 serum was fractionated by affinity chromatography on protein A agarose. SDS-PAGE analysis (Fig. 3A) showed the purity of the product, and confirmed that it is a protein A-specific IgG isotype. The immunoglobulin migrated behind the 130 kDa marker under non-reducing conditions (Fig. 3A, lane 2), while reduction of the sample produced two protein bands, of about 55 kDa and 22 kDa (Fig. 3A, lane 1), as expected for IgG. In western blot analysis the purified antibody reacted strongly with YKL-40 down to 0.175 mg/L, whereas the pre-immune serum showed no reaction (Fig. 3B).

Cross-reactivity of the purified antibody with related proteins was tested by the indirect ELISA technique. Fig. 4 shows binding of anti-YKL-40 IgG (50  $\mu\text{L}$ , 15.6  $\mu\text{g}/\text{L}$ ) to YKL-40 itself (red trace); the hyperbolic plot of the interaction signal with increasing antigen load in the micro-titer plate well is characteristic of a specific interaction. With human YKL-39 (green trace), AMCase (blue trace) and bacterial chitinase A (pink trace), no significant signal was obtained. The binding of each antigen was further tested with a fixed antigen load (50  $\mu\text{L}$ , 125  $\mu\text{g}/\text{L}$ ) and constant anti-YKL-40 (50  $\mu\text{L}$ , 15.6  $\mu\text{g}/\text{L}$ ). As evident from the summary of this test in Table 1, the signal for YKL-40 was about 11-, 12.5- and 50-fold larger than that for human YKL-39, human AMCase and bacterial chitinase, respectively. This confirmed that the purified antibody was highly specific for YKL-40 and thus suitable for use in electrochemical YKL-40 immunodetection.

#### 3.2. Sensor construction for capacitive YKL-40 immunosensing

The YKL-40 antibody was immobilized on Au disk working electrodes by covalent coupling with thiourea and glutaraldehyde. Even a small exposed conductive area on the Au disks would interfere with capacitance-based measurement of Ag binding, but blockage with 1-dodecanethiol produced an insulating monolayer that permitted pure capacitive current recordings in response to potential pulse application. Successful coating of the dielectric sensor was confirmed by cyclic voltammetry in electrolyte containing  $\text{K}_3[\text{Fe}(\text{CN})_6]$ : as shown in Fig. 5, the characteristic ferricyanide redox peaks obtained with untreated gold electrodes decreased progressively after exposure to thiourea, glutaraldehyde and antibody and were completely abolished by the final alkyl thiol treatment.

#### 3.3. YKL-40 immunosensor capacitance evaluation

In immunosensing tests 10 mM phosphate, pH = 7.0 was used as the running buffer, with a flow-rate of 0.1 mL/min for delivery of YKL-40 samples and standards from the injection point to the electrochemical flow cell, and then to the waste container. At distinct intervals during flow-cell operation, 50 mV potential pulses of 6.4 ms duration were applied to the working electrode. Fig. 6 shows a typical current response of a YKL-40 immunosensor to the transient potential change, as a plot of  $I(t)$  versus  $t$ . Since the running buffer was free of easily oxidizable or reducible compounds and the sensor effectively thiol-insulated, charge transfer through the cell was entirely capacitive in nature, the current therefore decaying exponentially with time.

**Table 3**

Parameter optimization for flow injection-based capacitive YKL-40 immunosensing: application to the running buffer type, pH and concentration, the injected sample volume and the applied flow rate.

Parameter	Property range	YKL-40 test concentration (g/L)	Revealed optimum <sup>b</sup>
Buffer solutions			
Type	10 mM phosphate buffer, pH = 7.0 10 mM HEPES buffer, pH = 7.0 10 mM Tris-HCl buffer, pH = 7.0	$10^{-7}$ to $10^{-3}$	10 mM phosphate buffer, pH = 7.0
pH <sup>a</sup>	6.0, 6.5, 7.0, 7.5, 8.0	$10^{-5}$	7.0
Concentration	5, 10, 50, 100 mM	$10^{-5}$	10 mM
Sample volume	100, 200, 300, 400 $\mu$ L	$10^{-5}$	200 $\mu$ L
Flow rate	50, 100, 200, 300, 400 $\mu$ L/min	$10^{-5}$	100 $\mu$ L/min

<sup>a</sup> pH = values valid at 25°.

<sup>b</sup> The original data responsible for completing this table is part of the Supplementary content and presented in Figs. S5–S9.

In redox mediator-free measuring buffer, the YKL-40 immunosensor responded to the application of a rectangular potential pulse of amplitude  $E_{(appl)}$  with an exponentially decaying current, which can be expressed as a function of time by:

$$\ln |I(t)| = \ln \left( \frac{E_{(appl)}}{R_s} \right) - t / (R_s C_{WE}) \quad (1)$$

where  $R_s$  represents the dynamic resistance of the recognition layer and  $C_{WE}$  the total capacitance of the immersed immunosensor/electrolyte interface. Accordingly, an experimental (extrapolated) quantity for  $E_{(appl)}/R_s$ , the y-axis intercept of the linear fit, can be derived from plots of  $\ln |I(t)|$  against  $t$  and with the known magnitude of the potential pulse this gives finite values of  $R_s$ ,  $R_s$ , and the slope of the linear fit then allow the calculation of  $C_{WE}$  for the particular sensor. In YKL-40 immunosensing trials  $C_{WE}$  values were determined every minute and, after scaling to the area of the carrier electrode ( $7.07 \times 10^{-4} \text{ cm}^2$ ), plotted as the area-normalized sensor capacitance,  $C$ , in  $\text{nF/cm}^2$ , against time. An example of this approach is shown in Fig. 7. At the beginning of this measurement the immunosensor surface was exposed to the running buffer and baseline values for  $C$  were recorded (Fig. 7, 0–5 min, here  $7544 \text{ nF/cm}^2$ ). The injection of, for instance, 200  $\mu$ L of 1 mg/L YKL-40 solution led to a readily detectable decrease in  $C$  on binding of YKL-40 to the immobilized antibody (Fig. 7, 6–10 min, here  $7480 \text{ nF/cm}^2$ ). As the YKL-40 antigen and antibody have molecular weights of about 40 and 150 kDa, the antigen is expected to be

considerably smaller than the antibody. However the routinely observed clear drop in  $C$  upon antigen sample injection proved that antigen bonding to immobilized antibody entities apparently spreads the double-layer arrangement at the immunosensor's liquid/solid interface significantly enough to let the change of surface state be detected via

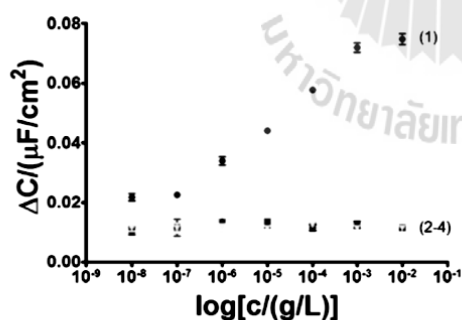


**Fig. 8.** Selectivity test for capacitive YKL-40 immunosensors. A YKL-40 antibody modified gold electrode was exposed either to its target antigen, YKL-40, or to the homologous proteins YKL-39 and AMCSe. The capacitance change,  $\Delta C$  (normalized to geometric electrode area) was evaluated for protein concentrations from  $10^{-8}$  to  $10^{-2} \text{ g/L}$ , under optimal assay conditions (flow rate 100  $\mu$ L/min, 200  $\mu$ L sample injection, running buffer 10 mM phosphate pH = 7.0, regeneration solution 3 mM HCl). 1, Red, YKL-40; 2, green, YKL-39; 3, blue, AMCSe; 4, yellow, blank. (For interpretation of the references to color in this figure legend, the reader is referred to the web version of this article.)

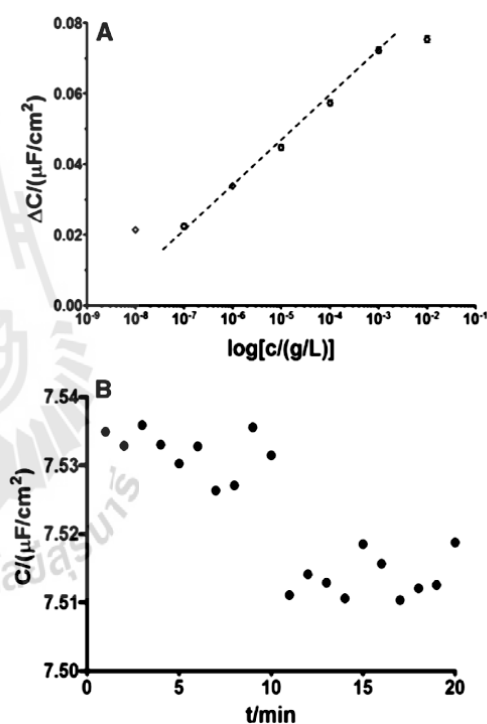


**Fig. 9.** A) Calibration of a YKL-40 immunosensor. Experimental parameters were: (1) running buffer, 10 mM phosphate pH = 7.0, (2) flow rate, 100  $\mu$ L/min, (3) regeneration solution, 3 mM HCl, (4) injected sample volume, 200  $\mu$ L and (5) measurement temperature 25°. Error bars are included in the calibration plot, but are about the size of the data points and so not easily visible. The linear regression equation for the fit of the data points between  $10^{-9}$  and  $10^{-3} \text{ g/L}$  was  $\Delta C(c) = \Delta C(c_{ref}) + b \cdot \log(c)$  with  $\Delta C$ , defined as  $C(\text{before sample injection}) - C(\text{after sample injection})$ ,  $\Delta C(c_{ref})$ , the value of the capacitance change for a sample concentration of zero (= the y-axis intercept of the linear regression line), computed as  $107.4 \pm 1.45 \text{ nF/cm}^2$ , and  $b$ , the concentration sensitivity, equal to  $12.28 \pm 0.27 \text{ nF/cm}^2$  per decade of concentration change. B) Immunosensor response to the injection of 0.1  $\mu$ g/L YKL-40. Experimental parameters were as listed in A).

**Table 4**  
YKL-40 detection in spiked serum samples: a comparison of the results from capacitive immunosensing with equivalent data from a standard ELISA screen.

Added/ $\mu\text{g/L}$	Immunosensor		ELISA	
	Found/ $\mu\text{g/L}^a$	Recovery/ $\%^{a,b}$	Found/ $\mu\text{g/L}^a$	Recovery/ $\%^{a,b}$
25.00	25.1 $\pm$ 1.2	100.4 $\pm$ 4.8	25.5 $\pm$ 0.8	101.9 $\pm$ 3.2
50.00	49.6 $\pm$ 3.4	99.2 $\pm$ 5.7	50.8 $\pm$ 0.7	101.5 $\pm$ 1.3
80.00	85.5 $\pm$ 1.9	106.7 $\pm$ 2.4	79.5 $\pm$ 0.3	99.4 $\pm$ 0.4
100.00	101.2 $\pm$ 3.5	101.2 $\pm$ 3.5	101.1 $\pm$ 0.5	101.1 $\pm$ 0.5

<sup>a</sup> Values represent average of triplicate assessments at  $T = 298 \text{ K}$  ( $25^\circ \text{C}$ ).

<sup>b</sup> Recovery defined as  $(\text{Found}/\text{Added}) \times 100$ .

electrical capacitance measurements in the voltage pulse mode. Subsequent injection of 200  $\mu\text{L}$  of an acidic regeneration solution (3.2 mM HCl) removed bound YKL-40 from the sensor surface and restored  $C$  to its original level (Fig. 7, 14–18 min, 7544  $\text{nF}/\text{cm}^2$ ). It should be noted that the total capacitance of the system increased during regeneration (Fig. 7, 10–13 min). This is because the capacitance of capacitive immunosensor surfaces increases with increasing ionic strength of the surrounding electrolyte solution [18,23]. A transient contact during regeneration with, for instance, 3 mM HCl exposes the sensing disk for a short period to an increased ionic strength, with a short but significant capacitance increase. However, return to the running buffer restores the capacitance of the immunosensor to the standard background level. As expected, repetition of the injection of the 200  $\mu\text{L}$  of 1 mg/L YKL-40 solution (Fig. 7, 19–23 min) produced virtually the same capacitance drop as was observed after the first injection.

#### 3.4. Parameter optimization and stability and selectivity tests for capacitive YKL-40 immunosensing

To obtain the best possible analytical performance, the experimental parameters affecting capacitive YKL-40 immunosensing were optimized. These were (i) the type, concentration and pH of the running buffer, (ii) the type and concentration of the regeneration solution, (iii) the injected sample volume and (iv) the flow rate. Individual trials assessed the capacitance changes in response to sequential injections of 10  $\mu\text{g/L}$  of YKL-40; measurements were performed in triplicate, varying one parameter while keeping all others fixed. Figs. S3–S9 in the Supplementary content show the original data while Table 2 and 3 summarize the optimization trials for the regeneration solution and the other specified factors. The optimal regeneration solution was 3.2 mM HCl ( $\text{pH} = 2.5$ ), while 10 mM phosphate buffer solution,  $\text{pH} = 7.0$ , 100  $\mu\text{L}/\text{min}$  and 200  $\mu\text{L}$  were selected for the running buffer, flow rate and sample volume, respectively.

When the equipment was operated with the optimal parameter set, a sequence of 45 injections of 10  $\mu\text{g/L}$  YKL-40, equally distributed over a period of 3 days, produced a capacitance change,  $\Delta C$ , defined as  $C(\text{before an injection}) - C(\text{after an injection})$ , that was reproducible to within  $\pm 5\%$  (see Fig. S10). This excellent signal stability and reproducibility accord with the previously reported performance of capacitive immunosensors with other Ab–Ag couples [11–13,15–22,24–28] and permit YKL-40 quantification in many samples.

The possibility of interference with the response of the capacitive YKL-40 immunosensors was also investigated. Two structurally related molecules, human YKL-39 and human AMCcase, were used to check the selectivity of the capacitive biosensor system. As seen in Fig. 8, YKL-39 and AMCcase at concentrations from  $10^{-08}$  to  $10^{-02}$  g/L produced no significant capacitance change, while the target antigen YKL-40 induced the expected concentration-dependent capacitance signal.

#### 3.5. Calibration trials with the optimized capacitive YKL-40 immunosensing assay

Sequential injections of YKL-40 standard solutions, of concentrations 0.01  $\mu\text{g/L}$  to 10 mg/L, in triplicate for each value and with intermediate

acidic regeneration steps, were used to produce a calibration curve and to determine the linear dynamic range of the assay. Fig. 9A shows the results of a typical calibration experiment, with the capacitance change,  $\Delta C$ , plotted against the logarithm of the YKL-40 concentration. A linear response was reproducibly obtained within the range 0.1  $\mu\text{g/L}$  to 1 mg/L. The linear regression equation for the test trial in Fig. 9 was  $C(c) = C(c_{\text{ref}}) + b \cdot \log(c)$  with  $C(c_{\text{ref}})$  equal to  $107.4 \pm 1.45 \text{ nF}/\text{cm}^2$ , for the onset of the linear approximation and  $b$ , the concentration sensitivity, equal to  $12.28 \pm 0.27 \text{ nF}/\text{cm}^2$  per decade of concentration change. Apparently, the sensor became saturated above 1 mg/L YKL-40, indicating that all immobilized antibody was occupied with antigen; and below 0.1  $\mu\text{g/L}$ , the amount of bound YKL-40 was insufficient to widen the ionic double layer detectably. The lower limit of detection was actually  $0.07 \pm 0.01 \mu\text{g/L}$ . A representative trace of the response of the sensor to 0.1  $\mu\text{g/L}$  YKL-40 is shown in Fig. 9B.

#### 3.6. Analysis of model and real samples

Triplicate quantifications of buffer solutions with added YKL-40 (0.5–100  $\mu\text{g/L}$ ) reproduced the set point levels with  $101.5\% \pm 5.4\%$  recovery (defined as  $[C_1/C_2 \times 100]$ , where  $C_1$  is the concentration of analyte measured in the spiked sample and  $C_2$  is the adjusted level of analyte). The applicability of the capacitive biosensor was tested further by measuring YKL-40 in human blood. Spiked samples with 25, 50, 80 and 100  $\mu\text{g/L}$  analyte concentration were prepared by mixing appropriate volumes of serum and YKL-40 standard and for final analysis these were diluted 5-fold with carrier buffer to minimize influence of the matrix effect on signal generation. The consequent reduction of the measured YKL-40 concentrations was not a problem because of the very low detection limit for the capacitive YKL-40 assay. Under these conditions, the sensitivities (slope of  $\Delta C$  vs.  $c$  plots) for measurements of standard YKL-40 solutions and spiked serum samples were identical, indicating that there was no interference by serum components and confirming the high specificity of the  $\Delta C$  signal for YKL-40, even after sample dilution. Table 4 summarizes the results of the serum performance test for capacitive YKL-40 immunosensing and compares the values obtained with those from conventional ELISA. For triplicate measurements of the same sample the standard deviation of the computed values of  $\Delta C$  was only  $\pm 1\%$ . Consistent with the observation for the samples in buffer, the recovery of YKL-40 in the four serum samples was 99–107%. Furthermore, the concentrations determined by the capacitive immunosensor system were found to be in good agreement with those from the ELISA technique, indicating that the label-free capacitive YKL-40 immunosensing assay is well suited for the analysis of real serum samples.

## 4. Conclusions

The first electroanalytical procedure for quantifying the disease marker YKL-40 is reported here. The novel detection scheme used gold disk working electrodes with target-specific antibody covalently attached to their thiol-modified surfaces. A linear correlation between the capacitance of the established electrochemical YKL-40 immunosensors and the analyte concentration was observed from  $10^{-07}$  to  $10^{-03}$  g/L; the

limit of detection was  $0.07 \pm 0.01 \mu\text{g/L}$ , which is about 300 times lower than is currently possible in routine optical YKL-40 ELISA assays. This significant improvement in performance was reached using a compact, low-cost electrochemical flow injection analysis system, simple probe fabrication and straightforward measuring procedures. Although electroanalysis is not yet used widely for clinical biochemical analysis, the great gain in sensitivity and the obvious possibility of improving the technique via system automation suggest that development and refinement of this approach are well worthwhile. A significant advance in YKL-40 analysis has already been realized and future work with this sensing strategy is expected to improve applications of trace YKL-40 screening for disease diagnosis and prognosis.

#### Acknowledgments

Wethaka Chaocharoen is grateful for the financial support from The Office of the Higher Education Commission, Thailand through a grant in the program "Strategic Scholarships for Frontier Research Network for the Ph.D. Program, Thai Doctoral degree" (grant no. CHE 510767). Financial support for the work came also through the Suranaree University of Technology grants to Wipa Suginta, Panida Khunkaewla and Albert Schulte, both personally and to their Biochemistry–Electrochemistry Research Unit (grant no. SUT1-102-54-36-06), and through the Prince of Songkla University funds for the Trace Analysis and Biosensor Research Center, Faculty of Science. All authors express their thanks to Dr. David Apps, Biochemistry Reader (retired), Centre for Integrative Physiology, Edinburgh University, Scotland for his critical manuscript reading and language improvements.

#### Appendix A. Supplementary data

Supplementary data to this article can be found online at <http://dx.doi.org/10.1016/j.bioelechem.2014.07.006>.

#### References

- [1] M. Harutyunyan, M. Christiansen, J.S. Johansen, L. Køber, C. Torp-Petersen, J. Kastrup, The inflammatory biomarker YKL-40 as a new prognostic marker for all-cause mortality in patients with heart failure, *Immunobiology* 217 (2012) 652–656.
- [2] K. Huang, L.D. Wu, YKL-40: a potential biomarker for osteoarthritis, *J. Int. Med. Res.* 37 (2009) 18–24.
- [3] J.S. Johansen, B.V. Jensen, A. Roslind, P.A. Price, Is YKL-40 a new therapeutic target in cancer? *Expert Opin. Ther. Targets* 11 (2007) 219–234.
- [4] J.S. Johansen, N.A. Schultz, B.V. Jensen, Plasma YKL-40: a potential new cancer biomarker? *Future Oncol.* 5 (2009) 1065–1082.
- [5] J. Kastrup, Can YKL-40 be a new inflammatory biomarker in cardiovascular disease? *Immunobiology* 217 (2012) 483–491.
- [6] M.H. Kazakova, V.S. Sarafian, YKL-40—a novel biomarker in clinical practice? *Folia Med.* 51 (2009) 5–14.
- [7] C.N. Rathcke, H. Vestergaard, YKL-40—an emerging biomarker in cardiovascular disease and diabetes, *Cardiovasc. Diabetol.* 8 (2009) 61.
- [8] J.S. Johansen, B.V. Jensen, A. Roslind, D. Nielsen, P.A. Price, Serum YKL-40, a new prognostic biomarker in cancer patients? *Cancer Epidemiol. Biomarkers Prev.* 15 (2006) 194–202.
- [9] S. Centi, S. Laschi, M. Mascini, Strategies for electrochemical detection in immunochemistry, *Bioanalysis* 1 (2009) 1271–1291.
- [10] V.M. Mirsky, M. Riepl, O.S. Wolfbeis, Capacitive monitoring of protein immobilization and antigen–antibody reactions on monomolecular alkythiol films on gold electrodes, *Biosens. Bioelectron.* 12 (1997) 977–989.
- [11] C. Berggren, B. Bjarnason, G. Johansson, Capacitive biosensors, *Electroanalysis* 13 (2001) 173–180.
- [12] C. Berggren, G. Johansson, Capacitance measurements of antibody–antigen interactions in a flow system, *Anal. Chem.* 69 (1997) 3651–3657.
- [13] W. Limbut, P. Kanatharana, B. Mattiasson, P. Asawatreratanakul, P. Thavarungkul, A comparative study of capacitive immunosensors based on self-assembled monolayers formed from thiourea, thioctic acid, and 3-mercaptopropionic acid, *Biosens. Bioelectron.* 22 (2006) 233–240.
- [14] P.B. Lippa, L.J. Sokoll, D.W. Chan, Immunosensors—principles and applications to clinical chemistry, *Clin. Chim. Acta* 314 (2001) 1–26.
- [15] C. Berggren, B. Bjarnason, G. Johansson, Instrumentation for direct capacitive biosensors, *Instrum. Sci. Technol.* 27 (1999) 131–140.
- [16] I. Bontidean, J. Ahlqvist, A. Mulchandani, W. Chen, W. Ba, R.K. Mehra, A. Mortari, E. Csöregi, Novel synthetic phytochelatin-based capacitive biosensor for heavy metal ion detection, *Biosens. Bioelectron.* 18 (2003) 547–553.
- [17] W. Limbut, P. Kanatharana, B. Mattiasson, P. Asawatreratanakul, P. Thavarungkul, A reusable capacitive immunosensor for carcinoembryonic antigen (CEA) detection using thiourea modified gold electrode, *Anal. Chim. Acta* 561 (2006) 55–61.
- [18] C. Berggren, B. Bjarnason, G. Johansson, An immunological interleukin-6 capacitive biosensor using perturbation with a potentiostatic step, *Biosens. Bioelectron.* 13 (1998) 1061–1068.
- [19] W. Limbut, P. Kanatharana, B. Mattiasson, P. Asawatreratanakul, P. Thavarungkul, A comparative study of capacitive immunosensors based on self-assembled monolayers formed from thiourea, thioctic acid, and 3-mercaptopropionic acid, *Biosens. Bioelectron.* 22 (2006) 233–240.
- [20] S. Loyprasert, P. Thavarungkul, P. Asawatreratanakul, B. Wongkittisuksa, C. Limsakul, P. Kanatharana, Label-free capacitive immunosensor for microcystin-LR using self-assembled thiourea monolayer incorporated with Ag nanoparticles on gold electrode, *Biosens. Bioelectron.* 24 (2008) 78–86.
- [21] A. Numnuam, P. Kanatharana, B. Mattiasson, P. Asawatreratanakul, B. Wongkittisuksa, C. Limsakul, P. Thavarungkul, Capacitive biosensor for quantification of trace amounts of DNA, *Biosens. Bioelectron.* 24 (2009) 2559–2565.
- [22] B. Wongkittisuksa, C. Limsakul, P. Kanatharana, W. Limbut, P. Asawatreratanakul, S. Dawan, S. Loyprasert, P. Thavarungkul, Development and application of a real-time capacitive sensor, *Biosens. Bioelectron.* 26 (2011) 2466–2472.
- [23] D. Jiang, J. Tang, B. Liu, X. Sheng, J. Kong, Covalently coupling the antibody on an amine-self-assembled gold surface to probe hyaluronan-binding protein with capacitance measurement, *Biosens. Bioelectron.* 18 (2003) 1183–1191.
- [24] J. Jantra, P. Kanatharana, P. Asawatreratanakul, B. Wongkittisuksa, C. Limsakul, P. Thavarungkul, Detection of staphylococcal enterotoxin A (SEA) at picogram level by a capacitive immunosensor, *J. Environ. Sci. Health A* 46 (2011) 560–568.
- [25] J.Y. Liao, Detection of human chorionic gonadotrophin hormone using a label-free epoxysilane-modified capacitive immunosensor, *Appl. Microbiol. Biotechnol.* 74 (2007) 1385–1391.
- [26] S. Suwansa-ard, P. Kanatharana, P. Asawatreratanakul, B. Wongkittisuksa, C. Limsakul, P. Thavarungkul, Comparison of surface plasmon resonance and capacitive immunosensors for cancer antigen 125 detection in human serum samples, *Biosens. Bioelectron.* 24 (2009) 3436–3441.
- [27] K. Teeparuksapum, M. Hedström, E.Y. Wong, S. Tang, I.K. Hewlett, B. Mattiasson, Ultrasensitive detection of HIV-1 p24 antigen using nanofunctionalized surfaces in a capacitive immunosensor, *Anal. Chem.* 82 (2010) 8406–8411.
- [28] L. Yang, W. Wei, X. Gao, J. Xia, H. Tao, A new antibody immobilization strategy based on electrodeposition of nanometer-sized hydroxyapatite for label-free capacitive immunosensor, *Talanta* 68 (2005) 40–46.

Chaocharoen, W., Ranok, A., Suginta, W. and Schulte, A. (2015). A microfluidic capacitive immunosensor system for human cartilage chitinase-3-like protein 2 (hYKL-39) quantification as an osteoarthritis marker in synovial joint fluid. **RSC Adv.** 5: 85410–85416.





Cite this: *RSC Adv.*, 2015, 5, 85410

## A microfluidic capacitive immunosensor system for human cartilage chitinase-3-like protein 2 (hYKL-39) quantification as an osteoarthritis marker in synovial joint fluid†

W. Chaocharoen,<sup>ac</sup> A. Ranok,<sup>ac</sup> W. Suginta<sup>\*acd</sup> and A. Schulte<sup>\*bcd</sup>

Worldwide, many people suffer from osteoarthritis, a painful condition that interferes with normal work and the enjoyment of life and is thus a serious personal and public problem. Good management of osteoarthritis requires methodologies for accurate and timely detection of disease onset, progression and response to treatment. Here, capacitive electrochemical immunosensors, using immobilized antibodies against the known osteoarthritis biomarker human cartilage chitinase-3-like protein 2, also known as hYKL-39, were used as novel tools for sensitive and selective osteoarthritis analysis. In the proposed procedure the current response of the sensor to a potential step application is measured; from the resultant traces, concentration-dependent capacitance changes, due to antigen binding, can be calculated. The linear range and detection limit of capacitive hYKL-39 immunosensing were respectively 0.1–1000  $\mu\text{g L}^{-1}$  and 0.074  $\mu\text{g L}^{-1}$ . This was better than the characteristics of the enzyme-linked immunosorbent assay (ELISA) with an optical readout, which is presently the standard practice for laboratory hYKL-39 screening. In synovial fluid samples from osteoarthritis patients, capacitive hYKL-39 immunosensing reported the expected elevated hYKL-39 biomarker levels in quantitative agreement with ELISA analysis. The improved detection limit and linear range of the electrochemical hYKL-39 immunoassay combined with the potential of cheap, simple, miniaturizable, portable and automatable equipment recommend this novel approach as a promising complementary tool and ideal reference assay for osteoarthritis diagnosis and monitoring, in particular when the aim is early detection.

Received 15th June 2015  
Accepted 28th September 2015  
DOI: 10.1039/c5ra11379b

www.rsc.org/advances

### 1. Introduction

Osteoarthritis (OA) is the degeneration of weight-bearing joints, and in its later stages it involves the breakdown of the cartilage layer at the terminals of the articulating bones; the consequential direct bone rubbing and abrasion result in acute or, in severe cases chronic, joint pain, tenderness, stiffness, locking and swelling.<sup>1</sup> Reduced usage of sore joints is a common reaction of people with OA, and muscle and ligament weakening around the affected sites are frequently found as secondary symptoms. Limiting painful body movements hinder chronic OA patients in their ability to work, move and exercise and result in

a diminished quality of life and also a burden to public health systems. Dealing with OA-related individual suffering and public socioeconomic issues involves disease management, medical care and the assessment of potential disease-modifying OA treatments, and so requires sensitive analytical methods for disease detection and clinical monitoring of the course of the disease. Presently, diagnosis of OA uses a combination of qualitative classification of the patient's pain levels and observation of clinical signs of joint movement reduction, joint enlargement/swelling and joint crepitus.<sup>2</sup> A positive medical check is usually followed by joint inspections using X-ray radiography or ultrasound scanning or by more expensive magnetic resonance imaging (MRI), computer tomography (CT) or radionuclide bone scans (RBS). Noticeable signs of, for instance, reduced joint space width and/or cartilage splintering, perforation or thinning confirm the presence of OA; however, with common imaging methods clear morphological changes in joint structure are only visible at advanced stages of OA, rather than at earlier stages, when therapeutic interventions would be most effective.

The drawbacks of clinical radiology in detecting premature and slowly changing OA states and the high costs and limited availability of MRI/CT/RBS OA diagnostic testing prompted

<sup>a</sup>School of Biochemistry, Institute of Science, Suranaree University of Technology, Nakhon Ratchasima 30000, Thailand. E-mail: wipa@sut.ac.th

<sup>b</sup>School of Chemistry, Institute of Science, Suranaree University of Technology, Nakhon Ratchasima 30000, Thailand. E-mail: schulte@sut.ac.th

<sup>c</sup>Biochemistry – Electrochemistry Research Unit, Suranaree University of Technology, Nakhon Ratchasima 30000, Thailand

<sup>d</sup>Center of Excellence on Advanced Functional Materials, Suranaree University of Technology, Nakhon Ratchasima 30000, Thailand

† Electronic supplementary information (ESI) available. See DOI: 10.1039/c5ra11379b

a search for alternatives for analysis of this defect. Progress in biomarker-based disease diagnosis and prognosis suggested that this type of approach might also be applicable to OA. Blood, urine and synovial fluid levels of the products of cartilage collagen and aggrecan metabolism, joint inflammation signalling molecules and joint glycoproteins, proteoglycans and glycation end-products have been reported as indicators of degenerative joint destruction.<sup>2–6</sup> More precisely, C-terminal telopeptide of collagen type II (CTX-II),<sup>7</sup> cartilage oligomeric proteins (COMPs),<sup>8</sup> matrix metallo-proteinases<sup>9,10</sup> and also hYKL-39 (ref. 11–13) were recognized as biomarkers for OA, through a combination of molecular biology, biochemistry and pathology. The routine method for detecting biomarkers in body fluids is the optical enzyme-linked immunosorbent assay (ELISA), which requires antibody against the indicator molecule and an enzyme-labelled secondary antibody for signal generation.

Detection of OA biomarkers using techniques other than ELISA is possible but has rarely been attempted. Examples are optical CTX-II and COMP microfluidic assays that work with antibody-conjugated fluoro-microbeads as functional components.<sup>14,15</sup> For COMP an immunochromatographic strip test, with gold nanoparticle-linked biomarker antibody immobilized on the sensing surface, was also reported.<sup>16</sup> To promote electrochemical signalling as an option for signal transduction in OA biomarker immunoassays we demonstrate here, for the first time, the suitability of flow-based capacitive immunosensing for reliable OA biomarker analysis. Because of experience in the preparation and structural and functional characterization of chitinase and chitinase-like proteins and also successful quantification of the cancer biomarker human chitinase-3-like protein 1 (hYKL-40) in blood serum,<sup>17</sup> hYKL-39 was chosen as the biomarker in this proof-of-principle study. The requisite electrochemical immunosensors were produced by fixing anti-hYKL-39 to a thin but insulating self-assembling monolayer of thiourea/1-dodecanethiol on gold electrodes. The concentration-dependent signal in hYKL-39 quantification was the exponentially decaying capacitive current response of completed hYKL-39 immunosensors to potential steps. The performance of capacitive hYKL-39 immunosensing was tested for the determination of the OA marker in 'spiked' samples spanning a pathologically relevant analyte concentration range, in lysates from various human cells and in synovial fluid samples from OA patients in a local clinic. Parallel assessments of duplicates of all these samples with conventional optical ELISA confirmed the data from the novel electrochemical hYKL-39 test, proving the validity of the methodology and promoting further applications for clinical osteoarthritis diagnosis. All relevant study details are presented hereafter.

## 2. Experimental

### 2.1 Chemicals and materials

Chemicals were of analytical grade and, unless otherwise specified, obtained from SM Chemical Supplies Co. Ltd (Bangkok, Thailand) or Italmar Co. Ltd (Bangkok, Thailand). The ultrapure water for electrode cleaning and buffer preparation came from a reverse osmosis/deionization purification system and was

passed through a cellulose nitrate membrane filter of pore size 0.20  $\mu\text{m}$  (Whatman, GE Medical Systems Ltd, Bangkok, Thailand) and degassed before use. YKL-39 antigen and hYKL-39 antibody preparation and purification followed procedures as described in detail earlier by Ranok *et al.* (2013).<sup>13</sup> Human cell lines used in this study were from the American Cell Culture Collection (Manassas, VA). Disk-shaped Au electrodes were prepared from crystalline Au rods of 3 mm diameter and 1 cm length and Au of 99.9% purity, obtained from a local gold shop (Tang Kim Heng Gold Shop, Nakhon Ratchasima, Thailand).

### 2.2 Capacitive hYKL-39 immunosensor preparation

Capacitive hYKL-39 immunosensors were made by a previously reported fabrication procedure.<sup>17–20</sup> The series of mechanical and electrochemical cleaning steps, amino-thiol monolayer formation and antibody immobilization by glutaraldehyde-assisted crosslinking is illustrated in the ESI in Fig. S1.† In brief, the exposed surface of the 3 mm-diameter gold disk working electrode (Au-WE) was first freed from surface dirt and polished by intense circular rubbing on soft polishing pads soaked with alumina slurries of decreasing particle size (5, 1 and finally 0.5 micron), then 15 min ultrasonication in water and drying in a stream of inert  $\text{N}_2$  gas. Polished and dried electrodes were further electrochemically cleaned in 0.5 M  $\text{H}_2\text{SO}_4$  with 25 repetitions of a 100  $\text{mV s}^{-1}$  potential scan from 0 to +1.5 V vs. an Ag/AgCl reference electrode. After rinsing in water and drying with  $\text{N}_2$ , the cleaned gold disks were immersed in 250 mM thiourea in water for 24 h at room temperature to allow formation of the required dense, covalently bound molecular thiol layer. This was followed by rinsing with water and drying in air in preparation for step 3, the coupling of anti-hYKL-39 to amine functionalities in the surface-anchored thiourea molecules, by glutaraldehyde-directed crosslinking. Thiolated Au-WEs were kept at room temperature for 20 min in a 5% (v/v) glutaraldehyde (GA) solution in 10 mM sodium phosphate buffer (PBS) pH 7.0. GA-treated sensors were rinsed with 10 mM PBS, pH 7.0, placed upside down in a suitable holder and 20  $\mu\text{L}$  of 1  $\text{mg mL}^{-1}$  anti-hYKL-39 in PBS placed on the top disk face. Antibody coupling was allowed to take place overnight at 4  $^\circ\text{C}$  and at completion the freshly modified sensor tips were thoroughly rinsed with PBS to remove reagent solution. Measurements of capacitive currents for hYKL-39 quantification require full insulation of the Au-WE, which is not usually achieved by simply coating with thiourea. Residual conductive gaps in the films can, however, be blocked with smaller thiols, so the anti-hYKL-39/glutaraldehyde/thiourea-modified Au-WEs were immersed for 20 min in a 10 mM solution of 1-dodecanethiol in ethanol. The success of the immunosensor preparation was checked by cyclic voltammetry of 5 mM potassium ferricyanide in 0.1 M KCl and electrochemical impedance spectroscopy (EIS) with a 5 mM mixture of ferro-/ferricyanide as redox probe in 25 mM PBS (pH 7.0).

### 2.3 Flow-based capacitive hYKL-39 quantification

Measurements of hYKL-39 with capacitive readout of antigen-antibody binding were executed in a microfluidic workstation as described in detail in an earlier publication<sup>17</sup> and also by

others.<sup>18–20</sup> System modules included a three-electrode potentiostat with its software and data acquisition system (EA 163/ED410, eDAQ, Australia), a three-electrode flow cell with opposite slots for the anti-hYKL-39-modified Au-WEs and the Ag/AgCl reference electrode (RE) and stainless steel (SS) connectors for the buffer influx and outflow tubing (the outlet SS canal served also as counter electrode), a peristaltic pump (Miniplus 3, Gilson, USA) offering a constant flow of running buffer and a 6-port injection valve (Biologic MV-6, Bio-Rad, USA) for injections of  $\mu\text{L}$ -sized samples.

In electrochemical experiments Au-WEs with well-insulating thiol films behave as electrical capacitors; one capacitor plate is the charged Au-WE surface, the other is the layer of electrostatically attracted ions and the dielectric is the thiol film in between. The capacitor capacitance is inversely proportional to the dielectric thickness. Antibody fixation to the thiol layer and later antigen capture inserts these units between the electrode face and the ion plane forming the Helmholtz double layer, producing a thickness increase and a capacitance decrease. This effect provides a very sensitive quantification of the binding of antibody to antigen. Baseline capacitances,  $C$ , of thiol/anti-hYKL-39-modified Au-WEs and capacitance changes,  $\Delta C$ , on binding of hYKL-39 to surface-anchored antibody can be quantified by the analysis of the exponentially decaying current ( $i$ ) in response to repetitive 50 mV potential steps of 6.375 ms duration, before and after antigen exposure. The value of  $i$  as function of time is given by the expression:

$$\ln i(t) = \ln E/R_s - (1/R_s \times C) \times t \quad (1)$$

where  $t$  is the time elapsed after the potential step was applied,  $R_s$  the dynamic resistance of the recognition layer, and  $C$  the total capacitance at the sensor/electrolyte interface. Linear least-squares plotting of  $\ln i(t)$  against  $t$  allows calculation of  $R_s$ , from the intercept of the regression line and the known value of  $E$ , and of  $C$ , from the slope. While buffer was passed continuously through the electrochemical cell, a typical sample measuring cycle used a sequence of 25 potential pulses for sensor capacitance assessments, one every minute. Usually, 10 pulses were applied before and 10 after sample injection. The last 5 pulses occurred after injection of regeneration solution. For all pulses, the current response allowed computation of corresponding  $C$  values, which, plotted *versus* time, gave the baseline, the change due to sample exposure, and baseline recovery after regeneration. The measured parameter was  $\Delta C$  on hYKL-39 capture, the difference between the  $C$  value after antigen exposure and the baseline. As shown earlier,<sup>16–19</sup>  $\Delta C$  scales with the concentration of injected antigen and construction of a calibration curve allows target quantification. Exposure of used hYKL-39 immunosensors to acidic regeneration buffer releases the antibody and the detector can then be reused.

Optimization trials with the capacitive hYKL-39 immunosensing procedure – for details and the data please refer to the ESI† – identified 25 mM phosphate buffer (pH 7.0), 3.2 mM HCl (pH 2.5), 100  $\mu\text{L min}^{-1}$  and 200  $\mu\text{L}$  as optimal running buffer, regeneration solution, flow rate and injected sample volume, respectively. System calibration under optimal conditions

revealed the analytical dynamic range, sensitivity and detection limit. Calibrated capacitive hYKL-39 immunosensors were used to quantify analyte concentrations in Jurkat, U937 and 293T cell lysates and in synovial fluid samples that were provided by the Department of Clinical Pathology at Maharat Nakhon Ratchasima Hospital, Nakhon Ratchasima, Thailand with the informed consent of patients with OA. However, synovial fluid from healthy individuals was not available from the hospital partner for desirable controls. All experiments in this study were performed in compliance with the relevant laws and institutional guidelines of Suranaree University of Technology and permitted by its Ethics Committee for Research Involving Human Subjects, which obeys international rules in reviewing and approving procedures involving humans and animals.

#### 2.4 ELISA assay for hYKL-39 determination

50  $\mu\text{L}$  of 0.5–500  $\mu\text{g L}^{-1}$  hYKL-39 in coating buffer (15 mM  $\text{Na}_2\text{CO}_3$ , 35 mM  $\text{NaHCO}_3$ , pH 9.6) were loaded into standard ELISA plate wells and the protein allowed to adsorb onto the well surfaces during overnight incubation at 4 °C. Coating buffer removal was followed by 1 h of exposure of the antigen-loaded wells to blocking buffer (2% skimmed milk in PBS, pH 7.0) at 25 °C; this filled vacant protein-binding sites and prevented non-specific binding of antibody. After removal of blocking buffer wells were rinsed four times with 200  $\mu\text{L}$  washing buffer (PBS with 0.05% Tween 20, pH 7.2, PBS-T) and then incubated for 1 h at 25 °C with 50  $\mu\text{L}$  of anti-hYKL-39 (15  $\mu\text{g L}^{-1}$  in blocking buffer). Wells were then washed four times with 200  $\mu\text{L}$  washing buffer and incubated for further 1 h at 25 °C with 50  $\mu\text{L}$  of horseradish peroxidase-conjugated goat anti-rabbit IgG (GenScript USA Inc., Piscataway, NJ), the stock (1 mg  $\text{L}^{-1}$ ) diluted 1 : 2000 in PBS, pH 7.2. Lastly, the plate was washed three times with 200  $\mu\text{L}$  washing buffer. Colour was developed by addition of 100  $\mu\text{L}$  3,3',5,5'-tetramethylbenzidine standard reagent solution (TMB, Invitrogen, Frederick, CA) and then 15 min dark incubation at 25 °C. The reaction was stopped by adding 100  $\mu\text{L}$  of 1 N HCl. The intensity of the developed colour was determined spectrophotometrically using a Biochrome Anthos MultiRead 400 Microplate Reader (Biochem, United Kingdom) at 450 nm.

### 3. Results and discussion

The protein hYKL-39 is often referred to as a pseudo-chitinase since it has structural and sequence similarity to bacterial chitinases, but although it binds chitooligosaccharides it has no catalytic activity.<sup>13,21</sup> A distinctive feature of hYKL-39 is its potential as OA biomarker, and the possible benefits of analysis of hYKL-39 in body fluids for understanding the onset and progression of OA has led to the search for hYKL-39 detection schemes. As mentioned above, ELISA is the standard means of hYKL-39 quantification. Here we explored the feasibility of hYKL-39 analysis by capacitive immunosensing, a technique that was previously shown to work well for other disease biomarkers. We first describe hYKL-39 immunosensor preparation and then discuss the parameters of the proposed

capacitive immunosensor scheme for specific hYKL-39 detection. We then report hYKL-39 analysis in synovial joint fluid from OA patients and in cell lysate, which was used to prove real sample quantification capability and clinical applicability either as an independent quantification scheme or as a novel auxiliary reference tool for the validation of measures obtained by standard optical ELISA screening.

### 3.1 Quality checks of hYKL-39 immunosensor

Ferricyanide cyclic voltammograms (CVs) for a Au-WE at different stages of modification are shown in the ESI as Fig. S2.† At the bare gold surface, forward and backward potential scans produced symmetrical current traces, indicating reversible analyte oxidation and reduction. Decreases in the cathodic and anodic peak currents were observed after reaction of the working electrode with thiourea, then glutaraldehyde and finally anti-hYKL-39, but even after immobilization of the bulky antibody the modified Au-WE retained significant electrochemical activity. To abolish current flow completely and limit electrode activity virtually to capacitive behaviour, the sensor surface was treated in a final step with 1-dodecanethiol, a linear thiol that filled the gaps left between anchored antibody molecules and established the tight insulation required for successful operation of capacitive immunosensing. The attainment of a proper interface for capacitive immunosensing was evident in CVs showing current lines with no significant redox current waves and in EIS measurements with ferro/ferricyanide as redox probe, which produced Nyquist plots typical of coated electrodes (ESI, Fig. S3†).

### 3.2 Analytical performance of capacitive hYKL-39 immunosensing

Fig. 1A shows the typical response of hYKL-39 immunosensors when sample (here:  $100 \mu\text{g L}^{-1}$  hYKL-39 in running buffer) is injected and the sensor capacitance,  $C$ , is recorded as a function of time. The two hYKL-39 additions produced well-defined stepped increases in  $C$ , indicating efficient capture of the antigen by immobilized anti-hYKL-39. Regeneration between individual injections effectively restored the baseline capacitance signal and the size of the capacitance change agreed well for the two additions. To identify the linear calibration range, hYKL-39 standard solutions of  $1 \text{ ng L}^{-1}$  to  $10 \text{ mg L}^{-1}$  were quantified by the immunosensor system, using the optimal condition parameter set. A typical calibration curve is shown in Fig. 1B, a plot of the capacitance change, normalized to the geometric sensor area, against the logarithm of hYKL-39 concentration. Triplicate measurements of all analyte concentrations showed linearity of the signal response between  $0.1$  and  $1000 \mu\text{g L}^{-1}$ ; the linear regression line drawn by standard software followed the equation  $y = (16.12 \pm 0.44)\log(x) + (137.2 \pm 2.45)$  with a correlation coefficient of  $0.99$ . As expected for binding to an immunosensor surface with a fixed number of adsorbed antibody molecules, the capacitance change in response to increasing antigen concentrations reached a plateau, here at concentrations above  $1 \text{ mg L}^{-1}$ . The limit of detection (signal-to-noise = 3) of capacitive hYKL-39 electroanalysis was  $0.074 \pm$

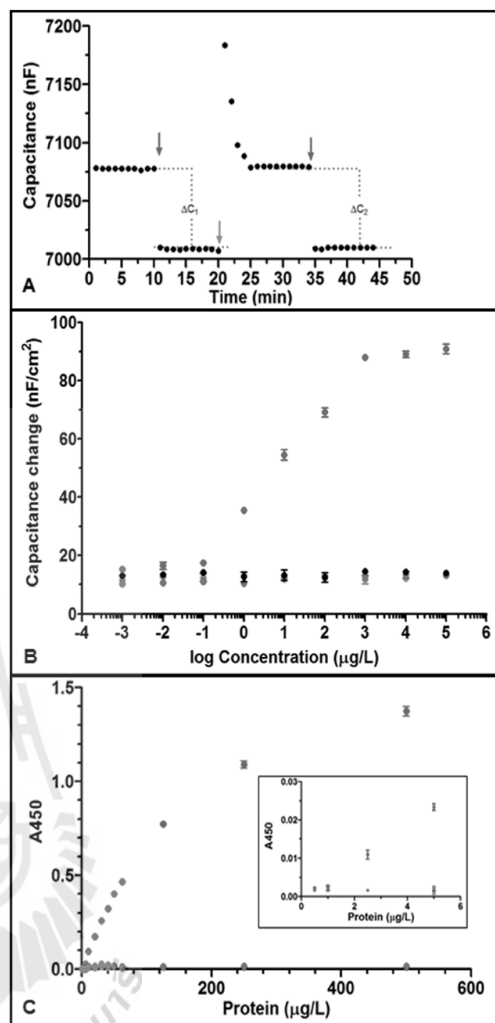


Fig. 1 (A) Capacitance response of anti-hYKL-39-modified electrode. The baseline signal of the carrier buffer is initially recorded. 1<sup>st</sup> injection of  $100 \mu\text{g L}^{-1}$  of hYKL-39 (left blue arrow) triggered antigen binding and a decrease of capacitance ( $\Delta C_1$ ). Injection of the regeneration buffer (red arrow) removed hYKL-39 from the immunosensor surface and the capacitance returned to initial baseline. 2<sup>nd</sup> injection of  $100 \mu\text{g L}^{-1}$  of hYKL-39 (right blue arrow) produced capacitance change  $\Delta C_2$ . (B) Concentration dependence of the capacitance change for a hYKL-39 immunosensor elicited by hYKL-39 (blue curve), hYKL-40 (red curve) and hAMCase (green curve) exposure. (C) Enzyme-linked immunosorbent assay (ELISA) of hYKL-39. Binding of anti-hYKL-39 IgG ( $50 \mu\text{L}$ ,  $15 \mu\text{g L}^{-1}$ ) to different amounts of immobilized hYKL-39 (blue trace), hYKL-40 (red trace) and hAMCase (green trace). The inset is a zoom of the signal response at low concentration of the antigens.

$0.02 \mu\text{g L}^{-1}$ . Two hYKL-39 homologues, hYKL-40 and hAMCase (human acidic mammalian chitinase), were tested in the capacitive immunosensor system for cross-reactivity in the

concentration range used for hYKL-39 (1 ng L<sup>-1</sup> to 10 mg L<sup>-1</sup>). Neither antigen produced a significant signal change over the concentration range tested (Fig. 1B). Interference even by closely related proteins could thus be excluded.

The specificity of the anti-hYKL-39 serum was also confirmed with a standard optical ELISA experiment. Fig. 1C shows binding of the hYKL-39 antibody to its target hYKL-39 and the reaction with hYKL-40 and hAMCase, for concentrations up to 500 µg L<sup>-1</sup>. For hYKL-39 (blue trace) triplicate recordings of the absorbance signal for the distinct biomarker levels showed linearity from 2.5–125 µg L<sup>-1</sup>, with a regression line correlation coefficient of 0.99 and pronounced levelling of the response at higher concentrations, typical of specific antibody–antigen interaction. In contrast hYKL-40 (red trace) and hAMCase (green trace) generated no signal above background level, excluding their recognition by anti-hYKL-39.

Obviously, the linearity of the electrochemical hYKL-39 screen extends at the upper and lower ends beyond those of the optical assay. The notably improved lower limit of linear response is a particular asset of the new procedure, as the OA biomarker can be quantified at concentrations beyond the reach of current ELISA. Detection closer to the onset of joint cartilage destruction thus is feasible and may permit better defect monitoring and control.

### 3.3 Signal stability of capacitive hYKL-39 immunosensing

Signal reproducibility and sensor stability over an extended time are crucial for analytical laboratory applications. The hYKL-39 immunosensors were therefore tested in the flow cell by monitoring, over 4 days, the capacitance changes for 57 sequential injections of 10 µg L<sup>-1</sup> hYKL-39. At the end of each measuring cycle 200 µL of 3.2 mM HCl was injected for sensor regeneration. The stability of the sensor was assessed from plots of the capacitance change recovery ( $(\Delta C_{\text{injection } \#(n+1)} / \Delta C_{\text{injection } \#n}) \times 100$ ) vs. injection number. An example of such a trace is shown as ESI Fig. S11.† For 49 sample injections the regeneration treatment was sufficient to maintain the response of a hYKL-39 sensor within 95% of the capacitance change for first antigen exposure; with subsequent sample injections, however, the response declined. Apparently, the electrode coating is able to withstand the mechanical impact of the buffer flow and the cyclic variations in the chemical environment from running to regeneration buffer for several days.

### 3.4 Capacitive and ELISA hYKL-39 immunosensing in test samples

The measured capacitance and absorbance changes for individual model samples spiked with hYKL-39 in the concentration range 0.5–150 µg L<sup>-1</sup> was used to derive their OA biomarker content, from pre-determined calibration curves. The averaged data from triplicate measurements of each sample, together with the equivalent information from ELISA, are listed in Table 1. Both methods offered recoveries close to 100%; however in contrast to capacitive immunosensing, ELISA failed to quantify hYKL-39 in samples at the lowest and highest analyte concentrations tested, as expected from the differences in detection limit and linear range seen in the calibration trials discussed in Section 3.2.

### 3.5 Capacitive and ELISA hYKL-39 immunosensing in synovial fluid

The hYKL-39 concentrations in synovial fluids from four OA patients, donated by a local hospital, were determined by capacitive immunosensing and ELISA, in comparative trials. Both procedures were also used for hYKL-39 analysis in lysates from Jurkat, U937 and 293t cells. The choice of cells was based on the facts that Jurkat and U937 cell lysates have been reported to contain detectable levels of expressed hYKL-39 while the 293t cell line does not show hYKL-39 secretion. Jurkat and U937 lysates thus offered a physiological matrix that exposed the hYKL-39 immunosensors not only to their target but also to a mixture of other biomolecules with the potential to affect the analytical signal. Analyte-free 293t cell lysates, on the other

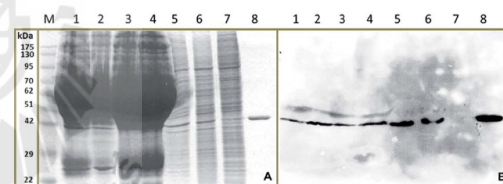


Fig. 2 Clinical sample and cell lysate electrophoresis on a 10% polyacrylamide-SDS gel. Lane: M, protein markers; lanes 1–4, synovial fluid from osteoarthritis patients; lane 5, Jurkat cell lysate; lane 6, U937 cell lysate; lane 7, 293t cell lysate; lane 8, pure hYKL-39 (2 µg). (A) Coomassie-blue stained gel. (B) Immunoblot detected with anti-hYKL-39 polyclonal antibody (1 : 10 000 dilution).

Table 1 Determination of hYKL-39 in model samples using capacitive immunosensor ( $n = 3$ ) and standard ELISA ( $n = 3$ ) quantification<sup>a</sup>

hYKL-39 concentration (µg L <sup>-1</sup> )	Detected hYKL-39 concentration (µg L <sup>-1</sup> )			
	Immunosensor	% recovery	ELISA	% recovery
0.5	0.5 ± 0.1	103.9 ± 1.4	n. d.	n. d.
2.5	2.6 ± 0.1	100.7 ± 1.1	2.5 ± 0.6	99.9 ± 2.2
5.0	5.1 ± 0.1	100.4 ± 3.8	5.1 ± 0.1	101.5 ± 2.6
50.0	51.2 ± 0.3	102.4 ± 0.6	49.6 ± 1.5	99.1 ± 3.0
150.0	149.9 ± 2.4	100.0 ± 1.6	96.4 ± 0.6	64.3 ± 0.4

<sup>a</sup> n. d. = not detected.

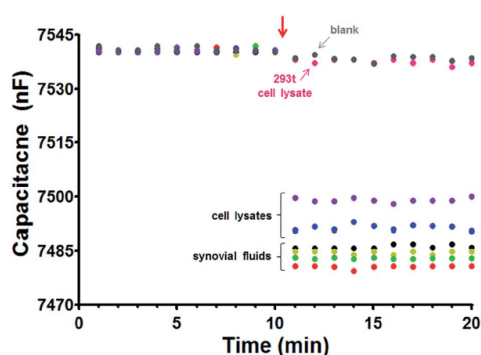


Fig. 3 Cell lysate and synovial fluid analysis, by capacitive immunosensing. Sample injection is marked by a red arrow. A decrease in the sensor capacitance indicates the presence of hYKL-39, the concentration of which can be determined from the calibration curve.

Table 2 Determination of hYKL-39 in clinical samples and cell lysates using capacitive immunosensor ( $n = 3$ ) and standard ELISA ( $n = 3$ ) quantification<sup>a</sup>

Sample	Detected hYKL-39 concentration ( $\mu\text{g L}^{-1}$ )	
	Immunosensor	ELISA
Synovial fluid #1	$59.4 \pm 2.4$	$58.3 \pm 3.4$
Synovial fluid #2	$106.3 \pm 0.8$	$107.0 \pm 2.5$
Synovial fluid #3	$68.1 \pm 1.3$	$67.7 \pm 1.2$
Synovial fluid #4	$89.0 \pm 2.7$	$88.8 \pm 1.6$
Jurkat	$26.4 \pm 0.4$	$25.2 \pm 3.1$
U937	$10.6 \pm 0.3$	$9.8 \pm 0.8$
293t	n. d.	n. d.

<sup>a</sup> n. d. = not detected.

hand, served as a useful negative control. Before biomarker quantification, samples were inspected by SDS-polyacrylamide gel electrophoresis (SDS-PAGE) and immunoblotting for hYKL-39 (Fig. 2). In each case Coomassie blue staining showed a band of the same mobility as pure hYKL-39 (Fig. 2A, lane 8) in the four synovial fluids and in Jurkat and U937 cell lysates, which was confirmed by immunoblotting (Fig. 2B). Only 293t cell lysates produced no hYKL-39 signal in the immunoblot. hYKL-39 was expected in the synovial fluid of joints from

positively diagnosed OA patients; its presence in the lysates of Jurkat and U937 cells, associated with innate and adaptive immune pathways, suggests that the protein may be involved in a defensive response to inflammation, however the exact mechanisms of this involvement are not yet clear and need further studies.

Synovial fluids and cell lysates are complex mixtures; they were therefore diluted 10-fold with 25 mM phosphate buffer, pH 7.0 before immunosensor and ELISA analysis, in order to minimize matrix interference with signal generation. The superimposed capacitances plotted in the left part of the traces in Fig. 3, up to 10 minutes, are the baseline values before sample injection, while the capacitances plotted in the left part of the traces in Fig. 3, up to 10 minutes, are the baseline values before sample injection when the hYKL-39 immunosensor is exposed to running buffer; 200  $\mu\text{L}$  aliquots of the diluted samples were then injected. In agreement with immunoblot analysis of the samples, a significant capacitance decrease was observed with all pathological synovial fluids and for the Jurkat and U937 cell lysates; synovial fluid from healthy people was not available for analysis. Injection of 293t lysate, on the other hand, led to the same small capacitance decrease as the injection of measuring buffer alone. Capacitance changes with individual samples were used to derive their content of hYKL-39, from previously determined calibration curves. The averaged data from triplicate measurements of each sample, together with the same facts from ELISA, are listed in Table 2. Regarding accuracy, the results from electrochemical hYKL-39 immunosensing were not significantly different (by  $t$ -test) from those of the ELISA immunoassay, standard deviations being small for both methods. The synovial fluid samples from the four different OA patients varied in their hYKL-39 contents, again with good agreement between electrochemical immunosensor and optical ELISA. The observed difference may be a reflection of variation in OA status of the individuals providing the samples.

The absence of hYKL-39 from 293t cell lysates allowed generation of samples with a genuine biological matrix but 'spiked' with known amounts of hYKL-39, for recovery measurements. hYKL-39 concentrations of 20 and 30  $\mu\text{g L}^{-1}$  were quantified and measurements with the capacitive immunosensor and control ELISA showed recoveries close to 100% in both cases (Table 3). Also included in Table 3 are trials with spiked synovial fluid samples. Based on a comparison with the values obtained for the non-spiked equivalents (Table 1) adequate recovery rates could

Table 3 Determination of hYKL-39 in spiked clinical samples and 293t cell lysate using capacitive immunosensor ( $n = 3$ ) and standard ELISA ( $n = 3$ ) quantification

Spiked concentration ( $\mu\text{g L}^{-1}$ )	Detected concentration ( $\mu\text{g L}^{-1}$ )			
	Immunosensor ( $\mu\text{g L}^{-1}$ )	Recovery (%)	ELISA ( $\mu\text{g L}^{-1}$ )	Recovery (%)
Synovial fluid #1 + 50 $\mu\text{g L}^{-1}$	$109.1 \pm 0.1$	$99.1 \pm 0.1$	$110.6 \pm 1.2$	$101.1 \pm 1.2$
Synovial fluid #2 + 50 $\mu\text{g L}^{-1}$	$155.1 \pm 1.0$	$99.2 \pm 0.6$	$156.7 \pm 0.8$	$99.8 \pm 0.4$
Synovial fluid #3 + 50 $\mu\text{g L}^{-1}$	$118.4 \pm 0.6$	$100.3 \pm 0.5$	$118.7 \pm 1.2$	$100.8 \pm 0.8$
Synovial fluid #4 + 50 $\mu\text{g L}^{-1}$	$139.6 \pm 0.4$	$100.4 \pm 0.3$	$141.6 \pm 1.2$	$102.0 \pm 0.7$
293t + 20 $\mu\text{g L}^{-1}$	$20.2 \pm 0.4$	$100.8 \pm 2.2$	$20.5 \pm 0.5$	$102.4 \pm 1.8$
293t + 30 $\mu\text{g L}^{-1}$	$29.7 \pm 0.2$	$99.1 \pm 0.7$	$30.4 \pm 0.5$	$101.2 \pm 1.2$

be computed for the entire set of measurements and confirm the absence of confounding matrix effects. The observed competitive analytical performance in all the comparative trials reported suggest that capacitive electrochemical immunosensing is a potentially valuable option for laboratories engaged in hYKL-39-based OA analysis, either as a reference tool or, especially for real sample levels down to 10-fold below the lower limit of linear range for ELISA testing, as a stand-alone approach.

The strongest argument for choosing the electrochemical over the optical strategy is the approximately 30-fold lower detection limit, as this would facilitate recognition of osteoarthritic joint degradation close to onset of the disease, when analyte levels are expected still to be very low. Simplicity, the low cost of instrumentation, convenience in operation, the portability of the small apparatus and the feasibility of fully automated measurements are additional features that make capacitive biosensing as described herein a recommendation for *in vitro* hYKL-39 determinations in body fluids and cell lysates.

#### 4. Conclusions

Attachment of an antibody directed against hYKL-39, a biomarker for osteoarthritis, to Au-WEs produced immunosensors that could measure sensitively the changes in capacitance on antibody-antigen binding, by analysis of current traces after the application of potential steps. Capacitive hYKL-39 immunosensing had a wider linear response range and, more importantly, a lower detection limit, than optical ELISA, which is currently the sole methodology for analysis of the biomarker in clinical and research laboratories. In synovial fluid from four different osteoarthritis patients the electrochemical screen detected and quantified hYKL-39 with values in accordance with those from routine ELISA. The quality of the analytical performance of this first non-optical hYKL-39 assay and the general benefits of electrochemical equipment – low cost, simplicity and ease of operation are offered together with the feasibility of automation, miniaturization, and portability – make capacitive hYKL-39 immunosensing worth further exploration, in the wide field of osteoarthritis research.

#### Acknowledgements

Wethaka Chaocharoen is grateful for grant CHE510767 from The Office of the Higher Education Commission, Thailand and the program “Strategic Scholarships for Frontier Research Network for the Ph.D. Program, Thai Doctoral degree”. Supporting funds came also through a Suranaree University of Technology (SUT) grant to Wipa Suginta (SUT1-102-57-24-19) and Albert Schulte (SUT1-102-57-24-01) and SUT budget allocations to the Biochemistry – Electrochemistry Research Unit and the Center of Excellence on Advanced Functional Materials. Sincere thanks go to Dr David Apps, Biochemistry Reader (retired), Centre for Integrative Physiology, Edinburgh University, Scotland for his critical manuscript reading and language improvement. We also acknowledge the support in general laboratory issues of the Biochemistry Laboratory of SUT's Center for Scientific and Technological Equipment and kind

advice of Associate Professor Dr Panote Thavarungkul and colleagues from the Trace Analysis and Biosensor Research Center, Prince of Songkla University, Thailand in questions about capacitive immunosensing.

#### References

- 1 S. Glyn-Jones, A. J. R. Palmer, R. Agricola, A. J. Price, T. L. Vincent, H. Weinans and A. J. Carr, *Lancet*, 2015, **386**, 376–387.
- 2 S. Sovani and S. P. Grogan, *Orthop. Nurs.*, 2013, **23**, 25–36.
- 3 M. Lotz, J. Martel-Pelletier, C. Christiansen, M. L. Brandi, O. Bruyère, R. Chapurlat, J. Collette, C. Cooper, G. Giacomelli, J. A. Kanis, M. A. Karsdal, V. Kraus, W. F. Lems, I. Meulenbelt, J. P. Pelletier, J. P. Raynaud, S. Reiter-Niesert, R. Rizzoli, L. J. Sandell, W. E. van Spil and J. Y. Reginster, *Ann. Rheum. Dis.*, 2013, **72**, 1756–1763.
- 4 F. J. Blanco, *Osteoarthritis Cartilage*, 2014, **22**, 2025–2032.
- 5 M. F. Hsueh, P. Önerfjord and V. B. Kraus, *Matrix Biol.*, 2014, **39**, 56–66.
- 6 M. Ishijima, H. Kaneko and K. Kaneko, *Ther. Adv. Musculoskeletal Dis.*, 2014, **6**, 144–153.
- 7 S. J. Kim, Y. M. Park, B. H. Min, D. -S. Lee and H. C. Yoon, *BioChip J.*, 2013, **7**, 399–407.
- 8 S. Y. Hong, Y. M. Park, Y. H. Jang, B. H. Min and H. C. Yoon, *BioChip J.*, 2012, **6**, 213–220.
- 9 A. C. Bay-Jensen, Q. Liu, I. Byrjalsen, Y. Li, J. Wang, C. Pedersen, D. J. Leeming, E. B. Dam, Q. Zheng, P. Qvist and M. A. Karsdal, *Clin. Biochem.*, 2011, **44**, 423–429.
- 10 S. Gargiulo, P. Gamba, G. Poli and G. Leonarduzzi, *Curr. Pharm. Des.*, 2014, **20**, 2993–3018.
- 11 E. Steck, S. Breit, S. J. Breusch, M. Axt and W. Richter, *Biochem. Biophys. Res. Commun.*, 2002, **299**, 109–115.
- 12 T. Knorr, F. Obermayr, E. Bartnik, A. Zien and T. Aigner, *Ann. Rheum. Dis.*, 2003, **62**, 995–998.
- 13 A. Ranok, P. Khunkaewla and W. Suginta, *Monoclonal Antibodies Immunodiagn. Immunother.*, 2013, **32**, 317–325.
- 14 S. Y. Song, Y. D. Han, S. Y. Hong, K. Kim, S. Y. Yang, B. H. Min and H. C. Yoon, *Anal. Biochem.*, 2012, **420**, 139–146.
- 15 Y. M. Park, S. J. Kim, K. J. Lee, S. S. Yang, B. H. Min and H. C. Yoon, *Biosens. Bioelectron.*, 2015, **67**, 192–199.
- 16 Y. Sun, X. Hu, Y. Zhang, J. Yang, F. Wang, Y. Wang, R. Deng and G. Zhang, *J. Agric. Food Chem.*, 2014, **62**, 11116–11121.
- 17 W. Chaocharoen, W. Suginta, W. Limbut, A. Ranok, A. Numnuam, P. Khunkaewla, P. Kanatharana, P. Thavarungkul and A. Schulte, *Bioelectrochemistry*, 2015, **101**, 106–113.
- 18 C. Berggren, B. Bjarnason and G. Johansson, *Electroanalysis*, 2001, **13**, 173–180.
- 19 C. Berggren and G. Johansson, *Anal. Chem.*, 1997, **69**, 3651–3657.
- 20 W. Limbut, P. Kanatharana, B. Mattiasson, P. Asawatreratanakul and P. Thavarungkul, *Biosens. Bioelectron.*, 2006, **22**, 233–240.
- 21 M. Schimpl, C. L. Rush, M. Betou, I. M. Eggleston, A. D. Recklies and D. M. F. van Aalten, *Biochem. J.*, 2012, **446**, 149–157.

## **CURRICULUM VITAE**

**NAME** Miss Wethaka Chaocharoen

**DATE OF BIRTH** 27 May 1987

**PLACE OF BIRTH** Bangkok, Thailand

**INSTITUTION ATTENDED**

Suranaree University of Technology, Nakhon Ratchasima, Thailand, 2005-2008, Bachelor of Science (Environmental Health)

Suranaree University of Technology, Nakhon Ratchasima, Thailand, 2009-2015, Doctor of Philosophy (Biochemistry)

**AWARDS AND SCHOLARSHIPS**

First class honors, Suranaree University of Technology, Nakhon Ratchasima, Thailand, 2008

Strategic Scholarships for Frontier Research Network for the Ph.D. Program, Thai Doctoral degree, from the Office of the Higher Education Commission 2009-2015